Institut für Biochemie und Biologie
AG Pflanzenphysiologie

Phosphorylation of polyglycans, especially glycogen and starch

Dissertation zur Erlangung des akademischen Grades
"doctor rerum naturalium"
(Dr. rer. nat.)

in der Wissenschaftsdisziplin "Biochemie"

eingereicht an der
Mathematisch-Naturwissenschaftlichen Fakultät
der Universität Potsdam

von
Felix Nitschke

Potsdam, den 30.04.2013

Published online at the
Institutional Repository of the University of Potsdam:
URL http://opus.kobv.de/ubp/volltexte/2013/6739/
URN urn:nbn:de:kobv:517-opus-67396
http://nbn-resolving.de/urn:nbn:de:kobv:517-opus-67396

To my parents who always believed in me.

Table of contents

List of tables

List of figures

List of abbreviations

ATP	Adenosine-5'-triphosphate
BSA	Bovine serum albumin
CBM	Carbohydrate binding domain
D_2O	Deuterium oxide (heavy water)
DP	Degree of polymerization
DQF-COSY	Double quantum filtered correlation spectroscopy
DSP	Dual specificity phosphatase domain
Epm2a	Gene encoding for the phosphatase laforin
Epm2b	Gene encoding for the ubiquitin E3 ligase malin
fFFF-MALLS-DRI	Flow field-flow fractionation coupled to multiangle laser light scattering and differential refractive index detection
FID	Free induction decay
GXP	Glucose X-phosphate (X = 1, 2, 3, 4, 6)
G6PDH	Glucose 6-phosphate dehydrogenase
GBE	Glycogen branching enzyme
GP	Glycogen phosphorylase
GS	Glycogen synthase
HMBC	Heteronuclear Multiple Bond Correlation
HMQC	Heteronuclear multiple quantum coherence
HSQC	Heteronuclear single quantum coherence
LB	Lafora body
LD	Lafora disease; epilepsy progressive myoclonic 2 (Epm2)
LDA	Limit dextrinase (pullulanase)
LSF1/LSF2	Like-SEX-Four1/Like-SEX-Four2
M6P	Maltose 6-phosphate
MTT	(3-(4,5-Dimethylthiazol-2-yl)-2,5-diphenyltetrazolium bromide
NAD^+/NADH	Oxidized/reduced form of nicotinamid adenine dinucleotide
$NADP^+$/NADPH	Oxidized/reduced form of nicotinamid adenine dinucleotide phosphate
NH_4OAc	Ammonium acetate
NMR	Nuclear magnetic resonance
6P-gluconate	6-Phosphogluconate
PMS	Phenazine methosulfate
SBE	Starch branching enzyme
SD	Standard deviation
SEM	Standard error of mean
SEX4	Phosphoglucan phosphates in plants (starch excess 4)
SHGL	>10 kDa fraction of plant water-soluble heteroglycans
SS	Starch synthase
UDP	Uridine diphosphate

1 Introduction

1.1 Glycogen and starch – animals and plants are facing similar problems

Living systems are characterized by a status far away from thermodynamic equilibrium. To maintain (against all odds) their vital biochemical and informational order they need a constant supply of energy that is used to fulfill one of the three tasks, mechanic work, transport of molecules and ions, and synthesis of (macro)molecules from simpler precursors (Lehninger *et al.*, 2001; Berg *et al.*, 2003). However, environment typically does not permanently provide sufficient energy that can immediately be used by a living system. Thus, environmental changes force living systems to accumulate some kind of storage of energy (as well as reduced carbon).

Since living systems consist of organic matter the backbone of which is always reduced carbon, the uptake of carbon from the environment is an additional necessity of life. The carbon is taken up in either reduced or oxidized form. Typically, animals import reduced carbon which implies a preceding reduction. Photosynthesis-competent organisms are capable of utilizing CO_2 and reducing the carbon by photosynthesis. Since photosynthetic carbon fixation requires light plants typically need to store light-derived energy and fixed carbon to maintain life during the night. Animals, by definition heterotrophs, are destined to take up chemical energy that has once been converted from light energy and carbon dioxide by autotrophs. For a variety of reasons, most animals do not have a continuous food supply and, therefore, need to store energy and carbon for those periods of time when food is not available.

Both animals and plants largely store energy and carbon both as lipids and as carbohydrates which serve different purposes according to their properties. As an example, lipids contain more energy per mass unit compared to carbohydrates but conversion of energy from lipids takes longer. Thus, organisms benefit from lipids for long-time storage of carbon and energy, such as in plant seeds and animal fat tissue. If a relatively fast or frequent mobilization of carbon and/or energy is required organisms typically utilize carbohydrates (Müller, 2004; Frayn, 2003; Taiz and Zeiger, 2007).

Almost all plants synthesize starch while most heterotrophic organisms rely on glycogen (Ball *et al.*, 2011). Both carbohydrate stores are chemically similar but differ in some important structural features: They almost exclusively comprise α-D-glucopyranose moieties (glucosyl residues; for minor constituents see 1.2.2) that when released as glucose can be either used for ATP generation and/or feed numerous metabolic pathways (Berg *et al.*, 2003). Both carbohydrate stores allow accumulation of lots of glucose moieties inside cells without severely affecting the osmolarity of the cell (Meléndez-Hevia *et al.*, 1993). The glucosyl residues in glycogen and starch are linked by only two types of glucosidic bonds, α-1,4- and α-1,6-linkages. The former are quantitatively dominant giving rise to helical chains and the latter constitute branching points. Native starch is a water-insoluble particle that consists of two types of α-polyglucans, amylopectin and amylose (Pérez and Bertoft, 2010). By contrast, glycogen is a hydrosoluble and relatively homogeneous biomolecule (Meléndez-Hevia *et al.*, 1993; Meléndez *et al.*, 1999). Amylopectin, like glycogen, possesses a relatively high degree of branching but, as opposed to glycogen, branchings are clustered rather than regularly distributed in the entire molecule.

Besides structural similarities the enzymology of starch and glycogen is also related (Ball *et al.*, 2011). In mammals, glycogen synthase (GS) and glycogen branching (GBE) enzymes are required for glycogen biosynthesis. In mammals GS repetitively transfers glucosyl residues from UDPglucose to non-reducing ends of α-glucan chains and GBE forms the α-1,6 branching points. Likewise, amylopectin synthesis is based on glucan elongating and branching reactions, although several starch synthase and starch branching isozymes participate in manufacturing the final structure. Moreover, starch synthases utilize ADPglucose as glucosyl donor as do glycogen synthases in some prokaryotic organisms. Glycogen breakdown is catalyzed by glycogen phosphorylase (GP), which mediates reiterating transfers of terminal glucosyl residues to orthophosphate yielding glucose 1-phosphate (G1P), and glycogen debranching enzymes (GDE), which cleave α-1,6 interglucose linkages. The dismantling of amylopectin is similarly driven by degradation of linear glucan chains and debranching. However, hydrolysis of α-(1,4) linkages in amylopectin is mainly mediated by β-amylases that release maltosyl residues from the non-reducing end, and the mode of debranching reactions is different between plants and animals (Roach *et al.*, 2012; Zeeman *et al.*, 2010; Ball *et al.*, 2011). Additionally, cycles of phosphorylation and dephosphorylation, the former by glucan water dikinase (GWD) and phosphoglucan water dikinase (PWD), the latter by the phosphatase SEX4 and SEX4-like proteins, obviously play an important role in amylopectin degradation (as well in mobilization of the entire starch granule; Ritte *et al.*, 2006; Kötting *et al.*, 2009; Santelia *et al.*, 2011). Mutant plants that lack GWD, PWD or SEX4 are compromised in starch turnover and exhibit a starch excess phenotype. It has been shown that phosphorylation at the starch granule surface facilitates the access of degrading enzymes by causing a transition of glucan chains from a highly ordered, insoluble to a less ordered state that facilitates solubilization (Hejazi *et al.*, 2008, 2009, 2010).

Both starch and glycogen contain a low proportion of phosphate. The steady-state level of starch phosphorylation varies widely depending on the plant species and/or the plant organs. In most cases less than 1% of the glucosyl residues carry monophosphate esters (Perez and Bertoft, 2010; Zeeman *et al.*, 2010). For glycogen, Lomako *et al.* (1994) reported ca. one phosphate per 650 glucosyl residues. The enzymology of glycogen phosphorylation is far less elucidated than that of starch and its physiological function is not at all clear. However, an important role of the phosphate residues in maintaining the structural integrity of glycogen has to be assumed since it became known that Lafora disease – a severe teenage-onset type of epilepsy – is largely caused by a non-functional α-glucan phosphatase, namely laforin, and that the knockout of laforin in mouse model leads to an increased phosphorylation of glycogen. In humans, the disease is characterized by gradual accumulation of an abnormal insoluble form of glycogen which is deposited in various tissues, including brain. In the latter, the insoluble glycogen is believed to gradually overtake neuronal dendrite cytoplasm provoking intractable and soon fatal seizures (Minassian, 2001; Turnbull *et al.*, 2011). Thus, controlled phosphorylation and dephosphorylation seem to be vital to functional metabolism of glycogen as well as of starch.

The functional similarity of plant and animal glucan phosphatases SEX4 and laforin, as demonstrated by the successful complementation of *Arabidopsis thaliana* SEX4 knockout mutants with laforin (Gentry *et al.*, 2007; Kötting *et al.*, 2009), suggest a close relation of the enzymology of starch and glycogen phosphorylation. However, *in silico* approaches did not reveal any enzyme in animals similar to plant GWD or PWD (Gentry *et al.*, 2009). Recently glycogen synthase has

been proposed to incorporate phosphate into glycogen via a circumstantially occurring side reaction, the assumed mechanism of which explains monophosphate esters at glucosyl carbon C2 and C3, but excludes C6 phosphorylation (Tagliabracci *et al.*, 2011) which is the predominant phosphorylation site in starch.

The proposed GS-mediated glycogen phosphorylation has some obvious implications. It requires a significant flexibility of the active site of GS, since it transfers chemically very different residues (glucosyl and phosphoglucosyl moieties) to the same acceptor site of the substrate (glycogen). Phosphorylation of glycogen being product of an inevitable side reaction is unlikely to be regulated and has no distinct physiological function but is rather an error that requires correction by laforin in order to keep glycogen metabolism functional. The question why some animal species lacking laforin (Gentry *et al.*, 2007) do not suffer from glycogen precipitation is left unanswered. Finally, starch and glycogen whose metabolism otherwise shares many similarities are very different with respect to enzymology and the physiological role(s) of polyglucan phosphorylation.

Based on these uncertainties, reassessment of substantial elements of glycogen phosphorylation seems justified because imprecise description of glycogen phosphorylation can erratically affect future Lafora disease research and impede the understanding of mechanisms that lead to the mentioned lethal disease and are usually the first step towards a cure.

This work aims to employ knowledge about starch phosphorylation and related methods to the field of glycogen. Due to the described structural similarities between starch and glycogen consumptive analytic methods were largely established using well characterized starch and were then transferred to glycogen.

After laying out a wider view over the topic, a more detailed introduction is given in the following sections.

1.2 Structure of starch and glycogen

Starch and glycogen are carbon and energy storages in plant and animal cells, respectively. While glycogen resides in the cyctosol starch in higher plants is found in plastidial compartments. Both are polymers almost exclusively comprising glucosyl monomers that allow the storage of vast amounts of glucose inside of cells, without significantly increasing the osmolarity of the cells (Meléndez-Hevia *et al.*, 1993).

Isolated glycogen is a polydisperse mixture of water soluble molecules. By contrast, isolated starch comprises a mixture of water insoluble semicrystalline particles (granules) heterogeneous in size. Structural parameters, determined for starch and glycogen, are, therefore, average values for a heterogeneous preparation that for the most part do not allow conclusions for individual particles.

Electron microscopy performed on rat liver glycogen revealed two types of particles: β-particles with a diameter of 10 to 60 nm and variable conglomerates of those particles with diameters up to 300 nm (α-particles; Drochmans, 1962; Wanson and Drochmans, 1968). The latter are so far described only for rat liver and are discussed to be formed by covalent linkage between β-particles (Manners, 1991; Sullivan *et al.*, 2010). Glycogenin, a protein that initiates the formation of glycogen molecules, resides in the centre of ß-particles (Roach *et al.*, 2012). Other proteins, among them many enzymes of the glycogen metabolism, are also present in the β-particles (Rybicka, 1996; Stapleton *et al.*, 2010).

Starch granules are composed of the two types of polymers, amylopectin and amylose. Depending on species and organ both the average size of the granules and the amylopectin to amylose ratio vary (Zeeman *et al.*, 2002; Lindeboom *et al.*, 2004; Buléon *et al.*, 1998a). However amylopectin typically accounts for more than 75% of the dry weight of starch granules (Zeeman *et al.*, 2010). Starch granules also contain small amounts of protein that reside both at the granule surface and in its interior parts (Perez and Bertoft, 2010).

1.2.1 Organization of glucan chains in starch and glycogen

Connected via α-1,4 glucosidic bonds, glucosyl residues of both glycogen and starch form glucan chains oriented with the non-reducing end towards the periphery of the polymer. Branching of the linear chains occurs by α-1,6 glucosidic bonds. While amylose is only lightly branched (Buléon *et al.*, 1998a) the abundance of branching points in amylopectin (4 to 6% of glucosidic bonds) and glycogen (8 to 10% of glucosidic bonds in mammals) is similar, although higher in the latter (Ball, 2002; Zeeman *et al.*, 2010). However, the distribution of branching points in amylopectin and glycogen differs and this difference is largely responsible for the different physicochemical properties of both storage products.

Branching points in amylopectin are discontinuously distributed which results in the lamellar structure of the starch granule characterized by concentric alternation of semi-crystalline and rather amorphous regions (periodicity of ca. 9 nm; Jenkins *et al.*, 1993). While in the latter branching occurs frequently, the semi-crystalline regions largely comprise clusters of unbranched double helices the glucan chains of which mainly consist of 12 to 15 glucosyl residues (Zeeman *et al.*, 2010). Longer chains occur less frequently and span two or three crystalline clusters (Hizukuri, 1986; Smith, 2001). The highly ordered arrangement of the double helices causes crystallinity of the region and determines the allomorph of the entire starch granule (Imberty *et al.*, 1991).

As revealed by X-ray diffraction analysis, native starches differ in the arrangement of double helices depending on their botanical source. For instance in wild type cereal starches double helices are arranged in flat layers and render the A-type allomorph more compact. By contrast, in the B-type allomorph the helices form a hexagonal cavity that contains water molecules (Imberty *et al.*, 1991). This allomorph characterizes starches from dicotyledonal storage organs (such as potato tubers) as well as for instance transitory leaf starch in *Arabidopsis thaliana* and potato (Gallant *et al.*, 1997; Hejazi *et al.*, 2008). A third allomorph, the C-type, describes a mixture of crystallite types A and B within a single granulum and is believed to be present in legume starches (Buléon *et al.*, 1998b). The fine structure of the starch granules is likely to have important biochemical implications. *In vitro* experiments demonstrated that the allomorph affects the performance of enzymes active on the carbohydrate as amylolysis of A-type starch proceeds faster than that of the B-type (Gérard *et al.*, 2001). Additionally, studies on maltodextrins crystallized in either A or B-type allomorph revealed that glucan solubilization in consequence of phosphorylation by PWD differs between both allomorphs and, hence, is dependent of the physical character of the phosphorylated substrate (Hejazi *et al.*, 2009).

Within the lamellar structure of amylopectin the largely linear chains of amylose are thought to be randomly spread. Individual amylose chains were attributed to both the semi-crystalline and the amorphous region and, thus, are likely to contribute to the physicochemical features of the granule (Perez and Bertoft, 2010).

Branching points in glycogen, as opposed to amylopectin, are believed to be more equally distributed in glycogen molecules. The widely accepted model of Whelan (Gunja-Smith *et al.*, 1970; Roach *et al.*, 2012) describes glycogen chains to be organized in tiers. The first tier exclusively contains the single glucan chain that is covalently bound to glycogenin and that, through branching, carries the chains of the next tier. Branched chains, mostly in the inner part of the molecule, were named B-chains, as opposed to A-chains in the outmost tier of the molecule that carry no further chains. It has been shown that in average A- and B-chains have degrees of polymerization (DP) of around 13 (Gunja-Smith *et al.*, 1971). Because by β-amylolysis ca. 50% of glycogen glucosyl residues can be released half of the glycogen chains were assigned to be unbranched A-chains (Marshall *et al.*, 1974). Since all chains (except the innermost one) arise from a branching point all branched B-chains consistently carry in average two A- and/or B-chains. In the model of Whelan, therefore, the number of chains per tier is doubled from one tier to the following (equation 1). This fits well to the findings obtained during β-amylolysis because according to equation (2) the amount of glucosyl residues in the outmost tier is approximately the half of all glucosyl residues in the molecule.

(1) $$C_n = 2^{(n-1)}$$

(2) $$\frac{1}{2} \cdot \sum_{n=1}^{n} 2^{(n_i-1)} \cong 2^{(n-1)}$$

C_n	Number of chains in tier n
n	Order of tier

The analysis of α-limit dextrins of glycogen revealed that the distance of the branching points is variable but in most cases at least four glucosyl residues (Roberts and Whelan, 1960). Goldsmith *et al.* (1982) modeled the steric dimensions of a DP 13 glucan chain upon X-ray diffraction data for maltoheptaose complexed with glycogen phosphorylase a. In their opinion within such a glucan chain the two branching points would be located on glucosyl residue 5 or 6 and 9 or 10, counted from the reducing end. For a spherical molecule of DP 13 glucan chains, branched according to equations (1) and (2), they compared the volume of the tier with that of the glucan chains within that tier. For that calculation they assumed a molecule radius of 20 nm (Wanson and Drochmans, 1968) and that for each tier the radius increases by the same increment. Furthermore, from average sedimentation coefficients (Wanson and Drochmans, 1968) they roughly estimated the molar mass of rabbit muscle glycogen to be ca. 10^7 g/mol which led them to ca. 55,000 glucosyl residues per molecule. Obviously, they assumed ca. 180 g/mol for each glucosyl residue while in glucans due to the loss of one H_2O per glucosidic bond the actual molar mass is ca. 162 g/mol (yielding 61,690 glc residues per molecule). However, the former number of glucosyl residues is supported by the equations (1) and (2) yielding 53,248 glucosyl residues per molecule when n = 12 and the glucosyl chain length is 13. Irrespective the actual amount of glucosyl residues per glycogen molecule, the calculations of Goldsmith *et al.* (1982) demonstrate that in tier 12 the volume of a 20 nm sphere is smaller than that of the chains comprised by the tier. Thus, it was assumed that glycogen particle growth is limited to 12 tiers by steric hindrance of glucosyl chains at the surface of the molecule (Goldsmith *et al.*, 1982).

However, this assumption is only true for the theoretical parameter set described above. Especially, when the sphere's radius increase per tier is not constant but for example slightly larger at higher tier numbers, than even in 20 nm particles the limit of tiers would increase. Furthermore, according to the calculations of Goldsmith *et al.* (1982), radii higher than 23.5 nm would allow a 13^{th} tier. It was reported that the diameter of glycogen β-particles is rather heterogeneous and obeys a Gaussian distribution between 20 and 60 nm for rabbit muscle glycogen (Wanson and Drochmans, 1968) or 10 to 40 nm in human muscle glycogen (Marchand *et al.*, 2002). Smaller radii indicate additional factors that limit the physiological size of glycogen particles. This is supported by the fact that glycogen particle size differs between compartments of the human muscle cell (Marchand *et al.*, 2002) and, thus, seems to be regulated.

The assumption of a uniform glucan chain length of DP 13 contradicts experimental data and, thus, strongly simplifies the current concept of glycogen structure. It has been shown that glycogen consists of glucan chains with more or less continuously distributed DPs of 4 to greater than 40 (Palmer *et al.*, 1983a). Sequential debranching revealed that exterior glycogen chains have a rather narrow distribution and on the average are shorter average of DP 13. By contrast, the distribution of B-chains is wider with a higher average DP (Manners, 1991). Palmer *et al.* (1983b) demonstrated that the DP of maltodextrins released from oyster glycogen with isoamylase increased as a function of the extent of isoamylolysis. They concluded that the glucan chain DP increases from the periphery to the centre of the glycogen molecule.

1.2.2 Minor components of starch and glycogen converge in phosphate esters

So far starch and glycogen have been described as branched homoglucans that both interact with proteins. However, it is long known that glycogen as well as starch contains some minor components besides glucosyl residues and protein. Some starches for instance contain low amounts of lipids that are thought to interact with the amylose fraction in the starch granule (Pérez and Bertoft, 2010).

Regarding glycogen it has been reported that during α-amylolysis small amounts of maltulose (glucopyranosyl-α[1,4]-fructopyranose) were released revealing the existence of fructose monomers in rabbit liver glycogen (Peat *et al.*, 1952; Roberts and Whelan, 1960). However, the amounts were very small and the possibility of analyzing contaminated glycogen preparations was considered in neither of the two publications. To the best of my knowledge, no further results have been published on that subject.

Later the group of Whelan demonstrated the presence of D-glucosamin in native rat and pig liver glycogen which can be released by either phosphorylase or amylase, yielding D-glucosamin 1-phosphate and glucosamine, respectively (Romero *et al.*, 1980; Kirkman and Whelan, 1986). While the amount of D-glucosamine in native glycogen was only 0.016 to 0.032 mmol/mol glucosyl residues it was shown that rat liver glycogen synthase incorporates D-glucosamin in to glycogen from chemically synthesized UDPglucosamin with a rate 12 times lower than with UDPglucose (Tarentino and Maley, 1976). A limited flexibility or selectivity of the active site of glycogen synthase has to be assumed since UDPgalactose, as opposed to N-acetyl glucosamin, serves also as monosaccharyl donor.

Starch and glycogen share another structural feature related to minor components. Both carbohydrates contain phosphate esters. In potato tuber starch monophosphate esters were

reported at glucosyl carbon C6, C3 and C2 (Hizukuri *et al.*, 1970; Tabata and Hizukuri, 1971). While the former two phosphorylation sites were confirmed by ^{31}P NMR (Lim and Seib, 1993; Ritte *et al.*, 2006), the site at C2 was deduced from two observations: first, under acid conditions a very small proportion of orthophosphate is released from α-limit phosphodextrins at a higher rate than determined for the release of orthophosphate from authentic G3P, and second, within glucan chains besides C6 and C3 only at glucosyl C2 a free hydroxyl group exists that permits esterification. However the amount of C2 phosphorylation was estimated to account for less than 1% of the glucan phosphate (Tabata and Hizukuri, 1971). For starches from potato tubers, *Curcuma* roots, cassava seeds, *Arabidopsis thaliana* leaves the ratio of C6:C3 phosphorylation was determined by quantitative ^{31}P-NMR or mass spectrometry techniques. C6 phosphorylation accounted for 72-89% (Blennow *et al.*, 2000a; Haebel *et al.*, 2008; Ritte *et al.*, 2006) and, thus, C6 is considered the most frequently used phosphorylation site. The steady-state phosphorylation of starch described in the literature is largely given as degree of C6 phosphorylation. The latter varies among starches from different plant organs and species (Table 1).

Table 1. C6 phosphate esters in starches of different origins

Organ	Species	C6 phosphate esters [mmol/mol glc]	References
Roots and tubers	*Curcuma*	9.5[1)]	
	Potato	2.8 - 4.6[2)]	Blennow *et al.*, 2000a, 2000b
	Cassava	0.41	
Leaf	Potato	0.43 - 0.73	Blennow *et al.*, 2000b; Ritte *et al.*, 2004
	Arabidopsis thaliana	0.65 - 1.4[3)]	Ritte *et al.*, 2006; Haebel *et al.*, 2008; Kötting *et al.*, 2009; Santelia *et al.*, 2011
Seed	Mung bean	0.57	Blennow *et al.*, 2000b
	Sorghum	0.15	Blennow *et al.*, 2000a, 2000b
	Rice	<0.02[4)]	Blennow *et al.*, 2000b; Tabata *et al.*, 1975
	Maize	<0.01[4)]	
	Wheat	<0.01	Tabata *et al.*, 1975
	Barley	n.d.	Blennow *et al.*, 2000b

1) Value given for *Curcuma zedoaria*
2) Value depending on the variety of *Solanum tuberosum*
3) Plants were grown under different light conditions; under long-day conditions C6 phosphorylation is higher
4) Only Tabata *et al.* (1975) were able to detect very small amounts of C6 phosphorylation

It has been shown very early that starch phosphate resides largely in the amylopectin fraction (Schoch, 1942). Furthermore Blennow *et al.* (2000a) located them mainly in the amorphous region of the amylopectin. The role of starch phosphate was addressed in many recent publications and will be described below (see 1.5).

The presence of phosphate in glycogen preparations was demonstrated by Fontana (1980) who fed fasted rats with glucose and radiolabeled orthophosphate and observed strict co-fractionation of glycogen and the labeled phosphate which was retained in several attempts of purification. Furthermore he isolated α-limit phosphodextrins some of which were labile when subjected to acid hydrolysis. One component of the hydrolysate, however, showed strong co-migration with glucose 6-phosphate in paper electrophoresis. The idea of two types of phosphate esters in glycogen, the more abundant one being acid labile, was seized by other researchers and confirmed for rabbit muscle and liver glycogen (Manners, 1991). Lomako *et al.* (1993) deduced from hydrolysis

experiments that the labile component must be a phosphodiester, bridging from C1 of one glucosyl residue to a carbon in another one. Many years later Tagliabracci *et al.* (2011) performed various NMR studies on rabbit skeletal muscle glycogen the results of which contradicted the previously published data. Glycogen was reported to be monophosphorylated at C2 and C3, while no evidence for any phosphodiester or a monophosphate at C6 was found. From early on the degree of glycogen phosphorylation is given as total phosphate, i.e. orthophosphate after hydrolysis of all phosphate esters. It has been studied in rat, rabbit, and mouse and varies depending on the tissue the glycogen is originating from (Table 2).

Table 2. Total phosphate content in glycogens of different origins

species	organ	total phosphate [mmol/mol glc]	References
Rat	Liver	1.9 – 3.2[1)]	Fontana, 1980
Rabbit	Liver	0.17	Manners, 1991
	Skeletal muscle	1.2 – 1.7	Lomako *et al.*, 1993; Manners, 1991
Mouse	Liver	0.4 – 0.5	Tagliabracci *et al.*, 2007; Turnbull *et al.*, 2010
	Skeletal muscle	0.6 – 1.0	Tagliabracci *et al.*, 2007, 2008; Turnbull *et al.*, 2010; Tiberia *et al.*, 2012

1) Calculated from 0.1 – 0.17% by weight (Fontana, 1980)

Concerning phosphorylation starch and glycogen are similar in two ways: first, they contain phosphate esters bound to glucosyl residues, and second, the degree of phosphorylation is within the same range (Tables 1 and 2). However, regarding the position of the phosphate at the glucosyl residues starch and glycogen seem to differ. Previous results for glycogen are, however, somewhat contradictory (see above). Especially the presence or absence of C6 phosphorylation in glycogen is decisive for considering phosphorylation of starch and glycogen as similar.

1.3 Starch metabolism

Photosynthesis is the basis of life in the biosphere. In higher plants it takes place in the chloroplasts of leaf mesophyll cells and comprises the light reaction at the thylakoid membrane and the reactions of the Calvin cycle in the stromal space. While the light reaction converts energy derived from light quanta to biochemically usable energy, i.e. generates ATP and reduction equivalents, namely NADPH, the Calvin cycle is the basis of all biochemical pathways in plant cells since thereby carbon dioxide is fixed and, utilizing the products of the light reaction, reduced organic carbon is synthesized. Glyceraldehyde 3-phosphate, one of the most commonly used intermediates of the Calvin cycle, is the elementary sugar phosphate that is employed for the synthesis of hexoses either in the chloroplast or in the cytosol. While in the chloroplast hexoses can be stored as glucosyl residues in leaf starch, sucrose is synthesized in the cytosol and transported to other plant organs, such as seeds, storage roots or tubers where storage starch is synthesized from sucrose-derived glucose.

Starch is storage of reduced carbon generated by photosynthesis and, as the oxidation of reduced carbon by cellular respiration yields ATP, likewise storage of energy. The mobilization of starch generally fuels cellular processes independently of photosynthesis. In chloroplasts of leaf mesophyll cells transient starch is synthesized during the day and degraded during the night in order to deliver reduced carbon and energy for essentially all cellular processes. For long-time storage

starch is built up in specialized plastids, named amyloplasts, in mostly non-photosynthetic storage organs of plants, such as seeds, roots and tubers (Zeeman *et al.*, 2010). It supplies reduced carbon and energy for non-photosynthetic phases of growth, such as the establishment of seedlings after germination (Fincher, 1989). Storage starch is also a major carbohydrate source of the human diet as the harvested parts of plants are mainly cereal seeds (such as rice, maize, wheat, barley, sorghum) and roots or tubers (such as potato or cassava). For details see Zeeman *et al.* (2007).

1.3.1 Starch synthesis

Starch synthesis includes the elongation of α-(1,4) glucan chains and the branching of linear glucans as well as the *de novo* synthesis of starch granule primers. However, to form the semi-crystalline clusters essentially lacking branching points in amylopectin more randomly occurring branching patterns have to be corrected by debranching. The initiation of starch granule synthesis appears to differ from that of glycogen initiation but has not yet been fully elucidated (Zeeman *et al.*, 2010).

In higher plants the elongation largely occurs through transfer of the glucosyl residue from ADPglucose to the non-reducing end of an α-(1,4) glucan primer. ADPglucose is either generated from intermediates of the Calvin cycle or, as in non-photosynthetic tissues, from sucrose-derived hexoses. Key enzymes are plastidial phosphoglucomutase and ADPglucose pyrophosphorylase that mediate the conversion of G6P to G1P and that of the latter to ADPglucose, respectively. Mutants lacking either of the enzymes contain only minimal amounts of leaf starch (Casper *et al.*, 1985; Lin *et al.*, 1988) indicating that leaf starch biosynthesis mainly utilizes the ADPglucose-dependent pathway (Ball *et al.*, 2011). Under some conditions reserve starch synthesis may however implicate a second pathway as there is evidence for a temperature-modulated phosphorylase-mediated glucosyl transfer into starch in potato tubers and rice endosperms (Satoh *et al.*, 2008; Fettke *et al.*, 2012).

The glucosyl transfer from ADPglucose is, however, executed by several isoforms of starch synthases that were assigned to the class of granule-bound synthases (GBSS) and several classes of soluble synthases designated as SSI, SSII, SSIII, and SSIV (Patron *et al.*, 2005). Analysis of mutant plants lacking one or more starch synthases revealed insight into their respective function.

One starch synthase encoded by the waxy locus (GBSS, granule bound SS) almost exclusively resides in the starch granule and cannot be removed by treatment of native starch granules with compounds such as detergent or protease (Rhaman *et al.*, 1995, Tanaka *et al.*, 1967). Starches from transgenic plants with reduced GBSS activity apparently contain less amylose as judged by iodine staining of solubilized or native starch granules (Visser *et al.*, 1991; Kuipers *et al.*, 1994; Tatge *et al.*, 1999). Thus, GBSS is assumed to play an essential role in amylose synthesis within the starch granule (Denyer *et al.*, 2001; Zeeman *et al.*, 2010; Fujita and Nakamura, 2012). However, it can not be excluded that the absence of GBSS also leads to alterations in amylopectin structure. The formation of the blue iodine-starch complex is dependent on the presence of long linear chains as predominant in amylose (Teitelbaum *et al.*, 1980). It has been shown that rice endosperm amylopectin also binds iodine (even if to a much lower extent than amylose) and that reduced GBSS expression results in amylopectin with lower iodine binding capacity and less chains with a very high degree of polymerization (DP; Takeda *et al.*, 1987; Umemoto *et al.*, 2002).

SS isoforms are either soluble in the plastid stroma or only partly bound to the starch granules. SSI, SSII, and SSIII seem to differ in their preference to elongate glucan chains with low, medium and high DPs (Jeon *et al.*, 2010; Zeeman *et al.*, 2010). SSI-deficiency leads to altered chain length distributions in amylopectin. Chains of the DP 8 to 12 are decreased, while those of DP 6 to 7 and 13 to 19 are increased. Thus, SSI appears to preferentially elongate chains of a DP 6 to 7. This was confirmed by *in vitro* studies comparing glucans with and without modification by SSI (Fujita *et al.*, 2006). In similar fashion SSII has been shown to mainly elongate chains of DP 6 to 11 (Zhang *et al.*, 2004) while SSIII contributes to the formation of long (DP exceeding 30) from intermediate chains (Fujita *et al.*, 2007). The relative expression levels of the isoforms SSI, II, and III vary among plant tissues and probably contribute to structural variations in starches from different origins (Zeeman *et al.*, 2010). SSIV seems to play a crucial role in the initiation of starch granule biosynthesis as plants lacking the isozyme show a decreased number of granules per chloroplast while the amount of starch per fresh weight remains largely unchanged (Roldán *et al.*, 2007). Additionally, it has been shown *in vitro* that SSIV has a high starch synthase activity when maltotriose, an intermediate of the plastidial starch degradation (see 1.3.2), is used as a primer (Szydlowski *et al.*, 2009). The function of all SS isoforms seems to be redundant to some extent. For instance, even the complete absence of SSI does not result in changes of crystallinity, shape, or size of starch granules (Fujita *et al.*, 2006); the loss or reduction of one SSIII isoform enhances the endogenous SSI (Fujita *et al.*, 2007); chloroplasts lacking SSIV are still capable of synthesizing starch granules (Roldán *et al.*, 2007). However, the simultaneous knockout of several SS isoforms often leads to severely impaired starch synthesis. As an example, *Arabidopsis thaliana* plants lacking SSIII and SSIV loose their ability to synthesize starch (Szydlowski *et al.*, 2009).

Branching of amylopectin glucan chains is catalyzed by branching enzymes (SBE) that fall into two classes, SBEI and SBEII. These enzymes exist as monomers capable of hydrolyzing α-(1,4) glucosidic bonds and reattaching the cleaved chain of 6 or more glucosyl residues to the same or to a proximate glucan chain forming an α-(1,6) glucosidic bond. SBEI and SBEII differ in their preference to branch polyglucans with different degrees of branching and in the preferred length of the transferred chain. SBEI mainly transfers longer chains (DP ≥ 16) from rather lowly branched polyglucans while SBEII acts on polyglucans with more branching points transferring glucosyl chains with DP ≤ 12. While these observations were made by *in vitro* studies using maize SBEI and SBEII expressed in E. coli (Guan *et al.*, 1997) starch of mutants lacking SBEI do not always show altered chain length distributions (Blauth *et al.*, 2002; Dumez *et al.*, 2006). However, amylopectin from rize endosperm lacking functional SBEI had less longer chains (DP >= 37). The concurrent observation of facilitated gelatinization points to a distinct role of SBEI in storage starch synthesis by forming long chains spanning semi-crystalline clusters (Satoh *et al.*, 2003).

The roles of isoforms within the SBEII class depend on plant species and organ. In rice and maize endosperm the absence of SBEIIb, which is specifically expressed in the endosperm, leads to major alterations in the amylopectin structure, short chains being strongly decreased while long chains are much more abundant (Nakamura, 2002; Yao *et al.*, 2004). SBEIIa does not largely compensate for the SBEIIb loss in the endosperm (Nishi *et al.*, 2001). Its absence almost exclusively affects the amylopectin structure of leaf starch (Blauth *et al.*, 2001). In *Arabidopsis thaliana* leaves three isoforms of branching enzymes were found, two of which (SBE2, SBE3) belong to class II of SBEs and are essential to functional biosynthesis of transitory starch. While their functions are redundant

to a great extend the knockout of both results in the depletion of starch and an accumulation of cytosolic α-maltose (Dumez *et al.*, 2006).

Debranching of amylopectin is catalyzed by three classes of isoamylases (ISA1, ISA2, and ISA3) and a limit dextrinase (LDA, also called pullulanase). All these enzymes carry out direct debranching by hydrolyzing α-1,6 interglucose bonds and releasing the entire formerly attached chain. That is opposed to indirect debranching as mediated by glycogen debranching enzyme during glycogen degradation in animals which consists of two consecutive steps (Wilson *et al.*, 2010; Ball *et al.*, 2011; see 1.4.2). Direct debranching in plants implicates the existence of a plastidial pool of soluble maltodextrins that are possible substrates of various starch-related enzymes.

While ISA3 and LDA are thought to mainly function during amylopectin degradation (see 1.3.2), ISA1 and ISA2 are implicated in amylopectin synthesis since loss of either of the two in *Arabidopsis thaliana* leaves and potato tubers leads to reduced starch contents and the accumulation of glycogen-like water soluble glucans (phytoglycogen) with more branching points and lower average chain length than normal amylopectin (Zeeman *et al.*, 1998; Hussain *et al.*, 2003). In *Arabidopsis thaliana* ISA2 the amino acids that are thought to be required for the catalysis of α-(1,6) hydrolysis are not conserved. In potato recombinant ISA2 did not show any catalytic activity (Hussain *et al.*, 2003). It has been shown, though, that ISA1 and ISA2 form heterooligomeric complexes in *Arabidopsis thaliana* leaves and potato tubers, while in rice endosperms also homooligomeric complexes of ISA1 are found (Hussain *et al.*, 2003; Delatte *et al.*, 2005; Utsumi and Nakamura, 2006). In leaves of *Arabidopsis thaliana* mutants lacking ISA2 the activity of ISA1 is also abolished which has shown to be due to the missing of the ISA1-ISA2 complex. Comparison of amylopectin from wild type and ISA1, ISA2, or ISA1-ISA2 double knockout plants revealed that in the mutants branching points are closer together, similar as in the phytoglycogen. Thus, it is reasoned that the complex of the two isoforms ISA1 and ISA2 facilitates crystallization of amylopectin by preferential hydrolysis or branching points that are close together (Delatte *et al.*, 2005). Debranching during starch biosynthesis is likely responsible for the occurrence of unbranched adjacent chains that form double-helices and give rise to semi-crystalline areas in starch, one of the basic characteristics of functional starch granules (Jeon *et al.*, 2010). However, a limited role of the ISA1-ISA2 complex in starch degradation was recently suggested. Small branched products of starch degradation as detectable in ISA3-LDA double knockout plants are apparently debranched by the complex, albeit at a slow rate (Streb *et al.*, 2012; see 1.3.2).

It should be noted that an incorporation of phosphate esters into starch occurs obviously also during starch biosynthesis which explains the rather invariant steady-state level of starch phosphorylation (Nielsen *et al.*, 2004; Ritte *et al.*, 2004). Two distinct dikinases with orthologs in almost all plants have been identified, glucan, water dikinase (GWD) and phosphoglucan, water dikinase (PWD) (Ritte *et al.*, 2006; Ball *et al.*, 2011). Plants lacking one of the enzymes exhibit strongly altered patterns of starch monophosphate esters and are compromised in growth. The observed starch excess in these mutants, indicates a important role of phosphorylation during starch turn-over (Kötting *et al.*, 2005; Ritte *et al.*, 2006; see 1.5).

The complex physicochemical structure of starch granules relies on the concerted implementation of chain elongation, branching and debranching. Each function is carried out by several partly interdependent isoforms all of which have more or less distinct substrate preferences. The

frequently observed redundancy of isoforms renders starch synthesis a very robust process of plant primary metabolism.

1.3.2 Starch degradation

The mobilization of energy and reduced carbon stored in starch is accomplished by starch degradation. The products of the plastidial starch degradation have to be provided to the cytosol of cells in order to maintain cellular function independent of photosynthesis. Several enzymes including isoforms are involved in dismantling the complex physicochemical structure of the starch granules. The vital process has been widely studied in leaves and cereal endosperm while the understanding of starch degradation in tubers, roots, and non-cereal seeds is yet rudimentary (Zeeman *et al.*, 2010). This paragraph will focus on leaf starch degradation and will leave the differences to endosperm starch degradation largely uncovered.

During starch degradation intact chloroplasts export mainly starch derived maltose and to some extend glucose (Weise *et al.*, 2004; Weber *et al.*, 2000). The concentration of maltose in *Arabidopsis thaliana* leaves is strongly increasing in line with the ongoing degradation of starch during the night (Niitylä *et al.*, 2004). The export of maltose is mediated by the transporter MEX located in the inner chloroplast envelope (Niitylä *et al.*, 2004). A glucose translocator in the chloroplast envelope has been functionally characterized (Weber *et al.*, 2000). *Arabidopsis thaliana* mutants lacking MEX possessed high levels of starch and very high maltose concentrations as compared to wild type. While the knockout of the putative plastidic glucose translocator does not result in a phenotype its knockout additional to MEX increases growth retardation and reduced starch turnover as compared with the MEX single mutant (Cho *et al.*, 2010). Thus, maltose is considered the major product of starch degradation which, together with minor amounts of glucose, is exported from the chloroplast and further metabolized in the cytosol.

It has been shown that degradation of transient starch is mainly driven by β-amylases which, being exo-amylases, release β-maltose from a non-reducing end of an α-(1,4) glucan chain that consist of at least 4 glucosyl residues (Zeeman *et al.*, 2010). *Arabidopsis thaliana* genome encodes for nine β-amylases-like proteins (BAM1 to BAM9) four of which are located in the chloroplast (BAM1 to BAM4) and should have access to the starch granule (Fulton *et al.*, 2008). Recombinant BAM1 and BAM3 show β-amylolytic activity. While of the two only the knockout of BAM3 leads to a moderate starch excess phenotype BAM1-BAM3 double mutants show severe starch excess and indicate that both enzymes are functional but, possibly, to a great extent redundant *in vivo*. Recombinant BAM2 showed a β-amylolytic activity 10 to 20 times lower than recombinant BAM1 or BAM3 and the *Arabidopsis thaliana* BAM1-BAM2-BAM3 triple mutant does not enhance the phenotype of the BAM1-BAM3 double mutant. Thus, no catalytic function of BAM2 in the degradation of starch could yet be assigned. However, though recombinant BAM4 is not catalytically active the knockout of BAM4 results also in elevated starch and decreased maltose levels at the end of the night period. Thus, it is speculated whether BAM4 might have regulatory functions and enhances starch degradation by interaction with other proteins involved in starch degradation (Fulton *et al.*, 2008).

Since β-amylases are not capable of hydrolyzing α-(1,6) glucosidic bonds β-amylolysis at the surface of starch granules will result in stubs of maltosyl or maltotriosyl residues that converge in branching points located in the amorphous regions of the starch granule (Zeeman *et al.*, 2010). Further degradation requires the action of debranching enzymes, such as isoamylase (ISA) and

limit dextrinase (LDA). As opposed to ISA1 and ISA2, both mainly involved in starch synthesis (see 1.3.1), ISA3 and LDA preferentially release short chains from branching points, such as in β-limit dextrins after β-amylolysis. *Arabidopsis thaliana* mutants lacking ISA3 show higher starch levels and a slower rate of starch degradation. The additional knockout of LDA increases this phenotype. It has, thus, been concluded that ISA3 and LDA dismantle the clusters of branching points in the amorphous region of the granules and make the linear chains of the following semi-crystalline granule region available to subsequent β-amylolysis (Delatte *et al.*, 2006).

Another important feature of starch degradation is reversible phosphorylation by glucan, water dikinase (GWD), phosphoglucan, water dikinase (PWD), as well as the phosphatase SEX4 and SEX4-like proteins (LSF). Knockout of either of the enzymes leads to strong impairment of starch degradation (Ritte *et al.*, 2006; Kötting *et al.*, 2009; Comparot-Moss *et al.*, 2010; Santelia *et al.*, 2011). There is profound evidence that by phosphorylation the packing of glucan double helices in the semi-crystalline regions of amylopectin is disturbed yielding a less ordered state of glucan chain arrangement (Hejazi *et al.*, 2008). It has been shown *in vitro* that the rates of granule degradation by hydrolytic enzymes are significantly enhanced with simultaneous phosphorylation and dephosphorylation (Kötting *et al.*, 2009). Dephosphorylation is required due to the inability of the hydrolases to cleave α-1,4 linkages in close vicinity of glucan bound phosphate esters (Kötting *et al.*, 2009). A detailed description of the role of starch phosphate can be found below (see 1.5).

The analysis of ISA3-LDA double mutants revealed that α-amylases may also contribute to starch degradation. This was based on two observations. First, the double mutant is capable of degrading most of the starch synthesized during the day. Second, the double mutant accumulates branched soluble dextrins with short side chains (Delatte *et al.*, 2006) which are only partly removed by the ISA1-ISA2 complex (Streb *et al.*, 2012). Both results imply circumventing the β-limit and would require α-amylases which are endo-acting α-1,4 hydrolases capable of cleaving in between branching points. This is consistent with an observed pleiotropic increase of AMY3 protein, one of the three α-amylases encoded in *Arabidopsis thaliana* genome, and α-amylase activity in the absence of ISA3 and LDA. AMY3 has been predicted to reside in chloroplasts and has a diurnal pattern of transcript level (Stanley *et al.*, 2002). Furthermore, the additional knockout of AMY3 in *Arabidopsis thaliana* plants lacking ISA3 and LDA increases the starch excess phenotype of the double mutant background (Streb *et al.*, 2012). The significance of α-amylolysis during starch degradation in *Arabidopsis thaliana* wild type is, however, hard to estimate but may be low (or, alternatively, it can be compensated by other degrading enzymes) since it was shown that *Arabidopsis thaliana* triple mutants lacking all three α-amylases did not exhibit an impaired starch degradation (Yu *et al.*, 2005). In other species the impact of α-amylase on starch degradation is obviously higher since for instance rice mutants with reduced plastidial α-amylase exhibit starch excess (Asatsuma *et al.*, 2005).

Products of the combined action of β-amylases and debranching enzymes on starch granules are maltose and maltotriose. The latter can not be exported to the cytosol but has to be further metabolized. This occurs by the action of the chloroplastic disproportionating enzyme (DPE1). It transfers maltosyl residues from maltotriose to other linear glucans elongating the latter and releasing glucose. Consequently the loss of DPE1 leads to an accumulation of maltotriose in leaves of *Arabidopsis thaliana* during starch degradation. Furthermore, the rate of starch degradation is

decreased leading to high starch levels at the end of the night period and emphasizing the significance of DPE1 for starch degradation (Critchley *et al.*, 2001).
Longer linear glucans as generated by the action of DPE1 are subject of β-amylolysis. Additionally in the presence of orthophosphate plastidial phosphorylase could release glucosyl residues in the form of glucose 1-phosphate (G1P). This pathway is considered of minor importance of for starch degradation since the latter is not impaired by the knockout of plastidial phosphorylase (Zeeman *et al.*, 2004).

1.3.3 Integration of starch metabolism into cytosolic pathways

Illuminated photosynthesis-competent cells fix carbon dioxide by the Calvin cycle recruiting energy and reduction equivalents (ATP and NADPH, respectively) generated in the photosynthetic light reaction. Plant tissues with net photosynthate consumption (sinks) rely on the supply of reduced carbon from tissues with net production (sources) via vascular connections. Thus, in photosynthesis-competent cells intermediates of the Calvin cycle are utilized to 1) maintain all vital cellular processes of cellular anabolism, 2) supply energy and reduced carbon to sink tissues, and 3) store energy and reduced carbon for periods of time when photosynthetic carbon fixation is not possible. Thereby, they continuously maintain the aforementioned tasks.
Most common compounds translocated between source and sink tissues are relatively inert non-reducing sugars the most prominent sugar being sucrose which is synthesized in the cytosol. Interconversion of pools of glucose 1-phosphate (G1P), glucose 6-phosphate and fructose 6-phosphate (F6P) are mediated by phosphoglucomutase and phosphoglucoisomerase, respectively. UDPglucose pyrophosphorylase transfers UDP to G1P yielding pyrophosphate and UDPglucose. The latter reacts with F6P mediated by sucrose 6-phosphate synthase yielding sucrose 6-phosphate and UDP. The final step in sucrose synthesis consists of removal of phosphate by sucrose 6-phosphate phosphatase (Lunn and MacRae, 2003). In heterotrophic tissue sucrose synthase or invertase mediate sucrose conversion to hexoses which feed both dissimilatory and assimilatory pathways (Abid *et al.*, 2009; Gilbert *et al.*, 2012).
In the natural day/night cycle the metabolic situation in photosynthetic competent cells undergoes dramatic changes. While in the light phase mainly triose phosphate is exported from the chloroplast the starch degradation products maltose and glucose are exported during the night (Weise *et al.*, 2004). Thus, biochemical pathways in the plant cell must utilize both, small phosphorylated sugars and neutral sugars.
Triose phosphate isomerase interconverts dihydroxyaceton 3-phosphate and glyceraldehyde 3-phosphate both of which form fructose 1,6-bisphosphate as catalyzed by fructose 1,6-bisphosphat aldolase. Fructose 1,6-bisphosphatase mediates the formation of fructose 6-phosphate which can feed sucrose synthesis (see above).
It is imaginable that at night maltose and glucose could be converted to glucose 6-phosphate recruiting an α-glucosidase that releases glucose from maltose and an additional kinase reaction. However, other cytosolic pathways involving both neutral sugars seem to be of indispensible value. Those pathways implicate the cytosolic isoforms of disproportionating enzyme (DPE2) and phosphorylase (Pho2 in plants except *Arabidopsis thaliana* where it is named PHS2). *In vitro* studies revealed that DPE2 transfers glucosyl residues between various substrates as glucosyl donors and acceptors. Utilizing maltose as donor it releases glucose and transfers one glucosyl

residue to glucose, maltose or a suitable glycan in a reversible reaction (Lu and Sharkey, 2004; Chia *et al.*, 2004). In *Arabidopsis thaliana* mutants lacking DPE2 starch degradation is largely impaired and maltose levels exceed that of wild type by two orders of magnitude (Chia *et al.*, 2004) indicating that cytosolic maltose conversion by DPE2 is indispensible for functional primary metabolism. Another kind of glucosyl transfer is mediated by the cytosolic phosphorylase which reversibly transfers a glucosyl residue from a non-reducing end of an appropriate poly- or oligosaccharide to orthophosphate yielding G1P (Schächtele and Steup, 1986).

Coupling the reactions of cytosolic disproportionating enzyme and phosphorylase would establish a possible pathway from maltose to G1P without the necessity of an ATP consuming kinase reaction. This requires an intermediate substrate to which DPE2 transfers glucosyl residues and that subsequently serves as glucosyl donor for the phosphorylase mediating the G1P formation. It has been shown that, as opposed to the plastidial phosphorylase, the cytosolic isoform preferable binds to highly branched glucan structures such as glycogen (Shimomura *et al.*, 1982).

While in the cytosol of plant cells glycogen has never been detected cytosolic water soluble heteroglycans were described in several plant species and organs (Fettke *et al.*, 2009b). They consist of monosaccharides linked via a wide variety of glycosidic bonds. Arabinose and galactose being the most prominent, additionally, glucose, fucose, mannose, and rhamnose are found. In *Arabidopsis thaliana* the cytosolic heteroglycans exhibit size distributions from 25 to 70 kDa (Fettke *et al.*, 2005a).

Both, DPE2 and Pho2/PHS2, selectively act on the cytosolic heteroglycans *in vitro* while neither do Pho1/PHS1 nor the mammalian glycogen phosphorylase a. *In vitro* experiments revealed that both cytosolic enzymes (DPE2, Pho2/PHS2) reversibly transfer glucosyl residues to the cytosolic heteroglycans (Fettke *et al.*, 2005a, 2005b, 2006).

Analyses of cytosolic heteroglycans throughout the diurnal cycle and in mutants permitted further insight into the *in vivo* carbon fluxes via the heteroglycans and reveal a close connection to the starch metabolism. In wild type leaves of potato the molar weight distribution shifts to higher masses during starch degradation in the dark (Fettke *et al.*, 2005b). In similar correlation to the starch metabolism the amount of cytosolic heteroglycans in *Arabidopsis thaliana* leaves was increased in the dark (Fettke *et al.*, 2005a). Interestingly, DPE2 and PHS2 also show changes in the diurnal expression levels since in some *Arabidopsis thaliana* accessions both enzyme activities are increased in the dark and decreased in the light enabling a higher turnover of glucosyl residues via the pool of heteroglycans when starch is degraded (Fettke *et al.*, 2009b).

The effect of DPE2 has been studied in leaves of *Arabidopsis thaliana* mutants that lack the aforementioned enzyme and, hence, exhibit starch and maltose excess (see above). Intriguingly, this is not directly reflected by diminished steady-state glucosyl contents in the cytosolic heteroglycans. Contrarily, the amount of glucosyl residues is increased which points to another path of glucosyl transfer to the cytosolic heteroglycans (Fettke *et al.*, 2006). However, in the DPE2 knockout mutants the level of PHS2 is increased several fold (Chia *et al.*, 2004). This emphasizes a close functional relationship of the two enzymes and could explain the increased glucosyl content when in the mutant the phosphorylase-mediated glucosyl transfer is favoured (Fettke *et al.*, 2009a). The absence of DPE1 (plastidial isoform), however, does not increase the amount of glucosyl residues in the cytosolic heteroglycans (Fettke *et al.*, 2006). This is consistent with the fact that the phosphorylase utilized G1P pool is fed by glucose that is exported from the chloroplast

after being released from starch degradation products by DPE1 (see 1.3.2). Accordingly, overexpression of the cytosolic phosphoglucomutase (cPGM) in potato leads to reduced glucosyl residues in the cytosolic heteroglycans due to a diminished pool of cytosolic G1P, and alterations of Pho2 levels in transgenic potato plants showed positive correlation of the glucosyl content in cytosolic heteroglycans from leaves and the level of Pho2 activity. Both observations confirm a possible *in vivo* carbon flux towards the heteroglycans mediated by the cytosolic phosphorylase (Fettke *et al.*, 2008).

The description of two enzymes acting on the cytosolic heteroglycans, however, cannot reflect the whole enzymology of the newly discovered plant carbohydrate. For instance the large set of glycosidic linkages requires many carbohydrate-active enzymes that are yet to discover (Fettke *et al.*, 2009b). Regarding the fact that starch and glycogen, however different in cellular compartmentation and physical properties, both contain significant amounts of glucosyl phosphate it is reasonable to assume that phosphorylation is a modification common for carbohydrates. However, phosphorylation has yet not been described in heteroglycans.

1.4 Glycogen metabolism

Whereas most plants store reduced carbon and energy as starch animals largely rely on glycogen as storage carbohydrate. All animals being heterotrophs rely on the ingestion of nutrients that once originated from photosynthetic carbon dioxide fixation. Human diet consists of around 60% carbohydrates the majority of which is taken up as starch. The remainder is ingested in the form of fats and proteins (Frayn, 2003). Starch derived glucose absorbed from the human intestinal tract after a meal would potentially raise the blood sugar concentration up to 8 fold which is far from being physiologically useful. Nevertheless glucose is a major source of energy since around 75% of the daily ingested carbohydrates are oxidized. Some tissues, such as brain, even exclusively rely on glucose as energy source (Schmidt and Thews, 1997). Thus, all cells must be constantly supplied with glucose since it is the major source of energy generated. Efficient mechanisms are required to keep the steady-state blood glucose concentration in a physiological range.

Glycogen serves as glucose depository in many tissues. While most glycogen is stored in the liver and skeletal muscle, many other tissues are capable of synthesizing glycogen (Roach *et al.*, 2012). The concentration of blood sugar is largely regulated by the insulin/glucagon ratio. At raising blood sugar concentration insulin stimulates glycogen synthesis in liver, skeletal muscle and adipose tissue. In the latter two tissues insulin additionally mediates the translocation of glucose transporters (type GLUT4) to the plasma membrane and, thus, increases the cellular glucose uptake from the blood. While insulin simultaneously inhibits glycogen degradation in the liver this process is stimulated by the antagonist of insulin, glucagon, in the postabsorptive state when no longer glucose is taken up from the intestinal tract, hence, the blood sugar concentration and the insulin/glucagon ratio decrease. While glucose derived from skeletal muscle glycogen is restricted to local catabolism, hexose liberated from liver glycogen is mainly released to the blood stream to maintain the physiological blood sugar concentration in times of nutritional restriction. It should be noted that besides insulin and glucagon other hormones, such as adrenalin and noradrenalin, are involved in the regulation of mammalian glycogen metabolism (Frayn, 2003).

1.4.1 Glycogen synthesis

Since glycogen (as well as starch) is a branched polyglucan biosynthesis generally requires elongation of α-1,4 glucan chains by glycogen synthase and branching of linear glucans by branching enzyme. However, it is assumed that the branching points in glycogen, as opposed to those in starch, are evenly distributed (Meléndez-Hevia *et al.*, 1993). Therefore, debranching is considered not necessary during glycogen synthesis as it is in starch synthesis (see 1.3.1).

Glucosyl donor of mammalian glycogen is typically UDPglucose which, as described for starch, is a nucleotide sugar. In fact UDPglucose is also utilized as glucosyl donor in the plant system for sucrose biosynthesis (see 1.3.3). Likewise some glycogen synthesizing prokaryotes exist that utilize ADPglucose for glycogen synthesis (Ball *et al.*, 2011).

In animal cells imported glucose is phosphorylated to G6P by hexokinase-type enzymes. Phosphoglucomutase mediates the conversion of G6P to G1P the glucosyl residue of which in the presence of UTP is transferred to UDP under pyrophosphate release as catalyzed by a UDPglucose pyrophosphorylase. Thus, the generation of glucosyl donors for polyglucan biosynthesis follows similar pathways in animals and plants (Berg *et al.*, 2003).

It has been shown that *de novo* synthesis of glycogen molecules usually requires the protein glycogenin (Krisman and Barengo, 1975). It catalyzes two distinct reactions: 1) apparent self-glucosylation by transferring a glucosyl residue from UDPglucose to a conserved tyrosine residue, and 2) glucosyl transfer to the non-reducing end of the already protein bound glucose residues forming a linear α-1,4 glucan chain of 6 to 16 residues which serves as substrate for subsequent chain elongation by glycogen synthase (Hurley *et al.*, 2006). The chemically very different acceptor sites glucosylated by glycogenin (hydroxyl in either tyrosine or glucosyl C4) and the distance between the transferase active site and the glucosyl acceptor (tyrosine) argue for two phases of the glycogenin reaction (Roach *et al.*, 2012): first, it starts with intermolecular glucosylation, one glycogenin glucosylating another until the attached glucan chains have a DP of 4 to 6, and second, intramolecular glucosylation occurs as glycogenin molecules become capable of glucosylation of their own glucan chain (Lin *et al.*, 1999; Hurley *et al.*, 2006).

In silico searches revealed several glycogenin-like genes in plants including *Arabidopsis thaliana*. Additionally for some glycogenin-like plant proteins self-glucosylation was demonstrated, but no relation to starch metabolism was observed (Qi *et al.*, 2005). In search of a similar protein that initiates starch granule formation a self-glucosylating protein, named amylogenin, was discovered that, however, only transferred one glucosyl residue to an arginine and had no sequence similarities with glycogenin. Moreover, any involvement in starch metabolism could not be proven (Singh *et al.*, 1995). Recently, evidence was found that initiation of starch granule synthesis is accomplished by isoforms of starch synthase IV that is capable of elongating glucan chains as short as maltotriose and the absence of which results in a severely reduced number of starch granules (see 1.3.1; Roldán *et al.*, 2007; Szydlowski *et al.*, 2009).

Glucosylated glycogenin is used as substrate by glycogen synthase (GS) that subsequently transfers glucosyl residues from UDPglucose to the glycogenin glucosyl chain (McVerry *et al.*, 1974). However, the active site of glycogen synthase is assumed to possess partial flexibility or selectivity as the transfer of D-glucosamin and galactose from the respective UDP derivatives into glycogen has been demonstrated using rat liver glycogen synthase (Tarentino and Maley, 1976).

While in higher plants several starch synthase isoforms exist that have different physiological functions in starch metabolism (see 1.3.1) only two genes encoding for GS were identified in mammals as well as in yeast. The expression of the two mammalian isoforms, GYS1 and GYS2, is tissue-dependent but GYS1 seem to be present in all cells capable of glycogen synthesis (Browner *et al.*, 1989; Nuttall *et al.*, 1994; Farkas *et al.*, 1991). Unlike in starch metabolism defects in one of the synthases involved in glycogen metabolism is not compensated by the other isoform. Thus, patients deficient in either synthase isoform suffer from the consequences of insufficient glycogen storage in liver or muscle (Kollberg *et al.*, 2007; Weinstein *et al.*, 2006; Cameron *et al.*, 2009).
Similarly severe effects are observed if the one known glycogen branching enzyme (GBE1) is defective (Raju *et al.*, 2008). Two diseases were described (Andersen's disease and adult polyglucosan body disease) that rely on mutation in human GBE1 gene (Cavanagh, 1999). Both are characterized by loss of the branching enzyme activity in cells of the patients. In consequence glycogen is formed that is less water soluble, containing relatively long outer chains and very few branching points, and has hence been described as being amylopectin-like (Brown and Brown, 1966). Functional GBE has been shown to be active on outer α-1,4 glucan chains that have been elongated by GS. It first cleaves an α-1,4 glucosidic bond at least 6 glucosyl residues apart from the non-reducing end. Forming an α-1,6 glucosidic bond the released chain is subsequently attached to either the same or an adjacent linear chain (Verhue and Hers, 1966). Each branching event generates one additional site for GS-mediated chain elongation. Branching concurrent with the action of GS seems to largely determine the structure of the glycogen since branching enzyme defects cause dramatic structural changes.
However, other factors seem also vital to structural functionality of glycogen. Glycogen synthesizing tissues of patients suffering from Lafora disease also accumulate insoluble polyglucans likely originating from abnormally structured glycogen (Tagliabracci *et al.*, 2008). One of the genes, if mutated causing Lafora disease, encodes for the phosphatase Laforin that is capable of removing phosphoesters from glycogen (Minassian *et al.*, 1998; Tagliabracci *et al.*, 2007). In mouse models lacking functional Laforin the accumulation of insoluble polyglucans increases in line with the glycogen phosphate (Tagliabracci *et al.*, 2008). While plant starch is phosphorylated by distinct dikinases it has recently been proposed that glycogen is phosphorylated in a side reaction of glycogen synthase (see 1.5.2; Tagliabracci *et al.*, 2011).
The enzymology of glycogen synthesis comprises, as does that of starch synthesis, chain elongation and branching but is believed to be relatively simple regarding the number of isoforms of glycogen acting enzymes and the fact that debranching is not required during glycogen synthesis. Nevertheless the regulation of glycogen synthesis appears complex. The synthesis rate is discussed to be mainly determined by the influx of glucose into the cell and the activity of glycogen synthase (Roach *et al.*, 2012). In muscle both processes are regulated by insulin. The reception of insulin causes the translocation of GLUT4 glucose transporters to the muscle cell membrane facilitating the influx of glucose a large part of which is subsequently metabolized to UDPglucose. GS activity is regulated on at least two levels: first, by the state of GS phosphorylation at multiple hierarchical phosphorylation sites mediated by protein kinases and phosphatases, and second, it is allosterically activated by G6P. The reception of insulin promotes the inactivation of one of the GS kinases (GSK3; Patel *et al.*, 2008) as well as the activation of GS targeted protein phosphatase (PP1) and, thus, causes activation of GS by lowering its state of

phosphorylation. Furthermore glycogen degradation in muscle is inhibited due to deactivation of glycogen phosphorylase through dephosphorylation by insulin-dependent PP1 (Dent *et al.*, 1990). Additionally the insulin-mediated massive glucose uptake in muscle results in activation of GS by raised intracellular G6P levels (Pederson *et al.*, 2000).

1.4.2 Glycogen degradation

Glycogen degradation implicates cleavage of α-1,4 and α-1,6 glucosidic linkages and is accomplished in two biochemical ways. In the cytoplasm glycogen is degraded by the concurrent action of phosphorylase and debranching enzyme, the former cleaving α-1,4 linkages of linear glucan chains, the latter cleaving branching points. The second form of glycogen degradation occurs in the lysosome employing the compartment-specific enzyme, acid α-glucosidase which is capable of hydrolyzing both types of α-glucosidic bonds present in glycogen (Matsui *et al.*, 1984). Defects in that enzyme lead to Pompe's disease characterized by lysosomal accumulation of glycogen in several tissues and typically leading to death through heart insufficiency within the first two years of life (Reuser *et al.*, 1995). Deficiency in functional muscle or liver phosphorylase leads to cytosolic glycogen accumulation described as glycogen storage diseases V (muscle) and VI (liver). Though clinical features are not as severe as in Pompe's disease it is assumed that glycogen mobilization is largely accomplished by the phosphorolytic pathway in the cytosol (Roach *et al.*, 2012).

The phosphorylase, acting on non-reducing ends of outer glycogen chains, releases glucose 1-phosphate in the presence of ortho- and pyridoxal phosphate, the latter serving as acid-base-catalyst (Berg *et al.*, 2003). While the liver isoform, being constitutively phosphorylated, is regulated only allosterically muscle phosphorylase, like glycogen synthase (GS), is regulated both allosterically and by covalent modification. As opposed to GS, phosphorylation leads to activation of the phosphorylase and is executed by phosphorylase kinase. The latter is activated by calcium ions (Cook *et al.*, 2005) and protein kinase A (PKA) the activation of which is induced following adrenalin or glucagon reception (Newsholme *et al.*, 1992; Berg *et al.*, 2003). PKA likewise inactivates protein phosphatase 1 and thereby mediates inactivation of GS (see 1.4.1). AMP activates the muscle phosphorylase allosterically irrespective of its phosphorylation state (Vereb and Bot, 1979).

Glycogen phosphorylase action is obstructed when a glucosyl residue is reached that is four residues away form a branching point (Walker and Whelan, 1960). Glycogen debranching enzyme is necessary for further glycogen digestion. As an example for bifunctional enzymes it comprises two active sites one of which, an α-1,4 glucanotransferase activity site, cleaves the α-1,4 glucosidic bond closest to the branching point and transfers the released maltotriosyl chain to an adjacent chain. Subsequently an α-1,6 glucosidase activity that is located on the same protein monomer releases the remaining α-1,6 linked glucosyl residue in the form of glucose (Nakayama *et al.*, 2001). The mode of debranching is therefore indirect as opposed to direct debranching in plants (see 1.3.1; Wilson *et al.*, 2010; Ball *et al.*, 2011). Defects in human glycogen debranching enzyme lead to Cori's disease characterized by elevated levels of glycogen which is enriched in short outer glucan chains (Cheng *et al.*, 2009).

Normally glycogen degradation mainly yields G1P which is converted to G6P by phosphoglucomutase. The latter can enter glycolysis and subsequent pathways to generate ATP

that is for instance required for muscle contraction. In liver glucose can be generated form G6P by glucose 6-phosphatase. In times of nutritional limitation the entire organism is supplied with glucose that is exported from the liver cells to the blood stream. Glucose and G6P are allosteric inhibitors of both liver (Ercan-Fang *et al.*, 2005) and muscle phosphorylase (Vereb and Bot, 1979) and trigger negative feedbacks that prevent glycogen degradation in excess of the metabolic demand and in times of nutritional abundance.

The enzymologies of glycogen and starch degradation differ in two major points. First, while glycogen is mainly degraded by phosphorolysis starch degradation employs hydrolysis, the major product of glycogen degradation being G1P as opposed to maltose and glucose in starch degradation. Second, as mentioned for glycogen synthesis, enzymes responsible for glycogen degradation do not occur as partially redundant isoforms. While plant mutants lacking one enzyme involved in starch degradation do not necessarily exhibit a phenotype defects in either of the few glycogen degrading enzymes promptly lead to severe diseases.

1.5 The role of phosphate in starch and glycogen metabolism

The carbohydrate stores starch and glycogen typically contain monophosphate esters (see 1.2.2). The glucose-based steady-state levels vary between species but are generally low. Being even undetectable in some starches they can reach values up to approximately 10 mmol per mol glucosyl residues. The pattern of phosphate esters is believed to be different in starch and glycogen. While in starch the majority of phosphate is linked to the glucosyl carbon C6, according to a recent publication (Tagliabracci *et al.*, 2011) no C6 phosphate is detectable in glycogen. The glucosyl carbons C2 and C3 are believed to be the major phosphorylation sites in glycogen whereas if even only traces of C2 phosphate are assumed to be present in starch which, however, also contains C3 phosphate (see 1.2.2). Regarding starch metabolism the significance of these covalent modifications became apparent when strong starch-related phenotypes in plant mutants were related to deficiencies in enzymes mediating starch phosphorylation or dephosphorylation (Zeeman *et al.*, 2010). In the glycogen context the subject of carbohydrate phosphorylation is even relevant to humans since it is known that deficiency in a functional carbohydrate phosphatase (Laforin) causes a severe type of epilepsy (Lafora disease; Gentry *et al.*, 2007). For both, starch and glycogen, evidence has accumulated that phosphate esters have a great influence on the physico-chemical properties of the carbohydrates. At least regarding starch those properties are closely related to physiological functionality (Hejazi *et al.*, 2012a; Tagliabracci *et al.*, 2008).

1.5.1 Incorporation of phosphate into starch

Starch monophosphate esters are formed at C6 and C3 by at least two different plastidial enzymes (Ritte *et al.*, 2006). The first enzyme proven to incorporate phosphate into starch is the glucan water dikinase (GWD; Ritte *et al.*, 2002). It exclusively phosphorylates the C6 carbon of glucans, as opposed to the second discovered dikinase, phosphoglucan water dikinase (PWD), which is specific for phosphorylation in C3 (Ritte *et al.*, 2006). The enzymatic basis of the minor C2 phosphorylation in starch has yet to be elucidated. A third gene encoding a putative starch-related dikinase has been identified, GWD2 (Glaring *et al.*, 2007). All three dikinases contain N-terminal carbohydrate binding moduls (CBM) that, however, vary in structure and sequence. While PWD and

GWD2 contain starch binding domains (SBD) assigned to CMB20 family, the SBD of GWD is attributed to CMB45 family members of which possess a relatively low affinity for α-glucans (Christiansen *et al.*, 2009). Furthermore all three dikinases utilize ATP transferring the β-phosphate to glucosyl carbon. The C-terminal ATP-binding motif shows significant homology to the respective site in the prokaryotic phosphoenolpyruvate synthase and the pyruvate, orthophosphate dikinase from maize (Yu *et al.*, 2001). Though GWD2 has been shown to phosphorylate the C6 carbon of α-glucan substrates under *in vitro* conditions two observations mainly exclude GWD2 from being relevant in diurnal starch metabolism: 1) GWD2 lacks a transit peptide and has been shown to reside in the cytosol, 2) high expression levels of GWD2, only observed at relatively late developmental states of the plant, are restricted to mesophyl cells in close vicinity to the vascular system (Glaring *et al.*, 2007). These observations indicate a temporal and spatial separation from diurnal starch metabolism in mesophyll cells.

By contrast, GWD is essential for functional diurnal leaf starch metabolism. *Arabidopsis thaliana* plants mutated in the SEX1 (starch-excess1) gene which encodes GWD massively accumulate starch and are severely compromised in growth. The mutant starch appears to be enriched in amylose and comprises very low amounts of both, C6 and C3, phosphate esters (Caspar *et al.*, 1991; Yu *et al.*, 2001; Ritte *et al.*, 2006). PWD-deficiency in *Arabidopsis thaliana* mutants also causes a starch excess phenotype, though not as pronounced as in SEX1 mutants, and has minor effects on growth. The amount of starch C3 phosphate is strongly reduced in relation to C6 phosphate (Kötting *et al.*, 2005; Baunsgaard *et al.*, 2005; Ritte *et al.*, 2006). Apparently, C6 phosphorylation by GWD can to some extent compensate for the lack of functional PWD, but *in vivo* PWD is typically dependent of prephosphorylation by GWD (Ritte *et al.*, 2006), hence the name PWD.

Resolving the molecular basis of these phenotypical findings was the aim of many studies in the last decade which thereby shed light on the role of phosphate esters in starch metabolism. The reaction mechanism underlying glucan phosphorylation by dikinases has been studied on GWD. The protein contains two sites of autophosphorylation, one being a histidine residue conserved in the dikinases (Ritte *et al.*, 2002; Mikkelsen *et al.*, 2004; Baunsgaard *et al.*, 2005; Kötting *et al.*, 2005; Edner *et al.*, 2007), the other remaining to be identified. Apparently the terminal γ-phosphate is first transferred from ATP to the unknown amino acid, followed by a subsequent transfer of the β-phosphate to the histidine residue yielding AMP and doubly phosphorylated GWD. From histidine the phosphate is transferred to the target glucosyl carbon (C6 in the case of GWD), while that of the unknown residue moves to water, yielding orthophosphate. However, it has been observed that other acceptors for phosphotransfer from the unknown residue are also functional, such as AMP or ADP (Hejazi *et al.*, 2012b).

The nature of the carbohydrate substrate utilized by either of the two starch-related dikinases was largely investigated using *in vitro* assays with recombinant proteins. GWD phosphorylates native starch granules of both, A and B, allomorphs. The heterogeneous chemical and physical structures in starches from different sources are assumed to be responsible for variations in substrate usability by GWD (Hejazi *et al.*, 2008). PWD is largely unable of phosphorylating native starch unless the starch was prephosphorylated by GWD (Kötting *et al.*, 2005). This concurs with the effects of GWD or PWD knockout mutants on the abundance of specific phosphate esters in the respective mutant starch. These effects indicate that *in vivo* PWD acts downstream of GWD (see

above). Both dikinases exhibit similar substrate specificities, as described for native starch granule, when crystalline maltodextrins are used as model compounds for the dikinase action on the surface of starch granules. Interestingly, crystalline maltodextrins are a much better substrate for GWD than native starch granules. PWD-mediated phosphorylation is, however, dependent of the degree of prephosphorylation by GWD. Maltodextrins and prephosphorylated maltodextrins solubilized by heat treatment are not noticeably phosphorylated by GWD and PWD, respectively (Hejazi *et al.*, 2008). This implies that the physical arrangement determines whether or not α-glucan chains are efficiently phosphorylated whereas the chemical structure of the substrate (which is not altered when crystalline [prephosphorylated] maltodextrins are solubilized) has little or no effect. It implies that both enzymes act on α-glucans at crystalline surfaces rather than in solution (Hejazi *et al.*, 2012a). GWD seems to preferably utilize highly ordered structures given in crystalline maltodextrins, to a lesser degree in native starch, but not in solubilized maltodextrin preparations. PWD at first sight seems to require a minimum of phosphate for being catalytically active on crystalline surfaces. One major effect of phosphate incorporation into crystalline maltodextrins is the solubilization of α-glucans at the surface. With increasing phosphorylation by both GWD and PWD maltodextrins are released into solution. Interestingly, upon GWD action most of the released chains have not been phosphorylated (Hejazi *et al.*, 2008; 2009). This implies that solubilization of glucan chains at crystalline surfaces only requires a few incorporated phosphate esters that assumingly disturb the tight packing of chains in the crystalline structure. This disturbance subsequently leads to the massive solubilization of maltodextrins. PWD action on prephosphorylated crystalline maltodextrins results in a large amount of solubilized monophosphorylated chains indicating that PWD is indeed able to phosphorylate neutral α-glucan chains but its action is merely dependent of a state of a somewhat reduced physical order which is for instance achieved by prephosphorylation (Hejazi *et al.*, 2009). This is consistent with results obtained when PWD activity was measured without prior prephosphorylation using starches isolated from transgenic potato and rice plants. PWD-mediated phosphate incorporation was independent of the amount of endogenous C6 or total phosphate. Thus differential activities of PWD are likely caused by variations in the physical order of surface chains in the starches of transgenic plants with altered expressions of various starch synthesizing enzymes (Fettke *et al.*, 2009a). Molecular modeling studies support the idea that phosphate esters interfere with the physical arrangement of α-glucan chains. While C6 phosphate is supposed to interfere with helix-helix interactions, phosphorylation in C3 is seemingly capable of breaking double helices (Hansen *et al.*, 2009; Blennow and Engelsen, 2010). Intriguingly, the solubilization of prephosphorylated crystalline maltodextrins by PWD is enhanced when the maltodextrins were crystallized in the B-type allomorph that comprises a less tight arrangement of double helices (Hejazi *et al.*, 2009).

The starch excess in both mutants deficient in either dikinase indicates that phosphorylation is required during starch degradation. This was confirmed by showing that the degree of phosphorylation at the periphery of potato leaf starch granules increased during starch degradation in dark (Ritte *et al.*, 2004). *In vitro* experiments revealed that starch degradation is facilitated by simultaneous starch phosphorylation. Degradation of leaf starch granules by β-amylase (BAM1 or BAM3, see 1.3.2) and debranching enzyme (ISA3, see 1.3.2) was massively accelerated in the presence of functional GWD and ATP. Additional PWD further enhanced the effect (Edner *et al.*,

2007). Furthermore it was shown that BAM3 preferably acts on solubilized maltodextrins while the activity on crystalline maltodextrins was two orders of magnitude lower (Hejazi *et al.*, 2008).
The phosphate-mediated alterations at the starch granule surface are therefore believed to lower the physical order of glucan chain arrangement and rendering the surface more suitable for starch hydrolyzing enzymes that preferably act on soluble glucans. Enzymatic hydrolysis occurs during starch degradation but is also part of starch synthesis as it is currently believed that debranching is necessary during starch synthesis to yield the clustered amylopectin branching pattern as a prerequisite to starch crystallization. It is not inconceivable that phosphate incorporation, also largely occurring during starch synthesis (Nielsen *et al.*, 1994; Ritte *et al.*, 2004), maintains surface properties suitable for synthesizing enzymes and avoids premature crystallization. However, the precise role of phosphate esters during starch synthesis has not yet been experimentally addressed.

1.5.2 Incorporation of phosphate into glycogen

The putative role of glycogen phosphate changed dramatically within the last decade. While from early on phosphate was found in preparations of glycogen it took a while until it was considered to be actually covalently bound to and a part of glycogen. In fact almost half a century ago phosphate was solely considered as contamination and the purity of glycogen preparations was evaluated upon the completeness of phosphate abolishment (Mordoh and Krisman, 1966; Wanson and Drochmans, 1968). Fontana (1980) was the first who published a study that addressed the glycogen phosphate itself. Glycogen and some phosphate strictly comigrated in several attempts of purification, indicative for a covalent interaction. Still the subject of glycogen phosphate was a matter of mere basic science concerned with describing the structure of glycogen without any obvious physiological relevance. Nevertheless the question arose, how the phosphate esters enter the glycogen. From rates of phosphoester hydrolysis Lomako *et al.* (1993) concluded a phosphodiester bridging from C1 of one glucosyl residue to a carbon in another. They postulated a UDPglucose:glycogen glucose 1-phosphotransferase and were apparently able to incorporate phosphate into glycogen when the latter was incubated with rabbit muscle extract and UDPglucose that was radiolabeled in the β-phosphate position (adjacent to the glucosyl residue). After acid hydrolysis of the glycogen the reaction products showed similar paper chromatographical behavior as G6P. They concluded that from UDPglucose the glucose 1-phosphate residue is transferred to the C6 carbon of a glycogen chain setting another type of branching where two glucosyl residues are linked via a phosphodiester. The ester bond to carbon C1, being labile, should account for the recovery of G6P after acid hydrolysis of the glycogen. The postulated enzyme was, however, never identified. Probably due to the partial lability of specific phosphate esters, phosphate contents in glycogen were ever since measured as total phosphate (see 1.2.2).
When a severe type of myoclonic epilepsy was described in 1911 by Lafora (Lafora and Glueck, 1911) the lack of technical possibilities and knowledge about glycogen precluded the discovery of a link between the disease and glycogen phosphate. Only when 1) one of the genes, if mutated being responsible for Lafora disease (LD), was identified (*Epm2a*; Minassian *et al.*, 1998; Serratosa *et al.*, 1999), 2) the gene product, named laforin, was found to encode for a phosphatase that was capable of dephosphorylating glycogen (Worby *et al.*, 2006; Tagliabracci *et al.*, 2007), and 3)

glycogen hyperphosphorylation was described as one cause for LD (Tagliabracci *et al.*, 2007, 2008), attention was drawn back to this minor component of glycogen.

The effects of hyperphosphorylation on glycogen have been studied using a mouse model with disrupted *Epm2a* gene. Viable homozygous laforin null mutants show formation of insoluble carbohydrates (Lafora bodies, LB) that correlate with neurodegeneration in an age-dependent manner which are key features of the human disease (Ganesh *et al.*, 2002). The phosphate content in muscle glycogen of *Epm2a*$^{-/-}$ mice increases with mice age, being four fold increased at three month of age and six fold increased at nine to twelve month as compared to wild type background where glycogen phosphate content remains unchanged as mice age from three to twelve month (Tagliabracci *et al.*, 2008). While the amount of muscle glycogen in wild type mice is unaffected by age, interestingly, the amount of muscle glycogen in mutant and wild type mice is similar at three month of age but severely increased in the older mutants. Alongside the age-dependent increase of phosphate, glycogen from *Epm2a*$^{-/-}$ mouse exhibits iodine staining properties that, with increasing mice age, become more similar to amylopectin. The authors conclude that the hyperphosphorylation correlates with decreased branching of mutant mice glycogen. Additionally, glycogen from nine to twelve month old mutant mice is less soluble in water but more in ethanol as compared to wild type mice glycogen of the same age. Furthermore the mutant glycogen is prone to aggregation as observed by electron microscopy. Aggregation and reduced water solubility apparently enables the sedimentation of a substantial part of the mutant glycogen by centrifugation at relatively low speed (Tagliabracci *et al.*, 2008). Interestingly, ethanol solubility and aggregation can seemingly be reverted to the level of wild type glycogen by treatment of the mutant glycogen with active recombinant laforin. The reduced water solubility is, however, unaffected by the phosphatase treatment. Also the aggregation of glycogen molecules does not occur in preparations from three month old mutant mice although the amount of glycogen phosphate is already strongly elevated as compared to wild type. The dramatic decrease in the number of branchings when mutant mice age from three to twelve month is, as considered by the authors, besides hyperphosphorylation another prerequisite for the decreasing water solubility of the mutant glycogen and its tendency to aggregate (Tagliabracci *et al.*, 2008). Both effects are assumed to cause the progressive formation of insoluble Lafora bodies that accumulate in tissues of LD patients. The occurrence of Lafora bodies in brain strongly correlates with neurodegeneration (Ganesh *et al.*, 2002; Chan *et al.*, 2004). Thus, the state of phosphorylation and the degree of branching seem to affect the physico-chemical properties of the glycogen as they do in starch (see 1.5.1).

Also in the lab of Roach the lead of Lomako *et al.* (1993) was followed and further experiments were conducted to identify the origin of glycogen phosphorylation. Incubating glycogen in the presence of $\beta[^{32}P]$ labeled UDPglucose with muscle lysates from mice they discovered that extracts from mice with non-functional GS did not lead to phosphate incorporation into glycogen (Tagliabracci *et al.*, 2011). Furthermore from *in vitro* experiments where glycogen was incubated with purified GS and UDP they concluded that UDPglucose apparently is the phosphate donor and glucosyl phosphate is incorporated into glycogen. However, they conducted a series of NMR experiments and identified the phosphorylated glucosyl carbons to be C2 and C3. The apparent absence of C6 phosphate and that of any phosphodiester contradicted the findings of Lomako (1993). Tagliabracci *et al.* (2011) postulated that within the active site of GS UDPglucose

undergoes the formation of intracyclic glucose phosphate where the former β-phosphate of UDPglucose bridges from C1 to C2 or C3 of the glucosyl residue. GS then transfers this intracyclic glucose phosphate to a nonreducing end of glycogen under cleavage of the C1 phosphoester bond yielding glycogen chains elongated by one glucosyl residue either phosphorylated in C2 or C3. The formation of intracyclic glucose phosphates has been reported previously (Paladini and Leloir, 1952; Khorana *et al.*, 1957). However, the utilization of such a molecule by GS requires a significant variability of the active site of the synthase. Tagliabracci *et al.* (2011) proposed that glycogen phosphate is merely the product of a fortuitous and very seldomly (1 phosphate incorporation per 10^4 glucosyl transfers) occurring side reaction of GS. Currently the view dominates that Laforin's role is merely the removal of the erratically introduced phosphate which otherwise accumulates with fatal consequences.

It should be noted that studies exist where glycogen phosphate is discussed to have a physiological function in glycogen metabolism. Rodriguez and Whelan (1985) observed phosphate esters on glucosyl chains that were in close vicinity of glycogenin, blocking the complete release of glycogen from glycogenin by amyloglucosidase. As discussed by Lomako *et al.* (1994) phosphate esters are likely to generally prevent the complete degradation of glycogen by exo-acting enzymes, such as glycogen phosphorylase. This could be relevant to prevent the complete disappearance of glycogen by phosphorolysis where this is undesirable. As opposed to liver glycogen deposits that can be almost completely removed by fasting, even after strenuous exercise a significant amount of residual glycogen remains in muscle (Brooks and Gaesser, 1980) where the glycogen phosphate is generally more abundant than in liver (see Table 2). Incomplete glycogen degradation in muscle would lead to exponentially more glucan chains at the glycogen surface that are accessible for chain elongation. This could facilitate a high rate of glycogen resynthesis as required for fast regeneration of the muscle (Conlee *et al.*, 1978).

Furthermore, Lomako *et al.* (1994) studied the ability of glycogen preparations containing different amounts of phosphate esters to act as primer for glycogen synthase. A glycogen preparation was fractionated the by anion exchange chromatography yielding fractions with different degrees of glycogen phosphorylation. They showed a positive correlation of chain elongation rate and phosphate content of the glycogen primer. However, it is speculative whether GS has a preference for phosphorylated chains. Likewise the phosphate alters the physico-chemical properties of the glycogen (see above). It is conceivable that those phosphate-mediated alterations increase the glycogen's priming ability.

1.5.3 Dephosphorylation of starch and glycogen

Phosphate esters are present in most plant starches and in glycogen from various sources (see 1.2.2). While amylopectin is phosphorylated by distinct enzymes, i.e. GWD and PWD, glycogen phosphate is currently believed to be the result of a catalytical error during glycogen chain elongation by GS (see 1.5.1 and 1.5.2). Besides that, the dephosphorylation of both types of carbohydrates is also necessary for functional metabolism of the respective carbohydrate store.

In *Arabidopsis thaliana*, as a model for higher plants, three enzymes (SEX4, Like-SEX-Four1 and Like-SEX-Four2) were identified that share the feature of an N-terminal dual-specificity phosphatase domain (DSP) and are closely related to starch metabolism. The DSP is common in a large family of protein phosphatases capable of dephosphorylating phosphoproteins at the amino

acid residues threonine/serine and tyrosine. In addition, some DSP-containing phosphatases act on various non-proteinaceous substrates (Pulido and Hooft van Huijsduijnen, 2008). First, the phosphatase SEX4 was discovered during the analysis of *Arabidopsis thaliana* starch excess mutants (Zeeman *et al.*, 1998; Niitylä *et al.*, 2006). Besides the DSP it contains a C-terminal carbohydrate binding module recently assigned to the family CBM48 (Santelia *et al.*, 2011). SEX4-deficient plants are retarded in growth and accumulate starch progressive with leaf age (Zeeman *et al.*, 1998; Kötting *et al.*, 2009). As compared to wild type the starch of these mutants exhibits a higher amylose to amylopectin ratio causing the slightly decreased starch phosphate due to the fact that starch phosphate is largely restricted to the amylopectin fraction of starch (Blennow *et al.*, 2002) and that the amylopectin phosphate is rather similar in wild type and SEX4-deficient mutant. Additionally SEX4 mutants accumulate intermediates of starch degradation, i.e. linear α-1,4 glucans phosphorylated at one or two glucosyl residues (Kötting *et al.*, 2009). *In vitro* assays with prephosphorylated maltodextrins revealed that SEX4 is capable of removing phosphate esters from both glucosyl C6 and C3 (Hejazi *et al.*, 2010).

The two enzymes Like-SEX-Four1 (LSF1) and Like-SEX-Four2 (LSF2) were discovered by computational analysis of the *Arabidopsis* genome due to their high DSP sequence similarity with SEX4. All three enzymes reside in the chloroplast but, as opposed to LSF1 and SEX4, LSF2 does not contain a carbohydrate binding module. However, it binds to starch and is capable of dephosphorylating glucosyl residues preferentially at carbon C3. The loss of LSF2 consequently leads to an altered pattern of starch phosphate, i.e. to a substantial increase in C3 phosphate (Santelia *et al.*, 2011). While the loss of LSF2 alone results in neither starch excess nor growth retardation the enzyme seems to participate in functional starch turnover. This is indicated by the starch levels in SEX4-LSF2 double mutants that are significantly elevated as compared to SEX4 single mutants. Accordingly, the growth retardation of SEX4 mutants is increased at the additional loss of LSF2. In contrast to LSF2, the LSF1 single mutant exhibits elevated starch levels and slightly retarded growth as compared to wild type but, similar to LSF2, the starch excess of SEX4 mutants is also increased at the additional knockout of LSF1. However, the growth retardation of the double mutants is similar to that observed in SEX4 knockouts. Both single mutants (LSF1 and LSF2) do not accumulate intermediates of starch degradation, as observed in SEX4 mutants indicating that functional SEX4 can at least partially compensate the loss of either LSF. Although all three phosphatases seem to be crucial for functional starch turnover, in contrast to SEX4 and LSF2, no evidence is yet provided that LSF1 dephosphorylates phosphorylated glucan chains. It is discussed that LSF1 might function as a protein phosphatase regulating the activity of other proteins involved in starch turnover (Comparot-Moss *et al.*, 2010; Santelia *et al.*, 2011).

Regarding the phenotypes of mutants lacking either starch phosphorylating enzymes or starch-related phosphatases emphasized the idea that both phosphorylation and dephosphorylation are crucial for functional starch metabolism. Indeed, previous studies revealed that a good portion of starch phosphate is rather transient indicating that the steady-state concentration of starch phosphate is a function of phosphate incorporation and dephosphorylation. In leaves of potato it was shown that starch phosphate increased at the surface of the granules during the first hours of starch degradation in the dark (Ritte *et al.*, 2004). Furthermore, when cells of the green alga *Chlamydomonas reinhardtii* were incubated with radiolabeled phosphate the label was introduced into the starch granules during both starch synthesis in the light and starch degradation in the

dark. However, while in the light labeling of starch was essentially constant, that in the dark was fast at the beginning (even exceeding that during illumination), slowing continuously down, and the labeling reaching its maximum after 90 minutes. Interestingly, a pulse-chase experiment revealed that the label introduced during net starch degradation diminished very fast after the chase indicating that, as opposed to starch biosynthesis, starch phosphate at the granule surface is rapidly turned over during starch degradation.

Evidence accumulated that the phosphate-mediated alterations at the starch granule surface lower the physical order of glucan chain arrangement and, thus, render the surface more suitable for starch degrading enzymes (Hejazi *et al.*, 2008, 2009; see 1.5.1). However, starch degradation is believed to be largely obtained by the action of β-amylases which are exo-amylases unable to release phosphorylated dextrins. If the hydrolysis of phosphate esters at the granule surface during starch degradation is largely impaired, as in SEX4-deficient mutants indicated by the major loss of glucan dephosphorylating activity, phosphorylated surface glucan chains become resistant to β-amylolysis. If not for the action of endo-acting hydrolases such as debranching enzymes or α-amylases which still can remove once incorporated phosphate from the granule by releasing phosphorylated glucan chains the starch degradation would be largely impaired. This is indicated by the fact, that double mutants lacking SEX4 and either ISA3 or AMY3 exhibit a dramatically increased starch excess as compared to SEX4 single mutants. Phosphorylated glucan chains as released by debranching enzymes or α-amylases in the absence of SEX4 can, however, not be completely converted to maltose and glucose, the main products of starch degradation, but are prone to accumulation as observed in SEX4 mutants (Kötting *et al.*, 2009).

It can be concluded that during starch degradation cycles of phosphorylation and dephosphorylation occur that both serve distinct purposes. The dikinase-mediated phosphate incorporation of phosphate esters renders the granule surface accessible for hydrolyzing enzymes while the dephosphorylation seems necessary for complete utilization of the starch derived glucosyl residues in the cell and to maintain sufficient rates of starch mobilization. The latter has been demonstrated in an *in vitro* experiment showing that the degradation of native starch granules by β-amylase (BAM3) and debranching enzyme (ISA3) is substantially enhanced by simultaneous phosphorylation. Additional dephosphorylation by SEX4 almost doubles the rate of starch degradation (Kötting *et al.*, 2009).

The significance of glycogen dephosphorylation is obvious considering the consequences of non-functional laforin, the so far only known enzyme that is capable of dephosphorylating glycogen. In humans laforin is encoded by the *Epm2a* gene positioned on chromosome six. Mutations in that gene lead to non-functional laforin and result in Lafora disease, a severe type of myoclonic epilepsy with onset in teenage years mostly leading to death within ten years through progressive neurodegeneration (Minassian *et al.*, 1998; Serratosa *et al.*, 1999).

Human laforin shares general structural features with SEX4 in plants. It also contains both a carbohydrate binding module (CBM) and a dual-specificity phosphatase domain (DSP) which makes it unique among all so far known about 130 human phosphatases (Zolnierowicz, 2000; Alonso *et al.*, 2004; Gentry *et al.*, 2007). Besides in mammals homologues of laforin were found in other classes of vertebrates (aves, amphibians, and osteichthyes) and as well in some protists, but it is considered absent in nonvertebrates. SEX4 is conserved in all land plants, but also found in the unicellular green alga *Chlamydomonas reinhardtii* (Gentry *et al.*, 2007). However, SEX4 and laforin

are not considered as orthologues for two reasons. First, the CBMs of both enzymes share a relatively low similarity and were assigned to different CBM families. As opposed to SEX4 (CBM48, see above) laforin contains a CBM of the same family as PWD (CBM20; Baunsgaard *et al.*, 2005; Gentry *et al.*, 2009). Second, the order of both domains is inverted as compared to SEX4, in laforin the CBM being N-terminal and the DSP being C-terminal (see above). Thus, the acquisition of laforin and SEX4 is likely to be based on separate evolutionary fusion events that connected phosphatase and carbohydrate binding domains yielding SEX4 or laforin homologues in the plant or animal kingdom, respectively (Gentry *et al.*, 2007).

Despite their distinct descent but derived from their structural similarity laforin and SEX4 were predicted to be functional equivalents. It has been shown *in vitro* that both enzymes are capable of dephosphorylating complex carbohydrates, such as amylopectin (Worby *et al.*, 2006). The expression of human laforin (fused with a SEX4 transit peptide) in SEX4-deficient plants complemented the starch excess phenotype and finally confirmed the prediction (Gentry *et al.*, 2007). Later, Tagliabracci *et al.* (2007) demonstrated that laforin liberates phosphate from glycogen as well. Furthermore, they isolated phosphoglucans from amylolytically treated rabbit muscle glycogen and incubated that with functional human laforin. They observed that laforin dephosphorylates phosphooligoglucans given the phosphorylated glucosyl chain had a minimum DP of three (Tagliabracci *et al.*, 2011).

The generation of laforin-deficient mice by disruption of the *Epm2a* gene facilitated the analysis of laforin function *in vivo* and its role in Lafora disease (Ganesh *et al.*, 2002). It has been observed that deficiency in laforin leads to elevated levels of phosphate in the glycogen prepared from the mutant mice (Tagliabracci *et al.*, 2007, 2008; see 1.5.2). This coincides with altered physico-chemical properties of the glycogen and the occurrence of insoluble polyglucan structures (Lafora bodies, LB) that are considered to be the cause for neuronal cell death and neurodegeneration (Tagliabracci *et al.*, 2008). Laforin's role is therefore thought to be the prevention of LB formation by removal of the malicious glycogen phosphate esters that were inadvertently introduced by one of the key enzymes of primary metabolism in animals, glycogen synthase (Tagliabracci *et al.*, 2011).

1.5.4 Lafora disease exemplifies the significance of glycogen phosphate

Epilepsy is regarded as the most common neurological disorder of children and has been currently diagnosed in around seven of thousand humans (World Health Organization, 2006). It is characterized by unprovoked recurring seizures mostly mediated by massive simultaneous excitation of populations of neurons (Silbernagl and Lang, 1998). Most seizures can be controlled medically (Minassian, 2001). One percent of all epilepsy cases are so called progressive myoclonic epilepsies (PME) with intractable rhythmic muscle contractions (myoclonus) during seizures and a progressive cortical degeneration. Lafora disease (LD) is a type of PME characterized by 'amyloid bodies in the protoplasm of ganglion cells' as described by Gonzalo H. Lafora in 1911 referring to results of iodine staining of post mortem brain tissue samples (Lafora and Glueck, 1911).

1.5.4.1 Clinical and pathological aspects of Lafora disease

The onset of the autosomal recessive hereditary Lafora disease is usually in adolescence between the ages of twelve to seventeen and is characterized by a first seizure (myoclonic as well as tonic-clonic or atonic; Minassian, 2001).

In the course of the disease the seizures progressively worsen, become increasingly intractable, and are often accompanied by other related symptoms, such as transient blindness, visual hallucinations or atypical absence. Soon after occurrence of the first symptoms a decline in the patient's cognitive skills becomes noticeable. Furthermore, the *status epilepticus* (a period of a continuous seizure or recurring seizures without regaining consciousness lasting longer than 5; Lowenstein *et al.*, 1999) becomes common. In advanced stages of the disease patients even exhibit continuous myoclonus. Patients usually die within ten years after the occurrence of the first seizure (Minassian, 2001).

Pathological (biopsy and post mortem) analyses revealed a substantial neuronal loss in the late stages of the disease but no demyelination such as observed in patients of Multiple sclerosis. The inclusion bodies, first described by Lafora (Lafora and Glueck, 1911) are already present in earlier stages of the disease. They stain dark violet with Schiff's reagent after oxidation with periodic acid which is characteristic for carbohydrates. Indeed it was demonstrated that these particles, named Lafora bodies (LB), mainly consist of rarely branched glucan chains (Yokoi *et al.*, 1968; Sakai *et al.*, 1970). Abundance of LBs increases in the course of the disease and they are present in many of the patient's tissues, such as brain, heart and skeletal muscle, liver, and sebaceous gland ducts within skin tissue (de Siqueira, 2010). Skin biopsy enabled a highly specific diagnosis of LD in patients suffering from epileptic symptoms, as described above, even before knowledge about the genetic reason of the disease (Carpenter and Karpati, 1981). Their diameter ranging from 3 to 40 µm, LBs in brain are largely confined to neurons where larger particles are perikaryally located while much smaller ones occur in dendrites. Thereby LBs can be distinguished from other insoluble glucan material found either under different pathologic conditions or as *Corpora Amylacea* occurring in relation with age (Minassian, 2001; Cavanagh, 1999).

For instance in patients deficient in glycogen branching enzyme (glycogen storage disease type IV, Andersen's disease, see 1.4.1) polyglucosan bodies are already found very early in many tissues as well as in brain, but in neurons they are restricted to the axons (Schochet *et al.*, 1970). Likewise *Corpora Amylacea* have been found in many tissues including brain, but have never been reported in neuronal cell bodies (perikaryal). While Andersen's disease usually leads to death within four years after birth, mostly due to hepatic cirrhosis, a mere reduction of glycogen branching enzyme activity also leads to axonal polyglucosan bodies and is related to mental deterioration (adult polyglucosan body disease). However, no cases of epileptic symptoms have been stated (Cavanagh, 1999). It is assumed that neuronal polyglucosan bodies potentially affect brain function but that seizures such as in LD are due to the perikaryal location characteristic for Lafora bodies (Minassian, 2001).

1.5.4.2 Genes responsible for Lafora disease

Mutations in two genes, in humans both on chromosome six, were identified as the genetic reason for LD (Minassian *et al.*, 1998; Chan *et al.*, 2003a). In approximately 48% of LD cases the gene *Epm2a* (encoding the protein laforin) is mutated while 40% of LD cases result from mutations in

Epm2b (encoding the protein malin). The remaining cases are either mutated in the non-coding region of either of the two genes or could be associated with mutations in a yet unidentified gene (Chan *et al.*, 2004a).

Laforin contains an N-terminal carbohydrate binding module (CBM20) and a C-terminal dual-specificity phosphatase domain (DSP, see 1.5.3). Malin is a single subunit E3 ubiquitin ligase containing a C-terminal RING domain and six NHL repeats towards the N-terminus (Chan *et al.*, 2003b). The RING domain is characteristic for one class of E3 ubiquitin ligases and named after the human gene RING1 encoding for the E3 ubiquitin ligase first discovered (Lovering *et al.*, 1998). The NHL repeats, named after the initials of three proteins that were first shown to contain this motif (Slack and Ruvkun, 1998), form a six-bladed β-propeller mediating protein-protein interactions (Edwards *et al.*, 2003).

Patients suffering from LD show mutations that are scattered all along the coding regions of the *Epm2a* and *Epm2b* genes. However, in laforin-deficient patients homozygous deletions for exon 2 of *Epm2a* are of highest recurrence, followed by nonsense mutations in exon 4. The former partly encodes for the CBM and the spacer connecting the CBM to the DSP while exon 4 mutations affect the DSP domain. In malin-deficient patients large deletions are rather rare. Highest recurrence is observed for a two-base pair deletion causing a frameshift after the first NHL repeat. Also quite abundant among malin-deficient patients is a missense mutation that affects the RING domain (Singh and Ganesh, 2009).

Several studies examined possible genotype-phenotype correlations in the LD affected families. While malin-deficient patients tend to live longer than those deficient in laforin it is discussed whether factors other than the genetic defects could be involved in modifying the disease's onset or its progression (Singh and Ganesh, 2012).

1.5.4.3 Absence of laforin or malin causes Lafora disease

Patients suffering from LD lack either functional laforin or malin. Pathology and symptoms are largely indistinguishable between both variants of the disease (Singh and Ganesh, 2012). However, both enzymes have completely different catalytic properties. Laforin is a dual-specific phosphatase that can bind carbohydrates via its CBM (Wang *et al.*, 2002; Girard *et al.*, 2006; Wang *et al.*, 2006) and is capable of removing phosphate esters from its substrates. Given the observation of accumulating insoluble polyglucans, i.e. Lafora bodies, in LD patients it is conceivable that laforin regulates enzymes of glycogen metabolism by altering their state of phosphorylation. Glycogen, as a soluble branched polyglucan, is constructed by the consecutive action of glycogen synthase (GS) and branching enzyme (GBE) (see 1.4.1). An alteration of the ratio between chain elongation and branching events leads to dramatic changes in glycogen structure and likely its physico-chemical properties. It has been shown that overexpression of GS in mouse muscle leads to polyglucosan structures that are similar to LB (Pederson *et al.*, 2003). Furthermore, these insoluble structures were observed in several disorders with disturbed glycogen branching, such as Andersen's and adult polyglucosan body disease (Cavanagh, 1999). The notions that GS as well as GS-regulating proteins are largely phospho-regulated and laforin is a phosphatase led to the suggestion that non-functional laforin may result in an imbalance between branching and chain elongation and, thus, in insoluble glycogen structures (Serratosa *et al.*, 1999). From cell culture experiments Lohi *et al.* (2005a) concluded that laforin interacts with and dephosphorylates (activates) GSK3, a GS kinase

that deactivates GS by phosphorylation. Since laforin is shown to bind strongly to LBs (Chan *et al.*, 2004b) the additional occurrence of GSK3 in LBs of malin-deficient, but not laforin-deficient, patients demonstrated the interaction of laforin and the GS regulator (Lohi *et al.*, 2005a). Laforin binding to LBs also gave rise to the hypothesis that laforin is involved in sensing the existence of LBs and subsequently mediates the down-regulation of GS to avoid accumulation of insoluble glycogen (Ganesh *et al.*, 2004). That laforin acts as protein phosphatase remained, however, controversial since another group concluded from *in vitro* experiments that laforin neither dephosphorylates GSK3 nor other proteins involved in glycogen metabolism or in the regulation of the same, such as GS or PTG (Worby *et al.*, 2006). Later Wang *et al.* (2007) confirmed in a mouse model of LD that the loss of laforin does not result in altered activities of GBE or GS and ruled out that the mere imbalance between the two enzymes is responsible for the occurrence of LB.

Following another approach, Worby *et al.* (2006) considered laforin as a phosphatase that does not just bind carbohydrates but also dephosphorylates them. They demonstrated that laforin can release phosphate from complex carbohydrates, such as amylopectin, and concluded that the DSP domain of laforin is unique among phosphatases since fusion products of laforin CBM and the DSP of a well characterized protein phosphatase did not show activity on amylopectin. The same group demonstrated the functional relation between the plant phosphoglucan phosphatase, SEX4, and laforin by complementation of SEX4 *Arabidopsis thaliana* mutants through expression of human laforin (Gentry *et al.*, 2007). Thus, attention was drawn to the minor component of glycogen phosphate and its role in glycogen metabolism. While most clinical features of LD are associated with impaired neuronal function, studies on glycogen phosphate were conducted on tissues, such as muscle and liver, where, as opposed to neuronal tissue, glycogen is much more abundant (Vilchez *et al.*, 2007). In mice lacking laforin (*Epm2a*$^{-/-}$) it was found that glycogen phosphate increases with age and that this is accompanied by decreased branching and hydrosolubility of the glycogen (Tagliabracci *et al.*, 2007, 2008). That and the observation that LBs are composed of glucan chains that are less branched and enriched in phosphate as compared to normal glycogen (Yokoi *et al.*, 1968; Sakai *et al.*, 1970) gave rise to the idea that LD is caused by phosphate accumulation in the glycogen leading to structural defects which cause polyglucosan precipitation and the accumulation of LB (Roach *et al.*, 2012).

Interestingly, the glycogen of malin-deficient (*Epm2b*$^{-/-}$) mice also exhibits elevated phosphate levels that likely underlie the LB formation in malin-related LD. However, glycogen hyperphosphorylation in *Epm2b*$^{-/-}$ mice is not as severe as in the absence of laforin. This indicates that hyperphosphorylation contributes to LB formation but is not its sole determinant (Turnbull *et al.*, 2010; Tiberia *et al.*, 2012). Since malin is not a glucan phosphatase the glycogen hyperphosphorylation in *Epm2b*$^{-/-}$ mice can only be explained by a close relation of malin and laforin.

Malin is an E3 ubiquitin ligase (see 1.5.4.2) and, acting as such, it is part of the multi-enzyme cascade that mediates protein ubiquitylation. This cascade involves the formation of thiol esters of ubiquitin with mostly three distinct types of enzymes: an ubiquitin-activating enzyme (E1), an ubiquitin-conjugating enzyme (E2), and an ubiquitin ligase (E3). Binding it covalently via a thiol ester bond E1 activates ubiquitin under ATP consumption. Forming another thiol ester bond ubiquitin is subsequently transferred to E2. The latter binds to E3 which also interacts with the target protein which finally is ubiquitylated under the formation of a stable isopeptide linkage

between a lysine residue of the target and the C-terminal glycan of ubiquitin (Hatakeyama and Nakayama, 2003). Ubiquitylated proteins are largely degraded utilizing the proteasome. However, it has been shown that ubiquitylation also plays a role in regulation of enzyme activity (Sun and Chen, 2004). The specificity of E3 enzymes, such as malin, enables selective degradation/modulation of target proteins (Chen and Dou, 2010). Thus, malin's role in LD is likely the regulation of the amount or function of distinct glycogen-related proteins.

Indeed, soon after its discovery it was shown to interact with and ubiquitylate laforin (Gentry *et al.*, 2005). This observation raised the question how the absence of malin-mediated laforin degradation via the proteasome would lead to glycogen hyperphosphorylation and LB formation, as seen in malin-related LD. Recent studies however shed some light on that matter.

It was observed that in the absence of malin laforin protein levels are elevated and that the increased laforin is associated with the LBs. The increased laforin protein levels are also present in very young mice when no LBs are detectable yet. This concurs with the fact that malin-mediated proteasome-dependent degradation of laforin is not functional in *Epm2b*$^{-/-}$ mice. While in very young *Epm2b*$^{-/-}$ mice only part of the laforin is associated with the yet soluble glycogen, at later stages, almost no laforin exists that is not associated to glycogen or LBs. The authors concluded that, in the absence of malin, laforin is increased which progressively binds to glycogen and finally leads to LB formation. This hypothesis was bolstered by the observation of LB-like structures in HEK293 cells with over-expressed laforin already 24 h after transfection. The formation of these polyglucosan structures was dependent of the presence of laforin with a functional CBM, but an non-functional DSP domain did not affect the accumulation (Tiberia *et al.*, 2012). The increasing hyperphosphorylation is assumed to be due to the absence of free laforin that is not associated with glycogen. Regarding its strong binding to glycogen (Wang *et al.*, 2002; Girard *et al.*, 2006; Wang *et al.*, 2006) it has been speculated that laforin once bound has to be removed from its target by ubiquitylation before another dephosphorylation event can take place (Gentry *et al.*, 2005). In the absence of malin the removal of laforin from glycogen is impaired and glycogen dephosphorylation is increasingly stalled due to the progressive association of laforin to glycogen (Tiberia *et al.*, 2012).

Similar to laforin in malin-deficient mice, the GS protein amount is largely increased in LBs both in the absence of laforin or malin (Tagliabracci *et al.*, 2008; Valles-Ortega *et al.*, 2011). It was shown that, in the presence of laforin, malin ubiquitylates GS and thereby mediates its proteasome-dependent degradation. In the same way laforin targets malin to PTG, one of the proteins that target PP1 to glycogen and enables PP1 to dephosphorylate (activate) GS (Vilchez *et al.*, 2007). In the absence of laforin or malin, GS, likely in a more active form, remains associated to glycogen and co-precipitates in LBs while GBE is seldom found in LBs (Tagliabracci *et al.* 2007, 2008). Thus, it is hypothesized that LB polyglucosan becomes less branched through GS-mediated elongation of glucan chains without adequate branching (Tiberia *et al.*, 2012).

The formation of LBs that are considered the reason for neurodegeneration in LD is obviously caused by hyperphosphorylation and/or by excess of laforin association to glycogen. GS, which, unlike branching enzyme, is trapped with the glycogen in the absence of functional laforin and malin, possibly contributes to the structural defects in glycogen. While LBs occur in several tissues clinical symptoms are largely caused by neuronal dysfunction. In brain, glial cells, being much more abundant than neurons, are considered to constantly provide energy equivalents to neurons

that, as apposed to glial cells, do not possess large glycogen stores (Vilchez *et al.*, 2007). It is conceivable that in LBs, present in both cell types, large amounts of immobile energy equivalents are stored and, thus, neurons die due to insufficient energy supply. Regarding their size (see 1.5.4.1) LBs could also cause blockages in intracellular transport which is maintained over relatively long distances in neurons as compared to cells in other tissues. Likewise the detrimental effects of LBs could be related merely with cell age. Since neurons abolish cell division shortly after differentiation (Currais *et al.*, 2009) the cell age is much higher in most neurons than in cells of other tissues. In humans it takes more than a decade for clinical symptoms to develop. Age-dependent and LB-related neurodegeneration could be the reason why relatively short-lived animal LD models, such as mice or even dogs, do not die from LD-related neurodegeneration although they show otherwise similar symptoms (Ganesh *et al.*, 2002; Lohi *et al.*, 2005b; Gentry *et al.*, 2009).

Neuronal cell death occurs relatively late in the course of LD and is likely related to the accumulation of LBs. The myoclonic seizures start, however, early becoming also more severe in line with LB accumulation. Among the diseases with glycogen derived polyglucosan inclusions, such as Andersen's disease or adult polyglucosan body disease (see 1.5.4.1) LD is unique due to the epileptic symptoms (Minassian, 2001). The latter seem to be confined to polyglucosan formation in relation to glycogen hyperphosphorylation.

The enzyme(s) responsible for glycogen phosphorylation have long been unknown. Many *in silico* genome searches did not reveal enzymes in vertebrates that resemble the plant dikinases GWD and PWD that incorporate phosphate into starch (Gentry *et al.*, 2009). Recently, Tagliabracci *et al.* (2011) reported that phosphate is incorporated via an inadvertent side reaction of GS itself. Glycogen phosphate, as opposed to that in starch, is therefore considered to have no specific function for the structure of the carbohydrate but rather is an error that has to be corrected by laforin.

1.6 Analysis of phosphate in polysaccharides

Among naturally occurring polysaccharides starch and glycogen have been shown to contain monophosphate esters. Within the last two decades evidence accumulated that phosphate esters have a great impact on physico-chemical properties of both storage carbohydrates. While the view, that starch phosphate occurs mainly at the glucosyl carbons C6 and C3, is widely accepted, the glucosyl carbons to which phosphate moieties are attached in glycogen is controversial. Fontana (1980) reported evidence of C6 phosphate besides some phosphate esters rather labile to acid hydrolysis. Lomako *et al.* (1993) concluded that the labile phosphate ester should be a phosphodiester, bridging from C1 of one glucosyl residue to a carbon in another one. The monophosphate esters present in glycogen they also assigned to carbon C6. The existence of C6 phosphate in glycogen was, however, rejected recently by Tagliabracci *et al.* (2011) who performed various NMR studies on rabbit skeletal muscle glycogen. They stated that glycogen phosphate exclusively occurs as monophosphate esters at the carbons C2 and C3.

In both plants and animals phosphatases have been identified that are capable of releasing phosphate from starch and glycogen, respectively. Furthermore the phosphatases laforin and SEX4 are functional equivalents, as laforin has been shown to complement *Arabidopsis thaliana* mutants lacking functional SEX4. It is even reasonable to assume that laforin can remove phosphate from

carbon C6 which is, as mentioned, the major site of starch phosphorylation. This function, however, would be irrelevant if glycogen does not contain monophosphate esters at carbon C6. Regarding dephosphorylation of the respective storage carbohydrate, plants and animals make use of rather similar enzymology.

While two starch phosphorylating enzymes have been described and to some extend characterized the enzymology of glycogen phosphorylation remained elusive until Tagliabracci *et al.* (2011) reported evidence for a phosphate incorporating activity of glycogen synthase, the key enzyme of animal primary metabolism responsible for chain elongation during glycogen synthesis. This implies a substantial difference in the mechanisms by which starch and glycogen are phosphorylated. The starch phosphorylating dikinases introduce phosphate specifically either at carbon C6 or C3. The existence of two non-redundant enzymes for starch phosphorylation supports the idea that the introduction of phosphate esters at different glucosyl carbons requires distinct enzymes.

An assessment of glycogen phosphate positions, especially addressing the possible phosphorylation site at carbon C6, is therefore essential mainly for two reasons: first, to judge the probability of distinct glycogen phosphorylating enzymes and second, to clarify whether starch and glycogen phosphorylation are different besides all so far known similarities regarding the physiological role of phosphate in both carbohydrates.

The following sections will introduce some methods currently available to analyze phosphate esters in carbohydrates.

1.6.1 Total phosphate quantification

Phosphate covalently bound to organic matter can be determined as orthophosphate after complete hydrolysis of phosphate ester bonds. Both the hydrolysis of ester bonds and the detection of orthophosphate are achieved by different methods.

Early studies on phosphate present in preparations of starch and glycogen, such as Mordoh *et al.* (1966) and Hizukuri *et al.* (1970) made use of the method of Fiske and Subbarow (1925). Nielsen *et al.* (1994) utilized the method of Morrison (1964), while later studies (see 1.5) almost exclusively employed the protocol of Hess and Derr (1975).

All three methods are similar with respect to the release of phosphate from organic matter in hot sulfuric acid with additional oxidants. However, the concentration of sulfuric acid varies between the methods as well as the type of oxidant. Fiske and Subbarow (1925) added small amounts of nitric acid, while Morrison (1964) and Hess and Derr (1975) rely on hydrogen peroxide and perchloric acid, respectively. After complete release of phosphate all three methods make use of the phosphate-dependent formation of phosphomolybdic acid at low pH. Some of the molybdenum atoms within this heteropolymolybdate complex are reduced by reducing agents, such as aminonaphtholsulfonic acid (Fiske and Subbarow, 1925) or ascorbic acid (Morrison, 1964), to yield phosphomolybdenum blue which can be detected photometrically at 822 nm. Hess and Derr (1975) took advantage of the discovery that at low pH the basic dye malachite green strongly changes its color from yellow to green (absorbance 620 to 650 nm) at relatively small concentrations of phosphomolybdic acid (Itaya and Ui, 1965). Thus, by the use of the malachite green the sensitivity of the molybdate-mediated quantification of phosphate could be improved several fold enabling the detection of 0.1 to 5 nmol phosphate per assay (Hess and Derr, 1975).

In a sample phosphate can be present as orthophosphate and phosphate bound to organic matter. The distinction between both can generally be made by performing the total phosphate assay with or without prior hydrolyzing the phosphate esters. However, it necessitates the stability of phosphoesters under the conditions of the orthophosphate determination which takes place at low pH (see above).

By total phosphate determination no information is gained about the origin the phosphate. Orthophosphate present in a sample can be derived from simple contamination with inorganic phosphate or be the product of inadvertent partial or complete hydrolysis of rather labile phosphoesters. Likewise, the assay gives no information about the quality and quantity of species of organic phosphoesters. Regarding starch and glycogen phosphoesters are supposedly formed at different hydroxyl groups of the glucosyl residues. The amount of phosphate bound to each distinct type of hydroxyl group can not be assessed by the total phosphate assay. Furthermore, even small contaminations with highly phosphorylated organic substances, such as nucleic acids, would largely overestimate the amount of phosphate bound to the carbohydrate. Contamination with nucleic acid is of special relevance for total phosphate determination in glycogen. Unlike native starch that is particulate and can be washed easily, native glycogen is hydrosoluble its purification mainly relying on ethanol precipitation repeated between various treatments to remove possible contaminations. Glycogen is routinely used as co-precipitant during the isolation of small amounts of DNA or RNA. This clearly points to an interaction between nucleic acids and glycogen which is unfavorable during the analysis of glycogen phosphate.

The determination of total organic phosphate is used as standard method to quantify the glycogen phosphate in glycogen preparations. The purity of the samples regarding for instance nucleic acids is, however, if even addressed rarely elaborated (Tagliabracci *et al.*, 2007).

1.6.2 Quantification of 6-phosphoglucosyl residues

The amount of glucosyl residues phosphorylated at carbon C6 can be determined specifically using an enzymatic assay. This is of special interest when analyzing polyglucans such as glycogen and starch. While in the latter C6 phosphate accounts for the majority of all phosphate esters present in the carbohydrate, the presence of C6 phosphate in glycogen remains controversial (see 1.2.2 and 1.5.2). Carbohydrates that are composed of monomers other than glucose, such as the plant cytosolic heteroglycan (see 1.3.3), can only be analyzed with respect to the phosphate being attached at carbon C6 of glucosyl residues.

The basis of glucosyl C6 phosphate determination in carbohydrates is the specific quantification of glucose 6-phosphate (G6P) in hydrolysates of the respective carbohydrate. An adequate hydrolysis is, therefore, required to cleave glucosidic bonds without hydrolyzing the phosphoester at carbon C6. Enzymatic hydrolyses using hydrolases would not fulfill this aim, since enzymes, such as α–amylase or amyloglucosidase, do not cleave glucosidic linkages in close vicinity of phosphorylated glucosyl residues (Takeda and Hizukuri, 1982; Wikman *et al.*, 2011). However, there are chemical (acid) hydrolysis methods available that quantitatively cleave glucosidic bonds irrespective of their relative vicinity to phosphorylated glucosyl residues and that maintain glucosyl 6-phosphomonoesters (Hizukuri *et al.*, 1970; Haebel *et al.*, 2008).

The enzymatic quantification of G6P relies on a principle described by Lowry and Passonneau (1972) where in the presence of excess $NAD(P)^+$ G6P is converted to 6-phosphogluconate by G6P

dehydrogenase (G6PDH). The reaction yields stoichiometric amounts of NAD(P)H which can be determined photometrically at 340 nm using the Lambert-Beer law and a known molar absorptivity (uncoupled assay, see 1.6.2.1). Another possibility is to enhance the signal by coupling the NAD(P)H, formed as described above, to a chain of redox reactions that finally yield a secondary product. By permanent cycling of the NAD(P)H the secondary product is built at a constant rate which only depends on the NAD(P)H concentration initially coupled to the redox chain. The rates of the secondary product formation are monitored photometrically. Via calibration using standard concentrations the initial amount of G6P can be calculated (see 1.6.2.2)

1.6.2.1 Uncoupled enzymatic assay

NAD(P)H, as opposed to $NAD(P)^+$, absorbs light at 340 nm with a molar absorptivity of 6,300 M^{-1} cm^{-1}. The complete conversion of G6P to 6-phosphogluconate by G6PDH in the presence of excess $NAD(P)^+$ yields amounts of NAD(P)H equal to that of the initial G6P. Thus, from the difference of absorbance values measured before and after enzymatic conversion of G6P the concentration of G6P in the sample can be deduced using the Lambert-Beer law.

Given the common photometric path length of 1 cm this assay requires concentrations of G6P in the cuvette higher than 3 µM for reliable measurements (Nisselbaum and Green, 1969). Performing the assay in a total volume of 1 ml would accordingly require at least 3 nmol G6P.

The abundance of phosphate esters in starch and glycogen is generally low. C6 phosphate, if present, is only a fraction of it (see 1.2.2). If direct (uncoupled) detection of NAD(P)H is used for determination of G6P in hydrolysates of carbohydrates the consumption of starting material (carbohydrate) is very high (Table 3).

Table 3. Minimum requirement of polyglucan for uncoupled determination of 6-phosphoglucosyl residues

Depending on the abundance of 6-phosphoglucosyl residues the minimum amount of polyglucan is calculated for reliable determination of G6P in polyglucan hydrolysates. Calculation is based on the following parameters: total volume per cuvette - 1 ml, molar mass of glucosyl residues – 162.1 g/mol, molar absorptivity of NAD(P)H at 340 nm – 6.300 M^{-1} cm^{-1}. ΔE – difference of absorbance values measured before and after enzymatic turnover of G6P

C6 phosphate [mmol/mol glc]	G6P per cuvette [nmol]	Glucose per cuvette [nmol]	Carbohydrate per cuvette [mg]	ΔE at complete enzymatic Conversion
10	3	300	0.05	0.019
1	3	3,000	0.49	0.019
0.1	3	30,000	4.86	0.019
0.01	3	300,000	48.63	0.019

If carbohydrates are analyzed having a very low glucose-based C6 phosphate content, if the amount of carbohydrate is limited, or if the glucosyl residues are only a small fraction of the carbohydrate, such as in the plant cytosolic heteroglycans (see 1.3.3), more sensitive methods are required.

1.6.2.2 Signal enhancement by NAD(P)H cycling

In the uncoupled enzymatic G6P assay (see 1.6.2.1) the stoichiometric amount of NAD(P)H, that is formed when G6P is turned over by G6PDH in the presence of $NAD(P)^+$, is directly measured photometrically. The sensitivity of such measurements is limited by the molar absorptivity of NAD(P)H. If the concentration of G6P in hydrolysates of carbohydrates is very small the equivalent amount of NAD(P)H may likely be below the detection limit.

Already in the middle of the last century researchers aimed to detect very small amounts of $NAD(P)^+$ or NAD(P)H in animal or plant tissue (Frunder, 1954; Holzer *et al.*, 1954). Assays have been developed that couple the coenzymes to redox reactions and, thereby, enhance the sensitivity of detection of the coenzymes.

Basically both oxidation states, NAD(P)H and $NAD(P)^+$, can be coupled to redox reactions. A general scheme of coupling possibilities is presented in Figure 1. During coupling, one coenzyme oxidation state (OX1) reacts with a second substance (substance_B). Thereby the oxidation states of both the coenzyme and of the substance_B are altered (OX1 to OX2) but coenzyme OX1 is continuously rebuilt (cycled) by a second reaction where coenzyme OX2 reacts with another substance (substance_A). This reaction is only limited by the concentration of coenzyme OX2. Thus, one oxidation state of the coenzyme (OX1) is continuously rebuilt and kept constant at a maximum concentration. This enables a constant reaction rate with substance_B. If the alteration of the substance_B oxidation state leads to changes in the absorption spectrum the ongoing reaction between coenzyme and substance_B can be photometrically determined as a rate of absorbance change (simple coupling). Substance_B, after being altered in its oxidation state by the coenzyme, can also participate in a redox reaction with another substance (substance_C). The alteration of the substance_C oxidation state can likewise be detected photometrically (two-step coupling). Since the initial oxidation state (OX1) of substance_A, _B, and _C are present in great excess the formation rate of the photometrically detected substance oxidation state (substance_B or substance_C) is only dependent on the amount of the coenzyme that was initially coupled to the redox reaction (Figure 1). Via calibration with known amounts of coenzyme unknown amounts of coenzyme can be calculated from photometrically detected formation rates.

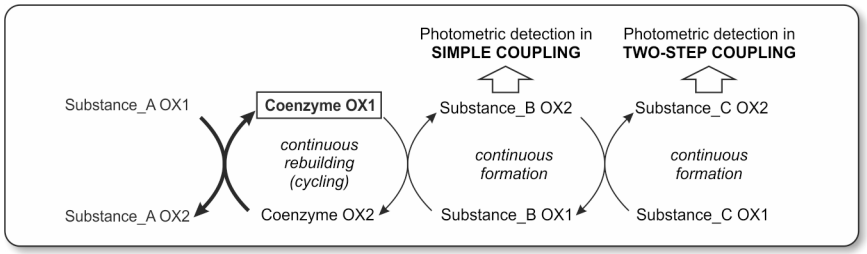

Figure 1. General scheme of signal enhancement by redox coupling of coenzymes

The coenzyme in oxidation state 1 (OX1) reacts with a substance (_B) altering its oxidation state from OX1 to OX2. Simple coupling, if the alteration of the substance_B is monitored; two-step coupling, if substance_B reacts with another substance (_C) which is detectable subsequent to its change in oxidation state. By continuous cycling of coenzyme OX1 the formation of the monitored substance (_B or _C) is maintained at a constant rate. This rate is only depending on the coenzyme OX1 concentration. The high capacity of the rebuilding reaction (marked by thick arrows) permits a constantly maximal concentration of coenzyme OX1. Thus, the initial amount of coenzyme determines the formation rate of the monitored substance.

Coenzyme being present in either oxidation state can be coupled to such redox system. However, the specific quantification of one coenzyme oxidation state implies the destruction of the other oxidation state before coupling. If OX2 is to be quantified OX1 has to be destroyed in the sample before coupling, and *vice versa*. Otherwise both oxidation states would contribute to the detected formation rate. NAD(P)H and $NAD(P)^+$ are labile under different conditions. This allows the specific destruction of one oxidation state while the other is retained. $NAD(P)^+$ can be destroyed at high pH and high temperature, conditions uncritical for NAD(P)H which is labile at low pH and room temperature, conditions, however, uncritical for $NAD(P)^+$ (Rover *et al.*, 1998).

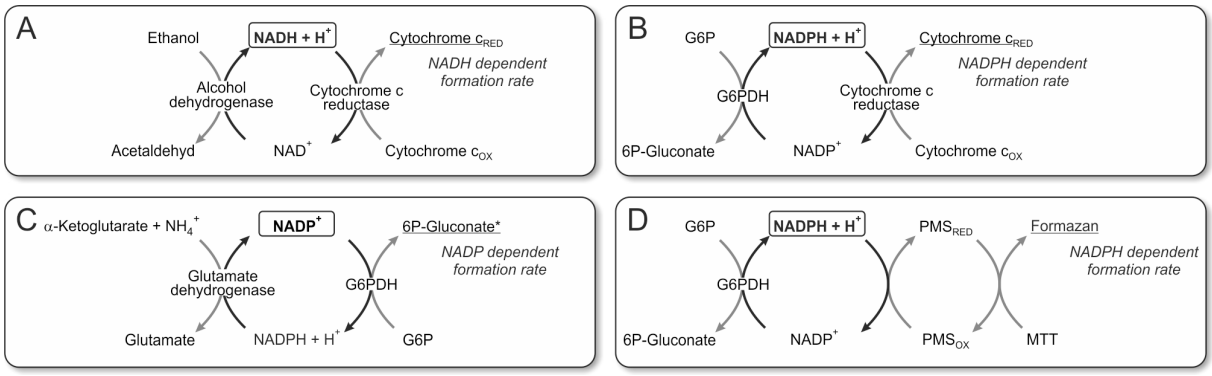

Figure 2. Variants of coenzyme cycling

Methods of Glock and McLean (1955; A and B, simple coupling), Lowry *et al.* (1961; C, simple coupling), and Nisselbaum and Green (1969; D, two-step coupling). The coenzyme oxidation state kept at maximum concentration in framed. Formation rates of underlined substances are detected. OX and RED indicate oxidized and reduced state of the substance, respectively. (*) While in (A), (B), and (D) the products are directly detected photometrically, 6-phosphogluconate (6P-gluconate) formation is stopped after a defined period of time and quantified by 6P-gluconate dehydrogenase-mediated conversion with excess $NADP^+$ and stoichiometric NADPH formation. The latter is subsequently detected photometrically at 340 nm. For substance abbreviations see list of abbreviations.

Figure 2 provides some examples of coenzyme cycling. While photometric detection of NAD(P)H without cycling requires at least 3 nmol of the coenzyme (see Table 3) the method of Glock and McLean (1955; Figures 2A and B) reduces that amount to about 70 pmol. Higher sensitivity is even reached using the methods of Lowry *et al.* (1961) or Nisselbaum and Green (1969) who both claim to enable detection of as less as 1 pmol NAD(P)H per assay.

An efficient cycling of NAD(P)H formed by G6PDH-mediated conversion of G6P present in hydrolysates of carbohydrates could, therefore, enhance the sensitivity of G6P determination by factor up to 3,000. This is promising since the amount of 6-phosphoglucosyl residues in carbohydrates, such as starch and glycogen, and thereby the concentration of G6P in hydrolysates of these is generally low.

Gibon *et al.* (2002) used NADPH cycling according to Nisselbaum and Green (1969) to determine G6P as metabolite in seeds of *Arabidopsis thaliana*. Furthermore they transferred the assay to 96 well format allowing the procession of a higher number of samples at a time. The G6P assay with NADPH cycling (cycling G6P assay) is outlined in Figure 3.

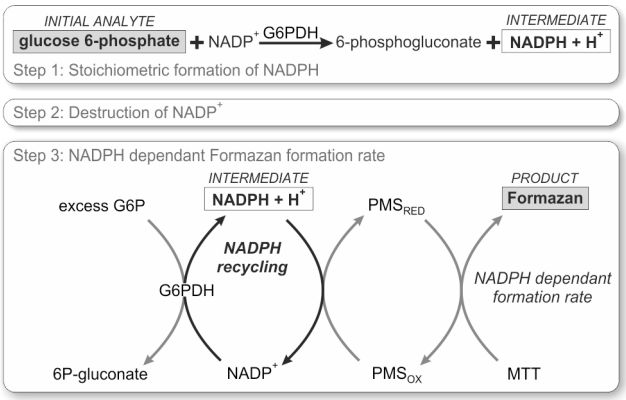

Figure 3. Experimental steps of the cycling G6P assay as described by Gibon et al. (2002)

For explanation see the text. For substance abbreviations see list of abbreviations and Figure 2.

Samples containing the initial analyte G6P are incubated with G6PDH and $NADP^+$. G6P is quantitatively converted to 6-phosphogluconate yielding stoichiometric amounts of NADPH

(Figure 3, Step 1; see 1.6.2.1). By heat treatment at high pH the excess $NADP^+$, added in Step 1, is destroyed while NADPH is retained (Figure 3, Step 2). After neutralization the mixture is transferred to 96 well plates for NADPH cycling largely according to Nisselbaum and Green (1969; Step 3). PMS_{OX} and MTT are added as well as G6PDH and G6P for continuous NADPH cycling. NADPH permanently reduces PMS the reduced form of which reduces MTT yielding the blue stain formazan. The rate of formazan formation recorded photometrically at 570 nm is proportional to the NADPH amount introduced to the cycling and, hence, to the initial amount of G6P applied to Step 1. Via calibration with G6P standards unknown concentrations can be calculated from rates of formazan formation.

1.6.2.3 Difficulties facing the quantification of 6-phosphoglucosyl residues

While the sensitivity of G6P detection can be enormously increased by cycling of NAD(P)H (see 1.6.2.2), such cycling assay is nonetheless based on the enzymatic conversion of G6P by G6PDH. G6P is released from 6-phosphoglucosyl residue containing carbohydrates by acid hydrolysis. However, due to the generally low abundance of 6-phosphoglucosyl residues, G6P is only a minor constituent of carbohydrate hydrolysates. Concentrations of the major carbohydrate monomer components exceed that of G6P by several orders of magnitude. In the case of polyglucans, such as starch or glycogen, hydrolysates contain mainly glucose and, if any, only very small amounts of the target compound G6P. In heteroglycans, such as those present in the plant cytosol, glucose accounts only for a very small proportion of all monomer constituents (Fettke *et al.*, 2005). Other neutral sugars, such as arabinose and galactose would dominate such hydrolysates and their concentrations would exceed that of G6P even more than that of glucose.

Applying hydrolysates of carbohydrates to a sensitive enzyme-based G6P assay implies that all reactions proceed in the presence of very high concentrations of non-target compounds. It is conceivable that those non-target compounds have an impact on the assay or parts of it.

For G6PDH an intrinsic glucose dehydrogenase activity (GDH) has been reported (Horne *et al.*, 1970). In the presence of high glucose concentrations GDH would strongly interfere with the selective enzymatic quantification of G6P since NADPH is generated in addition to that stoichiometrically formed by the G6PDH-mediated G6P conversion. G6P amounts derived from NADPH measurements (uncoupled or with a cycling assay) would be largely overestimated. The effect of high glucose concentrations (or that of other neutral sugars) on the G6PDH-mediated enzymatic G6P conversion has to be assessed and conditions of unbiased and sensitive G6P determination have to be established.

Likewise it is possible that high concentrations of neutral sugars as present in hydrolysates of carbohydrates affect the NAD(P)H cycling procedure. It has been reported that reducing sugars undergo various types of reactions at high concentrations in alkaline media (Yang and Montgomery, 1996). This could be the case during the destruction of excess $NAD(P)^+$ by heat and alkaline treatment before NAD(P)H cycling (Step 2, Figure 3). Any impact of putative degradation products formed during alkaline treatment has to be ruled out.

1.6.3 Determination of phosphoglucosyl residues by liquid chromatography and mass spectrometry

Depending on the carbon position of the phosphate ester, glucose phosphates exhibit differential physico-chemical properties which permit both, separation of different glucose phosphates by chromatographic approaches and distinction of different glucose phosphates using suitable techniques of mass spectrometry (MS).

Under appropriate conditions glucose phosphates differ in their retention on anion exchange chromatography columns and the specific phosphate position is assigned by comparing retention times with those of authentic standards. Quantification is possible after calibration of the detector response for each molecule species. However, inadvertent co-elution of more than one molecule species, as possible during the analysis of carbohydrate hydrolysates, can bias the quantification of the putative analyte (Ritte *et al.*, 2006).

Being structural isomers different glucose phosphates have identical molecule masses. Using MS without fragmentation of the analytes is therefore not appropriate for determination of specific glucose phosphates. However, fragmentation of glucose phosphate precursor ions, as obtained by collision-induced dissociation (CID) after electrospray ionization and precursor ion selection using tandem MS with ion trap, revealed that fragmentation patterns are characteristic for different glucose phosphates.

Techniques of tandem MS were described for the determination of G6P and glucose 3-phosphate (G3P) in hydrolysates of starch. They are used either without prior separation for determination of ratios between G6P and G3P (Haebel *et al.*, 2008) or, if they are coupled downstream of a suitable chromatography technique, for separate quantification of both glucose and glucose phosphates (Carpenter *et al.*, 2012). Chromatography with online quantitative MS combines quantitative and specific qualitative information about components eluting from chromatography columns. As opposed to high performance anion exchange chromatography coupled to pulsed amperometric detection (HPAEC-PAD), which is not suitable for MS coupling because of the usually high salt concentrations in the eluents used, by hydrophilic interaction chromatography (HILIC) glucose, G6P, and G3P are sufficiently separated using eluents rather MS compatible (Antonio *et al.*, 2008; Carpenter *et al.*, 2012). Carpenter *et al.* (2012) coupled HILIC to tandem MS where the HILIC derived eluate is constantly ionized by an electrospray source. Precursor ions of interest (glucose and glucose phosphate) are selected with an ion trap before they are fragmented by CID. G3P and G6P are determined by alignment of fragmentation patterns with those of authentic standards. Quantification of characteristic fragment ions allows the calculation of initial amounts of glucose and the respective glucose phosphates on the basis of calibration with known amounts of authentic standards.

The described chromatography- and MS-based methods are suitable for quantification of glucose phosphates provided they endure chemical hydrolysis of the carbohydrate. As opposed to starch, where the major glucosyl phosphates at carbon C6 and C3 are stable under appropriate hydrolysis conditions (Haebel *et al.*, 2008), a major proportion of glycogen phosphate has been reported acid labile (Fontana, 1980; Lomako *et al.*, 1993). Glucosyl phosphates that are acid labile, thus, can be neither quantified nor qualitatively analyzed by methods that rely on acid hydrolysis of the polyglucan. Milder conditions of polyglucan hydrolysis, such as during degradation using hydrolases, however, result in various species of phosphorylated oligoglucans. Chromatographic

and MS-based analysis of such degradation products is largely hampered since both methods rely on alignment with authentic standards which are practically unavailable in this case.

1.6.4 Determination of phosphorylated glucosyl carbons by NMR

Using techniques of nuclear magnetic resonance spectroscopy (NMR) glucosyl phosphates can be analyzed without acid hydrolysis of the polyglucans. Thus, by NMR, positions of phosphate esters on glucosyl carbons in polyglucans can be determined irrespective of their stability in acidic media. However, as will be explained in section 1.6.4.5 NMR is a rather insensitive method which requires relatively high amounts of analyte. This largely excludes NMR from being applied when only very small amounts of analytes are available.

1.6.4.1 Principles underlying NMR

The basis of NMR analysis is the occurrence of nuclei that possess a magnetic moment. This is realized in nuclei with a spin (spin quantum number I ≥ ½). The value of I in ^{1}H, ^{13}C, and ^{31}P nuclei is ½ which makes those nuclei relevant for NMR detection. Their magnetic moment vectors orient in external magnetic fields in two possible ways: along the direction of the external magnetic field (α-state), or against it (β-state). The magnetic moment vectors precess around the axis of the external magnetic field with the so called Larmor frequency. This frequency is dependent of the external magnetic field strength and the gyromagnetic ratio which is an isotope specific constant (equation 3). The energy difference ($\Delta E_{\alpha,\beta}$) between the two possible states (α or β) of nuclear magnetic moment vector orientation also depends on the external magnetic field strength and the gyromagnetic ratio (equation 4). This energy difference being generally small, compared to the average kinetic energy of samples at room temperature, implicates that α- and β-states are almost equally populated with a small excess of magnetic moment vectors oriented along the external magnetic field direction. The slight excess of magnetic moments in the α-state causes a macroscopic overall magnetization of the sample that is oriented in the direction of the external magnetic field.

(3) $$\nu_L = \frac{\gamma}{2\pi} \cdot B_0$$

(4) $$\Delta E_{\alpha,\beta} = \frac{\gamma}{2\pi} \cdot B_0 \cdot h = h \cdot \nu_L$$

$\Delta E_{\alpha,\beta}$	Energy difference between α- and β-state of magnetic moment vector orientation
ν_L	Larmor frequency
γ	Gyromagnetic ratio
B_0	External magnetic field strength
h	Planck's constant

If energy having a frequency matching the Larmor frequency is introduced at a right angle to the external field, the nuclei will absorb energy and magnetic moments will flip from α- to β-state, resulting in equal population of both energetic states (nuclear magnetic resonance). The overall magnetization vanishes.

Due to their different gyromagnetic ratios in a given external magnetic field different sorts of nuclei, such as ^{1}H, ^{13}C, or ^{31}P, exhibit largely different Larmor frequencies, which allows separate excitation of nucleus species by respectively adequate irradiation. Furthermore, within one species

of nuclei Larmor (and hence excitation energy) frequencies are slightly different because the effect of the external magnetic field on a nucleus is depending on magnetic shielding of the nucleus by its surrounding electrons. That means if the electronic constitution around nuclei of the same sort varies the effective external magnetic field strength and according to equation (3) and (4) the Larmor frequency as well as that of the adequate excitation energy differs. Since the electronic constitution around a nucleus is mainly determined by chemical bonds with other nuclei, even nuclei of the same sort are distinguishable by their nuclear magnetic resonance energy if their chemical surrounding differs (Friebolin, 1992; Günther, 1992).

1.6.4.2 Exemplification of 1D NMR measurements

In one-dimensional (1D) NMR experiments nuclei of one sort, e.g. ^{31}P, present in a sample are detected. In the external magnetic field the magnetic moments of these nuclei distribute between the two energetic states (α and β). $\Delta E_{\alpha,\beta}$ and the Larmor frequency is equal for all chemical equivalent nuclei but different for those with varying chemical surroundings. E.g. in a sample containing G3P and G6P ^{31}P exists as phosphate on carbon C3 or C6 of α- or β-glucopyranose (in this case α and β refer to the glucosyl anomers). Thus, four (C3α, C3β, C6α, C6β) groups of ^{31}P nuclei exist each group with a distinct Larmor and excitation energy frequency.

In modern NMR an electromagnetic pulse is applied in right angle to the magnetic field. This pulse contains a band of frequencies which permits the simultaneous excitation of all nuclei of one sort (in this example ^{31}P) irrespective their specific chemical surroundings. This pulse has two main effects. 1) In each set of ^{31}P nuclei, excitation causes magnetic moments to flip from α- to higher energetic β-state. The populations of magnetic moments in α– and β–state are equal and overall sample magnetization in the direction of the external magnetic field vanishes. 2) The right angle magnetic vector of the pulse forces nuclear magnetic moments, compatible in frequency, away from precessing randomly around the axis of the external magnetic field which causes an overall magnetization in right angle of the external magnetic field.

After irradiation a portion of the magnetic moments are 'bundled' in the direction transversal to the external magnetic field (coherence). They return to equilibrium (random precession around the axis of the magnetic field with overall magnetization along its direction) in spiral movement of the overall magnetization from right angle back to the axis of the external magnetic field. This spiral movement (relaxation) is registered as oscillating and decaying current (FID, free induction decay) in a receiver coil in right angle of the external magnetic field. The four sets of ^{31}P nuclear magnetic moments in the G3P/G6P sample (see above) relax with distinct spiral movements oscillating in correlation with their specific Larmor frequency. The FID in this example is therefore composed of induced currents from four overlapping relaxation processes. The four specific Larmor frequencies can be calculated. By Fourier transformation (FT) the FID is converted from the time domain to the frequency domain, resulting in a 1D ^{31}P NMR spectrum with four signals which represent the four groups of ^{31}P nuclei with respect to their Larmor or excitation energy frequency (signal position in x) and their abundance (signal intensity in y). Since the Larmor frequency is dependent of the external magnetic field, measured frequencies are compared to those of internal standards and given as chemical shift in parts per million (ΔHz per MHz) (Friebolin, 1992; Günther, 1992).

Similar to electronic shielding, the magnetic moment of one nucleus can affect the resonance frequency of another nucleus by altering the effective magnetic field strength the other nucleus is

exposed to (spin-spin coupling). In the example of G3P and G6P (see above) the effective external magnetic field at each ^{31}P nucleus is locally altered by ^{1}H nuclei that are connected via 3 chemical bonds (vicinal coupling; one hydrogen in the case of G3P, two in the case of G6P). Considering the magnetic moment of one α-state (excitable) ^{31}P nucleus in G3P, the resonance frequency that leads to excitation (transition to β-state) is increased when locally the external magnetic field strength is raised. Likewise it is decreased at diminished local magnetic field strength. The magnetic moment of the vicinal ^{1}H can either be in α- or in β-state. In both states it slightly alters the magnetic field at the neighboring ^{31}P with the same intensity but with different direction (increase or decrease). Since α- and β-state are always almost equally populated (see 1.6.4.1) half of the excitable (α-state) ^{31}P nuclei are exposed to a slightly higher, the other half to a slightly lower local magnetic field strength. This leads to excitation at two slightly different resonance frequencies and relaxation in accordance with slightly different Larmor frequencies (difference of frequencies is the coupling constant J) which results in splitting of the ^{31}P signals of both G3P anomers into doublets. In analogue fashion vicinal coupling with two chemically equivalent ^{1}H nuclei (as in anomers of G6P) leads to splitting of the ^{31}P signals into triplets. Thus, the splitting patterns of ^{31}P signals reveal whether the phosphate is connected to glucosyl C6 or to one of the carbons on the glucosyl ring. However, NMR spectra of many nuclei can also be recorded without coupling to nuclei of the same (homonuclear coupling) or a different species (heteronuclear coupling) (Friebolin, 1992; Günther, 1992; Berger *et al.*, 1993).

In 1D ^{1}H NMR the chemical shift of ^{1}H nuclei is affected by the position of the hydrogen on the glucosyl residue (carbon C1 to C6). Each position theoretically gives two signals according to anomer state of the glucosyl residue. The attachment of phosphate groups influences the chemical shifts of ^{1}H nuclei depending on the distance of phosphate and the respective hydrogen. Hydrogens connected vicinal to phosphorus (via 3 chemical bonds, i.e. bound to the same carbon) likely exhibit the most significant change in chemical shift. The attachment of phosphate to specific glucosyl carbons can principally be determined if hydrogen signals are assigned to their position on the glucosyl residue and vicinal phosphorus/hydrogen interaction is verified.

1.6.4.3 Principle of 2D NMR

The determination of homo- as well as heteronuclear couplings provides essential information about the connectivity of nuclei via chemical bonds. The couplings can be resolved by suitable techniques of two-dimensional (2D) NMR. For that matter FIDs are recorded after application of a sequence of electromagnetic pulses. These sequences usually consist of four stages: preparation period, evolution period t_1, mixing period, detection period t_2. Pulses applied during the preparation period result in sample magnetization transversal to the external magnetic field by 'bundling' the magnetic moment vectors in transversal direction. This coherence destabilizes during the evolution time according to the actual Larmor frequencies of the nuclear magnetic moments (relaxation) which are influenced by spin-spin coupling. During the mixing period another series of pulses is applied upon the partially relaxed magnetic moments. Subsequently the FID (transversal magnetization over time t_2) is recorded in the detection period. This pulse sequence is applied several times with incremented changes in t_1 so that the magnetization during mixing period is applied at differential states of magnetic moment coherence. Thus, as opposed to 1D NMR where

only identical FIDs are recorded and subjected to Fourier transformation, in 2D NMR several FIDs are obtained as a function of t_1.

After Fourier transformation of FIDs (conversion of the time domain t_2 to the frequency domain F_2) a second Fourier transformation is required to convert $F_2(t_1)$ to $F_2(F_1)$. Therefore, a 2D NMR experiment results in two frequency axes that derive from either of the two time variables t_1 or t_2 and represent a chemical shift. A plot of 2D NMR usually shows intensity values for a pair of frequency variables (F_1, F_2), the intensity being represented in a third dimension using contour lines (Martin and Zektzer, 1988; Friebolin, 1992).

1.6.4.4 Different correlations in 2D NMR experiments

In 2D NMR experiments the chemical shifts of the same or of different nuclei can be correlated.

^{1}H,^{1}H-COSY (COrrelation spectroscopY) spectra show chemical shifts of ^{1}H nuclei (protons) on both axes (F_1 and F_2). Some signals occur along the diagonal and correlate with identical chemical shifts in F_1 and F_2. The signal pattern on this diagonal is equivalent to that of the 1D ^{1}H spectrum. Coupling of protons with different chemical shifts results in crosspeaks (off-diagonal signals). In ^{1}H,^{1}H-COSY spectra ^{1}H,^{1}H correlations are detected when both nuclei are connected via three chemical bonds (vicinal coupling) or, provided they are chemically non-equivalent, via two chemical bounds (geminal coupling). In glucosyl residues hydrogen is bound either to carbon or to oxygen in hydroxyl groups. The chemical shifts of hydroxyl protons can be found over a wide range and is strongly depending on the acidity of a specific hydroxyl group. To simplify ^{1}H spectra measurements of carbohydrates are usually performed in D_2O. This way ^{1}H is quantitatively exchanged by ^{2}H (deuterium) which is not excited when ^{1}H-pulses are applied. Thus, hydroxyl protons are not detected and usually not visible in ^{1}H,^{1}H-COSY plots of carbohydrate compounds. For the analysis of glucosyl residues this type of experiment serves to assign signals in complex 1D ^{1}H NMR spectra to positions on the carbon backbone. The protons (H1) at glucosyl C1 exhibit the strongest chemical shift because they are de-shielded by two electronegative oxygen nuclei that are bound to the same carbon (Pomin, 2012). H1 couples vicinal with another proton the signal of which can consequently be assigned to H2. H2 reveals H3, etc., until all proton signals are assigned to their respective carbon (Friebolin, 1992; Martin and Zektzer, 1988).

Regarding phosphorylated glucosyl residues each ^{31}P nucleus is vicinal connected to hydrogen. Correlations of this type can be detected in ^{1}H,^{31}P-HMBC spectra (Heteronuclear Multiple Bond Correlation), where ^{1}H and ^{31}P chemical shifts are on the axes F_2 and F_1, respectively. Signals indicate connection of phosphate and a specific hydrogen nucleus to the same carbon.

Especially when the signal pattern in ^{1}H spectra is rather complex and various signals are very close to each other or even overlapping, 2D NMR that correlates hydrogen and carbon is useful to disentangle the complexity of the ^{1}H dimension. ^{1}H,^{13}C-HSQC (Heteronuclear Single Quantum Coherence) and ^{1}H,^{13}C-HMQC (Heteronuclear Multiple Quantum Coherence) spectra detect hydrogen-carbon correlations via one chemical bond. Thus, the proton signals in F_2 are separated along the ^{13}C chemical shift in F_1 and direct connectivity of hydrogens and carbons is indicated. By multiplicity editing signals that indicate methylene (-CH_2-) can be distinguished from those that point to methine (-CH-) or methyl groups (-CH_3). Since the latter do not occur in polyglucans, the multiplicity editing allows assignment of carbon and hydrogen signals to the position C6 (Friebolin, 1992; Martin and Zektzer, 1988).

1.6.4.5 Sensitivity of NMR requires high amounts of polyglucans

NMR relies on the detection of minimal changes in the magnetic field as induced by the excitation of specific isotopes in a sample. By irradiation small population differences of magnetic moments in α- and in β-state are equalized and brought to coherence which results in detected changes of the overall sample magnetization. These changes in sample magnetization depend on the absolute number of the specific isotope in the sample and on the extent of population differences between α- and β-state. The latter is dependent of the isotope species and the external magnetic field strength (see 1.6.4.1) which was improved in the last decades by the utilization of stronger magnets.

^{31}P is an NMR detectable isotope with 100% natural abundance. However, the abundance of phosphate in polyglucans is very low. Therefore, comparably huge amounts of polyglucans are required to enable the detection of the ^{31}P nuclei. When Lim and Seib (1993) analyzed phosphoesters in starch they used 1 g of starch. Ritte *et al.* (2006) consumed 225 mg of starch for similar NMR experiments. Even using such high substance amounts spectra of many repetitive measurements had to be accumulated to obtain acceptable signal to noise ratios. Thus, analysis of the rare phosphoesters in polyglucans by NMR is highly time and material consumptive.

1.7 Research objective

Both in animals and in plants energy and reduced carbon are stored in carbohydrates. While plants use starch animals usually synthesize glycogen. Starch is water insoluble residing in plastids, and the water soluble glycogen is mainly found in the cytosol. However, in plants carbohydrate polymers are also found in the cytosol as soluble heteroglycans that are physiologically related to starch metabolism.

The polyglucans starch and glycogen contain small amounts of covalently bound phosphate. These phosphoesters seem to play a significant physiological role in functional metabolism of the respective polyglucan. In plants insufficiency in both starch phosphorylation as well as dephosphorylation lead to disturbed starch turnover, progressive starch accumulation and usually growth retardation. Glycogen phosphate became even very relevant for humans as insufficient glycogen dephosphorylation is one reason for the severe form of neurodegenerative myoclonus epilepsy, Lafora disease (LD). Patients suffering from LD lack either the glycogen phosphatase laforin or an ubiquitin E3 ligase (malin). Interestingly in patients and mouse models of both forms of the disease the glycogen content is increased and insoluble particles are observed that accumulate progressive with age of patients or animals. Thus, considering both starch and glycogen, the function of phosphate esters seems closely related to the physico-chemical properties of the polyglucans. It is not inconceivable to assume that by phosphorylation of carbohydrates properties such as hydro-solubility are regulated. Besides in starch and glycogen, other carbohydrates, such as the plant heteroglycans, could also be affected by phosphorylation.

Regarding starch metabolism enzymes responsible for phosphorylation and dephosphorylation have been described. In glycogen metabolism until recently only laforin was known to alter the amount of glycogen phosphate. Especially the incorporation of phosphate into glycogen was unresolved for a long time. In starch at least two dikinases incorporate phosphate at distinct glucosyl carbons. Accordingly, the carbons C6 and C3 are the major phosphorylation sites in starch. Minor

phosphorylation at starch glucosyl C2 was postulated. By contrast, conflicting data is available about glycogen phosphorylation sites. While former publications state the existence of C6 phosphate, a recent publication exclusively declares the presence of phosphate at C2 and C3. Furthermore, glycogen phosphate is reported to be incorporated in an erratic side reaction of glycogen synthase via a mechanism that excludes the presence of C6 phosphate. As opposed to starch metabolism, it is currently believed that phosphate does not exert a specific function in glycogen metabolism, but is rather the result of an enzymatic error, that, if not corrected, has fatal pathological consequences. Thus, from the recent point of view the metabolism of phosphate in starch and glycogen seems to differ largely.

This work aims to clarify the view about glycogen phosphorylation sites. Since, the existence of C6 phosphate is a crucial point that could argue for or against the current view of glycogen phosphate metabolism a sensitive cycling assay is optimized and validated for specific measurement of G6P in hydrolysates of polysaccharides including glycogen. The assay is based on the enzymatic conversion of G6P and is therefore unaffected by phosphate containing contaminations. For higher sensitivity the stoichiometric amounts of NAD(P)H, formed in the enzymatic reaction, are coupled to redox reactions. The influence of high concentrations of neutral sugars, as present in hydrolysates of carbohydrates, is investigated and conditions are defined that enable reliable G6P detection. The high sensitivity of the cycling assay enables determination of G6P with very low sample consumption and in hydrolysates of carbohydrates with low C6 phosphorylation. In various carbohydrates, including starch and glycogen from several sources as well as preparations of the plant heteroglycan, the amount of 6-phosphoglucosyl residues will be determined. Likewise, the assay is versatile since cycling of NAD(P)H derived from other enzymatic reactions allows determination of other metabolites. Examples are provided in this work.

Various techniques of NMR (1D and 2D) are applied to finally elucidate the phosphorylated glucosyl carbons in glycogen. The well characterized and highly phosphorylated *Curcuma* starch serves for optimization of procedures. The phosphorylation sites as determined by NMR in *Curcuma* starch and several glycogen samples are compared.

If C6 phosphate exists in glycogen, the optimized cycling assay is a suitable tool to explore the distribution of C6 phosphate in glycogen molecules as well as possible correlations between C6 phosphate and other structural properties of glycogen such as chain length pattern and molecule size distribution. Studies on glycogen from mouse mutants defective in laforin and malin will be included and could elucidate a putative role of C6 phosphate and thereby of glycogen phosphorylation in general.

2 Experimental procedures

2.1 Chemicals, enzymes, and laboratory equipment

2.1.1 Chemicals

Acetic Acid	Cat. No. 3738.5, Roth, Karlsruhe, Germany
Ammonium acetate	Cat. No. 7869.1, Roth, Karlsruhe, Germany
Arabinose	Cat. No. A3131, Sigma, Taufkirchen, Germany
ATP (Adenosine-5'-triphosphate)	Cat. No. 10127523001, Roche, Mannheim, Germany
BCA (Na_2(2,2'-bichinolin-4,4'-dicarbonate))	Cat. No. D8284, Sigma, Taufkirchen, Germany
BisTris (buffer)	Cat. No. 9140.2, Roth, Karlsruhe, Germany
BSA (bovine serum albumin)	Cat. No. 8076.2, Roth, Karlsruhe, Germany
Copper sulphate	Cat. No. 1.02790, Merck, Darmstadt, Germany
D_2O (deuterium oxide)	Cat. No. 014100.2050, Armar Chemicals, Leipzig, Germany
DTT (dithiothreitol)	Cat. No. 6908.1, Roth, Karlsruhe, Germany
EDTA (Ethylenediaminetetraacetic acid)	Cat. No. 8043.2, Roth, Karlsruhe, Germany
Ethanol	Cat. No. 20821.321, VWR, Darmstadt, Germany
Fucose	Cat. No. F2252, Sigma, Taufkirchen, Germany
[^{14}C] glucose 1-phosphate	Cat. No. CFB128, GE Healthcare, Freiburg, Germany
G1P (glucose 1-phosphate)	Cat. No. G7000, Sigma, Taufkirchen, Germany
G2P (glucose 2-phosphate)	Kindly provided by Dr. P. Schmieder; prepared according to Zmudzka and Shugar (1964)
G3P (glucose 3-phosphate)	Kindly provided by Dr. G. Ritte; prepared as described in Ritte et al. (2002)
G4P (glucose 4-phosphate)	synthesized and purified by Dalton Pharma Services, Toronto, Canada
G6P (glucose 6-phosphate)	Cat. No. G7250, Sigma, Taufkirchen, Germany
Galactose	Cat. No. G0750, Sigma, Taufkirchen, Germany
Glucose	Cat. No. 1.08337, Merck, Darmstadt, Germany
HCl (hydrochloric acid)	Cat. No. 4625.1, Roth, Karlsruhe, Germany Cat. No. 4658, J.T. Baker, Deventer, Netherlands
Hepes (buffer)	Cat. No. 9105.3, Roth, Karlsruhe, Germany
Imidazole (buffer)	Cat. No. X998.3, Roth, Karlsruhe, Germany
KOH (potassium hydroxide)	Cat. No. 1.05033, Merck, Darmstadt, Germany
LiCl (lithium chloride)	Cat. No. 3739.2, Roth, Karlsruhe, Germany
L-Serin	Cat. No. 84960, Sigma, Taufkirchen, Germany
M6P (maltose 6-phosphate)	Kindly provided by Dr. G. Ritte; prepared as described in Ritte et al. (2006)
Magnesium chloride	Cat. No. HN03.1, Roth, Karlsruhe, Germany
Maltodextrin	Cat. No. 419672, Sigma, Taufkirchen, Germany

Mannose	Cat. No. M1134, Sigma, Taufkirchen, Germany
MTT (3-(4,5-Dimethylthiazol-2-yl)-2,5-diphenyltetrazolium bromide)	Cat. No. M2128, Sigma, Taufkirchen, Germany
NAD^+ (Nicotinamide adenine dinucleotide, oxidized form)	Cat. No. 10127981001, Roche, Mannheim, Germany
NADH (Nicotinamide adenine dinucleotide, reduced form)	Cat. No. 10107735001, Roche, Mannheim, Germany
$NADP^+$ (Nicotinamide adenine dinucleotide phosphate, oxidized form)	Cat. No. 10128058001, Roche, Mannheim, Germany
NaOH (sodium hydroxide)	Cat. No. 7067, J.T. Baker, Deventer, Netherlands Cat. No. 4689, J.T. Baker, Deventer, Netherlands
Perchloric acid	Cat. No. 1.00514, Merck, Darmstadt, Germany
Percoll	Cat. No. 17-0891-01, GE Healthcare, Uppsala, Sweden
PMS (phenazine methosulfate)	Cat. No. P9625, Sigma, Taufkirchen, Germany
p-Nitrophenyl phosphate	Cat. No. 107905, Boehringer, Mannheim, Germany
Potato starch	Cat. No. S2004, Sigma, Taufkirchen, Germany
QFF Sepharose	Cat. No. 17.0510.10, GE Healthcare, Uppsala, Sweden
Rhamnose	Cat. No. R3875, Sigma, Taufkirchen, Germany
Ribose	Cat. No. R7500, Sigma, Taufkirchen, Germany
Rothiszint eco plus	Cat. No. 0016.3, Roth, Karlsruhe, Germany
SDS (sodium dodecyl sulphate)	Cat. No. 4360.2, Roth, Karlsruhe, Germany
Sodium acetate	Cat. No. 71183, Sigma, Taufkirchen, Germany
Sodium azide	Cat. No. 822335, Merck, Darmstadt, Germany
Sodium bicarbonate	Cat. No. 1.06329, Merck, Darmstadt, Germany
Sodium carbonate	Cat. No. A135.2, Roth, Karlsruhe, Germany
Sodium citrate	Cat. No. 4088.2, Roth, Karlsruhe, Germany
Sodium nitrate	Cat. No. 1.06537, Merck, Darmstadt, Germany
Sulphuric acid	Cat. No. 1.00731, Merck, Darmstadt, Germany
TFA (trifluoroacetic acid)	Cat. No. P088.1, Roth, Karlsruhe, Germany
Tricine (buffer)	Cat. No. 6977.2, Roth, Karlsruhe, Germany
Tris (buffer)	Cat. No. 5429.2, Roth, Karlsruhe, Germany
Triton X-100	Cat. No. T9284, Sigma, Taufkirchen, Germany
Xylose	Cat. No. X1500, Sigma, Taufkirchen, Germany

2.1.2 Enzymes

Alkaline phosphatase	Roche, Mannheim, Germany Calf intestine, EIA grade, Cat. No. 10567744001
α-Amylase	Roche, Mannheim, Germany Pig pancreas, Cat. No. 10102814001
Amyloglucosidase	Sigma, Taufkirchen, Germany Aspergillus niger, Cat. No. 10115

G6PDH (glucose 6-phosphate dehydrogenase)	Roche, Mannheim, Germany Yeast grade I ('$G6PDH_{RI}$'), Cat. No. 10127655001 Yeast grade II ('$G6PDH_{RII}$'), Cat. No. 10127671001 *Leuconostoc* ('$G6PDH_{RL}$'), Cat. No. 10165875001 Sigma, Taufkirchen, Germany *Leuconostoc* ('$G6PDH_{SL}$'), Cat. No. G5760
HK (hexokinase)	Roche, Mannheim, Germany Yeast, Cat. No. 11426362001
Isoamylase	Sigma, Taufkirchen, Germany Pseudomonas spec., Cat. No. I5284
PGM (phosphoglucomutase)	Sigma, Taufkirchen, Germany Rabbit muscle, Cat. No. P3397
Phosphorylase a	Sigma, Taufkirchen, Germany Rabbit, Cat. No. P1261

2.1.3 Laboratory equipment

Standard laboratory equipment, such as test tubes, reaction vials, glassware, gloves, tips etc., is not specified below but was purchased from one of the following companies: Carl Roth GmbH + Co. KG (Karlsruhe, Germany), VWR International GmbH (Darmstadt, Germany).

96 well plates	Cat. No. 655001, Greiner Bio-One, Frickenhausen, Germany
Analytical balances	TE214S; Sartorius, Göttingen, Germany
Centrifuges	5417 and 5810R; Eppendorf, Hamburg, Germany EBA 12; Hettich, Tuttlingen, Germany 3-18K; Sigma, Osterode am Harz, Germany
fFFF-MALLS-DRI system	
Flow FFF instrument	F-1000; FFFractionation, Salt Lake City (UT), USA
Multiangle laser photometer	DAWN DSP; Wyatt Technology, Santa Barbara (CA), USA
Interferometric refractometer	Optilab DSP;
Fraction collector	Foxy Jr.; Teledyne ISCO, Lincoln (NE), USA
Half-micro cuvettes	Cat. No. Y199.1, Roth, Karlsruhe, Germany
HPAEC-PAD device	ICS3000; Dionex Thermo Fisher, Idstein, Germany
HPAEC-PAD separation columns	CarboPac PA1, CarboPac PA200; Dionex Thermo Fisher, Idstein, Germany
Hybridizer	HB-1D; Techne, Burlington (NJ), USA
Lyophilizer	Schrader, Friedland, Germany
NMR spectrometers	AVANCE III, DRX600, AV600; Bruker, Billerica (MA), USA
Nylon nets	neoLab, Heidelberg
Photometer	Cary 100; Varian, Darmstadt, Germany Genios Pro plate reader; Tecan, Männedorf, Switzerland
Pipettes	Labmate optima; Abimed, Langenfeld, Germany
Radiometer	QSL-2100; Biospherical Instruments, San Diego, USA
Rotator	Kisker-Biotech, Steinfurt, Germany
Scintillation counter	LS6500; Beckman Coulter, Krefeld, Germany

Software	Office 2003; Microsoft, Unterschleißheim, Germany Magellan 5; Tecan, Männedorf, Switzerland Topspin 2.1 and 3.0; Bruker, Billerica (MA), USA ASTRA, version 4.75; Wyatt Technology, Santa Barbara (CA), USA Chromeleon, version 6.8; Dionex Thermo Fisher, Idstein, Germany
SpeedVac	Savant SPDIIIV; Thermo Scientific, Langenselbold, Germany
Thermomixer	Compact; Eppendorf, Hamburg, Germany
Ultrafiltration units	Amicon (cut-off: 3, 10, 30, 100 kDa); Merck Millipore, Schwalbach, Germany
Vortex	MS1, IKA, Staufen, Germany
Water purification system	ELIX and MilliQ; Merck Millipore, Schwalbach, Germany

2.2 Biological material

Arabidopsis thaliana (Col-0) plants were grown under controlled conditions (14 h light/10 h dark, 22/17 °C, 70% RH, and approximately 100 µmol quanta m^{-2} s^{-1}). A homozygous GWD-deficient *Arabidopsis thaliana* mutant (SALK_077211, *sex1-8* (Ritte *et al.*, 2006)) was grown along side with the wild type control plants. Rhizomes from *Curcuma longa* L. were purchased from a local store and were stored frozen until use. Cell wall-deficient *Chlamydomonas reinhardtii* strain no. CC-503 cw92 mt+ was obtained from the *Chlamydomonas* Resource Center, University of Minnesota, USA.

2.3 Synchronized culture of the green alga *Chlamydomonas reinhardtii*

Cells of *Chlamydomonas reinhardtii* were grown according to Garz *et al.* (2012). The method is described briefly. After preculturing the cells (axenic conditions at room temperature for five days) aliquots were diluted in medium and grown for synchronization in glas tubes (3.5 cm inner diameter, 45 cm length; culture volume max. 300 ml) under axenic conditions. The medium [pH 7.4] in preculture and synchronization culture was the same and contained five macrocompounds (Sueoka, 1960) and microelements (Kuhl and Lorenzen, 1964) the latter reduced to 50% as compared to the original version. The glass tubes were placed in a water bath, kept at 34 °C, and illuminated from front and back side in a 12 h light/12 h dark regime. The cells were agitated by aeration with synthetic air supplemented with 2% [v/v] CO_2 (Kuhl and Lorenzen, 1964). Illumination, as measured inside the cell suspension using a radiometer (Quantum Scalar Laboratory Type QSL-2100; Biospherical Instruments Inc., San Diego, USA), was ca. 900 and 550 µmol m^{-2} s^{-1} at the beginning and the end of the light period, respectively. At the end of each dark period the suspension was diluted to ca. $7x10^5$ cells ml-1. After four days synchrony of the cell culture was reached. On the following day cells were harvested for the experiments described in this work.

2.4 Starch preparations

Commercial potato starch analyzed was obtained from Sigma (Cat. No. S2004; Taufkirchen, Germany). Endosperm starch from wild type rice kernels (Oryza sativa, Kinmaze) and those of the derived mutant line EM10 was isolated in the lab of Prof. Yasunori Nakamura (Akita Prefectural University, Akita City, Japan) and kindly provided. Starch granules were isolated according to Yamamoto *et al.* (1973, 1981). The endosperm of the mutant line EM10 is deficient in SBEIIb.

2.4.1 Isolation of starch from *Arabidopsis* leaves and *Curcuma* rhizomes

Native starch from *Arabidopsis thaliana* leaves and reserve starch from *Curcuma* rhizomes were isolated according to Ritte *et al.* (2000) and Kötting *et al.* (2005), with some modifications for the latter.

Frozen rhizomes were peeled, sliced and re-frozen in liquid nitrogen. Aliquots (~15 g) were ground in a mortar, transferred to a tube and resuspended in 25 ml extraction buffer (20 mM HEPES-KOH [pH 8.0], 0.2 mM EDTA, 0.5% [w/v] TritonX-100). After extensive mixing the suspension was passed through a nylon net (100 µm mesh width), centrifuged (5 min, 1,000 x g, 4 °C), and the supernatant was discarded. The pellet resuspended in 10 ml extraction buffer was passed successively through nylon nets with decreasing mesh width (60, 30 and 20 µm) and subsequently resuspended in 5 ml extraction buffer. The suspension was layered on top of a 10 ml cushion of 100% Percoll and was centrifuged for 15 min at 2,000 x g. After discarding the Percoll supernatant the pellet was resuspended in water and passed through Percoll once more. The pellet was subsequently washed three times with 5 ml 2% [w/v] SDS. The SDS was removed by washing the white pellet five times with cold water. Each washing step consisted of resuspending the particles, incubation on a rotator for 15 min, centrifugation (5 min, 1,500 x g), and discarding of the supernatant. Finally, the reserve starch granules were lyophilized and stored at -20 °C until use.

2.4.2 Isolation of starch from cells of *Chlamydomonas reinhardtii*

Starch granules of *Chlamydomonas reinhardtii* were isolated as follows. 25 ml of the synchronized cell culture were transferred to a tube containing 2.78 ml 50% [v/v] acetic acid on ice. After mixing the cells were collected by centrifugation (4 °C, 20,000 x g, 12 min), resuspended in 400 µl 5% [v/v] acetic acid and transferred to a 2 ml vial. 400 µl 5% [v/v] acetic acid were used to wash the tube and were finally added to the cell suspension. The latter was treated with an ultrasonic probe (for 60 s; setting: gain 55, cycle 4) and spun down followed by the addition of 200 µl 10% [w/v] SDS. After mixing the samples were frozen over night, thawed, vigorously mixed and incubated on a rotator for 20 min. After centrifugation (20,000 x g, 10 min) and discarding the supernatant the pellet was washed three times with 900 µl 2% [w/v] SDS, i.e. resuspending the pellet, incubation on a rotator (20 min), centrifugation (20,000 x g, 10 min), and discarding the supernatant. The pellet was then resuspended in 340 µl water and layered on 530 µl 100% Percoll (see above) followed by centrifugation (20 min, 2,000 x g, 4°C). Discarding the Percoll supernatant the pellet was resuspended in water and passed through Percoll a second time. Finally the starch granules were washed four times with 900 µl water (each time, 20 min incubation on a rotator and 10 min centrifugation at 4 °C and 20,000 x g), dried under vacuum, and stored at -80 °C.

2.5 Isolation of soluble heteroglycans from *Arabidopsis* leaves

According to Fettke *et al.* (2004) water soluble heteroglycans (SHG) were isolated from *Arabidopsis thaliana* wild-type leaves as follows. Immediately after harvesting the leaves were frozen in liquid nitrogen. The frozen leaves were ground yielding a fine powder using a liquid nitrogen cooled mortar. Subsequently aliquots of ~2 g were extracted with 20% [v/v] cold ethanol by using a vortex. By centrifugation (12 min, 4 °C, and 21,000 x g) insoluble compounds such as starch and cell debris were separated from water soluble compounds. The supernatant containing glycans of

the apoplast and symplast was passed through a nylon net (mesh width 70 µm) and subsequently heated for 8 min at 95 °C in a water bath. Cooled down to 4 °C on ice the extract was centrifuged (as above) and one more time passed through a nylon net (see above). The pellet of the first extraction was extracted a second time. The second extract was treated as the first. The two extracts were combined, lyophilized and are designated as total heteroglycan preparation (SHG_0). After dissolving the SHG_0 in 3 ml water (30 min shaking at 40 °C) SHG_L (>10 kDa fraction) was prepared from SHG_0 by ultrafiltration (regenerated cellulose membrane with 10 kDa cut-off). The retentate containing the SHG_L fraction was washed six times (with water), recovered from the filter, lyophilized, and dissolved in 800 µl water. SHG_L fractions were stored at -80 °C until use.

2.6 Glycogen isolation

Glycogen was isolated in the lab of Prof. Berge A. Minassian (Hospital for Sick Children, Toronto, Canada) from liver and skeletal muscle of wild type, *Epm2a*$^{-/-}$ and *Epm2b*$^{-/-}$ mice and from skeletal muscle of a male wild type rabbit (purchased at a local market). After the isolation according to Tagliabracci *et al.* (2008) the glycogen was transferred to Germany in a dry state. The glycogen was dissolved in water and stored frozen until use. Where stated, glycogen was five times precipitated in a mixture consisting of 66.6% ethanol [v/v] and 5.4 mM LiCl for 1 h at -20 °C, precipitated glycogen was collected by centrifugation (10 min at 20,000 x g), dissolved in water, and re-precipitated. Thereby, low molecular weight contaminants, such as G6P or phospho-oligoglucans, were removed. Rabbit glycogen was additionally washed 5 times using a membrane filter (100 kDa cut-off).

2.7 Acid hydrolysis of carbohydrates

Throughout this study, two procedures were applied. Procedure A aims the complete hydrolysis of both interglucose bonds and phosphate ester linkages and thereby converts all covalently bound phosphate to orthophosphate. For procedure A, samples were dried in highly clean glass vials under reduced pressure and subsequently dissolved in 40 µl consisting of 1.25 M sulphuric acid and 45% [w/v] perchloric acid. Samples were hydrolyzed at 190 °C for 26 min and then cooled to RT (Hess and Derr, 1975). After addition of 110 µl water each, the samples were ready for determination of total phosphate.

Procedure B was applied for acidic hydrolysis of interglucose bonds but retaining C3 and C6 monophosphate esters (Haebel *et al.*, 2008). Aliquots of starch, glycogen or plant soluble heteroglycan preparations were hydrolyzed in 2 M TFA for 3 h at 100 °C (hydrolysis B1). The volume of TFA was reduced to approximately 10 µl under reduced pressure, diluted with 1 ml of water followed by complete evaporation of the diluted TFA. Samples dissolved in water were analyzed. As a control, interglucose bonds of starch and glycogen were hydrolyzed in 0.7 M HCl for 3 h at 95 °C (hydrolysis B2). After cooling to RT and neutralization with KOH the hydrolysates were ready for glucose or G6P determination. The stability of G6P under either hydrolysis conditions (B1 or B2) was tested by using a G6P standard. Following 4 h hydrolysis recovery consistently exceeds 95%.

2.8 Quantification of reducing ends

Monosaccharide such as glucose, arabinose, galactose, rhamnose, mannose, xylose, ribose, and fucose possess an aldehyde group at carbon C1 (reducing end) when existing as open-chain state. This group can take part in redox reactions, e.g. it can donate electrons to a suitable electron acceptor reducing the latter while the aldehyde group is oxidized yielding a carboxyl group.

Carbohydrates that largely consist of monosaccharides with reducing ends, such as the plant cytosolic heteroglycans from *Arabidopsis thaliana* (Fettke *et al.* 2005), can be quantified following acid hydrolysis by using the method of Waffenschmidt and Jaenicke (1987). In this method Cu^{2+} is reduced to Cu^{+} ions at high pH which then form a photometrically detectable complex with BCA. L-serine forms a chelate complex with free Cu^{2+} ions remaining low concentrated and preventing precipitation as hydroxide.

A linear correlation between the concentration of reducing ends and the absorbance at 560 nm caused by the respective formation of the Cu^{+}-BCA complex enables the determination of unknown amounts of reducing ends. Calibration is done with standard concentrations of glucose. However, it should be noted that absorbance coefficients depend on the specific reducing sugar. If for instance equal molar amounts of glucose, galactose, and arabinose are separately subjected to the assay the resulting absorbance with galactose and arabinose is 85.6% and 71.6%, respectively, compared to that measured with glucose. Hence, relying on calibration with glucose, amounts of reducing ends can only be given as glucose equivalents which are only an estimation of the actual amount of reducing ends when the composition of the carbohydrate analyzed is quantitatively unresolved.

The assay was performed as follows:

Solution A:	5 mM	Na_2(2,2'-bichinolin-4,4'-dicarbonate)
	512 mM	sodium carbonate
	288 mM	sodium bicarbonate
Solution B:	5 mM	$CuSO_4$ x 5 H_2O
	12 mM	L-serine

Equal volumes of solutions A and B were mixed and kept on ice directly before adding 500 µl of the mixture to 500 µl of sample. The addition took place on ice. After mixing the complete reaction mixtures were incubated for 15 min at 100 °C and, subsequently, cooled in an ice bath followed by 5 min equilibration at RT. Absorbance is measured against a blank mixture containing water instead of sample.

The absorbance coefficients using standards of glucose, galactose, and arabinose were determined to be 0.0672, 0.0575, and 0.0481 ml $nmol^{-1}$ cm^{-1}, respectively, and are consistent with those previously published (Waffenschmidt and Jaenicke, 1987).

2.9 Determination of glucose and G6P using a conventional enzymatic assay

The conventional method to specifically determine glucose and G6P is based on an enzymatic assay according to Lowry and Passonneau (1972). In the presence of ATP Glucose is converted to G6P by hexokinase (HK). The G6P dehydrogenase (G6PDH) mediates oxidation of G6P to 6-

phosphogluconat and reduces $NAD(P)^+$ to NAD(P)H with a stoichiometry of unity. The latter is photometrically detected at 340 nm with an absorbance coefficient of 6.3 ml μmol^{-1} cm^{-1}. Polyglucans, such as starch and glycogen, can be quantified by quantifying of glucose after acid or enzymatic hydrolysis of all glycosidic bonds. The calculated amount is then given as glucosyl residues.

Both assays, for glucose and G6P, were performed in half-micro cuvettes or on 96 well plates. The latter format has the advantage of higher throughput and less sample consumption by measuring in a smaller volume. Taking the decreased path length into account the 96 well format still reduces the amount of sample needed approximately by factor 3.

Buffer (1) as well as ATP and $NADP^+$ stock solutions used for the enzymatic reactions in both formats were identical. ATP and $NADP^+$ were purchased from Roche (Mannheim, Germany) as well as G6PDH (from yeast, grade II) and HK.

Buffer 1	100 mM	imidazole-HCl [pH 6.9]
	1.5 mM	$MgCl_2$
ATP stock	0.1089 g/ml	in water (180 mM, stored at -20 °C)
$NADP^+$ stock	0.0886 g/ml	in water (112.5 mM, stored at -20 °C)

Table 4. Solutions for conventional glucose and G6P assay

Amounts are given for one sample. Final volumes are reached with buffer 1. Two test formats (designated as 96 well and Half-micro) are given. Enzymes are supplied as ammonium sulphate suspensions. Required volumes of the enzyme suspensions were centrifuged (14,000 x g and 4 °C). The supernatant was discarded and the pellet was dissolved in buffer as indicated.

		Glucose assay		G6P assay	
		96 well	Half-micro	96 well	Half-micro
Mix1	**ATP stock**	1 µl	6.67 µl	--	--
	$NADP^+$ stock	1 µl	6.67 µl	1 µl	6.67 µl
	G6PDH	1 U	2 U	--	--
	Final volume (buffer 1)	140 µl	800 µl	140 µl	800 µl
Mix2	G6PDH	--	--	1 U	2 U
	HK	1 U	1 U	--	--
	Final volume (buffer 1)	5 µl	5 µl	5 µl	5 µl

In the case of half-micro cuvettes 800 µl mix1 (see Table 4) was added to 5-200 µl of the samples that were transferred into cuvettes and adjusted with water to 200 µl. Following mixing the absorbance at 340 nm was monitored in a Cary 100 photometer (Varian, Darmstadt, Germany) at 30 °C against blinds containing no sample. After ca. 5 min 5 µl mix2 (see Table 4) was added each. To assure complete transfer of the enzyme solution the latter was first placed on a small plastic spatula that was subsequently used to mix the solution in the cuvette. Monitoring of absorbance was continued for ca. 10 min or until absorbance reached constancy.

In the case of 96 well format 140 µl mix1 was added to 5-30 µl of the samples placed onto the plate and adjusted with water to equal volumes. Absorbance at 340 nm was monitored at 30 °C and 1 measurement per minute in a plate reader for up to 30 min or until absorbance reached

constancy. Subsequently, 5 µl mix2 were added to each sample and absorbance was monitored as described before.
Calculation of glucose and G6P concentrations, respectively, is based on the difference of constant absorbance values before and after the addition of mix2. Since the path length in 96 well plate measurements depends on the final assay volume, the value of the absorbance coefficient for NAD(P)H as given for half-micro cuvettes does not apply. Hence, standard amounts of the respective analyte (0, 0.5-30 nmol per well) were included using the plate format.
Due to the large number of measurements performed on a single 96 well plate, it is unfeasible to determine manually the constant absorbance values for each measurement. Using the program Microsoft Excel, routines (macros) on the basis of Visual Basic for Application were programmed that determined the constant part of the recorded absorbance time function by iteration of an algorithm that consisted the following two steps:

1) Calculation of average over all yet undeleted absorbance values
2) Deletion of the single value that diverts most from the average

The iteration stopped when either the number of remaining values reached 8 or the standard deviation of the average absorbance was below 0.004. By iteration, the absorbance time function is also corrected for outliers such as occasionally caused by dust particles in wells. The average absorbance after applying the iterative algorithm is defined as constant absorbance and served for calculation of the difference in absorbance.

2.10 Quantification of sugars and sugar phosphates using a sensitive cycling assay

Any sugar or sugar phosphate that by a single reaction or by several consecutive steps are enzymatically converted to G6P can be quantified by determining the amount of NAD(P)H that stoichiometrically is formed when G6P is completely oxidized to 6-phosphogluconat by the action of G6PDH (Lowry and Passonneau, 1972).
Instead of directly measuring NAD(P)H at wavelength 340 nm, Nisselbaum and Green (1969) described a method to efficiently enhance signal intensity. Following destruction of residual $NADP^+$, NADPH is coupled to a series of redox reactions. First it reduces PMS which then reduces MTT yielding a blue stain, formazan. In the presence of saturating levels of G6P and G6PDH, NAD(P)H is permanently reduced maintaining the formation of formazan. The rate of formazan formation is constant in time and is directly proportional to the initial amount of NAD(P)H. Formazan formation is monitored photometrically at 570 nm. On the basis of calibration with standards unknown amounts of analyte can be determined.
After acid hydrolysis of carbohydrates (procedure B), G6P can be determined in the hydrolysates enabling the calculation of glucosyl C6 phosphate. As opposed to the analysis of metabolites, in hydrolysates of polyglucans G6P is quantified in the presence of large excess of glucose. In the case of hydrolyzed plant heteroglycans other monosaccharides, such as arabinose and galactose, also exceed G6P by several orders of magnitude. To rule out that these sugars bias the determination of C6 phosphate, the assay has been performed with mixtures of G6P and glucose, arabinose or galactose standards mimicking the hydrolysates of the glycans.

When applying the cycling assay to hydrolyzed polyglucans, an intrinsic glucose dehydrogenase (GDH) activity of glucose 6-phosphate dehydrogenase (G6PDH) is especially relevant (Horne *et al.*, 1970). The GDH activity also yields NADPH which strongly interferes with the specific enzymatic detection of G6P in these hydrolysates. In order to establish a reliable and selective enzymatic assay for G6P using the cycling assay, the effect of excess glucose during G6P determination has been tested using several commercially available G6PDH preparations.

2.10.1 Analysis of different preparations of G6PDH and their glucose dehydrogenase activities

The enzyme preparations used ($G6PDH_{RI}$, $G6PDH_{RII}$, $G6PDH_{RL}$, and $G6PDH_{SL}$) were first adjusted to equal G6PDH activities under the conditions of the cycling assay and in the absence of glucose. In a final volume of 1 ml, G6P and $NADP^+$ (1 µmol each) were incubated with G6PDH in buffer 2 (50 mM tricine-KOH [pH 8.0], 2.5 mM $MgCl_2$). The enzyme amount varied (0.01 and 0.005 U according to the manufacturers description) to test substrate saturation. The enzyme reaction was monitored as NADPH formation at 30 °C, and absorbance at 340 nm was recorded for 15 min in a CARY spectrophotometer. Absorbance rates were corrected by controls lacking G6P.

2.10.2 Solutions for the cycling assay

Buffer 2	200 mM tricine-KOH [pH 8.0] 2.5 mM $MgCl_2$
$NADP^+$ stock	4 mg/ml
ATP stock	10 mg/ml
BSA stock	6 mg/ml
G6PDH	from *Leuconostoc,* Roche, designated as $G6PDH_{RL}$ from *Leuconostoc,* Sigma, designated as $G6PDH_{SL}$
PGM	from rabbit muscle, Sigma
HK	from Yeast, Roche
HCl	0.5 and 0.25 M
Buffered HCl	0.5 M HCl : main buffer : water, 4 : 5 : 51 [v/v/v]
NaOH	0.5, 0.25, and 0.1 M

Table 5 shows the composition of solutions (mix1, mix2, mix3) needed for the cycling assay. The complete mix3 without glucose G6PDH is prepared freshly being only stable for a few hours. However, a convenient protocol for the preparation of two stable stock solutions ('EP' – containing EDTA and PMS; 'GMB' – containing G6P, MTT, and BSA) which are combined immediately before use has been established.

Preparation of 'EP' for approximately 1,000 assays: dissolve 0.285 g of EDTA in 16 ml main buffer, transfer 15.663 ml of the solution into a tube containing 0.0195 g PMS and add 3 ml of main buffer. Preparation of GMB for approximately 1,000 assays: dissolve the components separately in main buffer (0.162 g G6P/8 ml, 0.063 g MTT/16 ml, 0.0765 g BSA/9 ml). Combine the following volumes: 7.6 ml (G6P), 15.6 ml (MTT), 8.6 ml (BSA). Prepare aliquots of 1100 µl and 1850 µl for 'EP' and 'GMB', respectively, after completely dissolving the components, freeze the aliquots in liquid nitrogen, and keep them at -80 °C until use. The aliquots are stable for >1 year. Remainders of thawed 'EP' and 'GMB' stock solutions can be used again if frozen immediately in liquid nitrogen.

Table 5. Solutions for enzymatic cycling assay

Amounts are given for 1 assay. Enzymes are supplied as ammonium sulphate suspensions. Volumes equal to amounts of enzymes needed are taken from the suspension and added directly in the case of mix1 and mix2, or centrifuged (14,000 x g and 4 °C) and taken up in mix3 after discarding the supernatant. The composition of mix3 is identical for determination of G6P, G1P, and glucose.

		Analyte to be determined		
		G6P	**G1P**	**Glucose**
Mix1	Buffer 2	5 µl	5 µl	5 µl
	$NADP^+$ stock	1.28 µl	1.28 µl	1.28 µl
	$G6PDH_{RL}$	--	0.1312 U[1)]	0.1312 U[1)]
	Final volume (water)	20 µl	20 µl	20 µl
Mix2	Buffer 2	5 µl	5 µl	5 µl
	ATP stock	--	--	0.2281 µl
	BSA stock	0.0972 µl	--	--
	$G6PDH_{RL}$	0.1312 U[1)]	0.1312 U[1)]	0.1312 U[1)]
	PGM	--	0.6 U[1)]	--
	HK	--	--	0.2 U[1)]
	Final volume (water)	20 µl	20 µl	20 µl
Mix3[2)]	Buffer 2		27.86 µl	
	'EP' stock		18.66 µl	
	'GMB' stock		33.48 µl	
	$G6PDH_{SL}$		6 U[1)]	

1) referring to activities described by the supplier

2) For preparation of mix3 the enzyme is centrifuged in a small vial. The pellet is subsequently transferred with the premix of buffer 2, 'EP', and 'GMB' into a new tube.

All solutions were kept on ice until use.

2.10.3 Performing the cycling assay

The assay is based on the procedure described by Gibon *et al.* (2002) but was modified as described below.

Samples and standard amounts (0 – 40 pmol per assay) were adjusted with water to 25 µl and 20 µl of mix1 were added. Subsequently, samples were agitated at 30 °C for 10 min, except for G1P determination in plant extracts (30 min). In the latter, target levels are usually far below that of G6P which, therefore, was completely oxidized by G6PDH in mix1 (Table 5) to avoid erratic results for G1P. This is ensured by prolonging the incubation time.

Subsequently, NADPH is completely destroyed by acid treatment (Rover *et al.*, 1998). In the case of G1P or glucose determination this is essential to exclusively couple the NADPH to the cycling

reaction that derives stoichiometrically from G1P or glucose conversion after the addition of mix2 (Table 5). However, even during the determination of G6P this step was found valuable since it reduces deviations between technical replicas (see 3.1.2). The acid treatment is carried out by the addition of 10 µl 0.25 M HCl, 10 min incubation at 30 °C, and neutralization by the addition of 10 µl of 0.25 M NaOH.

Subsequently, mix2 is added to the vials placed in a suitable rack in an ice bath to avoid differences in the incubation times when the number of samples is high. Vials are incubated at 30 °C for 10 min before the immediate transfer back on ice. By the addition of 20 µl 0.5 M NaOH and heating (5 min at 99 °C) excess $NADP^+$ was destroyed (Rover *et al.*, 1998). However, NADPH is, although to a much lesser extent, also sensitive to the combination of high pH and heat treatment. Therefore heating time and conditions have to be equal for all samples. This is achieved by placing groups of samples into the heating block and back into an ice bath in the same order and with 3 s intervals.

After neutralization by adding 20 µl 0.5 M HCl, the reaction mixtures were transferred into 96 well plates in a cold room (4 °C). Subsequently, 80 µl of freshly prepared mix3 (Table 5) was added, the plate was centrifuged for 20 s at 1,500 x g, and absorbance at 570 nm was monitored in a Tecan plate reader for 120 min with 1 min^{-1} at 30 °C. Since, as mentioned, $NADP^+$ and NADPH are pH and temperature sensitive HCl and NaOH are added slowly while gentle mixing. As far as possible samples are strictly kept on ice and times of sample transfer are kept as short as possible. After each addition the samples are spun down for 15 s in a cooled centrifuge.

The procedure described above is suitable and valid for the determination of glc, G1P, and G6P, as long as the total amount of neutral sugars (including sugars other than those to be determined) per assay is below 80 nmol. G1P measurements are not affected by the presence of up to 120 pmol G6P. Considering G6P measurements the assay has been optimized for the analysis of starch or glycogen hydrolysates. In an excess glc, the neutral hexose does not interfere with the G6P measurements unless the glucose amount per assay exceeds 40 nmol (see 3.1.1.1).

When quantifying the 6-phospho glucosyl residues in plant heteroglycans, high amounts of the hydrolyzed carbohydrate have to be applied to the assay, since the heteroglycans mostly comprise of arabinose and galactose, and only a small proportion of the lowly abundant glc residues is assumed to be phosphorylated. High amounts of arabinose and galactose lead to erroneously increased rates of formazan formation, thus to overestimation of G6P. The critical step was identified to be the $NADP^+$ destruction at high pH and temperature which also leads to arabinose and galactose dependent browning of the assay mixture. To circumvent this effect for G6P measurements in hydrolysates of heteroglycans the cycling G6P assay is altered in the following way. Mix1 contained already G6PDH, thus was identical to mix1 for G1P measurements (Table 5). After incubation with mix1, excess $NADP^+$ was destroyed by the addition of 0.1 M NaOH and heating for 3 min at 95 °C. Subsequently, for neutralization 60 µl of buffered HCl was added. Transfer to 96 well plates and measurement of formazan formation were carried out as described above. By this alteration the tolerated amount of arabinose and galactose per assay could be raised fivefold and permit reliable measurements of G6P in hydrolysates of plant heteroglycans. However the variation of technical replicas was slightly higher as compared to polyglucans (see 3.1.1.2).

2.10.4 Automated well data processing

Depending on the number of standard amounts (5 – 6) and samples (up to 12) and their respective technical replicas (usually 3) a large data set is generated by one batch of cycling assays. The set consists of up to 54 subsets of 120 absorbance values representing the time-dependent formazan formation in a single well. At the onset of the reaction, absorbance versus time curves fairly followed a sigmoid pattern, showing low increase at the beginning (phase A) but with time increase linearly (phase B) and, finally, slope decreases (phase C). All three phases vary in length and intensity between samples of different concentrations and under different assay conditions during the process of optimization. To enable fast and objective data processing an automated algorithm has been developed on the basis of MS Excel and Visual Basic for Application that identifies the linear part (phase B) of the rates of formazan formation derived from all wells and uses that for calculation of mean rates. The latter are subsequently used for calculation of the amount of analyte initially applied to the assay.

For each well recorded absorbance values A_n (0 min ≤ n < 120 min; (n + 1) – n = 1 min) were converted to absorbance differences per minute ΔA_n by the following operation.

(5) $$\Delta A_n = A_n - A_{n-1} \qquad 0 < n < 120$$

Subsequently all negative ΔA_n were eliminated, and the remaining values were tested against the following criterion.

(6) $$\left|\Delta A_n - \overline{\Delta A}_{const}\right| > P \cdot \overline{\Delta A}_{follow12}$$

ΔA_n	Value tested
$\overline{\Delta A}_{const}$	Mean value of 15 successive ΔA_n values obtained in phase B (n manually assigned; for most measurements: n = 40 to n = 54)
P	Manually assigned constant for a measured batch of standards and samples (usually set to 0.7)
$\overline{\Delta A}_{follow12}$	Mean value of ΔA_n, n + 1 to n + 12 (twelve ΔA values succeeding ΔA_n)

If (6) for a ΔA_n is true the value deviates from $\overline{\Delta A}_{const}$ more than (P·100)% of $\overline{\Delta A}_{follow12}$, and was subsequently virtually labeled. By (6) values are more likely labeled if they are succeeded by ΔA_n obtained in phase C than if they are just outliers within phase B. Values ΔA_n were eliminated if 8 adjacent values were also labeled. Eliminations so far almost exclusively occurred at n in phase C (when the absorbance curve progressively flattens and thus ΔA_n get smaller). The average of the remaining ΔA_n was already very similar to the absorbance-time curve's slope in phase B.

Subsequently ΔA_n were eliminated if they met the following criterion.

(7) $$\left|\Delta A_n - \overline{\Delta A}_{remain}\right| > \frac{1}{Q}$$

ΔA_n	Value tested
$\overline{\Delta A}_{remain}$	Mean value of all remaining (not eliminated) ΔA_n derived from the same well
Q	Variable for iterative exclusion of outliers

Successive increase of Q was first achieved by iteration of n in (8).

(8) $Q_n = Q_0 + 10 \cdot n$ $Q_0 = 10$

As soon as a ΔA_n met criterion (7) the value was eliminated and did no longer contribute to mean value calculation. The iteration (8), thus, led to successive smoothing of the $\overline{\Delta A}_{remain}$ and stopped if within one data subset (data of the same well) either the number of ΔA_n reached a value below 60 (9) or the standard deviation of $\overline{\Delta A}_{remain}$ was below 10% of $\overline{\Delta A}_{remain}$ (10).

(9) $N_{remain} < 60$

N_{remain} Number of remaining values

(10) $\sigma_{remain} < 0.1 \cdot \overline{\Delta A}_{remain}$

σ_{remain} Standard deviation of all remaining ΔA_n derived from the same well
$\overline{\Delta A}_{remain}$ Mean value of all remaining ΔA_n derived from the same well

From the maximum value reached for Q_n during the first iteration 10 was subtracted, and a second iteration (11) was executed that increased Q in (7) with smaller increments.

(11) $Q_m = (Q_n - 10) + m$

Q_n Maximum Q_n reached in (8)

The second iteration (11) stopped if for one data subset one of the criteria (9) or (10) was met. The mentioned data subset was uncoupled from further smoothing. Yet coupled data sets were smoothed by further iterations of n in (8) and m in (11) as described above until all data subsets were finally uncoupled from smoothing, thus, met criterion (9) or (10).
After smoothing, $\overline{\Delta A}_{remain}$ was the mean slope of the linear part of the absorbance-time curve (phase B) form a certain data subset. Values derived from standard concentrations measured on the same 96 well plate served for calibration and, thus, for calculation of unknown amounts of analyte.

2.11 Laforin-mediated hydrolysis of glucosyl 6-phosphates

In a final volume of 75 µl (containing 100 mM NaOAc, 50 mM each bisTris and Tris, 4 mM DTT [pH 6.5]), 85 µg glycogen from *Epm2a*$^{-/-}$ mouse skeletal muscle was incubated at 37 °C for times indicated with 250 U isoamylase and laforin (equivalent to 0.3 mU when acting on p-nitrophenyl phosphate). Active human laforin was expressed in *E. coli* and kindly provided by Peixiang Wang (Hospital for Sick Children, Toronto, Canada). Where indicated, glycogen or enzymes were omitted as control experiments and replaced by water and buffer, respectively. Subsequently, all samples were heated (5 min, 95 °C) and subjected to acid hydrolysis (procedure B2). Glucose was determined using the conventional enzymatic assay according to Lowry and Passonneau (1972, see 2.9) and G6P was quantified utilizing the optimized cycling assay (see 2.10).

2.12 Amylolytical treatment of starch and glycogen prior to NMR analysis

Purified *Curcuma* starch was washed 3 times with 50 mM NH_4OAc buffer [pH 6.0] (for each washing step 1 ml buffer was added per 20 mg of starch, 20 min on a rotator). Subsequently, the starch was solubilized applying the following temperature program: 5 min 55 °C which then is increased to 95 °C during 8 min, 10 min 95 °C, and gradual cooling to 55 °C. Heating and cooling proceeded in the presence of a mixture of α-amylase and amyloglucosidase (50 U/ml of each enzyme in 50 mM NH_4OAc buffer [pH 6.0] and 20 mg/ml native starch). Subsequently, α-amylase and amyloglucosidase (each 2.5 U/mg starch) are added again, followed by 2 h incubation at 55 °C. Glycogen from *Epm2a*$^{-/-}$ mouse liver and rabbit muscle (see 2.6) was enzymatically hydrolyzed as described for *Curcuma* starch with the following modifications: Following the first addition of enzyme the glycogen was incubated 1.5 h at 37 °C. Subsequently the incubation was continued at 55 °C for 2 h after a second addition of enzyme. Enzymes, concentrations and buffer were exactly as described for *Curcuma* starch. Digestion of glycogen and *Curcuma* starch was terminated by 10 min heating at 95 °C.

After the enzymatic hydrolysis, glycogen and *Curcuma* starch samples were treated equally. Samples were centrifuged 10 min at 20,000 x g in order to remove precipitated protein and the supernatants were passed through 3 kDa membrane filters. Filtrates were lyophilized 1-3 times to reduce the amount of NH_4OAc and subsequently were dissolved in water. The 6-phosphoglucosyl residues were recovered in the filtrate by 95% as determined by the cycling assay after acid hydrolysis of aliquots taken before filtration as well as from the filtrate.

For 1D ^{31}P-NMR analysis without further enrichment of phosphoglucans digested samples of *Curcuma* starch (derived from ca. 20 mg starch powder) and mouse liver glycogen (ca. 100 mg) were taken up in 600 µl 50 mM NH_4OAc buffer [pH 7] containing 15% D2O.

2.13 Enrichment of phosphoglucans from starch and glycogen

The enrichment of phosphoglucans was performed in two scales. Up to 30 mg amylolytically treated glycogen or *Curcuma* starch were applied on a column with 300 µl bed volume of QFF Sepharose; larger amounts of carbohydrate were applied on 8 ml bed volume. Any cross-contamination of the phosphoglucans derived from starch and glycogen was avoided by performing the anion exchange chromatography on separate columns. Columns were washed with 8 column volumes (CV) 1 M NH_4OAc [pH 7.0] and equilibrated with 12 CV water. After sample application the column was washed with 8 CV water. Elution was achieved with at least 3 CV of increasing concentrations of NH_4OAc (0.02, 0.2, 1 M, or as indicated). Fractions were lyophilized, dissolved in water, and subjected to further analyses, such as determination of glucosyl residues, total phosphate, and C6 phosphorylation, along with aliquots that were taken during the process of enrichment. The enrichment of phosphoglucans was established using *Curcuma* starch and has been tested by HPAEC-PAD and ^{31}P-NMR (see 3.4.2). For HPAEC-PAD analysis 10-70 µg glucose equivalents or equal volumes of fractions were separated (separation mode 1, see Table 6).

The QFF-fractions eluting between 20 and 200 mM NH_4OAc contained the majority of the 6-phosphoglucosyl residues irrespective of the polyglucan analyzed. Those fractions that derived from ca. 340 mg *Epm2a*$^{-/-}$ mouse liver glycogen, ca. 150 mg rabbit muscle glycogen, and ca. 200 mg *Curcuma* starch, respectively, were dissolved in 600 µl D_2O and applied to NMR spectroscopy.

Curcuma phosphoglucans subjected to 1D ^{31}P-NMR were dissolved in 600 µl 50 mM NH_4OAc [pH 7] containing 15% D_2O.

2.14 Alkaline phosphatase treatment of phosphoglucans

Aliquots (50 µg glucose equivalents) of enriched phosphoglucans prepared from *Curcuma* starch were incubated with 4.5 U alkaline phosphatase (Roche) in 50 µl 20 mM Tris-HCl [pH 9.3], 5 mM $MgCl_2$, 0.1 mM $ZnCl_2$ for 2 h at 37 °C. The mixture was passed through a 10 kDa membrane filter. After reducing the filtrate volume, aliquots were applied to the HPAEC-PAD analysis (separation mode 2, see Table 6) along with an equal amount of phosphoglucans that had not been treated with alkaline phosphatase.

2.15 NMR experiments

All NMR measurements were run at Bruker 600 MHz spectrometers at 300 K using 5 mm sample tubes and D_2O as solvent. The phosphoglucan samples had aproximate concentrations of 6 mM phosphate (phosphoglucans derived from *Curcuma* starch), 0.5 mM phosphate (phosphoglucans derived from *Epm2a*$^{-/-}$ liver glycogen), and 2 mM phosphate (phosphoglucans derived from rabbit muscle glycogen). The 1D coupled ^{31}P NMR spectra were recorded at an AVANCE III spectrometer (measurements by Dr. Matthias Heydenreich, Institute of Chemistry, University of Potsdam). Typical acquisition data were: sweep width 3644 Hz, 12 k scans, 16 k data points, acquisition time 2.25 s, relaxation delay 1 s, 30° pulse angle (11.4 µs for 90°). Other experiments performed with *Curcuma* starch as well as the ^{31}P-HMBC of glycogen were recorded at a DRX600 using a (^{1}H,^{13}C,^{15}N,^{31}P)-QXI probe. Those performed with glycogen were recorded on a AV600 using a (^{1}H,^{13}C,^{15}N)-TXI cryoprobe. The ^{31}P-edited ^{1}H,^{13}C-HSQC of glycogen was recorded at the Center for Biomolecular Magnetic Resonance (BMRZ) at the Goethe-Universität in Frankfurt at a AV600 using a (^{1}H,^{13}C,^{31}P)-TXI cryoprobe. All probes were equipped with a one-axis self-shielding gradient. The measurements were performed by Dr. Peter Schmieder (Leibniz-Institute of Molecular Pharmacology, Campus Berlin-Buch, Robert-Roessle-Str. 10, 13125 Berlin, Germany).

For the three reference compounds without phosphorous (glucose, maltose, isomaltose, each 10mM in D_2O) a set of 2D experiments was recorded beside the conventional 1D: a DQF-COSY using 2048* x 256* data points, 8 scans and 204.8 msec and 30.7 msec as $t_{2,max}$ and $t_{1,max}$, respectively; a ^{13}C-HMQC using 512* x 256* data points, 16 scans and 51.2 msec and 35.8 msec as $t_{2,max}$ and $t_{1,max}$, respectively; a ^{13}C-HMQC-COSY using 512* x 256* data points, 32 scans and 51.2 msec and 35.8 msec as $t_{2,max}$ and $t_{1,max}$, respectively; a ^{13}C-HMQC-TOCSY using 512* x 256* data points, 16 scans and 51.2 msec and 35.8 msec as $t_{2,max}$ and $t_{1,max}$, respectively, and a mixing time of 80 msec; a ^{13}C-DEPT-HMQC using 512* x 256* data points, 32 scans and 51.2 msec and 35.8 msec as $t_{2,max}$ and $t_{1,max}$, respectively; a ^{13}C-HMBC using 2048* x 512* data points, 8 scans and 204.8 msec and 71.2 msec as $t_{2,max}$ and $t_{1,max}$, respectively and a ^{31}P-HMBC using 2048* x 64* data points, 8 scans and 204.8 msec and 51.2 msec as $t_{2,max}$ and $t_{1,max}$, respectively.

For those reference compounds with phosphorous (G1P, G6P, G4P, each 10 mM; G2P, approximately 8 mM; G3P approximately 7 mM; all in D_2O) the two 2D experiments to detect the interaction with phosphorous were recorded as well: a ^{13}C-HSQC using 512* x 1024* data points, 32 scans and 51.2 msec and 340.0 msec as $t_{2,max}$ and $t_{1,max}$, respectively, and a ^{31}P-edited-^{13}C-

HSQC recording carbon chemical shifts in the indirect dimension using 512* x 128* data points, 256 scans and 51.2 msec and 42.5 msec as $t_{2,max}$ and $t_{1,max}$, respectively. For those samples that had lower concentrations only the number of scans was varied if necessary.

For the experiments performed with *Curcuma* starch the following parameters were used: the multiplicity-edited HSQC was recorded with 512* x 256* points, 272 scans, $t_{2,max}$ = 51.25 msec and $t_{1,max}$ = 48.64 msec; the ^{31}P-edited HSQC was recorded with 512* x 256* points, 528 scans, $t_{2,max}$ = 51.25 msec and $t_{1,max}$ = 48.64 msec; the high resolution HSQC was recorded with 512* x 1024* points, 64 scans, $t_{2,max}$ = 51.25 msec and $t_{1,max}$ = 339.97 msec; the ^{31}P-HMBC was recorded with 2048* x 256* points, 8 scans, $t_{2,max}$ = 204.8 msec and $t_{1,max}$ = 256.0 msec; the DQF-COSY was recorded with 2048* x 512* points, 16 scans, $t_{2,max}$ = 204.8 msec and $t_{1,max}$ = 102.4 msec.

For the experiments performed with glycogen the following parameters were used: the multiplicity-edited HSQC was recorded with 512* x 256* points, 640 scans, $t_{2,max}$ = 51.25 msec and $t_{1,max}$ = 48.64 msec; the ^{31}P-edited HSQC was recorded with 512* x 150* points, 1344 scans, $t_{2,max}$ = 70.3 msec and $t_{1,max}$ = 28.5 msec; the high resolution HSQC was recorded with 512* x 1024* points, 256 scans, $t_{2,max}$ = 51.25 msec and $t_{1,max}$ = 194.56 msec; the ^{31}P-HMBC was recorded with 2048* x 64* points, 256 scans, $t_{2,max}$ = 204.8 msec and $t_{1,max}$ = 51.2 msec; the DQF-COSY was recorded with 2048* x 512* points, 48 scans, $t_{2,max}$ = 204.8 msec and $t_{1,max}$ = 85.0 msec.

1D spectra were processed using topspin 3.0 (Bruker) by zero filling up to 32 k data points and an exponential window function with a line broadening factor of 1 Hz. 2D spectra were processed using topspin 2.1 using squared sinebell window functions in both dimensions and resulting in a 4096 by 2048 data matrix.

2.16 High performance anion exchange chromatography coupled to pulsed amperometric detection (HPAEC-PAD)

By high performance anion exchange chromatography coupled to pulsed amperometric detection, mono- and oligosaccharides can be separated and quantified. Thus, the mono- and oligosaccharide patterns of mixtures can be analyzed. Mono- and oligosaccharides (in the mobile phase) interact with aminopropyl groups attached to pellicular matrices which form the immobile phase of the separation column. The retention time depends on the average negative charge of a molecule species that passes the positively charged column. Neutral mono- and oligosaccharides possess hydroxyl groups with relatively high pKa values (Sinnott, 2007). However, even at pH 7 only a small number of hydroxyl groups is deprotonated and negatively charged. Charges are randomly distributed over all hydroxyl groups with a similar pKa value. Many hydroxyl groups per molecule give raise to many negative charges within the molecule species at alkaline pH values. Thus, molecules with more hydroxyl groups interact stronger with the positively charged immobile phase and elute later. Consequently oligosaccharides are separated by degree of polymerization (DP) due to the increasing number of hydroxyl groups. Phosphorylation increases the net charge of a molecule species because of the lower pKa values of the phosphate groups. This results in increased proton dissociation, stronger interaction with the immobile phase, and longer retention times of phosphorylated oligosaccharides compared to neutral ones having the same DP.

Separated mono- and oligosaccharides are detected by a pulsed amperometric cell. A small proportion of the analyte is first oxidized at the surface of a gold electrode when a certain potential is applied. The resulting current is detected, the potential is shortly inverted (to avoid binding of oxidation products to the electrode surface), and the pulse sequence restarts. Signal intensity depends on the redox potential of the specific detected molecule species. The presence of reducing groups, such as in glucose and oligoglucans, facilitate oxidation and permit detection at a high sensitivity. However, the specific redox potential of reducing ends is influenced by many molecule-specific parameters. E.g. it slightly increases with the DP of an oligoglucan leading to decreased sensitivity for reducing ends of longer oligoglucans. Thus, for oligoglucans having varying DPs the signal intensities do not directly reflect the respective molarities.

Table 6. Separation modes applied during HPAEC-PAD analyses

Throughout this study several separation modes (#) were used for different applications. The mentioned separation columns (Col) refer to specifications of CarboPac columns from Dionex Thermo Fisher. Eluent program: uppercase letters refer to the eluents described above; percentages refer to total flow volume. FR – flow rate [ml min^{-1}], CT – column temperature [°C].

#	Col	FR; CT	Eluent program	Application
0	PA1	1; 25	Column wash step: 15 min, B 100% Equilibration: 20 min, A 100% Sample injection Isocratic: 60 min, A 100%	Monomers of plant heteroglycans (see 3.2)
1	PA1	1; 25	Equilibration: 10 min, C 99%, D 1% Sample injection Gradient: 30 min, C 99→0%, D 1→100% Isocratic: 10 min, D 100%	Enriched phosphoglucans from *Curcuma* starch (see 3.4.2)
2[1)]	PA1	1; 25	Equilibration: 10 min, C 99%, D 1% Sample injection Isocratic: 10 min, C 99%, D 1% Gradient: 30 min, C 99→0%, D 1→100% Isocratic: 10 min, D 100%	(Phospho)glucans after phosphatase treatment (see 3.4.2)
3	PA200	0.5; 30	Equilibration: 10 min, C 99%, D 1% Sample injection Gradient: 30 min, C 99→0%, D 1→100% Isocratic: 10 min, D 100%	Separation of linear α-glucans released from glycogen by isoamylase (see 3.6.1)
4[2)]	PA200	0.5; 30	Equilibration: 10 min, C 99%, D 1% Sample injection Gradient: 11 min, C 99→70%, D 1→30% Isocratic: 9 min, C 70%, D 30% Isocratic: 15 min, D 100%	Purification of G2P and G3P (see 2.17)

1) The isocratic step after sample injection ensures complete elution of Tris buffer before analytes and, thus avoids interference of both

2) Separation mode similar to that described by Ritte *et al.* (2006)

Throughout this study the HPAEC-PAD system ICS3000 and different CarboPac Columns from Dionex Thermo Fisher were used. For several applications different separation modes were used (Table 6). The ICS3000 system mixes the mobile phase if necessary from four eluents:

Eluent A: water
Eluent B: 200 mM sodium hydroxide
Eluent C: 100 mM sodium hydroxide
Eluent D: 100 mM sodium hydroxide, 500 mM sodium acetate

Gradients applied were always linear. Chromatograms were analyzed with Dionex Chromeleon Software (Version 6.8).

2.17 Purification of G3P and G2P

G3P was synthesized following a procedure of Perich and Johns (1988a, b) and a kind gift of Dr. Gerhard Ritte (Ritte *et al.,* 2002). G2P was synthesized in the lab of Peter Schmieder (Leibniz-Institute of Molecular Pharmacology, Campus Berlin-Buch, Berlin, Germany) according to Zmudzka and Shugar (1964). However, as standards for 2D NMR measurements both glucose monophosphate preparations had the disadvantage of containing impurities and required further purification which was achieved by a largely automated chromatographic approach.

The raw products of G2P and G3P were stored at -20 °C in dry state. Solutions of ca. 10 mM were prepared in water. While G3P dissolved completely during short shaking at 40 °C, it proved necessary to adjust the G2P solution to pH 5 (pH paper) by stepwise addition of diluted HCl. Supernatants obtained by centrifugation (to ensure removal of insoluble material) were repetitively applied to HPAEC-PAD. Per run 100-140 nmol of either compound were injected (injection volume: 95 µl), separated on a PA200 column (separation mode 4, see Table 6), and online desalted by a Dionex SRS desalter (500 mA). Putative G3P and G2P eluted at retention time 18 and 17 min, respectively.

Due to reproducible retention times it was possible to automatically collect the purified glucosyl monophosphates using a fraction collector. However, due to the construction of the chromatographic device sample collection was consistently delayed as compared to the detection. To permit automatic collection of the eluted sample the delay was determined experimentally.

During each of the consecutive chromatography runs (52 for G3P, 61 for G2P) a command-line within the chromatography control program triggered the collection of the peak of interest into 50 ml-tubes placed on ice. Subsequently the combined peaks were desalted 3 further times. The isocratic pump of the Dionex ICS3000 system was used to chromatograph the samples at a flow-rate of 0.5 ml min^{-1} through the desalter (see above). This allowed a reliable and largely autonomous desalting of large volumes (ca. 70 and 75 ml of collected G3P and G2P, respectively). The desalted samples were lyophilized and taken up in D_2O. Chromatography of equal volumes and comparison of peak area before and after purification revealed a recovery of ca. 90 and 80% for G3P and G2P, respectively. After purification the chromatograms of both monoglucosyl phosphates showed only one peak corresponding to the respective standard. NMR spectra revealed only one phosphorylated species in the sample.

2.18 Determination of molar mass distribution by fFFF-MALLS-DRI

Field-flow fractionation is a family of separation techniques whereby separation occurs due to different retentions of molecules or particles in a stream of liquid flowing through a thin channel. Since the flow profile of this laminar flow is parabolic, exhibiting highest velocity in the center of the channel and lowest near the walls, the position of a molecule within the channel determines its speed of channel passage. This position is affected by a field that is directed in right-angle to the channel flow (e.g. G force, flow, charge). Depending on molecule parameters (such as density,

diffusion coefficient, charge) the field differentially forces molecules into different regions of the laminar flow, affecting their channel passage speed. Molecules differentially affected by the field can be separated (Reschiglian *et al.*, 2005).

In flow FFF the two channel walls are permeable (frits) and allow the passage of the orthogonal cross-flow. The latter differentially drives molecules towards one frit (slow laminar flow region) that is covered by a membrane. The force the cross flow exerts on a molecule is negatively proportional to the molecules diffusion coefficient, (according to the Stokes-Einstein relation) the latter being negatively correlated with the hydrodynamic radius (Giddings, 1993). The real dimensions of a molecule in solution are not determinable and can deviate from the hydrodynamic radius, which is defined as the radius of a solid sphere that exhibits diffusion rates identical to the considered molecule. However, a constant field applied, time of channel passage is approximately proportional to the hydrodynamic radius, enabling a separation by molecule diameter only. Polydisperse polymer solutions with a wide range of molecule sizes elute from the channel without baseline separation due to the small size increments from degree of polymerization n to n + 1.

Coupling flow FFF with MALLS and DRI detection allows online determination of molar mass and concentration of small single fractions (slices) eluting from the fFFF channel. Those slices are considered as monodisperse and contain low concentration of the polymer. Thus, for homopolymers such as glycogen the following equation (12) from Zimm (1948) applies.

$$R_\theta = K \cdot \left(1 - \frac{32\pi^2}{3\lambda^2} \cdot \left[\sin\frac{\theta}{2} \right]^2 \cdot \left\langle r^2 \right\rangle \right) \cdot M_w \cdot c \qquad (12)$$

R_θ	Angle-dependent excess Rayleigh ratio (scattering intensity after subtraction of pure solvent scattering)
K	Optical constant, $K = 4\pi^2 n_0^2 (dn/dc)^2 \lambda_0^{-4} N_A^{-1}$; n_0 – refractive index of the solvent in vacuum, N_A – Avogadro's number, λ_0 – incident radiation wavelength in vacuum, dn/dc – refractive index increment with respect to changing solute concentrations
λ	Wavelength of polarized laser light (690 nm)
$\langle r^2 \rangle$	Gyration radius
M_w	Weight average molar mass
c	Concentration

The excess Rayleigh ratio, thus, positively correlates with weight average molar mass and concentration. Angle-dependent R_θ is slightly lowered in correlation with the gyration radius. Equation (13) shows an alternate form of equation (12), serves for plotting R_θ/Kc vs. $(\sin(\theta/2))^2$ (Debye plot) and indicates that M_w in a distinct slice can be obtained by extrapolation of $\theta \rightarrow 0$. The extrapolation takes place on the basis of a polynomial fit in $(\sin(\theta/2))^2$ which in the case of glycogen proved to be always first order.

$$\frac{R_\theta}{K \cdot c} = -M_w \cdot \frac{32\pi^2}{3\lambda^2} \cdot \left[\sin\frac{\theta}{2} \right]^2 \cdot \left\langle r^2 \right\rangle + M_w \qquad (13)$$

Thus, the simultaneous determination of concentration and molar mass in small fractions resolved by fFFF separation delivers the function of molar mass vs. elution volume (molar mass distribution). The weight average molar mass for a defined number of slices is calculated by equation (14).

(14) $$\overline{M}_w = \frac{\sum_{slices}(c_i \cdot M_{wi})}{\sum_{slices} c_i}$$

$\overline{M}_w$	Weight average molar mass for a defined number of slices
c_i	Concentration at slice i
M_{wi}	Weight average molar mass in slice i, determined in equation (13)

Molar mass distributions were determined by flow field-flow fractionation coupled to multiangle laser light scattering and differential refractive index detection (fFFF-MALLS-DRI) using a symmetrical flow FFF instrument (F-1000, regenerated cellulose membrane, cutoff 10 kDa; FFFractionation Inc., Salt Lake City, UT, USA), a multiangle DAWN DSP laser photometer (He-Ne-laser; Wyatt Technology Corporation [WTC], Santa Barbara, CA, USA), and an Optilab DSP Interferometric Refractometer (WTC).

Aliquots of glycogen preparations analyzed were transferred to the eluent used for fFFF-MALLS-DRI measurements (0.1 M sodium nitrate containing 0.05 % [w/v] sodium azide). This was usually achieved by washing the glycogen with eluent five to six times on membrane filters (10 kDa cut-off). Glycogen samples already washed with water on membrane filters (e.g. after gradual degradation with isoamylase or α-amylase) were mixed with equal volumes of doubly concentrated eluent. The injection volume was 220 µl. For the analysis of native wild type and Lafora disease glycogen ca. 180 µg of glycogen were applied. In the case of partially degraded glycogen the injected amount of remaining glycogen was ca. 120 µg.

Molar mass distribution and average molar mass were calculated from light scattering and DRI data by using the ASTRA software (version 4.75, WTC; extrapolation by Debye, first order). Among biological replica, mean values (and SEM) of the RI and molar mass data, respectively, were calculated at a given elution volume.

2.19 Analysis of linear side chain patterns of glycogen

In a final volume of 100 µl containing 3 mM NH_4OAc [pH 5] glycogen (200 µg) was incubated with 500 U isoamylase (Sigma) overnight at 37 °C. Subsequently the reaction mixture was heated (4 min 95 °C). After 10 min centrifugation at 20,000 x g 10 µg carbohydrate (supernatant) was applied to HPAEC-PAD analysis (separation mode 3, see Table 6). Linear glucan chains were separated by their degree of polymerization (DP; DP_{n+1} eluting later than DP_n) and correlated with linear chains of a maltodextrin standard. Baseline separation was achieved at least until DP of 40. Absolute DP peak areas were calculated with the Chromeleon software (Dionex) unless peak size or shape prevented valid calculation (i.e., when the peak intensity was too low). Relative peak areas were calculated for all DPs by the following equation (15). Peaks of high DPs that contributed less than 0.01% to the sum of absolute peak areas where omitted from relative peak area calculation.

(15) $$rA_{DPi} = \frac{A_{DPi}}{\sum A_{DPi}} \cdot 100$$

rA_{DPi}	Relative peak area of a distinct degree of polymerization i
A_{DPi}	Absolute peak area of a distinct degree of polymerization i

Mean relative peak areas of a DP i were calculated among biological replicates. For each DP i differences in mean relative peak areas between mutant and wild type were tested for significance by a T test and are given as ∆molar percent (equation 16).

$$\Delta P_{DPi} = \frac{\overline{rA}_{DPi,mut} - \overline{rA}_{DPi,wt}}{\overline{rA}_{DPi,wt}} \cdot 100 \quad (16)$$

ΔP_{Dpi} Difference of chain (DP i) abundance in percent (∆molar percent) between wild type and mutant

$\overline{rA}$ Mean relative peak areas of wild type (wt) or mutant (mut) at a given DP i

2.20 Gradual α-amylase degradation of glycogen

In a final volume of 1620 µl, 3600 µg of wild type mouse skeletal muscle glycogen was incubated at 37 °C with 0.65 U α-amylase (Roche, pig pancreas) using 28.3 mM NaOAc [pH 7] as buffer. A mixture lacking the enzyme served as control (0 min). At intervals (13, 30, 80 min) aliquots were withdrawn and heated for 10 min at 95 °C. All samples were subjected to membrane filtration (10 kDa cut-off) and washed 6 times with water to separate glucans released (filtrate) from remaining glycogen (retentate). Aliquots of the retentates were subjected to acid hydrolysis (procedure B2) and the glucosyl contents as well as the glucosyl 6-phosphate levels were determined and compared to respective amounts in untreated glycogen. Equal amounts (ca. 120 µg) of the remaining glycogen in the retentates were furthermore analyzed by fFFF-MALLS-DRI (see 2.18). The whole set of experiments was conducted twice with consistent results.

2.21 Gradual isoamylase degradation of glycogen

In a final volume of 438 µl, wild type mouse skeletal muscle glycogen (3.6 mg) was incubated with 3,000 U isoamylase at 37 °C in water. A mixture lacking the enzyme served as control (0 min). At intervals (2, 10, 40, 90 min, overnight) aliquots were withdrawn and heated for 5 min at 95 °C. Glucan chains released and remaining glycogen were separated as described in section 2.20, however, using a 30 kDa membrane filters to ensure separation of larger chains that are liberated from glycogen by isoamylase. Aliquots of the retentates were subjected to acid hydrolysis (procedure B2). In the hydrolysates glucose (see 2.9) and G6P (see 2.10) were quantified in order to calculate glycogen content and glucose-based C6 phosphate, both of which were compared to respective values in untreated glycogen solutions. In the retentate equal amounts of the remaining glycogen were further analyzed by fFFF-MALLS-DRI (ca. 120 µg; see 2.18) or debranched for a second time (10 µg glycogen; final volume: 50 µl, 50 U isoamylase [see 2.19], 37 °C overnight). After the second debranching 5 µg of the glucans were subjected to HPAEC-PAD analysis (separation mode 3, see Table 6). The whole set of experiments was conducted twice with consistent results.

2.22 Peripheral [^{14}C] labeling of glycogen by phosphorylase

In a final volume of 900 µl skeletal muscle glycogen (500 µg) prepared from wild type mice was incubated with phosphorylase a from rabbit (pho a, Sigma) in a mixture of 100 mM citrate [pH 6.5]

and 1 mM G1P. Two batches were prepared. Batch 1 contained 0.2 mg pho a and 5.96 Ci mol^{-1} [^{14}C] glucose 1-phosphate (G1P) (20 min incubation time). Batch 2 contained 2 mg pho a and 0.83 Ci mol^{-1} [^{14}C] G1P (4 min incubation time). The incubation was started by the addition of enzyme and stopped by heating for 10 min 95 °C. Subsequently 10 µmol non-labeled G1P were added, each batch was mixed, and centrifuged for 10 min at 2,000 x g. Aliquots (880 µl each) of the supernatants were passed through a membrane filter (10 kDa cut-off). The retentates were washed until the radiolabel in the filtrates reached background level. The retentates contained the labeled glycogen, an aliquot of which was used for determination of incorporated radiolabel. For radiolabel determination test solutions were mixed with an excess of scintillation liquid (Rothiszint eco plus, Roth, Germany) and counted for 10 min in a Beckman Coulter LS6500 scintillation counter. The absolute amounts of [^{14}C] label incorporated in batch 1 and 2 were similar.

2.23 Gradual α-amylase-mediated degradation of [^{14}C] labeled glycogen

In a final volume of 76.1 µl glycogen (169 µg each) either labeled with low or high pho a concentration (batch 1 or 2; see 2.22) was incubated in a hybridizer at 37 °C with 0.0305 U α-amylase (Roche, pig pancreas) using 28.3 mM NaOAc [pH 7] as buffer. The concentrations of glycogen, α-amylase, and buffer were, thus, identical to that of gradual α-amylase degradation as described in 2.20. A mixture lacking α-amylase served as control (0 min). At intervals (4, 8, 13, 30 min) aliquots were withdrawn and heated for 10 min at 95 °C. All samples were subjected to membrane filtration (10 kDa cut-off) and washed 6 times with water to separate carbohydrates released (filtrate) from remaining glycogen (retentate). In the retentates the glycogen content (as glucose after acid hydrolysis B2) as well as the radiolabel was determined. Decrease of radiolabel and glycogen content were calculated as percentage of the control (0 min). The trends of label and glycogen amount (decreasing with α-amylase incubation time) were similar using glycogen pre-labeled either in batch 1 or 2 (see 2.22).

2.24 Statistical methods

In this study often mean values are displayed that derive from measurements of either technical or biological replica. Values used for the calculation of the mean vary to some extend. Estimates of these variations are given either as 'average absolute deviation', as 'standard deviation' (SD), or as 'standard error of mean' (SEM). The latter two were calculated with Microsoft Excel functions. The following equations were employed.

(17) $$e = \frac{1}{n}\sum_{i=1}^{n}\left|x_i - \bar{x}\right|$$

(18) $$s = \sqrt{\frac{1}{n-1}\sum_{i=1}^{n}(x_i - \bar{x})^2}$$

(19) $$\sigma_n = \sqrt{\frac{1}{n^2 - n}\sum_{i=1}^{n}(x_i - \bar{x})^2}$$

e	Average absolute deviation
s	Standard deviation
σ_n	Standard error of mean
n	Number of values for calculation of mean
x_i	Single value of one replica
$\bar{x}$	Mean value of the n single values

Parameters measured in two groups of samples, e.g. the C6 phosphorylation in glycogen preparations from wild type mice (group 1) and LD mutants (group 2), and given as mean values calculated from replica can differ in the two groups. The significance of such difference has to be tested statistically. In this study Welch's T test was used, which is an adaption of an unpaired Student's T test that allows testing two groups with unknown or unequal variances considering the parameter measured (Sawilowsky, 2002). Since in most biological cases it is unknown whether a parameter's variance in two groups is similar this test is appropriate. The calculation the t value and degree of freedom was executed using the equations (20) and (21).

(20) $$t = \frac{\left|\bar{x} - \bar{y}\right|}{\sqrt{\frac{s_x^{\,2}}{n} + \frac{s_y^{\,2}}{m}}}$$

(20) $$\nu = \frac{\left(\frac{s_x^{\,2}}{n} + \frac{s_y^{\,2}}{m}\right)^2}{\frac{\left(\frac{s_x^{\,2}}{n}\right)^2}{n-1} + \frac{\left(\frac{s_y^{\,2}}{m}\right)^2}{m-1}}$$

t	t value
$\bar{x}$, $\bar{y}$	Mean values of each of the two groups of samples
s_x, s_y	Standard deviations of each of the two groups of samples (calculated as in equation [18])
ν	Degree of freedom
n, m	Number of values in each of the two groups of samples

Differences of mean values are considered as significant if the calculated t is greater than $t(1-\alpha, \nu)$ in a t-distribution at given significance level α and degree of freedom ν ($1-\alpha = 0.95$, *; $1-\alpha = 0.99$, **; $1-\alpha = 0.999$, ***).

3 Results

3.1 Cycling assay as a reliable method to determine C6 phosphorylation in hydrolysates of polysaccharides

Most plant starches contain small amounts of covalently bound phosphate the majority of which is located at carbon C6 of glucosyl residues. By contrast, C6 phosphorylation is reported to be absent in glycogen (Tagliabracci *et al.*, 2011). Whether or not cytosolic plant heteroglycans contain 6-phospho glucosyl residues has not yet been determined.

Generally, the specific quantification of the C6 phosphorylation is achieved by G6PDH-mediated turnover of G6P after acid hydrolysis of the polysaccharide. This enzymatic reaction yields NADPH which can either be determined photometrically at 340 nm (Lowry and Passonneau, 1972) or it can be coupled to a redox system as in the cycling NAD(P)H assay from Nisselbaum and Green (1969). NADPH concentrations are detected as rates of formazan formation which dramatically increases the sensitivity of the assay (see 1.6.2.2). The principle described by Nisselbaum and Green (1972) was adapted to the 96 well format by Gibon *et al.* (2002) who employed this method for high throughput quantification of metabolites in plant extracts.

When analyzing the C6 phosphorylation in carbohydrates it is reasonable to utilize a very sensitive assay in order to keep the amount of required source material in a practicable range. However, due to the low amount of C6 phosphorylation and consequently the low amount of G6P after acid hydrolysis of the carbohydrate quantification of G6P in hydrolysates of polysaccharides is always conducted at high levels of non-phosphorylated sugars which may affect the enzymatic target reaction. Any effect of those sugars on the G6P quantification would lead to analytical errors and has to be ruled out.

3.1.1 Impact of excess neutral sugars

Hydrolysates of starch and glycogen, both being homoglucans, comprise almost exclusively glucose besides small amounts of the target compound, G6P. In hydrolysates of plant heteroglycans the most abundant sugars are arabinose and galactose with only approximately 1% glucose some of which could be C6 phosphorylated. If present, other phosphorylation sites of glucosyl residues or other phosphorylated sugar residues cannot be detected by the enzymatic assays applied. The impact of sugar excess during G6P determination was investigated using standard solutions of glucose, arabinose, galactose and G6P.

3.1.1.1 Impact of glucose excess on cycling G6P determination

The cycling assay procedure can be divided into three steps: Step 1) G6PDH-mediated turnover of G6P resulting in stoichiometric formation of NADPH, Step 2) alkaline destruction of $NADP^+$ present in Step 1, and Step 3) coupling NADPH retained to a redox system leading to NADPH-depending rates of formazan formation (Figure 3).

Known amounts of G6P were mixed with different amounts of glucose and subjected to the whole cycling assay procedure (Step 1 through 3). NADPH-dependent rates of formazan formation determined in the presence and in the absence of high levels of glucose were compared. Under the assay conditions as described by Gibon *et al.* (2002) glucose amounts ≥1,000 pmol per assay

resulted in rates that massively exceeded those measured in the absence of glucose. The relative impact of glucose on the rates of formazan formation decreases at high G6P concentrations. Thus, correctness of G6P determination was affected by the initial concentrations of both, glucose and G6P (Figure 4A). Under these conditions, quantification of unknown G6P amounts in the presence of more than 1,000 pmol glucose used would lead to tremendous overestimation of G6P, especially when the G6P amount is small. It especially prevents reliable analysis of glucans with low degrees of C6 phosphorylation.

Anderson and Nordlie (1968) described a glucose dehydrogenase activity of G6PDH from yeast. This would result in a glucose-dependent NADPH formation during Step 1 of the cycling assay. To test this possibility the cycling assay was performed with different amounts of glucose that were added after Step 1. The acceleration of formazan formation as described above was only detectable when glucose was present in Step 1 of the cycling assay (Figure 4A and B).

Furthermore, it was examined whether shorter incubation times during Step 1 diminish the effect of glucose. The reduction of incubation time from initially 20 to 10 min is sufficient for complete G6P turnover (tested for up to 40 pmol G6P, see 2.10.3) but resulted in lower glucose-dependent rates of formazan formation (Figure 4C). Thus, the overestimation of G6P at high glucose levels is likely to be caused by the enzymatic side reaction described by Anderson and Nordlie (1968). It seems that the G6PDH-mediated oxidation of glucose (and simultaneous NADPH formation) is promoted in the absence or at low amounts of the preferred substrate (G6P).

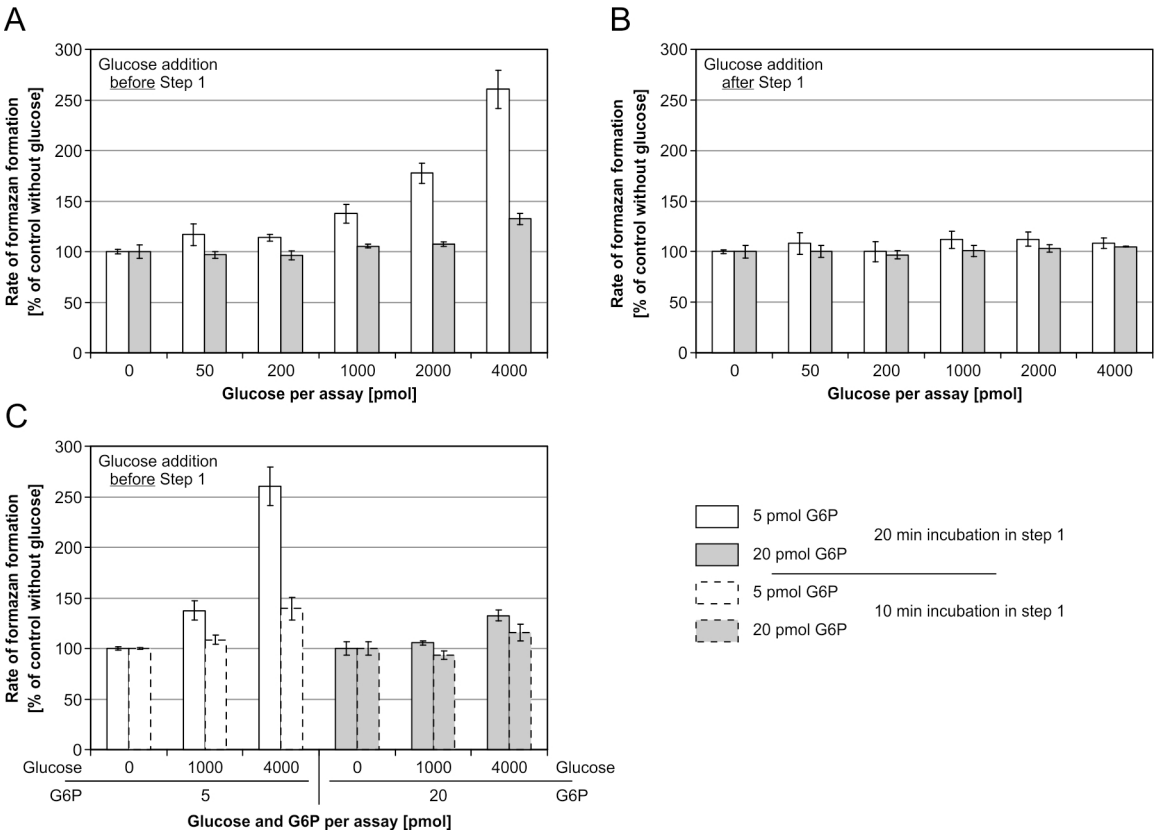

Figure 4. Impact of glucose on the rates of formazan formation in the cycling assay

Two levels of G6P were applied to the cycling assay procedure as described by Gibon *et al.* (2002) using G6PDH from Yeast (Roche, grade II). Rates of formazan formation were determined in the presence of varying amounts of glucose added either before (A) or after (B) Step 1 (Figure 3) of the cycling assay. Glucose increased formazan formation only if present during the enzymatic reaction in Step 1. Reduction of the Step 1 incubation time decreased the impact of glucose present in Step 1 (C). Rates were measured in triplicates (error: SD) and are given as percent of controls where glucose was omitted.

Since the source of the erratic impact of excess glucose on G6P determination is likely the G6PDH-mediated reaction, different commercially available enzyme preparations were tested for their apparent specific glucose dehydrogenase activity. For that purpose the four enzyme preparations used ($G6PDH_{RI}$, $G6PDH_{RII}$, $G6PDH_{RL}$, and $G6PDH_{SL}$; see 2.1.2) were first adjusted to equal G6PDH activities under the conditions of the cycling assay and in the absence of glucose (see 2.10.1). This step was found essential since enzyme activities *in situ* deviated differentially from those as described by the respective supplier. The enzyme preparations applied to the cycling assay were adjusted to 0.043 U (*in situ*).

Subsequently in the absence or in the presence of 5 pmol G6P varying amounts of glucose were applied to the cycling assay using either of the four G6PDH preparations (see above) in Step 1 of the assay. The apparent G6P content was determined by correlating the rates of formazan formation of glucose containing samples to G6P standards lacking glucose. The apparent glucose dehydrogenase activities of the enzyme preparations used differed largely. As an example, the excess of 10 nmol glucose per assay lead in the absence of G6P to rates of formazan formation that mimicked amounts of ca. 3 and ca. 6.5 pmol G6P when using $G6PDH_{RI}$ and $G6PDH_{RII}$, respectively. By contrast, the same excess of glucose resulted in rates of formazan formation indiscernible from those in the absence of glucose when using $G6PDH_{RL}$ and $G6PDH_{SL}$. However, considering all preparations tested in this study $G6PDH_{RL}$ (Roche, Leuconostoc) appears to be most suitable for G6P quantification by the cycling assay (Figure 5).

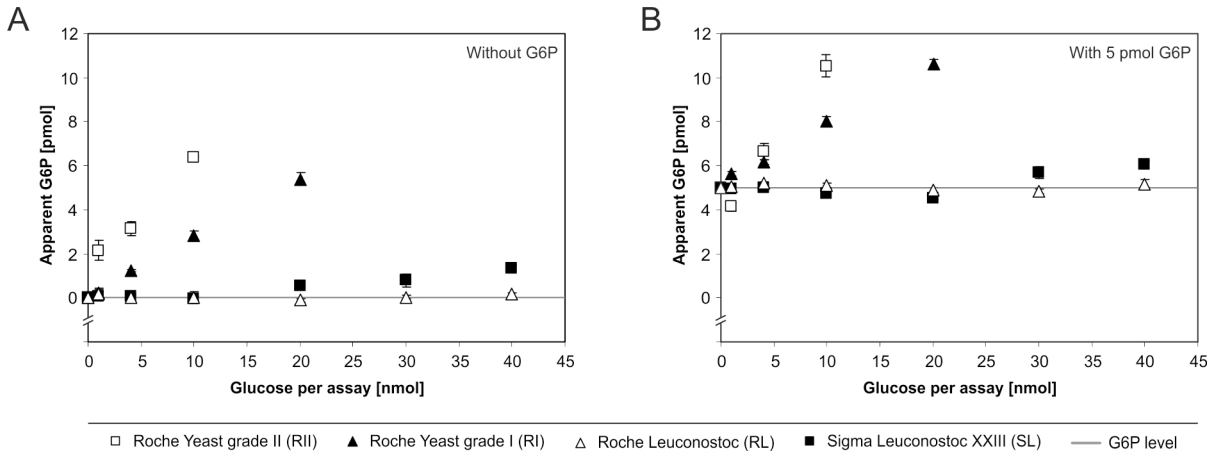

Figure 5. Impact of glucose on cycling assay using different preparations of G6PDH

Apparent glucose 6-phosphate (G6P) levels as measured at increasing glucose levels (up to 40 nmol per assay) using four commercially available G6P dehydrogenase (G6PDH) preparations in Step 1 of the cycling assay (see Figure 3) both in the absence of any G6P (A) and in the presence of 5 pmol G6P (B). All G6PDH preparations were adjusted to 0.043 U under the assay conditions (Step 1). In all assays, G6PDH from *Leuconostoc* (Sigma) was used in Step 3 (see Figure 3). In Step 1, G6PDH from yeast formed significant amounts of NADPH even in the absence of any added G6P. NADPH formation by grade I yeast G6PDH was lower but clearly interfered with G6P measurements in the presence of high glucose. Interference was much lower when using G6PDH from *Leuconostoc*. The enzyme preparation from Roche was superior to that from Sigma. The former G6PDH preparation was most suitable as for all glucose levels tested it did not cause any noticeable glucose-dependent NADPH formation.

While initially the cycling assay (see above) was conducted using $G6PDH_{RII}$ in Step 1 the impact of glucose on the G6P determination could be largely decreased by utilizing another enzyme preparation, namely $G6PDH_{RL}$. In all following cycling assays the amount of glucose was kept below 40 nmol per assay.

3.1.1.2 Impact of arabinose and galactose on G6P determination by using the cycling assay

Quantification of glucosyl C6 phosphate in cytosolic plant heteroglycans relies on the determination of G6P in hydrolysates of the glycans. In the case of cytosolic heteroglycans isolated from *Arabidopsis thaliana* those hydrolysates comprise concentrations of arabinose and galactose that together exceed that of glucose by 10 to 100 fold (Fettke *et al.*, 2006).

The impact of both sugars on the cyclic G6P determination has been studied first by applying mixtures with different amounts of G6P and arabinose or galactose to the complete cycling assay. The resulting rates of formazan formation were compared with respect to the applied amount of excess sugar. Amounts higher than 50 nmol per assay of either arabinose or galactose resulted in increased rates of formazan formation as compared to G6P standards without excess sugar. The relative increase in the rates of formazan formation was highest at low concentrations of G6P which would especially lead to overestimation of small unknown G6P amounts (Figure 6A and B).

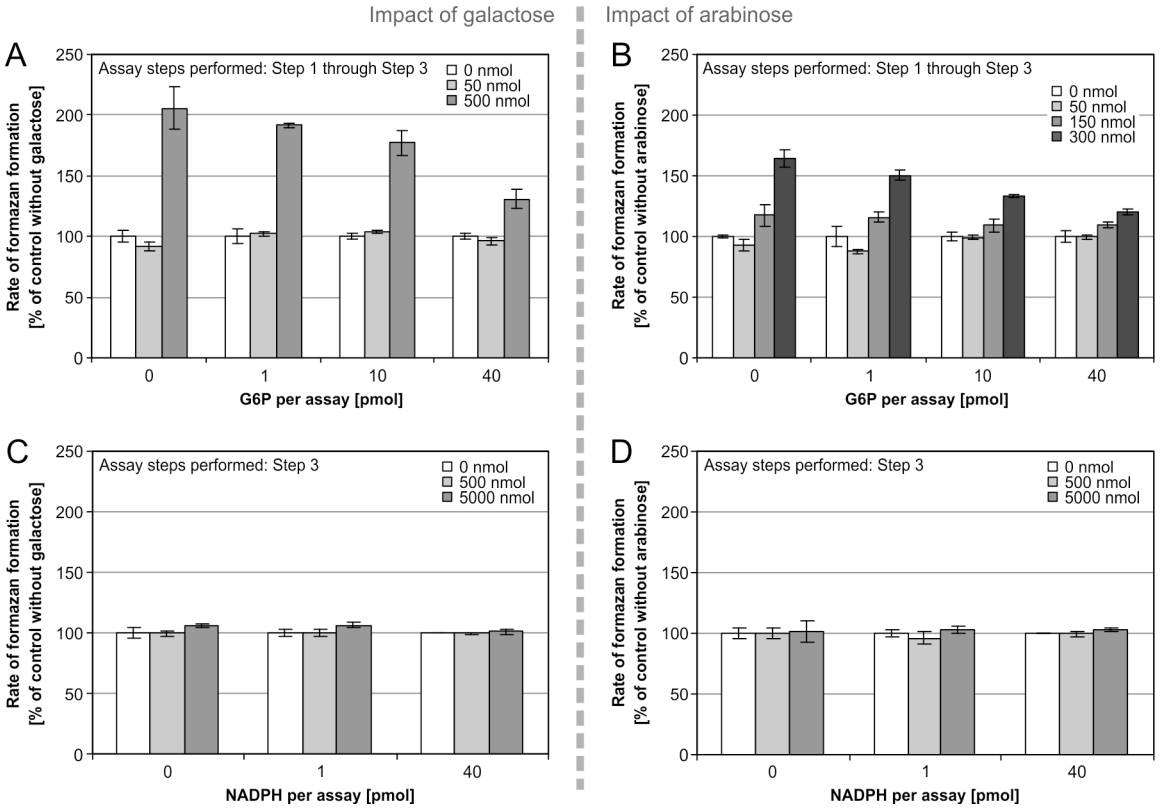

Figure 6. Impact of galactose and arabinose on absorbance rates in the cycling assay

Standards of galactose (A) or arabinose (B) were mixed with different amounts of G6P and subjected to the whole cycling assay procedure (Step 1 through Step 3; see Figure 3). Rates of formazan formation were determined depending on the presence of different amounts of the respective sugar. In the presence of more than 50 nmol of either sugar absorbance rates are increased. The relative acceleration of the rate increases with decreasing amounts of G6P. To investigate the impact of both sugars on the NADPH cycling (Step 3 of the cycling assay; see Figure 3) galactose (C) or arabinose (D) were mixed with NADPH standards and subjected to Step 3 of the assay. Even very high levels of both sugars do not affect the NADPH cycling as judged again by the rate of formazan formation. All rates were measured in triplicates (error: SD) and are given as percent of controls where any neutral sugar was omitted.

It has been examined which step of the cycling assay procedure (Figure 3) is the basis for the erratic effect of high levels of arabinose or galactose. To investigate a putative impact on NADPH cycling in Step 3 (Figure 3), different amounts of NADPH and arabinose or galactose were mixed

and subjected to NADPH cycling in Step 3. During cycling all total volume and concentrations of all assay constituents were similar as when the assay procedure was conducted completely. NADPH-dependent rates of formazan formation were recorded and lacked any effect of authentic arabinose and galactose on NADPH cycling. At this stage it was concluded that excess of both authentic sugars does not influence formazan formation directly. The sugars need to be converted to something (or support the conversion of something) in cycling assay Step 1 or during the $NADP^+$ destruction (Step 2) that later (in Step 3) promotes acceleration of formazan formation.

Conducting the whole cycling assay procedure it was observed that assay mixtures containing very high amounts (5,000 nmol) of galactose or arabinose lead to rapid formazan formation even at 4 °C. 1 min after the addition a mix 3 (containing the constituent for NADPH cycling; see 2.10.2) the optical density at 570 nm in all cases exceeded the value 2; some were even out of the photometer's detection range. However, this rapid darkening effect of both sugars was exploited in a very simple experiment to examine whether galactose leads to G6P-independent NADPH formation during incubation in Step 1. The incubation in Step 1 was carried out either in the presence or absence of 5,000 nmol galactose. Additionally, either one, both, or none of the constituents G6PDH and $NADP^+$ were omitted from the reaction mixture in Step 1. Subsequently the mixtures were subjected to $NADP^+$ destruction at high pH and temperature (Step 2). Following neutralization the mixtures underwent Step 3 (NADPH cycling). All samples that contained galactose immediately turned dark blue irrespective the presence or absence of G6PDH or $NADP^+$ in Step 1 of the cycling assay. Mixtures lacking galactose did not change noticeably (Figure 7A). Hence, the galactose- and arabinose-dependent effect on the formation of formazan is independent of the G6PDH reaction in Step 1.

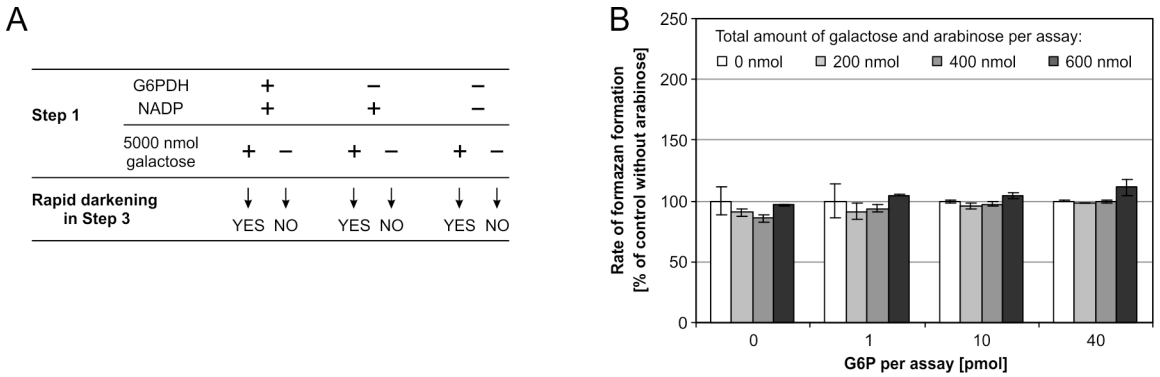

Figure 7. Optimized $NADP^+$ destruction increases galactose and arabinose tolerance of the cycling assay

(A) The complete cycling assay was performed without any G6P but with alterations in the reaction mixture in Step 1 of the cycling assay (Figure 3). Very high amounts of galactose present in Step 1 resulted in rapid darkening of the assay mixture in Step 3 (NADPH cycling; Figure 3) irrespective of the presence of G6PDH and $NADP^+$ in Step 1. This indicates that the impact of galactose on the formazan formation does not rely on G6PDH-mediated NADPH formation in Step 1. Rapid darkening (optical density at 570 nm > 2) occurred at 4 °C within less than 1 min after adding mix 3 (containing the constituents needed for NADPH cycling; see 2.10.2). Mixtures lacking galactose did not noticeably darken. (B) After optimization of Step 2 (alkaline destruction of $NADP^+$ derived from Step 1) the impact of galactose and arabinose on the G6P determination using the cycling assay was determined. Equal amount of both sugars (sum of both indicated as total amount) were mixed with different amounts of G6P, subjected to the whole assay procedure, and rates of formazan formation were determined. All rates were measured in triplicates (error: SD) and are given as percent of controls where any sugar was omitted.

Assay mixtures containing very high amounts of galactose or arabinose tend to develop a slight reddish-brown coloring during the alkaline and heat treatment in Step 2, indicating chemical reactions under these conditions in the presence of the sugars excess. Products of these chemical

reactions could be the reason for the higher rates of formazan formation. The alkaline and heat treatment is essential for destruction of $NADP^+$ prior to NADPH cycling. Conducting the cycling assay for quantification of metabolites Gibon *et al.* (2002) added a defined amount of 0.5 M NaOH to the assay mixtures and incubated 5 min at 100 °C. To achieve higher tolerance of the cycling assay for galactose and arabinose while maintaining $NADP^+$ destruction sufficient attempts were made to optimize the alkaline treatment. Tthe parameters length of treatment and concentration of sodium hydroxide applied were altered while volume and temperature remained as described in Gibon *et al.* (2002). The combination of 3 min incubation with 0.1 M sodium hydroxide fulfilled the need for completeness of $NADP^+$ destruction and NADPH conservation. This was observed by strictly linear correlations between G6P added to Step 1 and the resultant rates of formazan formation. The coefficient of determination R^2 was consistently above 0.995. Furthermore, the alterations in Step 2 decreased the arabinose- and galactose-dependent impact on the rates of formazan formation and, thus, enabled the reliable detection of G6P in cytosolic plant heteroglycans unless the combined amount of arabinose and galactose exceeded 400 nmol (Figure 7B). However, the modifications in Step 2 seemed to result in slightly increased deviation between technical replicas. Therefore, the modified Step 2 was exclusively used when samples were analyzed that contained high amounts of galactose and arabinose such as in hydrolysates of the plant heteroglycans.

3.1.2 Improving the sensitivity of G6P determination by the cycling assay

The reliability of the quantification of very low amounts of G6P in hydrolyzed glycans is determined by two factors: 1) the maximum amount of carbohydrate that can be applied to the assay without erratic side effects of highly abundant neutral sugars, and 2) the minimum G6P amount that can be reliably detected (detection limit). For the cycling G6P assay the first factor has been addressed above. The maximum amount of carbohydrate per assay was substantially increased in the case of both homoglucans (relevant for glycogen and starch) and heteroglycans. The second factor, however, is equally essential and was the objective of the optimization described below.

Considering quantification of analytes the detection limit is determined by the sensitivity and the precision of a method. For the cycling assay the change of the rate of formazan formation per mol G6P (or NAD(P)H) would be a good measure of sensitivity, while the deviation of technical parallels reflects the cycling assay's precision. The following optimizations aimed both to increase the NAD(P)H-dependent rate of formazan formation and to decrease the deviation of technical parallels.

In Step 3 of the cycling assay NAD(P)H is coupled to a chain of redox reactions. The rate of formazan formation is depending on the steady-state concentration of NAD(P)H which is determined by two chemical reactions: 1) NAD(P)H oxidation during the reduction of PMS, and 2) $NAD(P)^+$ reduction by G6PDH-mediated G6P oxidation (recycling). For instance at a given amount of G6P in Step 1 of the cycling assay the highest rate of formazan formation (highest sensitivity) is, thus, achieved when recycling of the reduced coenzyme is maximal.

Two commercial preparations of G6PDH were tested for effectiveness of coenzyme recycling. Both were from *Leuconostoc* and used either NAD^+ or $NADP^+$ as coenzyme. First, solutions were prepared that contained varying amounts of NADH and all constituents present in a reaction mixture that underwent Step 1 and 2 of the cycling assay. Mix 3 (see 2.10.2) was added to couple

the NADH with the chain of redox reactions. For both commercial G6PDH preparations, rates of formazan formation were recorded using different enzyme amounts per assay either in the presence or absence of 40 pmol NADH (highest amount of standard used for the cycling assay). The difference between rates of formazan formation recorded in the absence and in the presence of NADH is a measure of recycling effectiveness and, hence sensitivity of coenzyme determination (Figure 8A). Using low amounts of enzyme the preparation from Roche ($G6PDH_{RL}$; see 2.1.2) resulted in much higher rate differences as compared to the Sigma preparation ($G6PDH_{SL}$; see 2.1.2).

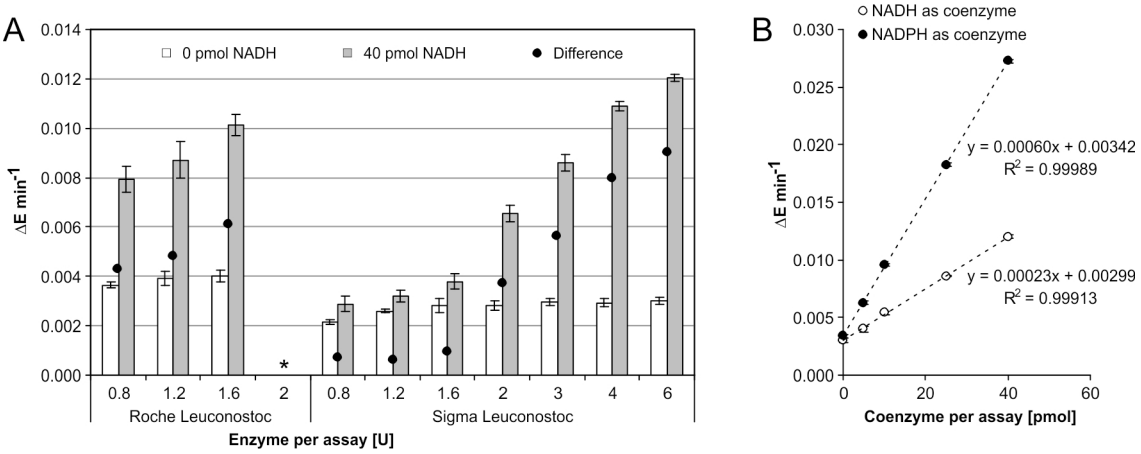

Figure 8. G6PDH concentration and type of coenzyme affect sensitivity of NAD(P)H cycling

(A) NADH-dependent rates of formazan formation were determined using preparations of *Leuconostoc* G6PDH from Roche ($G6PDH_{RL}$) or Sigma ($G6PDH_{SL}$). In the presence of different enzyme amounts per assay rates were measured either in the absence of NADH or with 40 pmol of the coenzyme. The rate difference was calculated as a measure of sensitivity. (*) Amounts of the Roche enzyme higher than 1.6 U resulted in strong formazan formation in mix 3 containing all constituents for NAD(P)H cycling even in the absence of any coenzyme and when stored at 4 °C (see text). (B) In the presence of 6 U $G6PDH_{SL}$ rates of formazan formation were determined dependent of the amount of either NADH or NADPH. Rates are strictly dependent of the coenzyme amount applied to cycling as judged by coefficients of determination (R^2) after linear regression (equations given). All rates (in A and B) were measured in triplicates (error: SD).

G6PDH from Roche could not be added to the mixture (Step 3) more than 1.6 U per assay as preparations of mix 3 (see 2.10.2), which contained the enzyme and all constituents for coenzyme cycling, became unstable. Even when stored on ice and in the absence of any NADH, mix 3 containing 2 U per assay rapidly darkened indicating a coenzyme-independent formazan formation. By contrast, the amount of *Leuconostoc* G6PDH form Sigma could be raised up to 6 U per assay without affecting the stability of mix 3 preparations. Furthermore, the rates of formazan formation in the absence of coenzyme were consistently smaller when using the G6PDH preparation from Sigma, and higher G6PDH concentrations did not result in significantly increased rates. Using 6 U of the Sigma enzyme preparation per assay, the rates of formazan formation in the presence of NADH exceeded those using the highest possible amount of the Roche enzyme. This resulted in an increased sensitivity of coenzyme determination as judged by the rate difference between measurements in the presence or in the absence of NADH (Figure 8A).

Since the *Leuconostoc* G6PDH preparation from Sigma ($G6PDH_{SL}$) can reduce both coenzymes (NAD^+ and $NADP^+$) it was examined whether selection of coenzyme has an effect on the concentration-dependent rate of formazan formation and, hence, on the sensitivity in Step 3 of the cycling assay. Solutions were prepared containing varying amounts of either of the two coenzymes

and buffer identical to that of reaction mixtures (Step 1 and 2) of the cycling assay. After the addition of mix 3 containing 6 U $G6PDH_{SL}$ the rates of formazan formation were determined. The sensitivity, measured as the coenzyme concentration-dependent rate of formazan formation, was approximately 2.6 fold higher when NADPH was used as coenzyme (Figure 8B).

In addition attempts were made to improve linearity of absorbance recorded during formazan formation. Linear parts of the absorbance time curves served for calculation of the rates of formazan formation. With number of values in the linear part of the curve the reliability of the determined rates (and consequently the quantified amounts of analyte) increases. Absorbance curves recorded as described by Gibon *et al.* (2002) exhibited a flattening increase at the end of the recording and occasionally even strong fluctuations of the absorbance which is due to the precipitation of insoluble formazan. By the addition of BSA to mix 3 and by increasing the volume of mix 3 that is added for NADPH cycling in Step 3 of the cycling assay, the time-dependent absorbance change was largely constant for at least 2 hours. Even high concentrations of NADPH during Step 3 did not result in formazan precipitation (Figure 9).

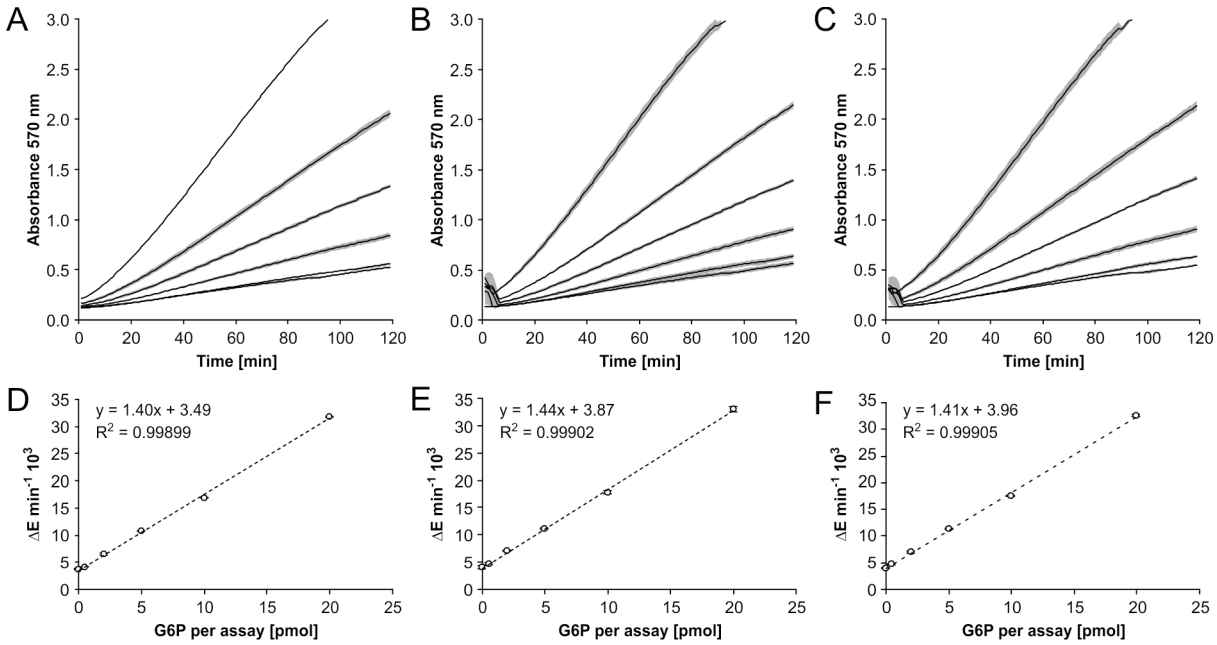

Figure 9. Formazan formation as measured during G6P determination using the optimized cycling assay

G6P standards were subjected to the complete and optimized cycling assay procedure (Step 1 through 3). Formazan formation in Step 3 is photometrically measured at 570 nm. Absorbance curves were determined in 3 individual experiments (A, B, C) with 3 technical replicas for each G6P amount (n in pmol). Mean absorbance values at each time point were calculated from technical replicas (SD depicted as *grey shadow*). Rates of formazan formation in (A), (B) and (C) were determined and plotted in (D), (E) and (F), respectively, against the G6P amount applied in Step 1 of the cycling assay. Rates were determined separately for each technical replica and mean values as well as SD were calculated subsequently. Note, that due to small rate deviations SD is sometimes imperceptible. Calibration curves and equations were determined by linear regression. Irregularities in absorbance within the first 10 min of formazan formation detection (B and C) occasionally occur when complete 96 well plates are transferred from a cold room (4 °C) to the plate reader (30 °C ambient temperature) due to water condensation on the well bottom.

In order to increase the precision of the cycling assay by smaller deviations of the rates of formazan formation in technical replica an additional pH-related step was introduced to the assay procedure. According to the method described by Gibon *et al.* (2002) G6P standards or samples are immediately incubated with $NADP^+$ and G6PDH, yielding NADPH which is subsequently coupled to the redox chain in Step 3 after destruction of excess $NADP^+$ in Step 2. The alteration of this procedure comprises the separate addition of buffered $NADP^+$ (mix 1; see 2.10.2) to standards and

samples followed by short equilibration at room temperature. Subsequently mixtures are subjected to an acid treatment at 30 °C (see 2.10.3) followed by neutralization. Only then mix 2 (see 2.10.2) containing G6PDH is added and the turnover of G6P is executed. The acid treatment prior to enzymatic G6P turnover significantly reduces the average standard deviation of technical replica by (ca. factor 2.6). The effect is likely caused by the destruction of contaminations of NADPH that are derived from the $NADP^+$ preparation and that are differentially preserved when the $NADP^+$-containing buffer is added to different replica of the same sample or standard.

After optimizing precision and sensitivity of the cycling assay, formazan formation measured as absorbance-time curves in Step 3 of the cycling assay is exemplarily shown in Figure 9. At given amounts of G6P (applied in Step 1 of the cycling assay) absorbance curves exhibited very small deviations in the rates of formazan formation which allowed detection of G6P amounts as small as at least 0.5 pmol.

Moreover, sensitivity of the cycling assay was highly reproducible as observed by the similar calibration curves of independent measurements (Figure 9D through F). This was achieved by the development of a new method for preparation of mix 3, which contains all constituents for NAD(P)H cycling (PMS, MTT, EDTA, BSA, G6P, G6PDH). As already noted by Nisselbaum and Green (1969) the complete mix 3 is only stable for a few hours and needs to be prepared freshly for each measurement. That is time consuming, and variations of mix 3 constitution between independent preparations are almost inevitable. However, mix 3 can conveniently be prepared from 2 stock solutions that are combined and mixed with G6PDH immediately before measurement (see 2.10.2). One of the stock solutions contains PMS that is dissolved in EDTA-containing buffer. The other contains G6P, MTT and BSA. Both stock solutions, frozen in liquid nitrogen and stored at -80 °C until use, are stable for at least 6 month as they do neither show any noticeable change in color nor deficiency in NAD(P)H cycling.

3.2 The cycling assay as a versatile method for metabolite quantification

Cycling assays can be used to quantify any analyte that can enzymatically be converted under stoichiometric NAD(P)H formation. Figure 10 exemplarily displays procedural schemes for enzymatic quantification of glucose, glucose 1-phosphate, and fructose 6-phosphate using NADPH cycling. When G6P is quantified as metabolite a cycling assay can be used as described for the measurement of G6P in hydrolysates of carbohydrates.

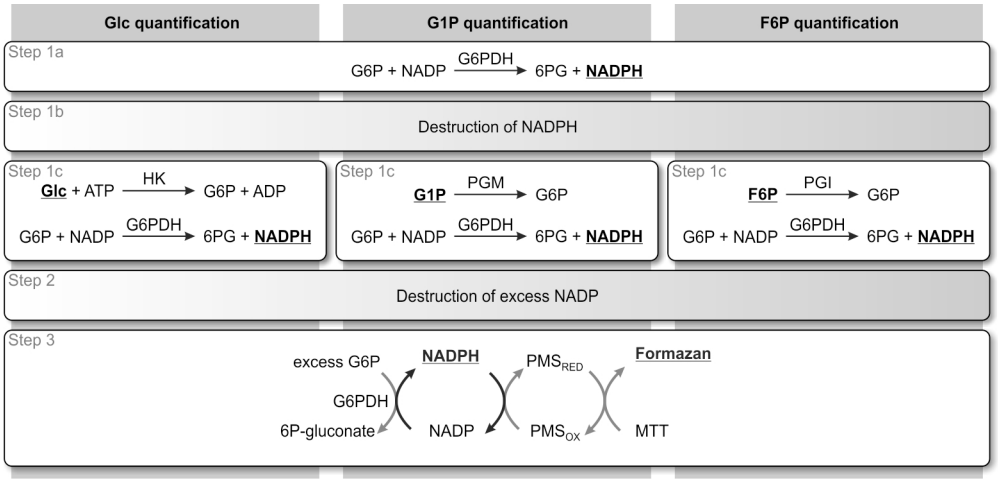

Figure 10. Schemes for determination of metabolites using a cycling assay

Metabolites such as glucose (Glc), glucose 1-phosphate (G1P), and fructose 6-phosphate (F6P) can be determined with high sensitivity using a variant of the cycling assay depicted in Figure 3. The presence of G6P in a sample would also lead to NADPH formation and would therefore interfere with the quantification of either metabolite. In a first incubation (Step 1a) G6P has to be enzymatically converted by G6PDH. NADPH formed during this reaction is destroyed by acid treatment (Step 1b). Subsequently the respective metabolite is enzymatically converted to G6P which, utilizing G6PDH, leads to NADPH formation equimolar to the amount of initial metabolite (Step 1c). After destruction of excess $NADP^+$ deriving from Step 1, NADPH is coupled to the cycling reactions (see Figure 3) resulting in rates of formazan formation that depend on the amount of NADPH formed in Step 1c and can, thus, be correlated with the amount of initial metabolite. HK – hexokinase, PGM – phosphoglucomutase, PGI – phosphoglucoisomerase, 6PG – 6-phosphogluconate, see also list of abbreviations.

A cycling assay procedure was established for G1P quantification in leaf extracts from *Arabidopsis thaliana* ecotype Columbia. A commonly used method for extraction of sugar phosphates with perchloric acid (Stitt *et al.*, 1989) was used and performed by Dr. Irina Malinova.

G1P and G6P were separately quantified in extracts of 6 biological parallels using an enzymatic assay either with conventional NADPH detection at 340 nm or with additional NADPH cycling as described in Figures 3 and 10, respectively. In both G1P assays G6P present in the sample has to be completely converted to 6-phosphogluconat by G6PDH. In the conventional method NADPH formation is monitored during G6P conversion. After completion of G6P conversion the NADPH concentration is constant. Subsequently phosphoglucomutase is added which converts G1P to G6P. Utilizing again G6PDH, NADPH is formed equimolar to initial G1P. Using the cycling assay complete G6P conversion is ensured by incubation in Step 1a (Figure 10) for 30 min. The resulting NADPH is destroyed by acid treatment (Step 1b) before NADPH is formed following the conversion of G1P to G6P in Step 1c. Unknown G1P amounts are calculated using a calibration curve with authentic G1P as exemplarily depicted in Figure 11A.

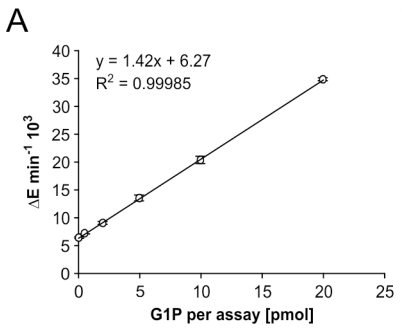

C

Minimum amount required	Conventional assay	Cycling assay
G6P and G1P per assay	3 nmol	0.5 pmol
FW per G6P assay	30 mg	5 µg
FW per G1P assay	300 mg	50 µg

Figure 11. Quantification of G1P and G6P in leaf extracts of *Arabidopsis thaliana*

(A) Several amounts of authentic G1P were applied to the respective cycling assay procedure depicted in Figure 10. Calibration curves are derived by plotting rates of formazan formation against the amount of G1P per assay. One representative measurement is shown (mean of 3 technical replicas, error: SD). (B) In leaf extracts of 6 biological parallels G6P and G1P were determined either with an adequate cycling assay or using the conventional enzymatic assay with NADPH detection at 340 nm. During both cycling assays rates of formazan formation were recorded for equally treated standards and samples that simultaneously underwent the assay procedure. Standards (3 technical replicas) served for calibration and unknown sugar phosphate amounts in samples were calculated and subsequently based on fresh weight (FW). Error: SD (n = 6). (C) Comparison of fresh weight consumption using the conventional and the cycling assay for either G6P or G1P quantification. The minimum amounts of sugar phosphate required are based on the molar absorptivity of NADPH (conventional assay, 6.300 M^{-1} cm^{-1}) and on the lowest standard amount used in the cycling assay. Required fresh weight per assay is calculated using 0.1 and 0.01 µmol per gramm fresh weight for G6P and G1P, respectively.

Essentially the same fresh weight-based levels of both G6P and G1P are obtained by both methods (Figure 11B) but the cycling assay requires only very small amounts of fresh weight per assay (Figure 11C). For instance using the cycling assay, quantification of G1P was performed utilizing

extract volumes equivalent to ca. 1.5 mg fresh weight, and G1P amounts measured exceeded the lowest G1P standard (0.5 pmol per assay) by 30 fold. For conventional G1P determination at least 100fold higher amounts of fresh weight were used, and the G1P amounts measured were at the limit of detection. This difference may be also relevant if a compound is quantitatively extracted more easily when using small amounts of tissue.

A cycling assay was established for glucose quantification with high sensitivity. This enabled precise determination of glucose even if the analyte is limited. In the case of heteroglycans prepared from *Arabidopsis thaliana* leaves glucosyl residues account only for a small proportion of the monomers. The amount of heteroglycans per fresh weight is much lower than that of starch. Thus, analyses of the glucosyl content in plant heteroglycans are immensely facilitated by highly sensitive methods. According to Figure 10 glucose is converted to G6P by hexokinase in the presence of ATP. The stoichiometric amount of NADPH formed is coupled to redox reactions as described in Figure 3 and 10. Step 1a in Figure 10 removes G6P from the sample that could interfere with the glucose determination. If this step is omitted glucosyl residues are determined irrespective whether they are phosphorylated in C6. Glucose standards that are subjected to the adequate cycling assay lead to rates of formazan formation that strictly correlate to the amount of standard applied per assay (Figure 12A).

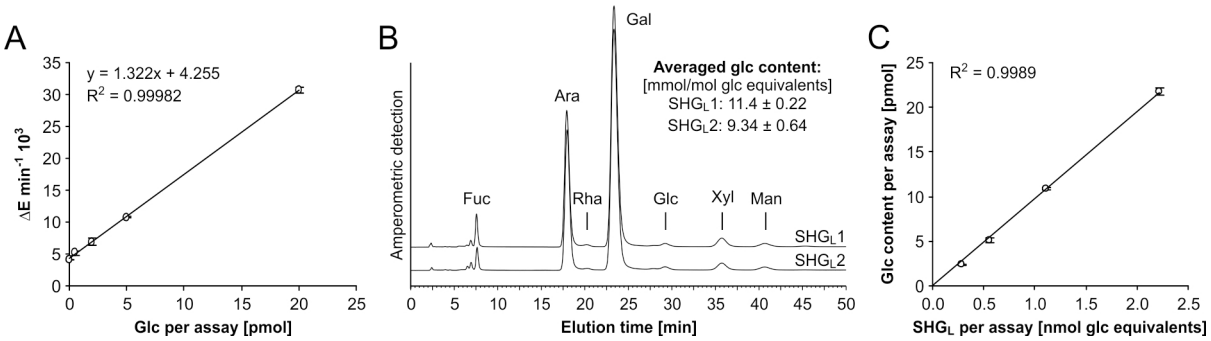

Figure 12. Glucose determination in plant heteroglycans using the cycling assay

(A) Several amounts of authentic glucose (Glc) were applied to the respective cycling assay procedure depicted in Figure 10. Calibration curves are derived by plotting the rates of formazan formation against the amount of glucose per assay. One representative is shown (mean of 3 technical replicas, error: SD). (B) Monosaccharide patterns two individual preparations of SHG_L (1 and 2). The latter were subjected to acid hydrolysis followed by the application of 5 µg each to the column utilizing separation mode 0 (see 2.16). Monosaccharides were identified using authentic standards (Fuc – fucose, Ara – arabinose, Rha – rhamnose, Gal – galactose, Xyl – xylose, Man – mannose). The cycling assay was used to quantify the amount of glucose (mean of 3 technical replicas, error: SD) based on glucose equivalents as determined by a reducing ends test. (C) Different amounts of SHG_L2 were applied to the cycling assay and revealed a strictly linear correlation between carbohydrate applied to the assay and glucose determined as judged by coefficients of determination (R^2) after linear regression (graphs given). For each SHG_L amount triplicates were measured (error: SD).

Heteroglycans were isolated from *Arabidopsis thaliana* leaves harvested from two individually grown batches of plants. The total heteroglycans (SHG_0) were prepared according to Fettke *et al.* (2004) and were subjected to ultrafiltration. SHG_L (> 10 kDa) was recovered and subject of further analyses. After acid hydrolysis (procedure B1) the amount of carbohydrate was estimated by determination of reducing ends. Since for calculation a calibration curve is used that derived from glucose standards, carbohydrate amounts are given as glucose equivalents (see 2.8). The monosaccharide patterns of the two individual SHG_L preparations (SHG_L1 and SHG_L2) were analyzed by HPAEC-PAD (Figure 12B). As shown in a previous publication (Fettke *et al.*, 2005a) galactose and arabinose are the major monomers while especially glucose is only a small

proportion. To determine the exact amount of glucosyl residues aliquots of the hydrolyzed SHG_L fractions were subjected to the cycling assay. In both preparations glucose accounted for ca. 1% of the carbohydrate (Figure 12B). Furthermore, the detected amount of glucose was strictly depending on the amount of SHG_L subjected to the assay as observed when different amounts of the same hydrolysate were applied. This indicates that the rates of formazan formation measured are exclusively dependent of the amount of glucose initially applied to the assay.

3.3 Quantification of glucosyl 6-phosphate quantified in polysaccharides

The cycling assay has been established and optimized for reliable quantification of G6P in hydrolysates of polysaccharides (see 3.1). Subsequently the assay was used to quantify glucosyl 6-phosphate in *Arabidopsis thaliana* heteroglycans as well as in starch and glycogen isolated from various sources.

3.3.1 Heteroglycans from leaves of *Arabidopsis thaliana*

The >10 kDa fraction of heteroglycans (SHG_L) isolated from *Arabidopsis thaliana* leaves contains only a small proportion of glucosyl residues (see Figure 12B; Fettke *et al.*, 2005a). If glucosyl residues exist that carry a phosphate at carbon C6 (6-phosphoglucosyl residues) these residues are likely to represent only a fraction of all glucosyl residues. To be able to measure G6P with the cycling assay comparably high amounts of hydrolyzed carbohydrate have to be applied to the assay which results in very high concentrations of arabinose and galactose in the assay mixture. The impact of these neutral sugars was analyzed and the assay procedure was altered for determination of G6P in the presence of up to 400 nmol arabinose and galactose per assay (see 3.1.1.2). When hydrolysates of heteroglycans were applied to the cycling assay it was ensured that the total amount of carbohydrate per assay was below this limit.

Two individual preparations of heteroglycans (SHG_L1 and 2) were subjected to acid hydrolysis (procedure B1) and various amounts of carbohydrate were applied to the cycling assay. Rates of formazan formation where recorded and G6P amounts calculated using a calibration curve derived from G6P standards that underwent the assay procedure simultaneous with the hydrolysates. Determined amounts of G6P were proportional to the amount of carbohydrate applied to the assay. This correlation was very similar in both SHG_L preparations and ruled out an overestimation of G6P at higher concentrations of arabinose and galactose (Figure 13A).

As the SHG_L is obtained as the retentate after extensive ultrafiltration (cut-off 10 kDa) G6P was at the limit of detection when acid hydrolysis was omitted indicating that the measured G6P is derived from 6-phosphoglucosyl residues of the heteroglycans.

After quantification of glucosyl residues in both SHG_L preparations (see Figure 12) the glucose-based amount of glucosyl 6-phosphate was calculated independently for each preparation and carbohydrate amount applied to the G6P assay (Figure 13B). In both independent preparations of SHG_L the glucose-based amount of glucosyl 6-phosphate is very similar at different levels of applied carbohydrate, ranging from 2.5 to 3 (SHG_L1) and 3.25 to 3.6 (SHG_L2) mmol per mol glucose, respectively. The slight difference between both preparations reflects small variations in the amount of glucosyl residues in both carbohydrate preparations (see Figure 12B).

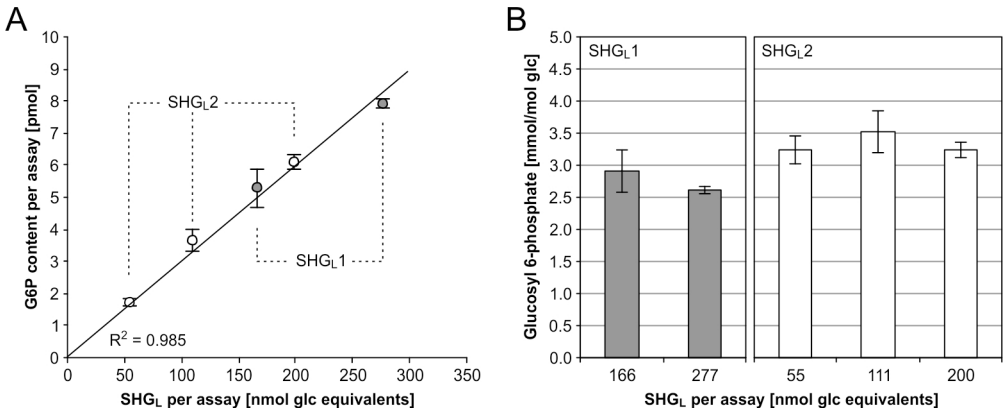

Figure 13. G6P determination in hydrolysates of plant heteroglycans using the cycling assay

(A) Heteroglycans preparations independently isolated from *Arabidopsis thaliana* leaves were subjected to acid hydrolysis and various amounts of carbohydrate (determined as glucose equivalents using a reducing ends test, see 3.2) were subjected to a cycling assay for G6P determination as described in 3.1.1.2. G6P amounts per assay are calculated after calibration with G6P standards that underwent the cycling assay simultaneous with the samples. Measured G6P per assay is plotted against the carbohydrate applied to the assay and proves to be proportional to the amount of carbohydrate. For illustration linear regression was performed (graph and coefficient of determination R^2 displayed) including the measurements of both preparations (SHG$_L$1 and 2). All G6P determinations were done in triplicates (error: SD). (B) For each carbohydrate amount applied in (A) glucose-based glucosyl 6-phosphate is calculated. The amount of glucosyl residues in SHG$_L$1 and 2 were 11.4 and 9.34 mmol per mol glucose equivalent, respectively (see Figure 12B).

According to the data presented here approximately 3 out of 1,000 glucosyl residues of the heteroglycan SHG$_L$ fraction carry a monophosphate ester at carbon C6. The glucose-based amount of glucosyl 6-phosphate is comparable to that of potato tuber starch and, hence, comparably high (see 1.2.2). Since glucosyl residues in SHG$_L$ account for only around 1% of all monomers the monomer-based amount of glucosyl 6-phosphate is very small. However, this does not exclude a physiological role of phosphate in heteroglycans. Since most of the glucosyl residues of SHG$_L$ are part of the cytosolic subfraction (Fettke *et al.*, 2005a) it is likely that cytosolic enzymes exist mediating phosphorylation of cytosolic heteroglycans.

3.3.2 Starch from various botanical sources

3.3.2.1 Commercial starch

Potato starch was obtained from Sigma and used for validation of the C6 phosphate quantification by the cycling assay optimized as described in 3.1.1.1. In two individual experiments 30 mg of starch were extracted twice with 80% ethanol under continuous agitation at 80 °C to remove any soluble low molecular weight contaminants. Subsequently the starch was washed with cold water, dried, and subjected to acid hydrolysis (procedure B1). In the resultant hydrolysate glucose concentration was determined using the conventional enzymatic assay according to Lowry and Passonneau (1972). NADPH was photometrically determined at 340 nm and the NADPH concentration was calculated using a molar absorptivity of 6,300 M^{-1} cm^{-1}. G6P was determined in the hydrolysate using both the enzymatic cycling assay and the conventional enzymatic assay.

Varying amounts of the hydrolyzed starch were applied to the cycling assay procedure (see Figure 3) along with equally treated G6P standards which served for calibration in order to calculate G6P amounts in hydrolysates from rates of formazan formation. In both individual experiments G6P amounts detected per assay showed a strictly linear correlation with the amount of starch applied to the assay over the whole range of G6P detection (0 to 40 pmol per assay; Figure 14A).

For each starch amount applied the glucose-based C6 phosphate was calculated the average of which is given in Figure 14B. The presented data show that starch C6 phosphate is reliably quantified using the cycling assay as C6 phosphate values determined with the cycling are indiscernible from those of the conventional method (Figure 14B).
However, due to high sensitivity of the cycling assay the required amount of starch for reliable determination is at least 3 orders of magnitude smaller.

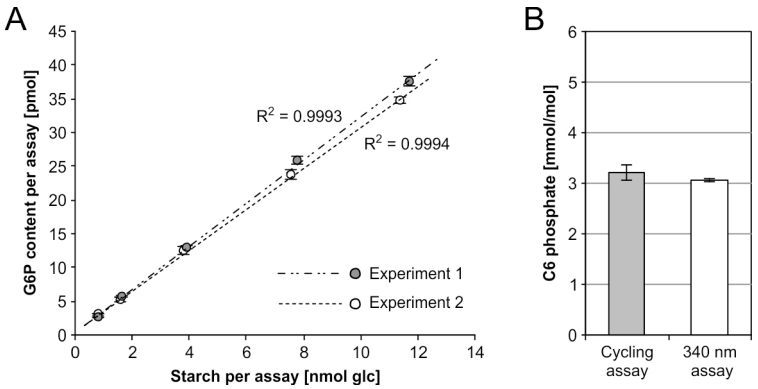

Figure 14. C6 phosphate determination in commercial starch using the cycling assay
Commercial potato tuber starch was subjected to acid hydrolysis after extraction with 80% ethanol to remove soluble contaminations. Different amounts of starch derived from either of two individual experiments were subjected to the cycling assay optimized as described in 3.1.1.1. (A) G6P content per assay was calculated after calibration with simultaneously processed G6P standards and plotted against the amount of starch applied to the assay. For each starch amount applied 3 technical replicas were measured (Error: SD). Linear correlation is illustrated by linear regression (graph and coefficient of determination shown). (B) Averaged glucose-based C6 phosphate as calculated from the values in (A) are compared to values determined by the conventional method with NADPH detection at 340 nm (averaged value of all technical replicas in two experiments).

3.3.2.2 Starch from *Arabidopsis thaliana* leaves and *Curcuma* rhizomes

Native starch was isolated from *Curcuma* rhizomes as well as from leaves of *Arabidopsis thaliana* including both wild type and mutant plants lacking GWD (encoded by the gene *sex1*; line *sex1-8,* Ritte *et al.*, 2006) the enzyme phosphorylates amylopectin specifically at glucosyl carbon C6. While *Curcuma* starch is known to possess relatively high amounts of C6 phosphate (see 1.2.2) it is almost lacking in starch from GWD-deficient *Arabidopsis* plants (Ritte *et al.*, 2006; see 1.5.1).
Aliquots of the starches were hydrolyzed using two hydrolysis conditions. For determination of total phosphate all phosphate esters were hydrolyzed using procedure A. For determination of C6 phosphate hydrolysis procedure B2 was used which maintains phosphate esters at glucosyl C6 (Haebel *et al.*, 2008). In the hydrolysate of procedure A orthophosphate was determined by the malachite green assay. C6 phosphate was determined as G6P in the hydrolysate of procedure B2 using the cycling assay. As shown in Table 7 *Curcuma* starch possesses the most covalently bound phosphate, around 70% of which are bound at glucosyl C6. Wild type *Arabidopsis* leaf starch contains almost 10 times less phosphate than *Curcuma* starch. However, the ratio of C6 to total phosphate is similar in both starches. The lowest amount of total phosphate was detected in transitory starch of *sex1-8* plants. Even using the sensitive cycling assay C6 phosphate was consistently below the limit of detection even when maximal amounts of starch (equivalent to 40 nmol glucose per assay; see 3.1.1.1) were applied to the assay.

The values determined for both total phosphate and C6 phosphate in the respective starch concur with data previously published (see 1.2.2; Ritte *et al.*, 2006). Furthermore, the optimized cycling assay (see 3.1.1.1) does not show false positive results due to G6P overestimation at high glucose concentrations as is the case when starch hydrolysates of *sex1-8* plants are applied to the cycling assay.

Table 7. Total phosphate content and C6 phosphate of starch from Curcuma and *Arabidopsis*

Total phosphate content was determined by the malachite green assay following exhaustive acid hydrolysis (procedure A) of the starch. C6 phosphorylation was determined as G6P by a cycling assay after acid hydrolysis of glucosidic bonds (procedure B2). Mean values ± SD are given (n - number of biological replicas). n.d. - below the limit of detection.

Biological source	Glucose-based total phosphate [mmol/mol]	Glucose-based C6 phosphate [mmol/mol]	C6 phosphate as fraction of total phosphate [%]
Curcuma longa rhizome *wild type*	11.02 ± 0.56 (n = 6)	7.73 ± 0.14 (n = 4)	70.2
Arabidopsis thaliana leaves *wild type*	1.31 ± 0.14 (n = 4)	0.86 ± 0.18 (n = 6)	65.5
Arabidopsis thaliana leaves *sex1-8*	0.24 ± 0.08 (n = 3)	n.d. (n = 4)	n.d.

3.3.2.3 Starch from *Chlamydomonas reinhardtii*

One convenience of the sensitive cycling assay is the possibility of experiments with high temporal resolution. When starch phosphate is to be examined, utilization of the conventional method for G6P determination necessitates the isolation of sufficient amounts of starch from plant material that has usually been pooled before isolation. The consumption of plant material is, thus, very high when samples sufficient in size are taken in high number for temporal analysis of starch phosphate. As an example for the suitability of the cycling assay in experiments with high temporal resolution C6 phosphate in starch of a cell wall-deficient line of *Chlamydomonas reinhardtii* is monitored over time. The unicellular alga is cultured under photoautotrophic conditions with a strict light-dark-cycle. This and daily dilution to a defined cell density induces synchronization and, thus, increases homogeneity of the cell culture because each cell has permanent access to all nutrients and is exposed to similar illumination.

For one experiment aliquots were withdrawn from the same algae suspension and immediately brought to 5% acetic acid to stop any cellular enzymatic activity. Samples were taken from 4 hours before the beginning of the dark phase (light/dark switch) to 2 hours within the dark phase, temporal resolution being increased in the vicinity of the light/dark switch. Two independent experiments were performed. After isolation the native starch was subjected to acid hydrolysis (procedure B1) and quantified as glucose using the conventional enzymatic assay (Lowry and Passonneau, 1972; see 2.9). The cycling assay was used to determine C6 phosphate at each time point in both experiments.

In the algae suspension starch content as well as that of C6 phosphate increase in the light phase indicating that phosphate is indeed incorporated during starch synthesis as previously stated (Nielsen *et al.*, 1994; Ritte *et al.*, 2004). However, while the amount of starch reaches maximum right at the end of the light phase declining in the first hours of the dark phase, C6 phosphate is still increasing after the light/dark switch, reaching its maximum in the dark phase (Figure 15A). This is reflected by the slight increase of glucose-based C6 phosphate at the beginning of the dark

phase (Figure 15B) possibly caused by phosphorylation of the starch surface during the initialization of starch degradation (see 1.5.1). The overall change of the glucose-based C6 phosphate during the monitored time period is, however, relatively small ranging between 0.45 and 0.55 mmol/mol. While starch phosphorylation is apparently necessary for functional starch turn-over, including starch degradation and synthesis, the steady state level of phosphate in starch seems rather invariant over time.

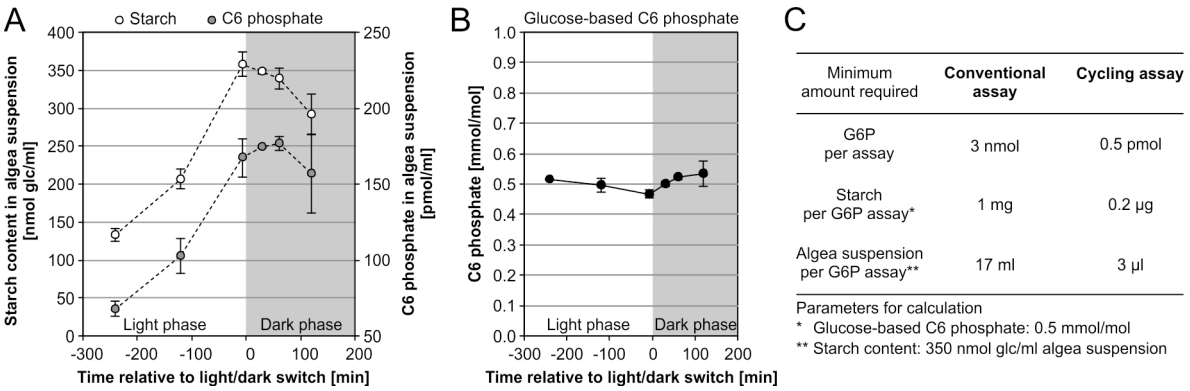

Minimum amount required	Conventional assay	Cycling assay
G6P per assay	3 nmol	0.5 pmol
Starch per G6P assay*	1 mg	0.2 µg
Algea suspension per G6P assay**	17 ml	3 µl

Parameters for calculation
* Glucose-based C6 phosphate: 0.5 mmol/mol
** Starch content: 350 nmol glc/ml algea suspension

Figure 15. Starch and C6 phosphate determination in synchronized cultures of *Chlamydomonas reinhardtii*

Cells of *Chlamydomonas reinhardtii* were harvested at different time points surrounding the light/dark switch and starch was isolated, hydrolyzed and quantified using a conventional enzymatic assay (Lowry and Passonneau, 1972). Furthermore G6P was determined in starch hydrolysates using a cycling assay optimized as described in 3.1.1.1. (A) Averaged values of two individual experiments (error: average absolute deviation) for starch content and C6 phosphate in the algae suspension is plotted against time. (B) For each experiment and time point the glucose-based C6 phosphate is calculated separately. Averaged values of the two individual experiments are given (error: averaged absolute deviation). (C) The minimum required amount of algae suspension for a single C6 phosphate determination is calculated for both the conventional (see 1.6.2.1) and the cycling assay. Calculation is based upon the starch content and glucose-based C6 phosphate in the algae suspension at time point 0 as well as on the detection limit of both assays.

For this time-resolved experiment 25 ml algae suspension (10% of the total culture volume) were harvested at each time point. As illustrated in Figure 15C using the cycling assay the temporal resolution of such an experiment could easily be increased by several folds, while it is already too high for C6 phosphate determination using the conventional enzymatic assay.

3.3.2.4 Endosperm starch from rice

Endosperm starch from rice (*Oryza sativa*) has been shown to contain no or only little phosphate. The endosperm of the rice mutant line EM10 is deficient in starch branching enzyme IIb (SBEIIb ko). In the EM10 starch the amylopectin structure is strongly altered, short chains being strongly decreased while long chains are much more abundant (Nakamura, 2002; Yao *et al.*, 2004; see 1.3.1). C6 phosphate as another structural feature of starch granules was analyzed in starch isolated from wild type (Kinmaze) and EM10 endosperm. Starch isolation was performed in the lab of Prof. Yasunori Nakamura (Akita Prefectural University, Akita City, Japan) according to Yamamoto *et al.* (1973, 1981).

Subsequent to acid hydrolysis (procedure B1) starch of wild type and mutant was subjected to the cycling assay for determination of C6 phosphate. The amount of starch per assay was altered and furthermore rates of formazan formation were determined in the absence or in the presence of 3 pmol authentic G6P (internal standard). After calibration with standards G6P amounts per assay were calculated from rates of formazan formation. Using starch hydrolysates from wild type rice

endosperm the rates of formazan formation were neither in the presence nor in the absence of internal G6P significantly depending on the amount of starch applied to the assay (Figure 16A). The amount of G6P per assay was below the limit of detection. By contrast, both in the absence and in the presence of internal standard using SBEIIb ko starch G6P was clearly detectable, the amount per assay being proportional to the amount of starch applied.

As a control SBEIIb ko starch was extracted twice with 80% ethanol prior to acid hydrolysis. The treatment, however, did not significantly change the amounts of G6P in the hydrolysate indicating that G6P derived from 6-phosphoglucosyl residues of starch and not from contamination of the starch sample (Figure 16A).

The glucose-based C6 phosphate was calculated for each G6P measurement after subtraction of internal standard (Figure 16B). In endosperm starch from wild type rice glucose-based C6 phosphate is too low to be reliably determined which concurs with data previously published on rice endosperm starch (see 1.2.2). C6 phosphate in the starch of the SBEIIb-deficient mutant is, however, comparably high and reaches values similar to *Arabidopsis thaliana* leaf starch (see above and 1.2.2). The increase of starch phosphate as a consequence of insufficient branching indicates a relation between the two processes of starch metabolism, branching and phosphorylation.

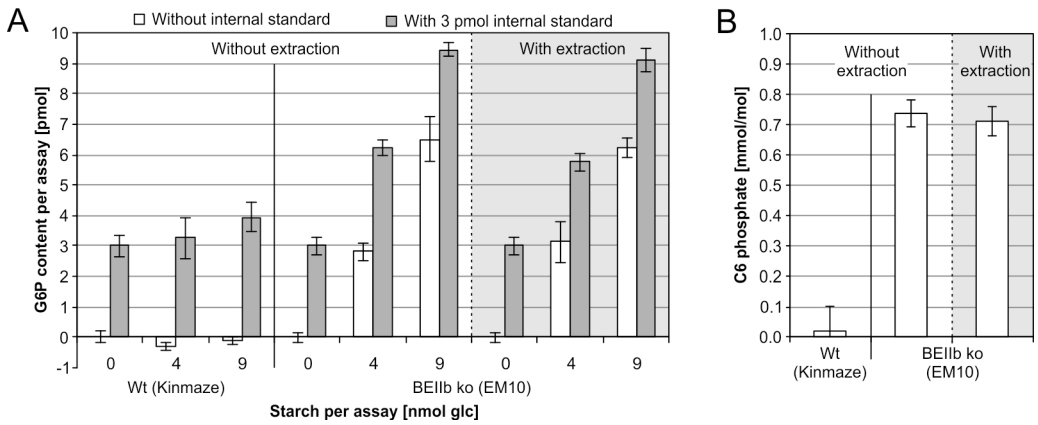

Figure 16. C6 phosphate determination in rice endosperm starch using the cycling assay

Native endosperm starch isolated from kernels of wild type (Wt) and SBEIIb-deficient rice (SBEIIb ko) was subjected to acid hydrolysis (procedure B1). (A) Different amounts of hydrolyzed starch were mixed with authentic G6P (internal standard) applied to the cycling assay. G6P amounts per assay were calculated from rates of formazan formation after calibration with external G6P standards that simultaneously underwent the assay procedure. Negative G6P values are due to rates of formazan formation that were slightly lower than that of the lowest calibration standard (0 pmol per assay). All measurements were done in triplicates (error: SD). G6P in hydrolysates of SBEIIb ko starch was additionally quantified after extraction of the starch granules with 80% ethanol. G6P amounts detected were similar without and with extraction indicating that G6P derived from 6-phosphoglucosyl residues in the starch and not from low molecular weight contamination. (B) After subtraction of internal standards glucose-based C6 phosphate was calculated. Averaged values are derived from measurements of different amounts of starch and internal standard per assay (error: SD, n = 4).

3.3.3 Glycogen from mouse tissue

When Tagliabracci *et al.* (2011) performed NMR studies on rabbit skeletal muscle glycogen they exclusively found monophosphate esters at the glucosyl carbons C2 and C3. Unlike starch, they reported absence of phosphate at glucosyl carbon C6. In amylopectin, the C6 carbon is critical to the entire phosphorylation/dephosphorylation cycle of starch. To verify absence of C6

phosphorylation in glycogen, it was isolated from tissues of wild type rabbit and wild type as well as Lafora disease mice in the lab of Prof. Berge A. Minassian (Hospital for Sick Children, Toronto, Canada) and kindly provided. Following acid hydrolysis (procedure B) glucose was determined using the conventional enzymatic assay (Lowry and Passonneau, 1972) while glucose 6-phosphate (G6P) was quantified using the enzymatic cycling assay which was carefully optimized for G6P measurements in the presence of the large excess of glucose as generated by the hydrolysis of glycogen (see 3.1). Hydrolysates of glycogen from rabbit skeletal muscle and mouse skeletal muscle and liver all contained G6P, indicating that glucosyl 6-phosphate and therefore C6 phosphorylation is actually present in glycogen (Table 8).

The glucose-based C6 phosphate in glycogen varied between the two species and organs, rabbit muscle glycogen possessing the highest (0.36 mmol/mol glucose) (Table 8) and glycogen from mouse liver the lowest (0.008 mmol/mol glucose). In the latter it was at the limit of detection. To obtain unambiguous evidence for or against glucosyl 6-phosphate in liver glycogen, glycogen of several animals was pooled and digested with α-amylase and amyloglucosidase. From the resultant low molecular weight glucans the fraction of putative phosphoglucans was separated by ion exchange chromatography using QFF Sepharose. Following acid hydrolysis the fractions were assayed for glucose and G6P. A large amount of glucosyl 6-phosphate in this enriched fraction (17.7 mmol/mol glucose, Table 8) confirmed its presence in liver glycogen.

Table 8. Glucosyl 6-phosphate residues of glycogen from indicated sources

In hydrolysates of glycogen from various sources glucose was determined using a conventional enzymatic assay (Lowry and Passonneau, 1972). G6P was quantified by the cycling assay optimized as described in 3.1. Mean values of glucose-based C6 phosphate are given (error: SD, n - number of biological replicas), n.d. - not detectable.

Species	Source organ	Glucose-based C6 phosphate [mmol/mol glc residues]
Rabbit *Wild-type*	Skeletal muscle	0.36 ± 0.01 (n = 6)
Mouse *Wild-type*	Skeletal muscle	0.081 ± 0.019 (n = 8)
	Liver	0.008 ± 0.0017 (n = 4)
	Enriched phosphoglucans[1]	17.7
Mouse *Epm2a*$^{-/-}$	Skeletal muscle	0.64 ± 0.08 (n = 6)
	Liver	0.055 ± 0.007 (n = 5)
	Enriched phosphoglucans[1]	51.0
Mouse *Epm2b*$^{-/-}$	Skeletal muscle	0.66 ± 0.16 (n = 5)

[1] For the enrichment of phosphoglucans, glycogen from several animals was pooled

Glycogen in the mouse model of Lafora disease is characterized by progressive increased phosphorylation (Tagliabracci *et al.*, 2007, 2008). As an example, at the age of 9-12 months the phosphate content of skeletal muscle glycogen isolated from the *Epm2a*$^{-/-}$ (laforin-deficient) LD mouse model, is sixfold elevated compared to that of wild type mice (Tagliabracci *et al.*, 2008). To date, only total phosphate of LD glycogen had been determined via an orthophosphate assay following exhaustive acid hydrolysis of purified glycogen. Using the enzymatic cycling assay, glucosyl 6-phosphate content in glycogen of 9-12 month-old *Epm2a*$^{-/-}$ and *Epm2b*$^{-/-}$ (malin-deficient) mice was quantified and found to be eightfold increased in muscle of both LD mice and

sevenfold in laforin-deficient liver (Table 8). This indicates that an increased C6 monophosphate content contributes to the elevated levels of total glycogen phosphate and, therefore, to the disturbed glycogen phosphorylation in LD.

The glucosyl 6-phosphate residues as measured in all the above experiments were originally an integral part of glycogen and not attributed to contaminants. This is confirmed by the following observations. Repeated ethanol precipitation of glycogen which would at least diminish water soluble low molecular weight contaminants does not alter the measured glucose-based C6 phosphate content (Figure 17A). When glycogen was subjected to 100 kDa ultrafiltration using membranes of regenerated cellulose, the retentate being washed 5 times, the majority of the glycogen remained in the retentate. C6 phosphate as measured after acid hydrolysis of the fractions using the cycling assay distributed on both fractions almost identically (Figure 17B). By contrast, low molecular weight phosphoglucans containing glucosyl 6-phosphate residues were generated only by endoamylolytic glycogen degradation (see above). Thus, neither by repeated precipitation nor by ultrafiltration intact glycogen and C6 phosphate could be separated indicating that the measured C6 phosphate is indeed derived from 6-phosphoglucosyl residues in glycogen.

A

Species	Source organ	Glucose-based C6 phosphate [mmol/mol glc residues]	
		Before precipitation	after 5 precipitations
Rabbit *Wild type*	Skeletal muscle	0.36 ± 0.01 (n = 3)	0.38 ± 0.01 (n = 3)
Mouse *Wild type*	Skeletal muscle	0.09 ± 0.018 (n = 5)	0.095 ± 0.011 (n = 5)
Mouse *Epm2a*$^{-/-}$	Liver	0.047 ± 0.001 (n = 2)	0.045 ± 0.003 (n = 2)
	Skeletal muscle	0.67 ± 0.05 (n = 5)	0.67 ± 0.09 (n = 5)

B

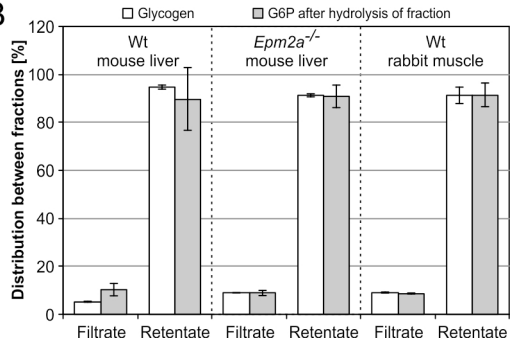

Figure 17. C6 phosphate co-precipitates and co-fractionates with glycogen

(A) Glycogen preparations derived from independent isolations were precipitated 5 times in 66.6% [v/v] ethanol with 5.4 mM LiCl (final concentration each) and aliquots were subjected to acid hydrolysis (procedure B2) before and after precipitation. Glucosyl 6-phosphate residues were determined in the hydrolysates by the enzymatic cycling assay and are related to the glucosyl content. Mean values ± SD are given (n - number of biological replicas). (B) Glycogen preparations from different sources and independent isolations were subjected to membrane filtration (100 kDa cut-off). The retentates were washed 5 times with water each. Filtrates and retentates were recovered and subjected to acid hydrolysis. Subsequently the amounts of glycogen and of G6P were determined in the fractions and expressed as percent of the sum of both fractions. Mean values of independent preparations are given (error: SD, n = 3).

3.3.4 Laforin treatment of glycogen from muscle of *Epm2a*$^{-/-}$ mice

Tagliabracci *et al.* (2007) showed that laforin *in vitro* releases phosphate from rabbit skeletal muscle glycogen. They achieved a quantitative hydrolysis of phosphate esters when glycogen structure was concurrently disrupted by α-amylase and amyloglucosidase. As the released phosphate was determined as orthophosphate using the malachite green assay no information is available about the specific glucosyl carbons the phosphate was formerly attached to. Since glucosyl C6-phosphate is increased in glycogen from laforin-deficient mice it is conceivable that laforin is also capable of removing phosphates from glucosyl carbon C6.

In this study it was tested whether active laforin hydrolyses phosphate esters in 6-phosphoglucosyl residues of glycogen isolated from laforin-deficient mice *in vitro*. According with the findings of Tagliabracci *et al.* (2007) glycogen was incubated with laforin during concurrent disruption of the

polyglucan structure. After incubation in the presence of absence of laforin the glucose-based C6 phosphate was determined using the sensitive cycling assay after acid hydrolysis of the reaction mixtures (Figure 18A).

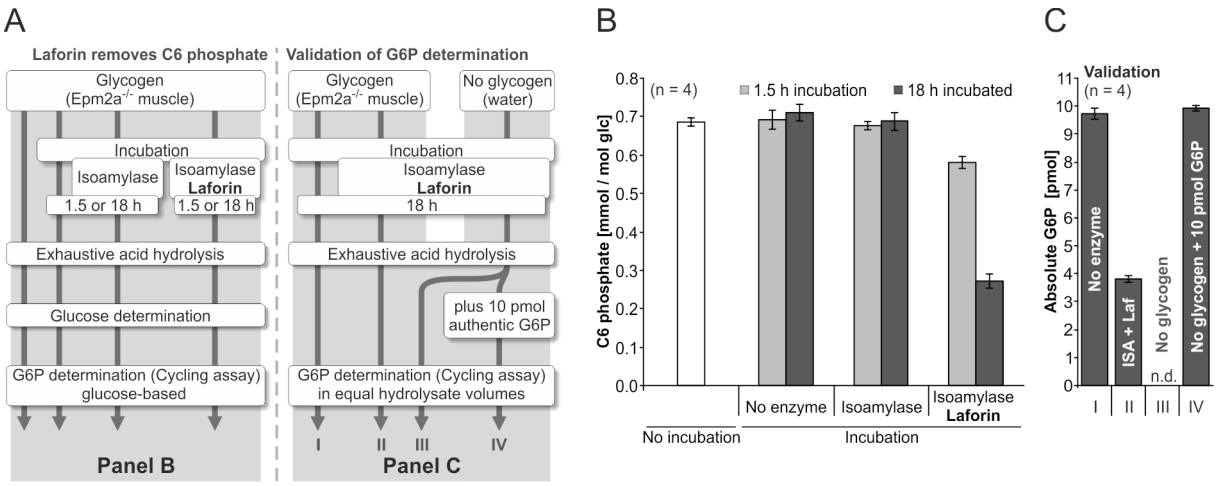

Figure 18. Dephosphorylation of glucosyl C6 phosphate residues in glycogen by laforin

(A) Experimental outline. Left: Glucose-based C6 phosphate was determined using hydrolysates of *Epm2a*$^{-/-}$ mouse skeletal muscle glycogen that was either omitted from incubation or incubated for different times with none, one, or both of the enzymes isoamylase and laforin. The results are depicted in (B). Right: for Validation of G6P determination in hydrolysates G6P was additionally measured when glycogen was omitted from the incubation (both enzymes, 18 h). These water controls were treated exactly as samples containing glycogen. To all G6P assays equal volumes of hydrolysates were applied. Results are shown as indicated in (C). (B) Glucose-based C6 phosphate of glycogen treated as described in (A, left). Only incubation with laforin substantially decreased phosphorylation at glucosyl C6 in time-dependent manner. (C) Absolute amount of G6P as measured by the cycling assay in equal hydrolysate volumes (8 µl) of experiments as illustrated in (A, right). Averaged glucose concentration in glycogen containing hydrolysates: 1.76 ± 0.01 nmol/µl. The G6P determination is valid since no G6P is detectable when glycogen is omitted but the expected amount of G6P is measured when authentic G6P is added. n - number of individual experiments (Error: SD), ISA - isoamylase, Laf - laforin, n.d. - not detectable.

When glycogen was incubated for 1.5 or 18 hours either lacking any enzyme or exclusively with isoamylase the resultant glucose-based C6 phosphate was in all cases indiscernible from glycogen that underwent no incubation at all. By contrast, when laforin was added to the incubation mixture the glucose-based C6 phosphate decreased in time-dependent manner, being reduced by ca. 63% after 18 hours incubation (Figure 18B).

In a second set of experiments the G6P determination was validated. Samples that lacked glycogen (water controls) were treated exactly as glycogen containing samples, and incubation was performed for 18 hours in the presence of both isoamylase and laforin. Additionally glycogen was incubated without any enzyme. Following acid hydrolysis equal volumes of all hydrolysates were applied to the cycling assay. While in glycogen containing hydrolysates G6P was present according to whether or not glycogen was treated with laforin, in hydrolysates derived form water controls G6P was not detectable. However, the presence of laforin and isoamylase did not affect the validity of the G6P measurements as the addition of authentic G6P to water control hydrolysates resulted in detection of exactly the expected amount of internal standard (Figure 18C).

3.4 NMR analysis of *Curcuma* starch and of various glycogen preparations

G6P determination in hydrolysates of mammalian glycogen using the optimized cycling assay revealed that G6P is clearly present in glycogen preparations. These results, however, do not

concur with previously published data that state the absence of 6-phosphoglucosyl residues in glycogen (Tagliabracci *et al.* 2011; Roach *et al.* 2012). For a further characterization of the phosphorylation pattern of glycogen a detailed NMR analysis was performed. NMR techniques permit the determination of any position of phosphate esters on glucosyl residues without requiring all glucosidic bonds to be hydrolyzed. However, due to the low abundance of phosphate residues in both glycogen and starch, relatively high amounts of the α-polyglucans are needed. As compared to other starches, *Curcuma* starch is highly phosphorylated and most of the phosphate groups are located at C6 (see Tables 1 and 7). *Curcuma* starch was used to optimize sample pretreatment prior to NMR to keep consumption of mouse glycogen as low as possible.

3.4.1 1D ^{31}P-NMR of starch and mouse glycogen

Prior to NMR analysis, pretreatment of *Curcuma* starch and glycogen was essentially the same but the isolated glycogen underwent five cycles of precipitation in a mixture of 66.6 % [v/v] ethanol and 1.5 mM LiCl (final concentrations each) followed by dissolving in water. The repetitive precipitation aimed to remove potential contaminations of the glycogen preparation, such as (phospho-)oligoglucans or nucleic acids. *Curcuma* starch and mouse liver glycogen were enzymatically hydrolyzed using a mixture of α-amylase and amyloglucosidase. The resultant α-limit dextrins were subjected to membrane filtration (3 kDa cut-off) to remove the proteins. The filtrate was lyophilized, dissolved in D_2O containing buffer, and applied to ^{31}P-NMR, 80% phosphoric acid serving as external standard. Spectra were recorded either with or without proton-decoupling (see 1.6.4.1).

In proton-decoupled ^{31}P spectra of *Curcuma* starch and *Epm2a*$^{-/-}$ liver glycogen 4 signals are detected (Figures 19A and B). The signal to noise ratio is quite low in the case of glycogen even though 5 times more glycogen was applied to NMR as compared to *Curcuma* starch. By contrast, the signals in the *Curcuma* starch sample are clearly distinguished from background due to its high amount of glucosyl phosphate.

Proton-coupling reveals the number of hydrogens that are connected with the phosphorus via 3 chemical bounds (vicinal coupling). In the *Curcuma* starch sample one signal splits into a doublet (Figure 19C, signal 1; one vicinal hydrogen), two into a triplet (Figure 19C, signals 2 and 3; two vicinal hydrogens) and one is retained as a singlet (Figure 19C, signal 4; no vicinal hydrogen). As glucosyl phosphates show vicinal connectivity either to one (when phosphate is attached to any of the carbons C1 through C4) or two hydrogens (when phosphate is attached to carbon C6), signal 4 is assigned to orthophosphate. Due to the low signal intensity in the glycogen sample the splitting patterns are less clear. At least patterns of signal 2 and 3 are interpreted as triplets (Figure 19B). As in the *Curcuma* starch sample, signal 4 shows no splitting (not shown) and is likewise assigned to orthophosphate. When liver glycogen prepared from wild type mice was used no signals were detected except that of orthophosphate (not shown).

Since the absolute signal position in ^{31}P-NMR is depending on the sample concentration (Twyman, 2005) it is useless to compare the position of the signals 1 through 4 in the samples of *Curcuma* starch and *Epm2a*$^{-/-}$ liver glycogen. However, for further assignment of the signals 1 through 3 and to determine whether the signals 1 through 4 in both samples correspond to the same phosphate species mixing experiments were performed.

First, authentic G6P and maltose 6-phosphate were sequentially added to the glycogen sample, spectra being recorded after each addition. The phosphate signals of both internal standards clearly overlap with signal 2 in the glycogen sample (Figure 19D). It should be noted that G6P causes two phosphate signals in agreement with the presence of two glucosyl anomers, while the phosphate group in maltose 6-phosphate, being apparently attached to the non-reducing glucosyl residue, results in one signal.

Second, an aliquot of the *Curcuma* starch sample was added to the glycogen sample already containing the internal standards. Subsequently 4 signals emerge that correspond in chemical shift with the signals in the glycogen sample (Figure 19E).

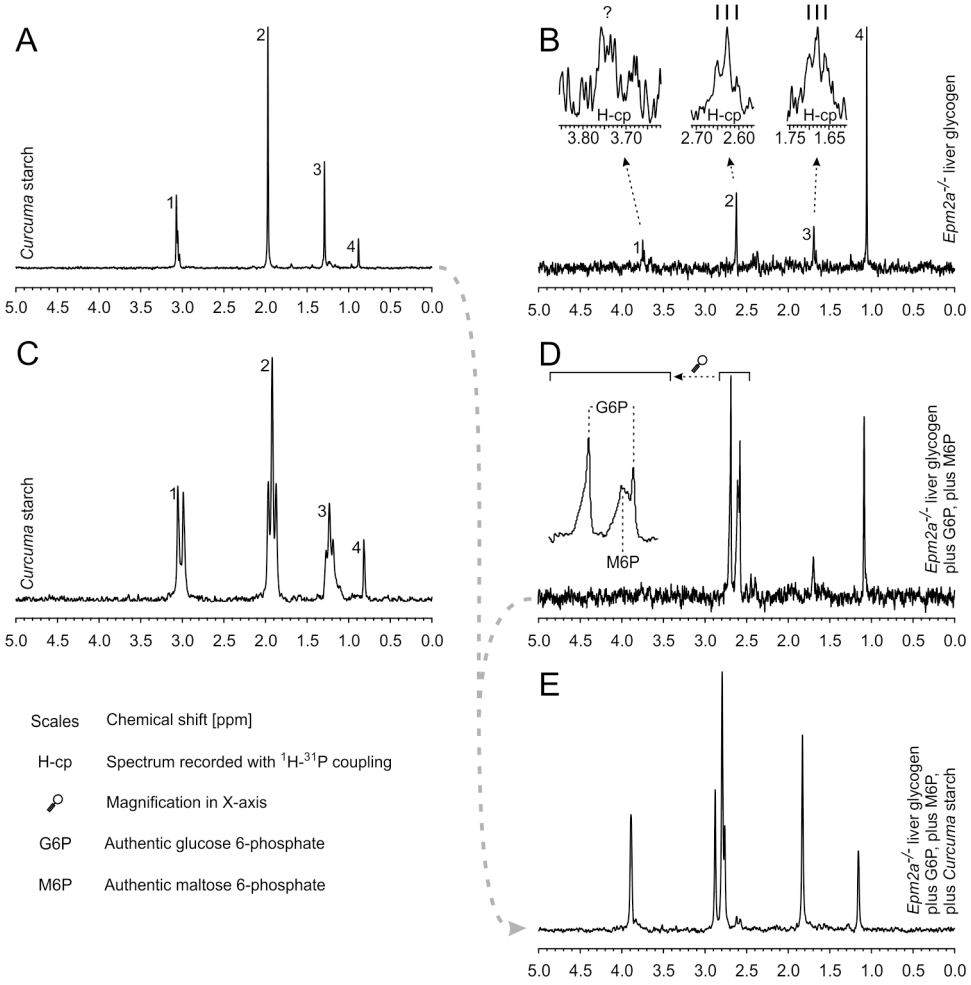

Figure 19. ^{31}P-NMR spectra of *Curcuma* starch and liver glycogen from *Epm2a*$^{-/-}$ mice

α-Limit dextrins were prepared from *Curcuma* starch (20 mg) and liver glycogen (100 mg) that was isolated from *Epm2a*$^{-/-}$ mice. After removal of hydrolytic proteins, samples were subjected to ^{31}P-NMR. (A) Proton-decoupled spectrum of *Curcuma* starch. (B) Proton-decoupled spectrum of glycogen. For the signals 1 through 3 details are shown in a spectrum recorded with proton-coupling. (C) Spectrum of *Curcuma* starch with proton-coupling. (D) Proton-decoupled spectrum. Glycogen sample as in (B) but after the addition of authentic G6P and maltose 6-phosphate. The signals of the internal standards are additionally shown with magnification. (E) Proton-decoupled spectrum. Glycogen sample as in (D) but after the addition of *Curcuma* starch α-limit dextrin (equivalent to ca. 5 mg starch).

Thus, from the data presented in Figure 19 one can conclude that *Curcuma* starch and glycogen contain species of phosphate esters that have similar nuclear magnetic properties. At least one type of phosphate ester shows similar chemical shifts as G6P and maltose 6-phosphate (signal 2). Furthermore, this signal splits into a triplet when spectra are recorded with proton-coupling, which

is consistent with the assignment of signal 2 to phosphorylation in glucosyl C6 where phosphate is connected to two hydrogens via 3 chemical bonds. In the glycogen sample orthophosphate is the most prominent phosphate species which could be the result of phosphate ester hydrolysis during sample preparation.

Neither signal 1 nor signal 3 could be assigned by the addition of authentic G3P, G4P and G1P as phosphate signals of these standards did not show similarity in chemical shift with the detected signals in samples of *Curcuma* starch and glycogen. However, as glucosyl C3 has been reported to be a phosphorylation site in starch it is conceivable that signal 1 is caused by α-limit dextrins phosphorylated in glucosyl C3. The occurrence of another triplet signal (signal 3) argues for the existence of another type of phosphate ester with two vicinal hydrogens, such as in a phosphodiester that spans between hydroxyl groups on two different glucosyl carbons. While such type of phosphate ester has never been reported in starch Lomako *et al.* (1993) suggested their existence in glycogen (see 1.2.2).

3.4.2 Enrichment of phosphoglucans from starch and glycogen

For further investigation of the phosphorylation sites in starch and glycogen, phosphoglucans of α-limit dextrin preparations derived from both polyglucans (see 3.4.1) were enriched by anion exchange using a QFF Sepharose column (8 ml total volume). After equilibration of the column with water α-limit dextrins were applied. Neutral oligoglucans were removed from the column by washing with water. Compounds bound to the column were eluted with in creasing concentrations of NH_4OAc, lyophilized, dissolved in water, and subjected to further analysis.

The conditions of the enrichment were optimized using α-limit dextrins from *Curcuma* starch. As outlined in Figure 20A, one-step elution from QFF Sepharose was conducted with 300 mM NH_4OAc. The derived fraction (0-300 mM; 'All SF' in Figure 20A) was split into two equal volumes one of which was applied to proton-coupled 1D ^{31}P-NMR without further fractionation. The second aliquot was resolved into subfractions using HPAEC-PAD (designated as SF1 though 3; Figure 20A). The spectrum of the non-fractionated eluate ('All SF') showed 4 signals with the characteristic splitting patterns as already observed when α-limit dextrins were analyzed without prior phosphoglucan enrichment (Figure 20B). HPAEC-PAD chromatograms (separation mode 1) of 'All SF' revealed a complex peak pattern that was resolved between 13 and 30 min retention time. During several consecutive runs of HPAEC-PAD the subfractions SF1, SF2, and SF3 (Figure 20C) were collected, desalted, dried, and dissolved in 40 µl of water. Subsequently, each subfraction was sequentially added to the one-step eluate (containing all subfractions). After each addition the sample was analyzed by 1D ^{31}P-NMR as in Figure 20A. After the addition of each subfraction peak areas were calculated for the 4 phosphorus signals in the ^{31}P-NMR spectrum. While SF1 and SF3 did not change the signal intensities significantly, addition of SF2 results in a large increase in the peak areas of all 4 signals (Figure 20D). Thus, phosphoglucans from *Curcuma* starch are exclusively recovered in SF2. However, the increase in peak area by the addition of SF2 is around 65% that of the 'All SF'-aliquot which had the same volume but was not resolved into subfractions. This reflects a loss of phosphoglucans during subfraction preparation.

Other batches of digested *Curcuma* starch were used to enrich phosphoglucans by QFF Sepharose chromatography using different concentrations of NH_4OAc. SF3 eluted from QFF Sepharose with

200-300 mM (Figure 20C). Phosphoglucans from *Curcuma* starch, as detected in SF2 by ^{31}P-NMR, elute from QFF Sepharose in 30 to 200 mM NH_4OAc (Figure 20E).

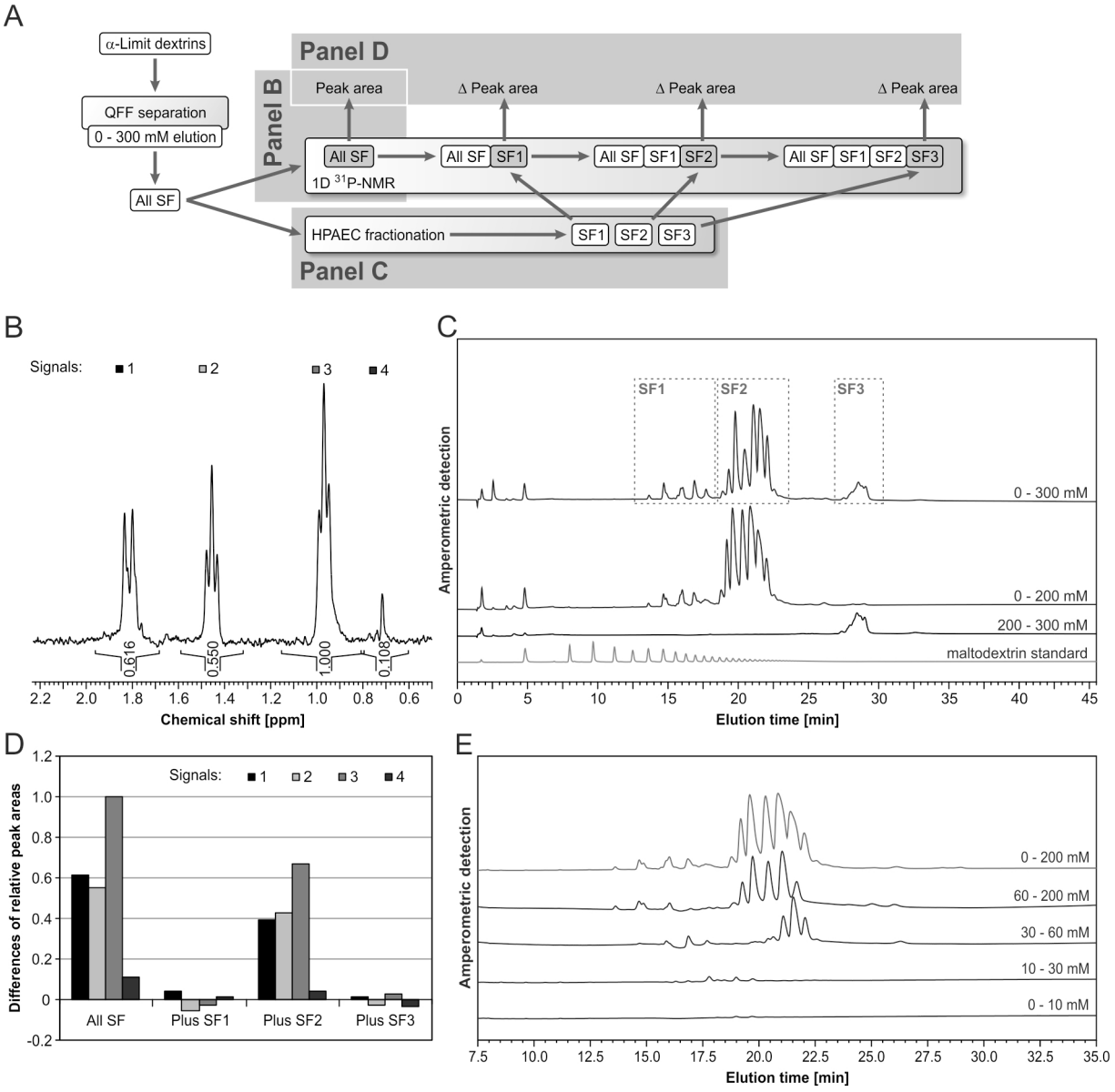

Figure 20. Enrichment of phosphoglucans of α-limit dextrins derived from *Curcuma* starch

(A) Outline of the experiments leading to the panels (B), (C), and (D). For details see text. (B) Proton-coupled 1D ^{31}P-NMR spectrogram of phosphoglucans derived from *Curcuma* starch eluted by one step (0-300 mM NH_4OAc). Four signal groups were detected. The peak area reflects the relative amount of the respective phosphate species. (C) HPAEC-PAD chromatograms of phosphoglucans from *Curcuma* starch eluted by NH_4OAc (two modes, as indicated). By HPAEC-PAD an aliquot of the one-step eluate (0-300 mM, 'All SF') was resolved into three subfractions, designated as SF1, SF2, and SF3 (as indicated). Other batches of *Curcuma* α-limit dextrins were used to enrich phospho-oligoglucans by QFF Sepharose chromatography but the column was eluted first with 0-200 mM (elution of SF1 and SF2) and then with 200-300 mM NH_4OAc (elution of SF3). (D) SF1 to SF3 collected after several applications of 'All SF' to HPAEC-PAD were desalted, dried and dissolved in 40 µl of water. Subsequently, each subfraction was sequentially added to the one-step eluate ('All SF'), and after each addition samples were analyzed by 1D ^{31}P-NMR as in (B). For the four phosphorus signals, the peak areas were determined as affected by the addition of a single subfraction. 'All SF' means the four peak areas of signals 1 through 4 without any addition (derived from the spectrum in (B)). Differences in peak areas after the addition of each subfraction are calculated. (E) HPAEC-PAD chromatograms of phospho-oligoglucans from *Curcuma* starch that were eluted from the QFF Sepharose either by several steps (as indicated) or by a single elution (0-200 mM). All fractions eluted from QFF Sepharose were brought to equal volumes. Subsequently, equal fraction volumes were applied to the HPAEC-PAD system except for the two fractions eluted with the lowest NH_4OAc concentration (fourfold fraction volume applied to HPAEC-PAD). Chromatograms show that phospho-oligoglucans from *Curcuma* starch, as detected in SF2 by ^{31}P-NMR (C, D), elute from QFF Sepharose in 30 to 200 mM NH_4OAc.

Phosphoglucans as enriched by anion exchange using QFF Sepharose are a complex mixture of phosphorylated linear and branched oligoglucans. This is revealed by HPAEC-PAD analysis of QFF Sepharose eluate fractions that were treated with alkaline phosphatase (Figure 21).

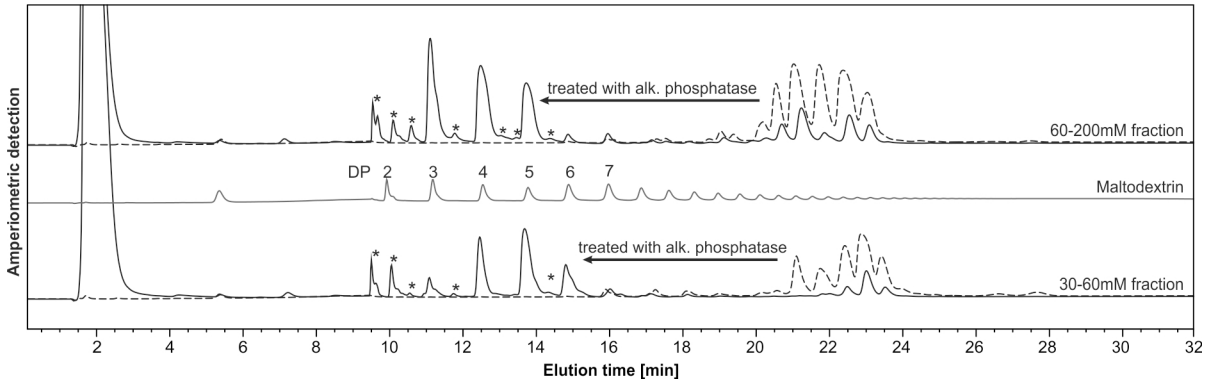

Figure 21. Alkaline phosphatase treatment of phosphoglucans derived from *Curcuma* starch

Phosphoglucans eluted by 30-60 and 60-200 mM NH_4OAc (see Figure 20E) were treated with alkaline phosphatase. Aliquots were analyzed by HPAEC-PAD before and after the phosphatase treatment. A mixture of maltodextrins served as standard. Following enzymatic dephosphorylation, maltodextrins having a degree of polymerisation (DP) ranging from 2 to 7 were observed. However, some analytes (marked with *) result in peaks that do not match those of the constituents of the maltodextrin standard indicating the occurrence of α-1,6 glucosidic bonds.

After optimization of the enrichment procedure using *Curcuma* starch α-limit dextrins, phosphoglucans were enriched from α-limit dextrins of liver glycogen isolated from *Epm2a*$^{-/-}$ mice. However, the preparation of glycogen α-limit dextrins was slightly altered to avoid the release of labile phosphate esters that was indicated by the results of 1D ^{31}P-NMR studies (see 3.4.1). Following amylolysis, the 3 kDa filtrate was not lyophilized but diluted to approximately 10 mM NH_4OAc and directly applied to QFF Sepharose. A separately prepared column was used to avoid any cross-contamination of the phosphoglucans derived from starch and glycogen. During sample application and the stepwise elution of the glycogen-derived phosphoglucans aliquots were taken from each fraction and glucosyl content, total phosphate, orthophosphate as well as G6P were determined (Figure 22).

Recovery of total phosphate and G6P was 88 % and 68 %, respectively. Prior to anion exchange chromatography the preparation contained only a small proportion of (free) orthophosphate, which was, however, increased during chromatography by factor 1.7. Therefore, a small proportion of the phospho-oligoglucans releases phosphate during the enrichment procedure.

Most of the compounds that contain covalently bound phosphate were eluted by a two-step gradient of ammonium acetate ranging from 20 to 200 mM (first step) and from 200 to 1,000 mM (second step). The total phosphate is distributed over both fractions but consistent with the results for the enrichment of phosphoglucans derived from *Curcuma* starch, the fraction of the first step almost exclusively contains oligoglucans carrying a monophosphate ester at C6 (Figure 22). Therefore, the two-step elution partially enriches C6 phosphorylated glucan chains and leads to an increased probability of their detection by NMR. For both, phosphoglucans derived from *Curcuma* starch and those of *Epm2a*$^{-/-}$ mouse liver glycogen, the 20-200mM fraction was analyzed by NMR.

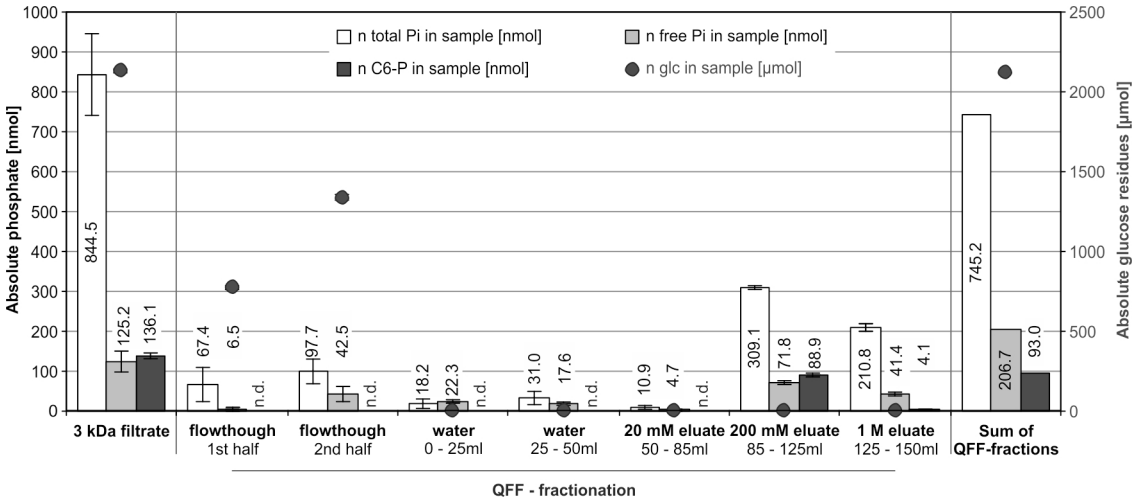

Figure 22. Phosphoglucans enriched from liver glycogen of *Epm2a*$^{-/-}$ mice.

Following amylolysis and membrane filtration, the 3 kDa filtrate was applied to a separately prepared QFF Sepharose column. After extensive washing with water, the column was eluted using three steps (0-20, 20-200, and 200-1,000 mM NH_4OAc). Eluates were collected during sample application (designated as 'flowthrough', as indicated) and during washing ('water', as indicated). Subsequently, the three fractions obtained by elution with NH_4OAc were collected separately. In each fraction the amounts of glucose (after acid hydrolysis [procedure B2], right scale), G6P, total phosphate and orthophosphate (all three on left scale) were quantified. Values were compared with those of the sample prior the QFF chromatography. N.d. – not detectable. Error bars represent SEM of technical replica. As observed in starch-derived phospho-oligoglucans, glucosyl 6-phosphate residues elute mostly between 20 and 200 mM NH_4OAc. Elution of glucosyl 6-phosphate residues differs from that of total phosphate; glucosyl 6-phosphate residues are enriched in the eluate 20-200 mM NH_4OAc. Due to the distribution of the total phosphate over two fractions, 20-200 mM and 200-1,000 mM, the glucosyl 6-phosphate is partially enriched in the former fraction. The phosphoglucans in the 20-200 mM fractions derived from *Curcuma* starch and glycogen were analyzed by NMR.

3.4.3 2D NMR experiments

Various approaches of two-dimensional NMR were conducted to further elucidate the phosphorylation patterns in mouse glycogen and to compare them to those of *Curcuma* starch. First, samples of various standard compounds were analyzed. Subsequently suitable NMR experiments were conducted with phosphoglucans prepared from *Curcuma* starch and glycogen.

3.4.3.1 Analysis of standard compounds

First glucose, being the monomer of both starch and glycogen, was examined. In aqueous solution glucose is present as a mixture of α- and β-glucose. For both anomers the $^{1}H,^{13}C$-HMQC reveals several signals all of which represent H,C correlations via one chemical bond (Figure 23A). However, in a rather simple spectrum such as this all resonances can be assigned to their carbon position utilizing the information of a $^{1}H,^{1}H$-COSY spectrum (Figure 23D). The anomeric hydrogens usually resonate at the most downfield (highest chemical shift) region of the spectra (Pomin, 2012) and, hence, give a good starting point for assignment of the remaining hydrogens. The assignment is illustrated in Figure 23D (for details see figure legend).

In the $^{1}H,^{13}C$-HMQC for each of the glucosyl carbons 1, 2, 3, and 5 two H,C correlations are observed reflecting the influence of the anomeric state on the chemical shift of the respective carbons and hydrogens. By contrast, H4,C4 correlation signals of α- and β-glucose are overlapping and occur as one signal in the spectrum. The two hydrogens at carbon C6 (H6) are diastereotopic, i.e. substitution of either of the two would result in diastereoisomers. Therefore, for each anomer of glucose two H6,C6 signals emerge. In the case of α-glucose the two H6,C6 signals exhibit similar

^{1}H-shifts, thus, appear as one broadened signal while the respective correlations in β-glucose are clearly separated (Figure 23A).

Furthermore maltose and isomaltose were examined. Both consist of 2 glucose monomers one of which (possessing the reducing end, designated as glucosyl ring I; see Figure 23E) can occur as α- or β-glucose while the other (possessing the non-reducing end, designated as glucosyl ring II; see Figure 23E) exclusively exists as α-anomer. The number of H,C correlations detected in a ^{1}H,^{13}C-HMQC increases as compared to glucose (Figures 23A through C). The chemical shifts of H,C correlations depend on the carbon position in the glucosyl residue (C1 through C6), on whether the glucosyl carbon belongs to glucosyl ring I or II, and on the anomeric state of glucosyl ring I. Furthermore, shifts of H,C correlations are significantly influenced at carbon positions at or in close vicinity of the glucosidic bond. E.g. the H4,C4 correlation of glucosyl ring I in maltose shifts very differently as compared to H4,C4 in glucose. The same can be observed when H1,C1 of glucosyl ring II in maltose or H6,C6 of glucosyl ring I in isomaltose are compared with the respective H,C correlation in glucose. However, examinations of longer oligodextrins such as maltotriose and maltotetraose revealed that shifts of H,C correlations at specific glucosyl carbons on glucosyl residues with larger distance from the reducing end only slightly differ from those of glucosyl ring II in maltose. Regarding the phosphoglucan preparations of *Curcuma* starch and glycogen very complex signal patterns can be expected due to the simultaneous presence of branched and linear phosphoglucan varying in length as well as position of phosphate and branching points.

The influence of phosphate on the shifts of H,C correlations was examined in ^{1}H,^{13}C-HMQC spectra of glucose X-phosphate standards (X = 1, 2, 3, 4, 6). Highly pure G1P and G6P were purchased from Sigma. G4P was synthesized and purified by Dalton Pharma Services (Toronto, Canada). G2P, G3P were not available commercially. G2P was synthesized from base G1P using the procedure described in Zmudzka and Shugar (1964). G3P was synthesized following a procedure of Perich and Johns (1988a, b) and a kind gift of Dr. Gerhard Ritte (Ritte *et al.,* 2002). G2P and G3P were additionally purified using anion exchange chromatography.

In Figure 24 ^{1}H,^{13}C-HMQC spectra of monoglucosyl phosphates are overlaid with that of glucose. Obviously H,C correlations are shifted downfield in both dimensions (towards higher ppm) when phosphate is bound in close vicinity. In G1P the correlation H1,C1 exhibits the highest change in chemical shift. The same is true for H2,C2 and H3,C3 in G2P and G3P, respectively, as well as for H4,C4 in G4P and H6,C6 in G6P. Except for G1P this phosphate induced change in chemical shift similarly affects H,C correlations of both anomers. In G1P the glucosyl ring is fixed in its α-anomeric form due to esterification at C1. Hence, no H,C correlations are detectable for the β-anomer.

Using ^{1}H,^{31}P-HMBC NMR the coupling of hydrogen and phosphorus is detected. In Figure 24 the ^{1}H,^{31}P-HMBC spectra are additionally aligned with ^{1}H,^{13}C-HMQC spectra of the monoglucosyl phosphates. The H,P correlation signals clearly correspond to the H,C signals previously determined to be shifted most as compared to the respective H,C signal in glucose (see above). However, when more crowded spectra are analyzed as expected for phosphoglucan preparations of starch and glycogen (see above) unambiguous assignment of H,P correlations to H,C correlations might be difficult due to overlapping hydrogen resonances which is for instance observed in the ^{1}H,^{13}C-HMQC of G4P, where the signals of αH5, αH3, and α/βH4 exhibit similar 1H chemical shifts while only the latter is attached to a phosphorylated carbon.

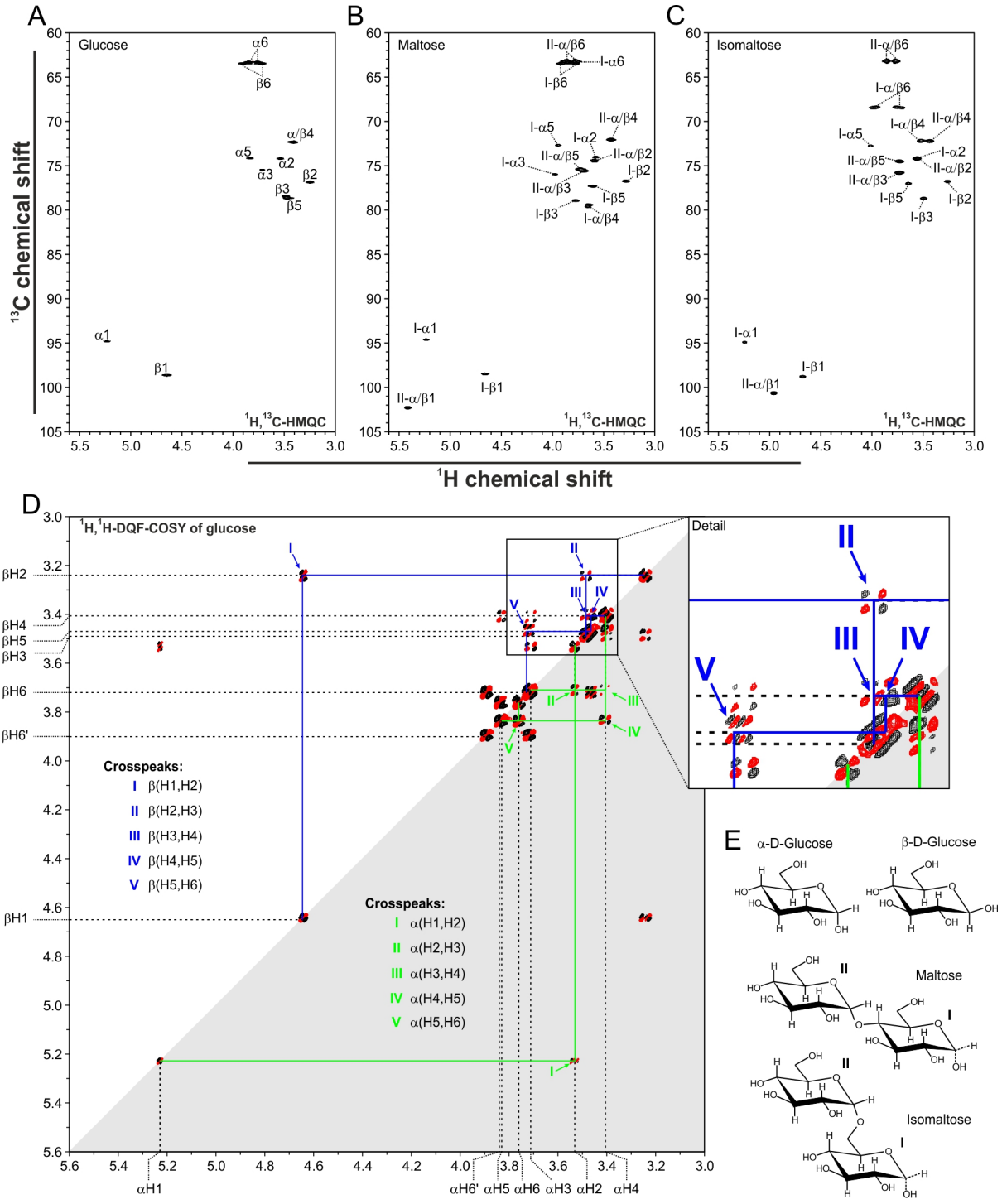

Figure 23. NMR spectra of glucose, maltose and isomaltose

(A through C) ^{1}H,^{13}C-HMQC spectra were obtained for glucose, maltose, and isomaltose. All chemical shifts are given in ppm. Signals reflect connectivity of carbon with hydrogen via one chemical bond. H,C correlations are labeled according to their specific glucosyl carbon positions. While in the spectrum of glucose only the two anomers α and β can be distinguished, signals in the spectra from maltose and isomaltose additionally derive from two glucosyl residues (I and II denoted as in (E)) one of which (I) can occur as α- or β-anomer. Thus, the label of signals includes 'I' or 'II' to mark the glucosyl ring the carbon is attached to. Often signals of H,C correlations in glucosyl ring II show the same position irrespective of the anomeric state of glucosyl ring I in the same molecule. As an example: II-α/β2 denotes the position of two overlapping C,H correlation signals, one representing C2H2 on ring II while ring I occurs as α-anomer, the second representing C2H2 on ring II while ring I occurs as β-anomer. The assignment of hydrogen and carbon positions has been achieved by additional spectra, such as ^{1}H,^{1}H-COSY (as shown in (D) for glucose) and ^{1}H,^{13}C-HMQC-COSY (data not shown). (D) Assignment of hydrogen positions in glucose using a ^{1}H,^{1}H-DQF-COSY spectrum. On both axes hydrogen chemical shift is given. The spectrum is divided by a diagonal upon which signals occur that reflect the signals of a 1D ^{1}H-NMR spectrum. So called crosspeaks occur apart from the diagonal, appear mirrored along the diagonal, and reflect coupling of hydrogens via 3 or less chemical bonds. A crosspeak is always aligned with two signals on the diagonal, derived from the coupling hydrogens. For better visualization the crosspeaks of the α-anomer are marked in the grey shadowed half of the spectrum while those of the β-anomer are marked in the white

half. Alignment of crosspeaks is indicated by green (α-anomer) and blue (β-anomer) lines. Furthermore crosspeaks are marked with arrows and roman numbers (assignment of coupling hydrogens is given in the spectrum). The H1 signals of both anomers are most downfield shifted on the diagonal and are, thus, a good starting point for the assignment of other hydrogens. H1 is aligned with a crosspeak (I) that reveals the position of H2, which again is aligned with another crosspeak (II) which reveals H3, etc. This way all hydrogen positions of both glucose anomers can be assigned to values of ^{1}H chemical shift. To compensate for the low signal dispersion between 3.35 and 3.55 ppm a range has been cut out and shown in greater detail (as indicated). (E) Representation of glucose (both anomers), maltose, and isomaltose in chair conformations. For the latter two the glucosyl residues were indexed with respect to the reducing end. Glucosyl ring I contains the reducing end and can, thus, occur as α- or β-anomer indicated by the dashed bonds at the anomeric carbon.

Two types of $^{1}H,^{13}C$ experiments can, however, be used to find out which positions in a molecule have phosphorus attached. In a conventional $^{1}H,^{13}C$-HSQC that has been recorded with high resolution those proton/carbon pairs in which a scalar coupling (via chemical bonds) to phosphorus is present exhibit an E.COSY-type pattern, i.e. a splitting of crosspeak signals is induced by additional H,P and C,P coupling. The pattern results from the fact that no phosphorus pulses are applied and, thus, the phosphorus spins involved in the coupling do not change their spin state during the experiment. Figure 25A exemplarily shows such a spectrum for G3P. The signals of the carbon positions 2, 3, and 4 were processed with high resolution and are shown in Figures 25D through H. Regarding carbon position 3 the typical tilt of split signals (E.COSY pattern) is visible. This is indicative for C,P coupling via 2 chemical bonds ($^{2}J_{C,P}$) and H,P coupling via 3 chemical bonds ($^{3}J_{H,P}$). In the split signals corresponding to carbon position 2 only the C,P coupling via 3 chemical bonds ($^{3}J_{C,P}$) gives rise to a visible splitting, while H,P coupling via 4 chemical bonds ($^{4}J_{H,P}$) is below the limit of detection, and hence no tilt of split signals is observed. A similar pattern can be observed for carbon position 4 in G3P.

Since it can be difficult to unambiguously identify these patterns in more crowded $^{1}H,^{13}C$-HSQC spectra, a second spectrum can provide additional information. In this triple-resonance experiment (^{31}P-edited $^{1}H,^{13}C$-HSQC) the scalar carbon-phosphorus coupling is used to identify carbons carrying a phosphate group and to combine this information with the superior signal dispersion of the $^{1}H,^{13}C$-HSQC. The resulting spectrum, thus, corresponds to a $^{1}H,^{13}C$-HSQC but contains only resonances of carbons that exhibit a detectable scalar coupling to phosphorous. The ^{31}P-edited $^{1}H,^{13}C$-HSQC spectrum of G3P is shown in Figure 25B and contains all peaks that show crosspeak splitting due to C,P coupling in the high resolution $^{1}H,^{13}C$-HSQC (Figure 25).

High resolution $^{1}H,^{13}C$-HSQC and ^{31}P-edited $^{1}H,^{13}C$-HSQC spectra were additionally recorded for G1P, G2P, G4P, and G6P. Table 9 shows for which C,H correlations peaks are visible in the ^{31}P-edited spectra of the respective monoglucosyl phosphate. Furthermore the values for J are given regarding both C,P and C,H couplings as derived from the tilts of E.COSY type signals in the high resolution $^{1}H,^{13}C$-HSQC of the respective monoglucosyl phosphate. $^{3}J_{H,P}$ values are consistently larger than $^{4}J_{H,P}$ values, which are often close to zero. Thus, those carbon positions that directly carry the phosphate group exhibit two tilted peaks (exhibiting the $^{2}J_{CP}$ and the $^{3}J_{HP}$ scalar coupling) and can generally be distinguished from those carbons that couple to phosphorus via more than 2 chemical bonds where only the $^{3}J_{CP}$ coupling leads to a detectable crosspeak splitting (see above).

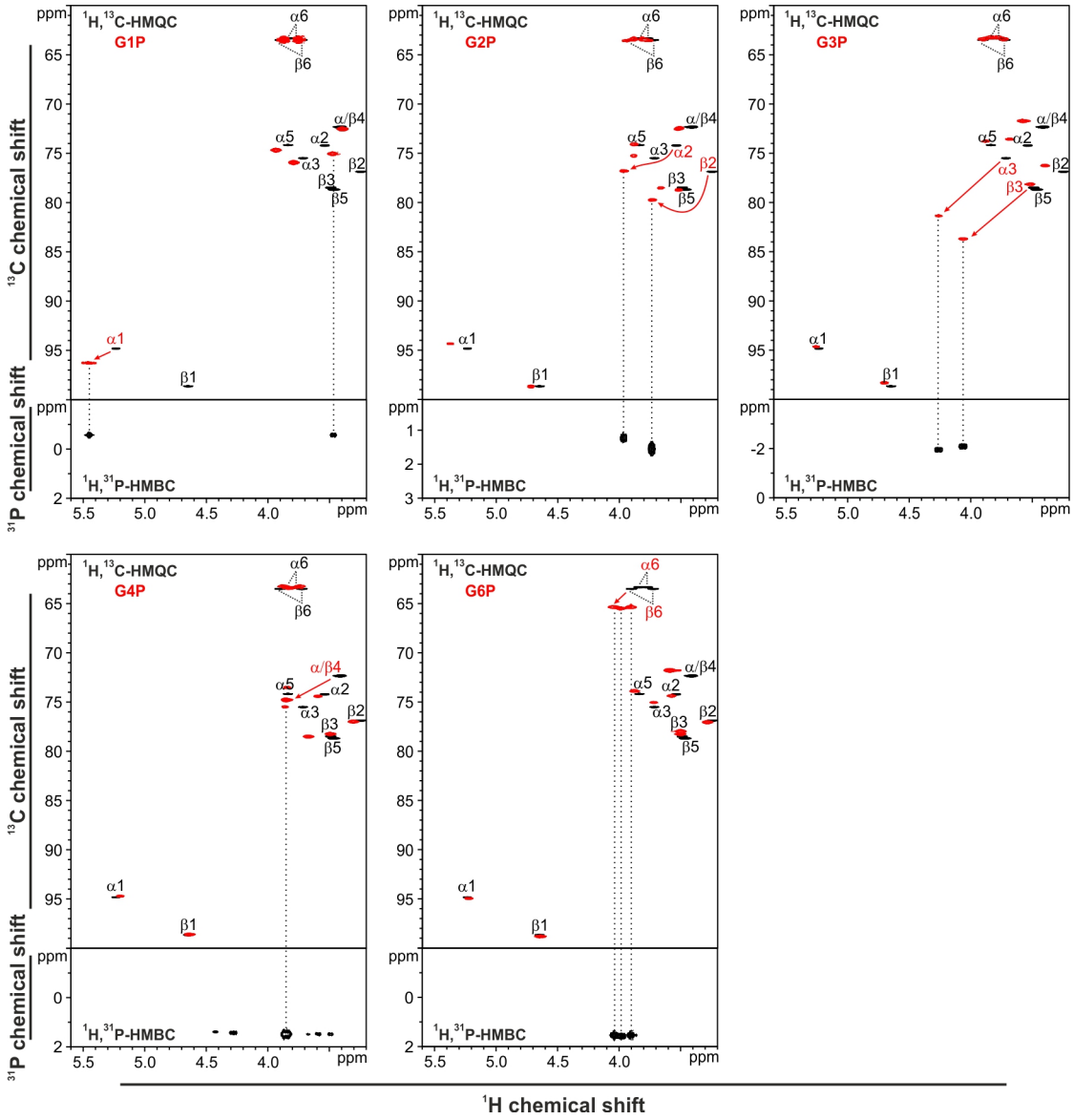

Figure 24. NMR spectra of monoglucosyl phosphates

^{1}H,^{13}C-HMQC spectra are aligned with ^{1}H,^{31}P-HMBC spectra of G1P, G2P, G3P, G4P, and G6P (as indicated). Red signals in the ^{1}H,^{13}C-HMQC spectra represent H,C correlations of the respective monoglucosyl phosphate. Black signals derive from ^{1}H,^{13}C-HMQC of glucose (assignment of signals as in Figure 23A). H,C signals of monoglucosyl phosphates were assigned utilizing additional spectra, such as ^{1}H,^{1}H-COSY (as shown in Figure 23D for glucose) and ^{1}H,^{13}C-HMQC-COSY (data not shown). H,C signals exhibit downfield offset (in both dimensions) from the respective signal of glucose when phosphate is attached (offset is indicated by red arrows). Signals with most offset in ^{1}H,^{13}C-HMQC spectra align with H,P signals in the ^{1}H,^{31}P-HMBC, verifying direct phosphate connection. Usually the ^{1}H,^{31}P-HMBC only shows signals when hydrogen and phosphate are bound to the same carbon ($^{3}J_{H,P}$ coupling) because signal intensity is depending on the coupling constant, and coupling via 4 chemical bonds ($^{4}J_{H,P}$) is usually too small to cause signals. However, in the case of G1P the coupling of ^{31}P at C1 with H2 ($^{4}J_{H,P}$) is relatively strong (see Table 9), thus, causing an additional signal.

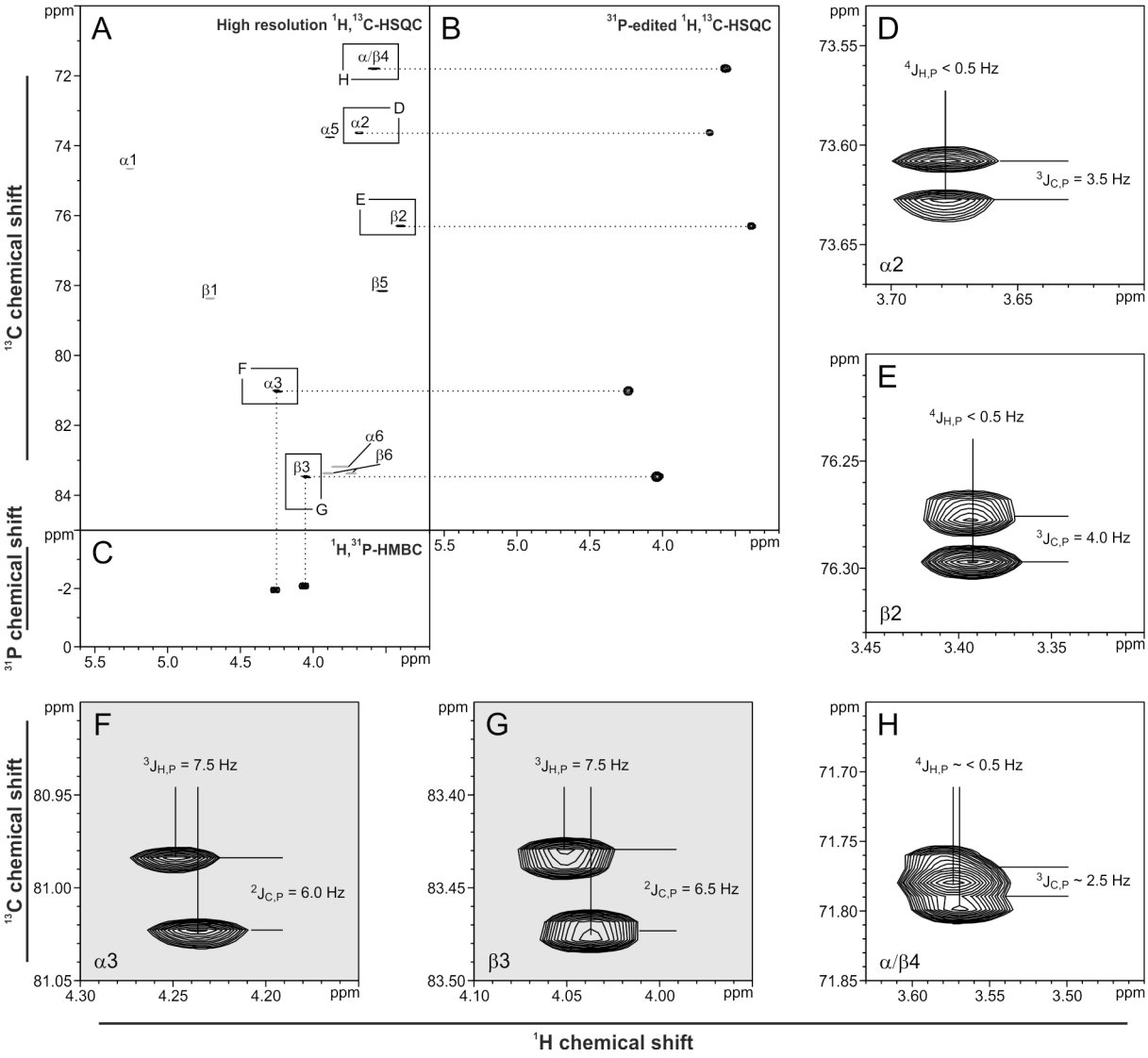

Figure 25. High resolution and ^{31}P-edited $^{1}H,^{13}C$ HSQC of glucose 3-phosphate

High resolution $^{1}H,^{13}C$-HSQC spectrum (A), ^{31}P-edited $^{1}H,^{13}C$-HSQC spectrum (B), and $^{1}H,^{31}P$-HMBC spectrum (C) of authentic G3P. H,C signals at glucosyl carbon position C3 in (A) align with H,P signals in (C) indicating the attachment of phosphate at carbon C3. Due to high resolution data sampling, signals of H1,C1 and H6,C6 correlations (grey) were outside the sampling range and are folded into the spectrum with opposite sign. Signals in (B) indicate H,C correlations where additional C,P coupling is detected. The signals in (A) that show C,P coupling in (B) are marked with the letters D through H, processed with high resolution, and shown in greater detail in the panels (D) through (H). The H,C signals exhibit an E.COSY-type pattern and split in ^{13}C dimension due to C,P coupling. The tilt of the split signals is induced by H,P coupling. Coupling constants J are given in Hz for C,P coupling via 2 ($^{2}J_{C,P}$) or 3 ($^{3}J_{C,P}$) chemical bonds and for H,P coupling via 3 ($^{3}J_{H,P}$) and 4 ($^{4}J_{H,P}$) chemical bonds. $^{4}J_{H,P}$ as in the case of H3,C3 signals of G3P (F and G) are always significantly smaller then $^{3}J_{H,P}$. Thus, connection of phosphate and hydrogen to the same carbon can be proven by the inspection of the H,P coupling induced tilt of E.COSY-type C,H signals.

Table 9. E.COSY type signals in high resolution $^{1}H,^{13}C$-HSQC spectra of monoglucosyl phosphate standards

Glucosephosphate		Carbon position					
		C1	C2	C3	C4	C5	C6
G1P	Signals present in ^{31}P-edited HSQC[1]	**α**	α	-	-	-	-
	$J_{H,P}$	**$^{3}J_{H,P}$ 7.5 (α)**	$^{4}J_{H,P}$ 2.5 (α)				
	$J_{C,P}$	**$^{2}J_{C,P}$ 5.5 (α)**	$^{3}J_{C,P}$ 7.0 (α)				
G2P	Signals present in ^{31}P-edited HSQC[1]	α, β	**α, β**	-	-	-	-
	$J_{H,P}$	$^{4}J_{H,P}$ <0.5 (α) <0.5 (β)	**$^{3}J_{H,P}$ 9.0 (α) 7.5 (β)**				
	$J_{C,P}$	$^{3}J_{C,P}$ 4.0 (α) 4.5 (β)	**$^{2}J_{C,P}$ 5.0 (α) 5.0 (β)**				
G3P	Signals present in ^{31}P-edited HSQC[1]	-	α, β	**α, β**	α, β	-	-
	$J_{H,P}$		$^{4}J_{H,P}$ <0.5 (α) <0.5 (β)	**$^{3}J_{H,P}$ 7.5 (α) 7.5 (β)**	$^{4}J_{H,P}$ <0.5 (α,β)[2]		
	$J_{C,P}$		$^{3}J_{C,P}$ 3.5 (α) 4.0 (β)	**$^{2}J_{C,P}$ 6.0 (α) 6.5 (β)**	$^{3}J_{C,P}$ ≈2.5 (α,β)[2]		
G4P	Signals present in ^{31}P-edited HSQC[1]	-	-	-	**α, β**	α, β	-
	$J_{H,P}$				**$^{3}J_{H,P}$ ≈8.0 (α,β)[2]**	$^{4}J_{H,P}$ <0.5 (α) <0.5 (β)	
	$J_{C,P}$				**$^{2}J_{C,P}$ ≈5.0 (α,β)[2]**	$^{3}J_{C,P}$ 6.5 (α) 6.5 (β)	
G6P	Signals present in ^{31}P-edited HSQC[1]	-	-	-	-	α, β	**α, β**
	$J_{H,P}$					$^{4}J_{H,P}$ <0.5 (α) <0.5 (β)	**$^{3}J_{H,P}$ 5.5 / 7.5 (α)[3] ≈ 6.5 (β)[4]**
	$J_{C,P}$					$^{3}J_{C,P}$ 7.0 (α) 7.5 (β)	**$^{2}J_{C,P}$ 4.5 / 4.5 (α)[3] 4.0 / 4.0 (β)[3]**

1 The anomer is given for which at an indicated carbon position a H,C signal is present

2 E.COSY patterns of C4,H4 correlations in α- and β-anomers are overlapping; no exact determination of J

3 H6 hydrogens are diastereotopic and result in two H,C correlations for each anomer

4 Two H6 signals (see [3]) of the β-anomer are overlapping; no exact determination of J

3.4.3.2 Analysis of phosphoglucans prepared from glycogen and starch

Curcuma starch, or glycogen, was enzymatically converted to glucose, oligoglucans and phosphoglucans. Subsequently, the latter were enriched by ion exchange chromatography (see 3.4.2). The derived sample is complex in several aspects. As an example, the enriched phosphoglucans derived from *Curcuma* starch possess a degree of polymerization (DP) ranging from 2 to 7 (i.e. glucan chains of 2 to 7 glucosyl residues; Figure 21), and phosphate esters can be attached at different glucosyl carbons within one glucosyl residue and/or at different glucosyl residues within a phosphoglucan chain. Due to the complexity of the sample, complete assignment of all resonances to specific positions in the oligosaccharides is impossible and the low dispersion of the ^{1}H and ^{31}P resonances prevents an unambiguous identification of phosphorylation sites in one- or two-dimensional approaches that include only ^{1}H and/or ^{31}P resonances. Therefore two-dimensional ^{1}H,^{13}C correlation spectra were obtained utilizing cryogenic probes. Because of the superior signal dispersion, these spectra provide far more detailed information. As shown for samples of authentic monoglucosyl phosphates (see 3.4.3.1) phosphorylation sites in phosphoglucan preparations are also determined by assigning the resonances in the ^{1}H,^{13}C correlation spectra to positions in the sugar moieties and identifying those positions that have a phosphate attached.

Assignment can be based on ^{1}H,^{1}H-DQF-COSY spectra to obtain information about the positions 1, 2, and 3 and on multiplicity editing in ^{1}H,^{13}C correlation spectra to identify the carbons in position 6. In Figure 26 ^{1}H,^{1}H-DQF-COSY spectra of phosphoglucans from *Curcuma* starch and *Epm2a*$^{-/-}$ mouse glycogen are shown. In these spectra signals indicate vicinal coupling hydrogens, i.e. hydrogens on adjacent glucosyl carbons couple via 3 chemical bonds. Concurring with the information about ^{1}H resonances in glucose, maltose, and isomaltose, signals of H1,H2 coupling are found separate from most of the other H,H signals due to the significant downfield offset of the anomeric hydrogen. One of the α(H1,H2) signals in the glycogen sample is even more downfield shifted than the others. It reveals the position of one αH2 (bound to carbon C2 in an α-anomeric glucosyl residue) at 4.01 ppm which is exactly that of αH2 in α-G2P (see Figure 24). This signal is missing in the phosphoglucan preparation of *Curcuma* starch. However, in both samples one αH2 couples with αH3 at approximately 4.5 ppm, significantly downfield offset from the αH3 position in glucose, maltose, and isomaltose but remarkably resembling the position of αH3 in α-G3P.

In Figures 27A and D multiplicity-edited ^{1}H,^{13}C-HSQC spectra of phosphoglucans from *Curcuma* starch and *Epm2a*$^{-/-}$ mouse liver glycogen, respectively, are shown. Grey signals indicate methylene groups, i.e. carbons that carry two hydrogens as in glucosyl carbon C6. Black signals represent methine groups, i.e. carbons each bound to one hydrogen such as those that are part of the pyranose ring. Regarding the pattern of the signals, similarities between *Curcuma* and glycogen preparations are obvious. In both samples a bulk of methylene signals appears at 62-64 ppm (^{13}C chemical shift) and 3.70-4.00 ppm (^{1}H chemical shift). The position of these signals, being similar to H6,C6 signals in glucose and maltose (see Figure 23), implies that they are caused by methylene groups (C6 carbons) of glucosyl residues that neither carry phosphate nor another glucosyl residue at C6. Other methylene groups result in signals that are offset from the bulk. As seen during the analysis of authentic isomaltose and G6P (see 3.4.3.1) an offset of H6,C6 signals can be induced either by α-1,6 branching or phosphorylation at C6. Signals of methylene groups are more disperse in the glycogen preparation which could be due to the higher abundance of

branching points in glycogen as compared to starch. However, in both samples of phosphoglucans, regarding position and pattern, some of these methylene signals (circled in Figure 27) are similar to H6,C6 signals in G6P.

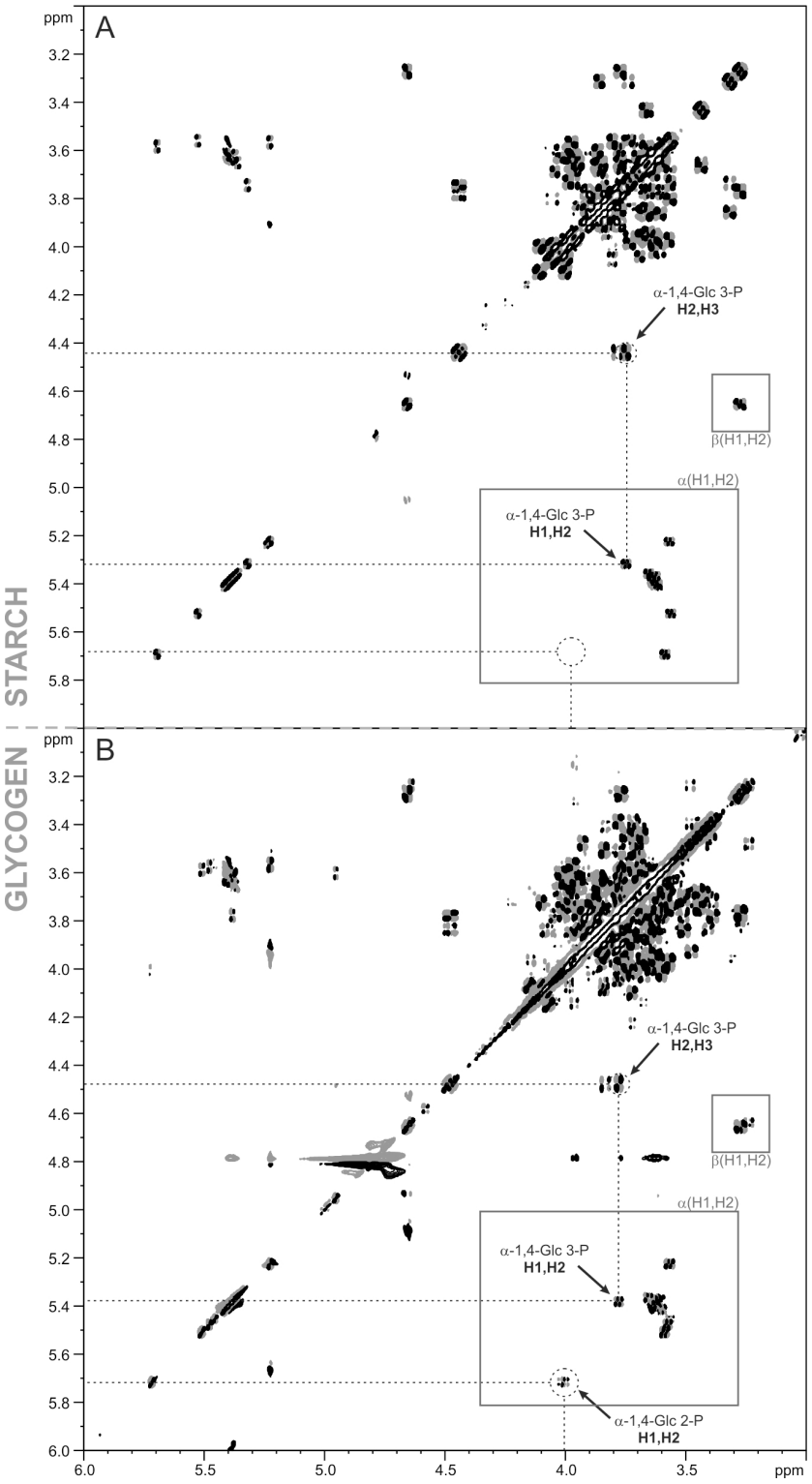

Figure 26. DQF-COSY spectra of phosphoglucans from curcuma starch and *Epm2a*$^{-/-}$ mouse liver glycogen

^{1}H,^{1}H-DQF-COSY of phosphoglucans derived from *Curcuma* starch (A) and *Epm2a*$^{-/-}$ mouse liver glycogen (B). Crosspeaks indicate correlations of vicinal hydrogens on glucosyl residues existing either as α- or β-anomer. Between 5.00 and 5.80 ppm (y-axis) αH1 couple with αH2 occurring between 3.50 and 4.10 ppm (x-axis). βH1 at 4.65 ppm (y-axis) couple with βH2 at 3.28 ppm (x-axis). Circles highlight the hydrogen correlations that are strongly downfield shifted as compared to their counterparts in glucose, maltose, and isomaltose (see Figure 23). The offset resonance of αH2 resides at 4.01 ppm, is only visible in the glycogen sample, and is exactly that of αH2 in α-G2P indicating that the offset H1,H2 signal is caused by α-1,4-glucosyl 2-phosphate residues. That of αH3 occur at 4.44 and 4.47 ppm in starch and glycogen, respectively, resembling the position of αH3 in α-G3P (see Figure 24) indicating that the offset H2,H3 signal is caused by α-1,4-glucosyl 3-phosphate residues.

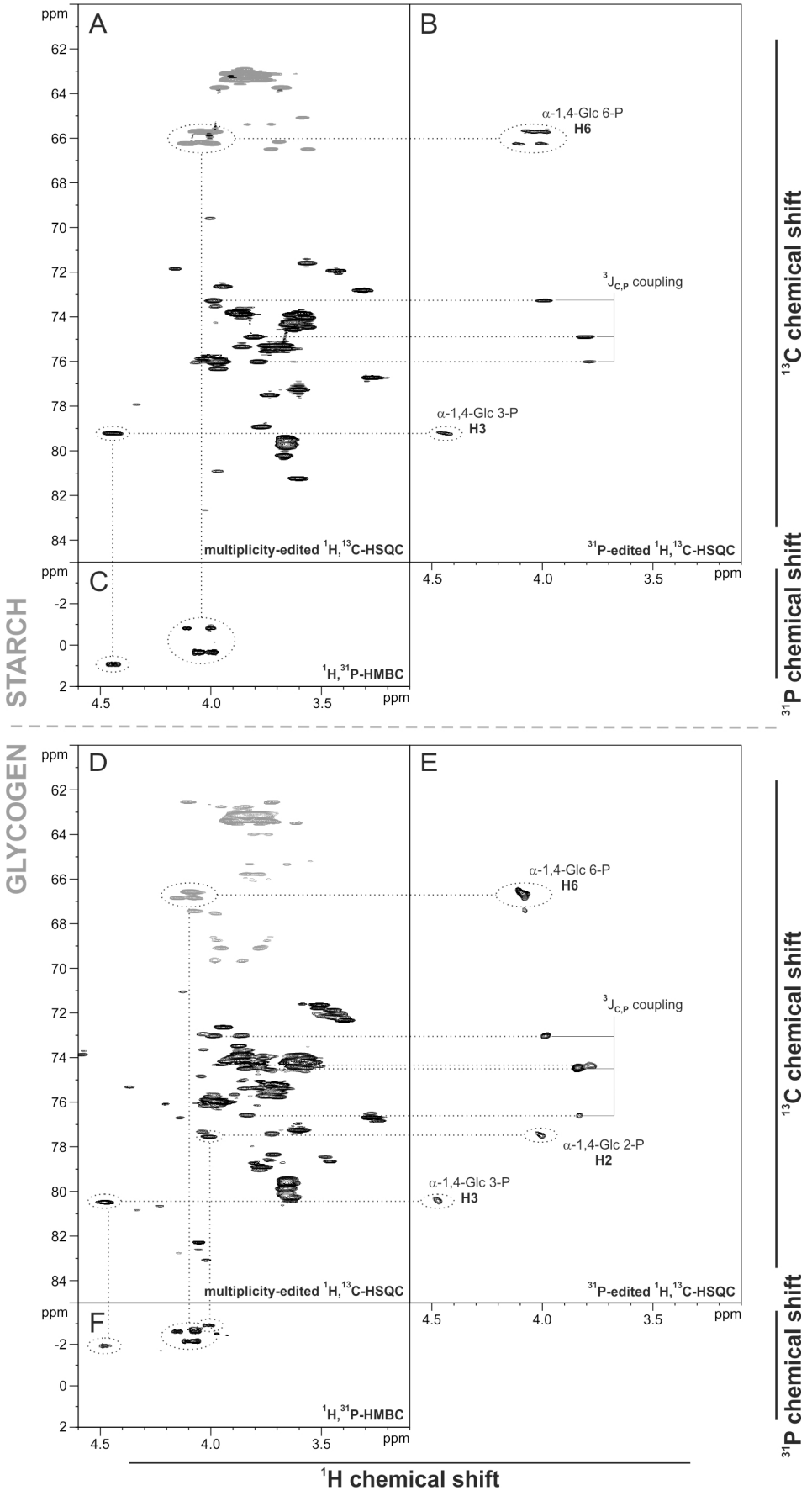
STARCH
GLYCOGEN
A
B
C
D
E
F
α-1,4-Glc 6-P
H6
α-1,4-Glc 3-P
H3
α-1,4-Glc 2-P
H2
$^{3}J_{C,P}$ coupling
multiplicity-edited $^{1}H,^{13}C$-HSQC
^{31}P-edited $^{1}H,^{13}C$-HSQC
$^{1}H,^{31}P$-HMBC
ppm
^{13}C chemical shift
^{31}P chemical shift
^{1}H chemical shift

Figure 27. NMR spectra of phosphoglucans derived from glycogen and *Curcuma* starch

Enriched phosphoglucans of *Curcuma* starch and *Epm2a*$^{-/-}$ mouse liver glycogen (see Figure 22) were analyzed. The region of glucosyl carbon-hydrogen correlations is shown without the anomeric range. (A and D) multiplicity-edited $^{1}H,^{13}C$-HSQC: grey signals indicate methylene groups, black signals point to methine groups. (B and E) ^{31}P-edited $^{1}H,^{13}C$-HSQC: occurring signals indicate either $^{2}J_{CP}$ or $^{3}J_{CP}$ coupling. The former proves connection of phosphate and hydrogen to the same carbon (dotted circles) while the latter occurs when hydrogen and phosphate are bound to adjacent carbons. The assignment to either of the two possibilities was obtained by alignment with signals occurring in the respective $^{1}H,^{31}P$-HMBC and by high-resolution HSQC (see Figure 28). The assignment of H2 and H3 is based upon $^{1}H,^{1}H$-DQF-COSY NMR (see Figure 26). (C and F) $^{1}H,^{31}P$-HMBC: signals indicate vicinal correlation of phosphate and hydrogen.

The attachment of phosphate to carbon atoms is initially detected by $^{1}H,^{31}P$-HMBC spectra and confirmed by ^{31}P-edited $^{1}H,^{13}C$-HSQC spectra. While only the protons directly attached to the carbon carrying the phosphate group are visible in the $^{1}H,^{31}P$-HMBC (Figures 27C and 27F), correlations from these carbons as well as potentially their neighbors are visible in the ^{31}P-edited-$^{1}H,^{13}C$-HSQC. Combining the assignment information of these spectra leads to the identification of the phosphorylated positions (see 3.4.3.1). The $^{1}H,^{31}P$-HMBC spectra (Figures 27C and 27F) reveal that in both phosphoglucan preparations one phosphate is coupling with a hydrogen at around 4.50 ppm. These ^{1}H resonances have been assigned to carbon position 3 using the information of the DQF-COSY spectra (see Figure 26). They also occur in the ^{31}P-edited $^{1}H,^{13}C$-HSQC spectra of both preparations verifying their proximity to phosphate. Likewise both the ^{31}P-edited $^{1}H,^{13}C$-HSQC and the $^{1}H,^{31}P$-HMBC indicate that phosphate is bound to some of the methylene groups whose signal appear offset from the H6,C6 correlations without phosphate association. However, another H,P correlation exclusively appears in the glycogen sample at 4.01 ppm (^{1}H chemical shift). This ^{1}H resonance has been assigned to carbon position 2 using the information of the DQF-COSY spectra (see Figure 26).

Signals appearing in the ^{31}P-edited $^{1}H,^{13}C$-HSQC indicate C,H correlations where the carbon either directly carries a phosphate group ($^{2}J_{C,P}$ coupling) or is the neighbor of an adjacent phosphorylated carbon ($^{3}J_{C,P}$ coupling). Combining the assignment information of $^{1}H,^{31}P$-HMBC and ^{31}P-edited $^{1}H,^{13}C$-HSQC spectra already indicates which signals arise from direct connectivity of phosphate and carbon. This was, however, verified by inspecting the pattern of peaks from the high-resolution $^{1}H,^{13}C$-HSQC spectra as shown in Figure 28. Signals that occur in the respective ^{31}P-edited $^{1}H,^{13}C$-HSQC are marked in the high resolution spectra of phosphoglucans from *Curcuma* starch and glycogen and shown in greater detail. As observed during the analysis of monoglucosyl phosphates (see 3.4.3.1) those carbon positions that directly carry the phosphate group exhibit tilted crosspeaks (exhibiting the $^{2}J_{CP}$ and the $^{3}J_{HP}$ scalar coupling), while the correlations of carbons adjacent to phosphorylation sites show two peaks almost aligned in the ^{1}H direction, as the $^{4}J_{HP}$ coupling is usually quite small and only the $^{3}J_{CP}$ coupling leads to a detectable splitting. Observation of tilted crosspeaks in the high resolution $^{1}H,^{13}C$-HSQC is consistent with the occurrence of peaks in the $^{1}H,^{31}P$-HMBC spectra.

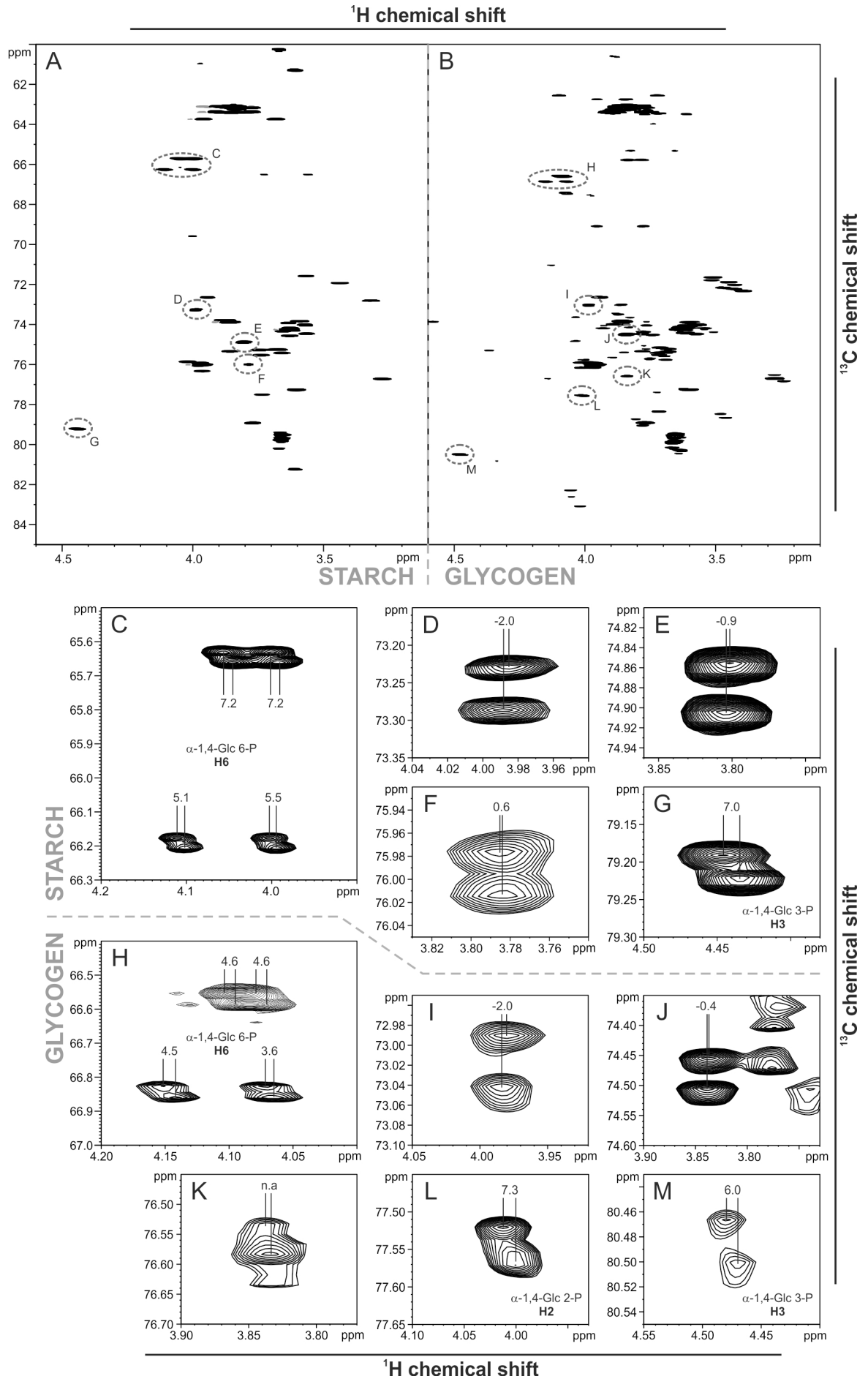
^{1}H chemical shift
^{13}C chemical shift
A
B
C
D
E
F
G
H
I
J
K
L
M
STARCH
GLYCOGEN
α-1,4-Glc 6-P
H6
α-1,4-Glc 3-P
H3
α-1,4-Glc 2-P
H2
n.a
ppm

Figure 28. High-resolution HSQC of phosphoglucans from *Curcuma* starch and *Epm2a*$^{-/-}$ mouse liver glycogen

Enriched phosphoglucans of *Curcuma* starch and *Epm2a*$^{-/-}$ mouse liver glycogen (see Figure 22) were analyzed. Signals that occur in the ^{31}P-edited ^{13}C,^{1}H-HSQC (Figures 27B and 27E) are marked in the high-resolution ^{1}H,^{13}C-HSQC spectra of *Curcuma* starch (A) and *Epm2a*$^{-/-}$ mouse liver glycogen (B). (C to M) The marked signals (C through M) in the panels (A) and (B) are processed with high resolution and shown in greater detail. The phosphorus induced tilt in the hydrogen dimension of each signal is given in Hz. Larger values for $^{3}J_{H,P}$ coupling indicate that phosphate and hydrogen are connected to the same carbon. The assignment of H6 is done with respect to the multiplicity-edited ^{13}C,^{1}H-HSQC (Figure 27) showing a methylene group at that position. H2 and H3 are assigned by ^{1}H,^{1}H-DQF-COSY experiments (Figure 26).

The presence of C6 phosphorylation in *Epm2a*$^{-/-}$ liver glycogen and *Curcuma* starch can be conclusively demonstrated by the occurrence of phosphorylated methylene groups. *Curcuma* starch, as well as glycogen, contains an additional phosphate at position C3. For glycogen, a third phosphorylation site exists at C2. However, monophosphate at C2 is below the limit of detection in phosphoglucans from *Curcuma* starch.

Additionally phosphoglucans were prepared from wild type rabbit skeletal muscle. H,C correlations showing phosphate coupling are identical to those of *Epm2a*$^{-/-}$ mouse liver glycogen (Figure 29). Thus, rabbit glycogen is phosphorylated similarly at carbon C2, C3, and C6. This proves that the presence of C6 phosphate in glycogen is neither species specific nor restricted to Lafora disease.

The NMR data presented here reveals no evidence for the occurrence of phosphodiesters in phosphoglucan preparation of starch and glycogen. Using 1D ^{31}P-NMR a phosphate signal was detected that revealed coupling of phosphate with two hydrogens but that differed in chemical shift from phosphate in G6P. However, the presence of this additional phosphate signal can be explained comparing the ^{1}H,^{13}C-HSQC (or HMQC) and ^{1}H,^{31}P-HMBC spectra of phosphoglucans from *Curcuma* starch and glycogen with those of G6P. The HMQC of G6P shows 4 signals of phosphorylated methylene groups, two of which are aligned in the ^{13}C dimension. This indicates the presence of two diastereotopic H6 in both anomers of G6P. The phosphate signals of the α- and β-anomer of G6P have a similar ^{31}P chemical shift as observed in the ^{1}H,^{31}P-HMBC. Thus, they appear close together in a 1D ^{31}P-NMR spectrum. The phosphorylated methylene groups in the phosphoglucan preparations also consist of 4 signals, two of which are aligned in ^{13}C dimension. This indicates that in the phosphoglucan preparations some of the C6 phosphates are connected to the glucosyl residue containing the reducing end enabling the distinction between signals of α- and β-anomeric states. However, phosphate signals at C6 of the α- and β-anomeric glucosyl residues exhibit substantially different ^{31}P chemical shift. Thus, they appear as two remote signals in 1D ^{31}P-NMR spectra, both showing vicinal connection to 2 hydrogens. Furthermore, no phosphate signals were observed that correlate with two hydrogens at different glucosyl carbon positions. This verifies the absence of phosphodiester bonds.

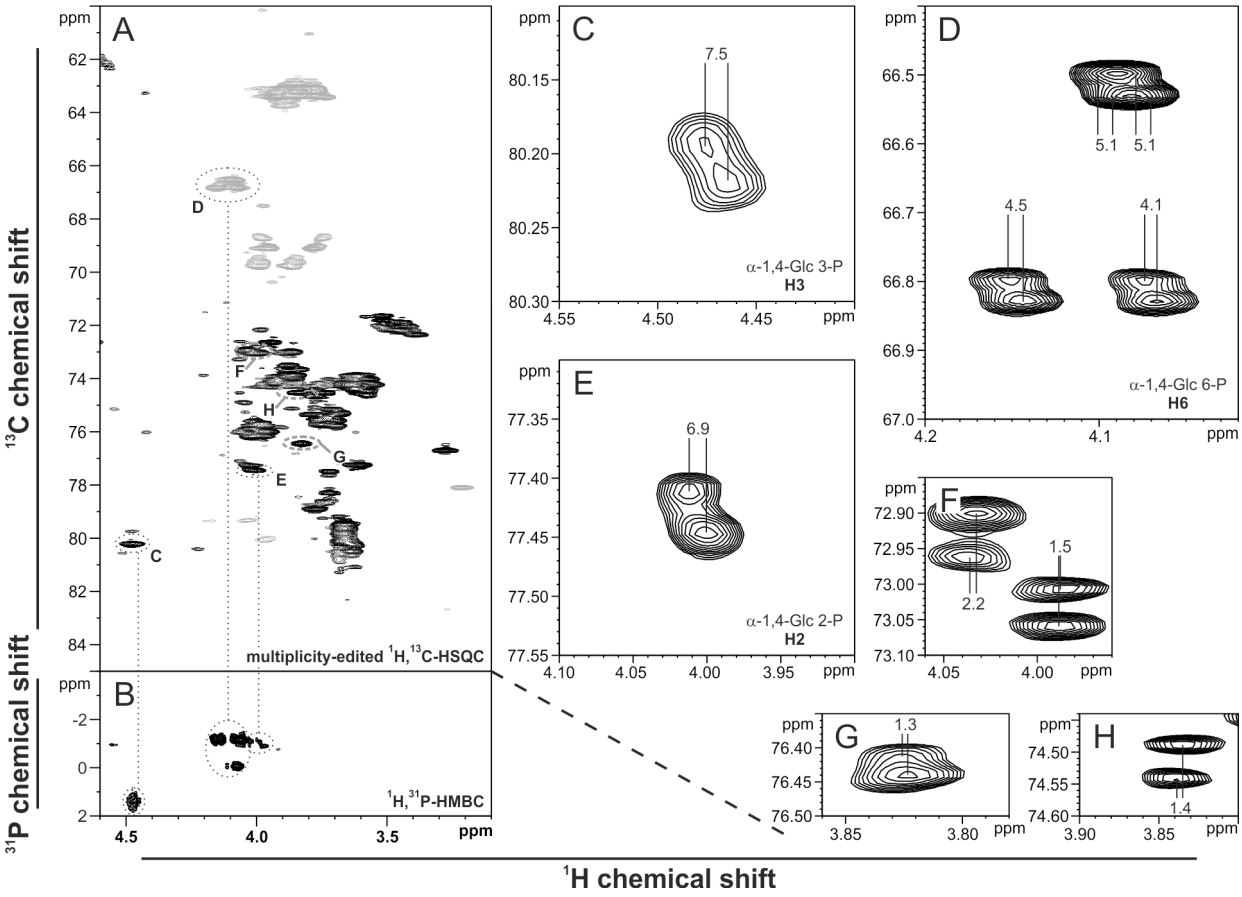

Figure 29. NMR spectra of phosphoglucans from wild type rabbit muscle glycogen

Phosphoglucans of wild type rabbit skeletal muscle glycogen were enriched by anion exchange chromatography. Fractions eluting between 20 and 200 mM NH_4OAc were analyzed. The region of glucosyl carbon-hydrogen correlations is shown without the anomeric range. (A) Multiplicity-edited ^{1}H,^{13}C-HSQC: grey signals indicate methylene groups (H6), black signals point to methine groups (hydrogens at the glucosyl ring). Signals showing carbon phosphorus coupling in ^{31}P-edited ^{1}H,^{13}C-HSQC spectra of phosphoglucans prepared from *Epm2a*$^{-/-}$ mouse liver glycogen (Figure 27E) are labeled ($^{2}J_{C,P}$ – black dotted circles, $^{3}J_{C,P}$ – grey dashed circles) and indexed (letters C through H, referring to the panel caption). (B) ^{1}H,^{31}P-HMBC: signals indicate vicinal correlation of phosphate and hydrogen ($^{3}J_{H,P}$) strictly correlating with the $^{2}J_{C,P}$ coupling signals in (A). (C to H) Labeled signals in (A) are shown in a high-resolution ^{1}H,^{13}C-HSQC spectrum and zoomed in. The phosphorus induced tilt in the hydrogen dimension of each signal is given in Hz. Larger values for $^{3}J_{H,P}$ coupling indicate that phosphate and hydrogen are connected to the same carbon. The assignment of H6 is done with respect to the multiplicity-edited ^{13}C,^{1}H-HSQC (A) showing a methylene group at that position. H2 and H3 are assigned by their identical position in the spectra of phosphoglucans prepared from *Epm2a*$^{-/-}$ mouse liver glycogen (Figures 26 and 27).

3.5 Size Distribution and Side Chain Pattern of Wild Type and Lafora Disease Glycogen

The results in this study show that C6 phosphate at least in skeletal muscle is elevated by factor 8 in both types of LD. Relationships between the amount of C6 phosphate and other structural features of glycogen, such as molecule size distribution and linear side chain pattern, were studied using muscle glycogen isolated from wild type as well as the two LD mouse models, *Epm2a*$^{-/-}$ and *Epm2b*$^{-/-}$.

To determine the size distribution of glycogen molecules equal amounts of glycogen were applied to flow Field-flow fractionation (fFFF) with multi-angle laser light scattering (MALLS) and differential refractive index (DRI) detection. Using this technique, molar mass and concentration are

simultaneously determined during elution of glycogen molecules separated by size. Concentration and molar mass are typically plotted over elution volume to display size distribution.

Size distribution data from 6 biological parallels for each genotype was obtained. At equal elution volumes averaged DRI as well as molar mass values were calculated among biological parallels. The averaged size distributions of muscle glycogen from wild type, *Epm2a*$^{-/-}$, and *Epm2b*$^{-/-}$ mice are displayed in Figure 30A while the average molar mass is shown in Figure 30B. Both reveal that glycogen from LD mice differs significantly from that of the wild type control. However, size distribution does not correlate with hyperphosphorylation as glycogen from *Epm2a*$^{-/-}$ mice is smaller than that of wild type while size in *Epm2b*$^{-/-}$ mice exceeds that of wild type glycogen.

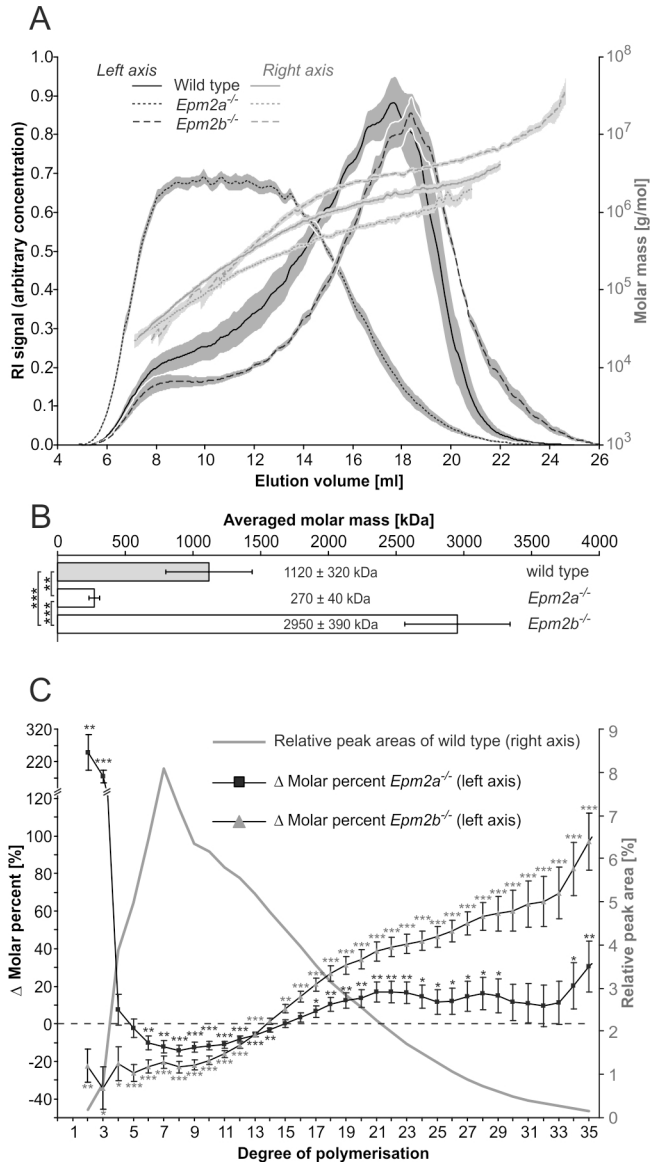

Figure 30. Molar masses and chain patterns of muscle glycogen in wild type and LD mice

(A) Averaged size distributions of muscle glycogen isolated from wild type, *Epm2a*$^{-/-}$, and *Epm2b*$^{-/-}$ tissue as determined by fFFF-MALLS-DRI. *Grey shadows* reflect SEM (n = 6 biological replicas). The left scale reflects concentration (DRI signals, black lines); the right scale displays molar mass (grey lines). (B) Averaged molar masses of the three types of glycogen. Error: SD (n = 6 biological replicas). (C) Linear side chain patterns of skeletal muscle glycogen isolated from wild type, *Epm2a*$^{-/-}$, and *Epm2b*$^{-/-}$ tissue as determined by HPAEC-PAD (separation mode 3) following exhaustive isoamylolysis. Mean relative peak areas of each chain length was calculated (n = 6 biological replicas per genotype) and are given for wild type glycogen. Δmolar percent was calculated: [$area_{mutant}$ - $area_{wild\ type}$] / $area_{wild\ type}$ * 100. It reflects the quantitative change of a particular chain length in a mutant as compared to the abundance in wild type (100%). A T test was used to test significance of the quantitative change at each chain length in comparison to wild type. Error: sum of SDs from wild type and mutant.

Furthermore, glycogen of wild type and LD mice was completely debranched by over night incubation with isoamylase from *Pseudomonas*. Linear α-glucans released were separated by HPAEC-PAD (separation mode 3). The degree of polymerization (DP) of the linear glucans derived from wild type glycogen ranges from 2 to over 30 glucosyl units, with DPs of 5 to 15 being most prominent. Chain patterns from LD glycogen differ but deviations are complex: laforin-deficient

glycogen is increased in very short side chains (DP2 and DP3) as compared to wild type control. Medium-sized chains (DPs 3 to 13) are less frequent but long chains (DP ≥15) are more abundant than in the control. Glycogen from malin-deficient mice is to some extent similar to laforin-deficiency but clearly deviates in the very short chains, which are less abundant than in wild type glycogen. Abundance of larger side chains (DP ≥15) is even higher than in laforin-deficiency (Figure 30C).

Thus, in both LD mutants glycogen structure appears profoundly altered. However, the alterations do not always align with hyperphosphorylation. This implies that phosphorylation is only one of the parameters that determine the glycogen structure.

3.6 Localization of 6-phosphoglucosyl residues in glycogen molecules

In this study it has been shown that glucosyl carbon C6 is a major phosphorylation site in glycogen. Using skeletal muscle glycogen isolated from wild type mice attempts were made to determine the distribution of 6-phosphoglucosyl residues in glycogen. This distribution could be even or uneven among glycogen molecules of different sizes. Likewise within glycogen molecules 6-phosphoglucosyl residues could be distributed even or uneven between periphery and core regions. Furthermore the chain length pattern could be different or equal in glycogen molecules of different sizes. As outlined in Figure 31 three approaches were used to examine these possibilities.

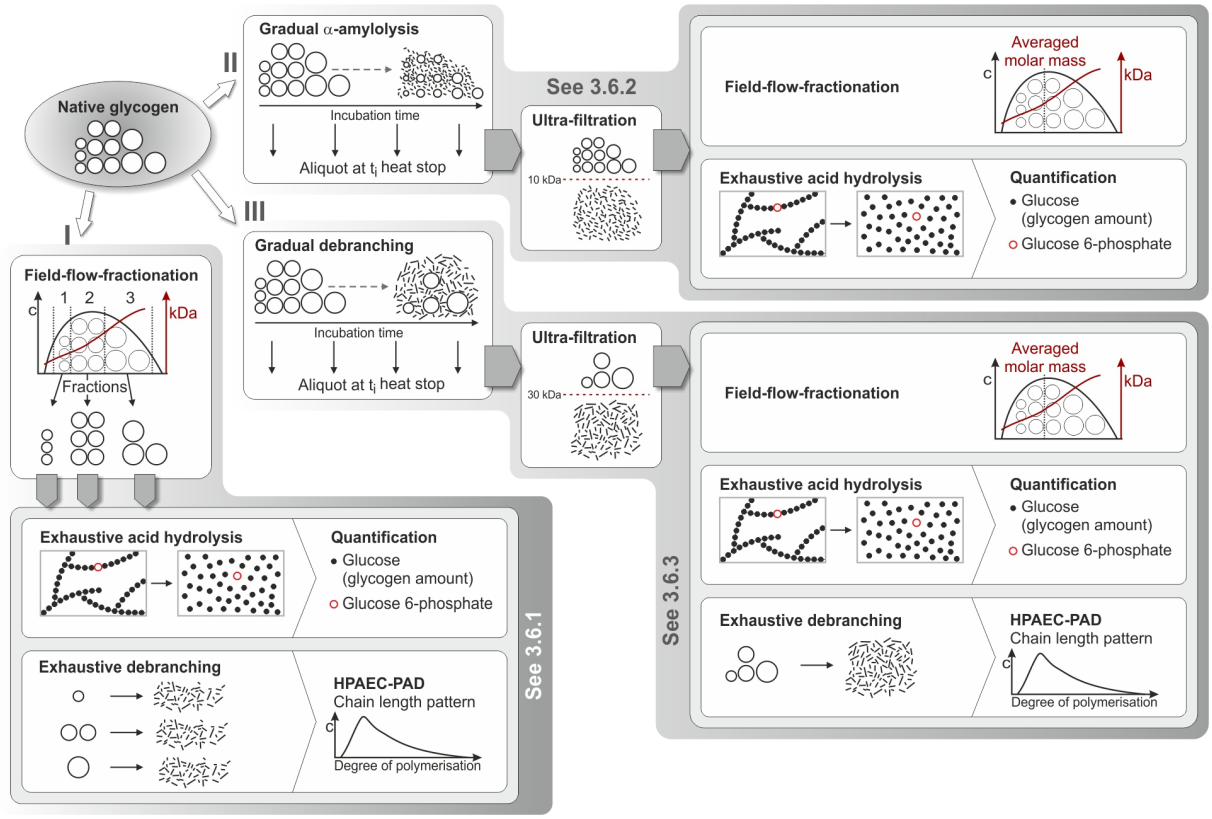

Figure 31. Distribution analysis of glucosyl 6-phosphate residues in glycogen – design of experiments

Three approaches are outlined. (I) Fractionation of native glycogen into three fractions by fFFF-MALLS-DRI and subsequent analyses regarding 6-phosphoglucosyl residues and linear side chain patterns. Gradual α-amylolysis (II) and isoamylolysis (III) of native (non-fractionated) glycogen and carbohydrate analyses following membrane filtration. The results of the approaches are shown in the sections indicated.

In the first, the possibility was investigated that C6 phosphate is enriched either in smaller, intermediate or bigger glycogen molecules. Likewise it was examined whether molecules of different sizes have altered abundance of distinct linear chains lengths. Therefore glycogen was resolved into three fractions containing different averaged molecule sizes (small, intermediate, large). The fractions were subsequently analyzed with respect to glucose-based C6 phosphate and linear chain length distribution.

The second approach aimed to investigate the distribution of 6-phosphoglucosyl residues between molecule periphery and core by gradual α-amylolytic glycogen degradation and quantification of C6 phosphate after differential removal of glucose from the molecule periphery.

The third approach is similar to the second despite that gradual degradation of glycogen was achieved by debranching with isoamylase.

3.6.1 C6 phosphorylation and chain length distribution are independent of glycogen molecule size

Native skeletal muscle glycogen isolated from wild type mice was subjected to fFFF-MALLS-DRI. During elution three fractions were collected that contained small, medium, and large size glycogen molecules whose averaged molecular weight differs by more than one order of magnitude (Figure 32A). Following exhaustive acid hydrolysis (procedure B2), the glucose-based G6P content was determined enzymatically. In all three fractions it was found similar (Figure 32A) indicating that glycogen size does not noticeably correlate with the relative G6P content.

Additionally, aliquots of each glycogen fraction were exhaustively debranched by isoamylase followed by determination of chain length distribution using HPAEC-PAD. As shown in Figure 32B the three fractions have similar chain patterns. Thus, neither glucose-based G6P content nor chain length distribution varies with molecule size of native glycogen.

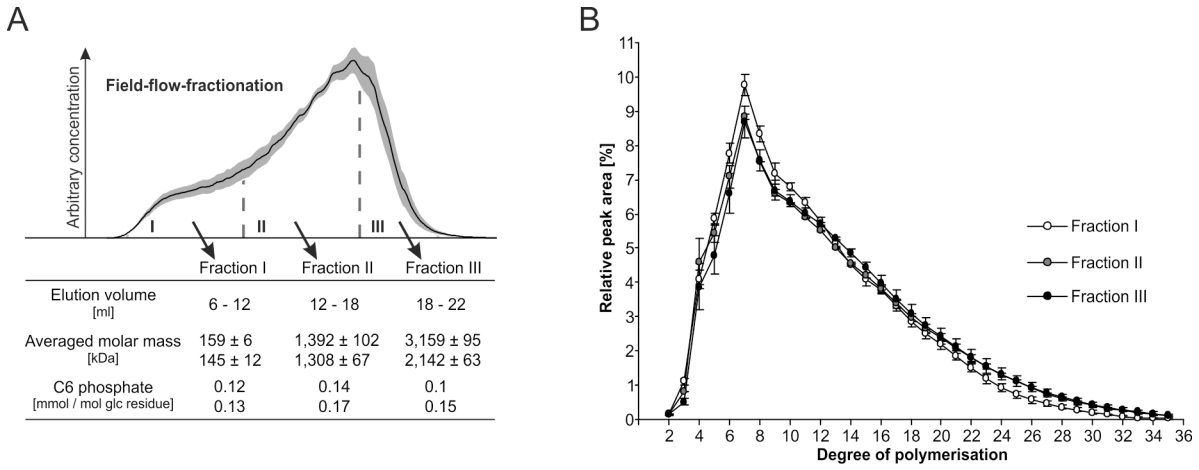

	Fraction I	Fraction II	Fraction III
Elution volume [ml]	6 - 12	12 - 18	18 - 22
Averaged molar mass [kDa]	159 ± 6 145 ± 12	1,392 ± 102 1,308 ± 67	3,159 ± 95 2,142 ± 63
C6 phosphate [mmol / mol glc residue]	0.12 0.13	0.14 0.17	0.1 0.15

Figure 32. 6-Phosphoglucosyl residues and side chain pattern with respect to glycogen molecule size

The experimental design is outlined in Figure 31 (first approach). (A) Two preparations of skeletal muscle glycogen independently isolated from wild type mice applied to fFFF-MALLS-DRI was collected in three fractions (I, II, III). Fractions I, II, and III obtained in 3 consecutive applications of the same glycogen preparation were combined and mean averaged molar mass was calculated for each fraction (error: SD of 3 applications). In the three fractions, glucose-based G6P content was determined (two values for two experiments carried out on two individual glycogen preparations). (B) Following exhaustive debranching, chain patterns of the glycogen fractions were determined by HPAEC-PAD. Relative peak area is given at each DP representing the average of two experiments with individual glycogen preparations (error: absolute deviation).

3.6.2 C6 phosphorylation is largely found in the center of glycogen molecules

In a second approach (see Figure 31) native glycogen was gradually degraded by α-amylase, an endo-acting enzyme capable of cleaving interglucose bonds in chains exceeding 3 residues from a branching point or from a phosphate ester (Posternak, 1951; Hizukuri *et al.*, 1970; Roberts and Whelan, 1960). Thus, the action of α-amylase on glycogen is not significantly affected by branchings and essentially not limited by the rare phosphoesters present in glycogen.

At intervals, aliquots of the reaction mixture containing glycogen and α-amylase were withdrawn and stopped by heat treatment. Using membrane filtration (10 kDa cut-off) the remaining glycogen was separated from α-amylolytically released glucose and oligoglucans. The remaining glycogen residing in the retentate was further analyzed. Size distribution was determined by fFFF-MALLS-DRI and, following acid hydrolysis (procedure B2), both glucose and G6P were quantified.

During α-amylolysis the size distribution of glycogen changes (Figure 33A). The molecules gradually elute earlier from the fFFF channel corresponding to their gradual decrease in averaged molecule size. Interestingly, the amount of remaining glycogen decreases in remarkably similar fashion. When after 13 min incubation around 50% of the initial glycogen has been released the averaged molecule size is reduced by around 40%. Likewise after 30 min incubation 70% of the glycogen has been converted to a size smaller than 10 kDa and the averaged molecule size is about 30% of the initial. Finally, both parameters reach values between 5 and 13% of the respective initial after 80 min incubation (Figure 33B).

During α-amylolysis the total amount of C6 phosphate determined as G6P in the glycogen hydrolysate also decreases indicating that glucan chains phosphorylated at C6 are to some extent also released by α-amylase. However, both glycogen amount and averaged size decrease more strongly than G6P and, consequently, glucose-based G6P levels increase several-fold in the partially degraded glycogen molecules (Figure 33B).

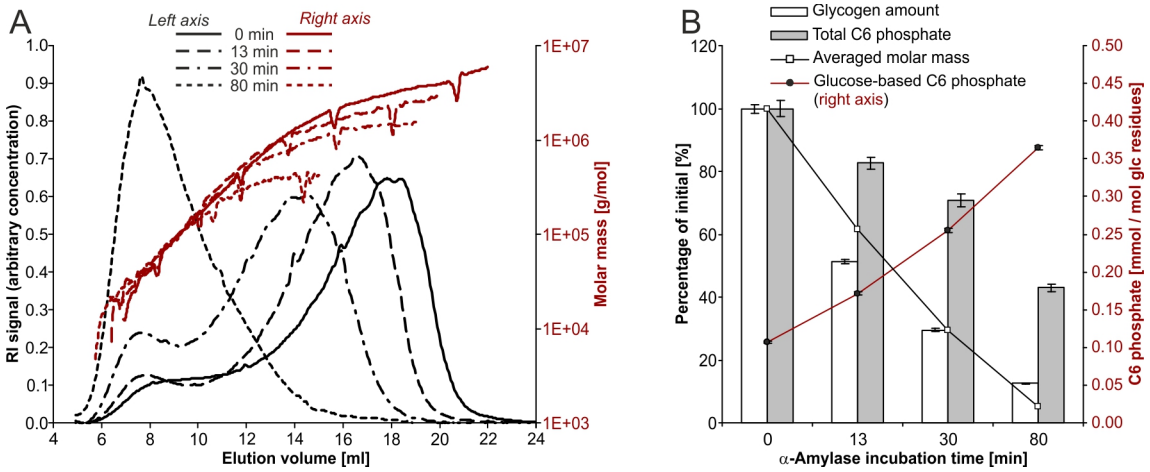

Figure 33. Molecule size and glucose-based C6 phosphate during gradual α-amylolysis of glycogen

The experimental design is outlined in Figure 31 (second approach). (A) Molar mass distributions (fFFF-MALLS-DRI) of glycogen partially degraded by α-amylase but retained by the 10 kDa filter. DRI signal intensities (black lines, left axis) and molar masses (red lines, right axis) are given. (B) Averaged masses and amounts of glucosyl and G6P residues (each given as % of the initial values of glycogen; left scale) and glucose-based G6P levels (right scale) of the partially degraded glycogen. Mean ± SD (n = 3, technical replica; one of two independent experiments is shown).

Similar results would be obtained making two assumptions: 1) α-amylase preferably digests larger glycogen molecules and 2) smaller glycogen molecules, being, thus, enriched during α-amylolysis, contain significantly more 6-phosphoglucosyl residues than larger molecules, which are degraded first. However, since native glycogen did not show a correlation between size distribution and glucose-based G6P levels (see 3.6.1), the increased glucose-based G6P levels at later stages of α-amylolysis are not due to preferential degradation of distinct glycogen molecule sizes by α-amylase.

Thus, the data strongly suggest that 6-phosphoglucosyl residues are unevenly distributed within glycogen molecules. Their location being largely in interior parts of the molecules prevents release of glucosyl and 6-phosphoglucosyl residues with similar probability and, thus, leads to the observed increase of glucose-based C6 phosphate during gradual α-amylolysis.

It was furthermore considered that α-amylolysis might not be equally effective on all parts of the glycogen molecule surface. Therefore, in a separate experiment the glycogen surface was labeled and, during subsequent α-amylolysis, degradation of glycogen as well as the release of label was monitored.

Muscle glycogen from WT mice was pre-labeled by incubating with [^{14}C]glucose 1-phosphate and phosphorylase a (pho a) from rabbit muscle. For sterical reasons, the catalytic action of pho a is likely to be restricted to the periphery of glycogen molecules. For pre-labeling two incubation mixtures (Batch 1 and 2 in Figure 34A) were used in which the amounts of phosphorylase and the specific radioactivities of glucose 1-phosphate varied by one order of magnitude (high phosphorylase level at low specific radioactivity of G1P and *vice versa*). This way, different amounts of glucosyl residues were transferred to the glycogen surface while the incorporated label was similar (Figure 34A). Following termination of the reaction, glycogen was purified by exhaustive membrane filtration (10 kDa cut-off).

A

^{14}C-labeling of glycogen by phosphorylase a

Conditions of phosphorylase a incubation		
	Batch 1	**Batch 2**
Pho a in batch [mg/ml]	0.22	2.2
[^{14}C] glucose 1-phosphate [µCi]	5.36	0.75
Results after incubation with phosphorylase a		
	Batch 1	**Batch 2**
Incorporated label in glycogen [µCi]	0.45	0.30
Percentage of used G1P [%]	8.5	40.0
Δ Glucosyl residues in glycogen [%]	2.4	11.5

B

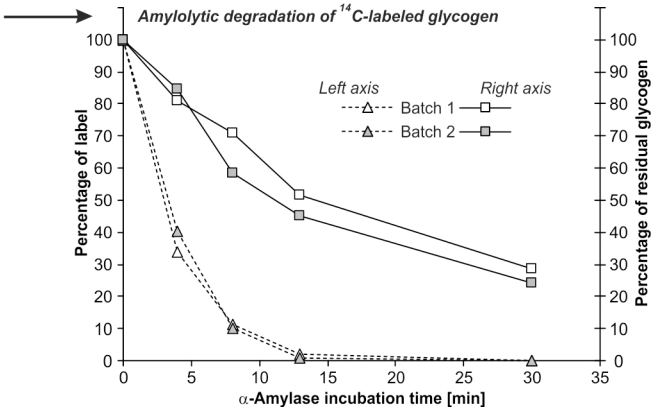

Figure 34. α-Amylolytic degradation of [^{14}C] pre-labeled glycogen

(A) Muscle glycogen from wild type mice was pre-labeled by incubating with [U-^{14}C]glucose 1-phosphate and phosphorylase a from rabbit muscle using two incubation mixtures with varying amounts of phosphorylase and specific radioactivities of glucose 1-phosphate (batch 1 and 2). Following termination of the reaction, glycogen was purified by membrane filtration (10 kDa cut-off) with exhaustive washing of the retentate. Label in the retentate was quantified using a scintillation counter. (B) Aliquots of the pre-labeled glycogen preparations (batch 1 and 2) were digested with α-amylase. At intervals, aliquots of the reaction mixtures were heat treated followed by removal of liberated α-glucans by ultrafiltration. Contents of [^{14}C] label and the remaining glycogen were quantified. The [^{14}C] label as well as the glycogen content is given as % of that of the pre-labeled glycogen before the onset of α-amylolysis.

Aliquots of the pre-labeled glycogen preparations were digested with α-amylase applying identical conditions (including glycogen and α-amylase concentration) as when glycogen was gradually degraded without pre-labeling. At intervals, aliquots of the reaction mixtures were heat treated to denature the hydrolases. Following removal of the liberated α-glucans by ultrafiltration, contents of [^{14}C] label and, after acid hydrolysis, glucose equivalents in the remaining glycogen were quantified. In both pre-labeled glycogen preparations, the amounts of glucosyl residues transferred during pre-labeling vary depending on the phosphorylase activity. However, using both pre-labeled glycogen preparations, [^{14}C] label is consistently released much faster as compared to non-labeled glucosyl residues. The relative [^{14}C] labeling declines to the limit of detection during 13 min of α-amylolysis indicating that the action of the α-amylase starts at the periphery which is largely degraded before regions are reached that were originally placed in central parts of the glycogen molecules (Figure 34B).

3.6.3 C6 phosphorylation is correlated with long glycogen side chains

In a third approach (see Figure 31), native glycogen prepared from wild type mice was gradually debranched by isoamylase and at intervals aliquots of the reaction mixtures were passed through a 30 kDa filter to remove released linear chains from non-degraded glycogen remaining in the retentate. Aliquots of the latter were analyzed by fFFF-MALLS-DRI or subjected to exhaustive acid hydrolysis (procedure B2) followed by glucose and G6P quantification. Furthermore, aliquots of the partially degraded glycogen underwent a second debranching which was executed overnight with higher isoamylase concentration to ensure completeness. The resultant chain patterns were analyzed by HPAEC-PAD.

As with α-amylase, isoamylase treatment results in gradually decreasing glycogen content. However, as demonstrated in two independently performed experiments, the averaged glycogen size does not decrease in the fashion observed during α-amylolysis (Figures 35 and 37A). Following a decrease to ca. 75% within the first 10 minutes, the averaged molecule size remains largely constant throughout the remaining incubation, while the degradation progresses, as demonstrated by the further decreasing glycogen content.

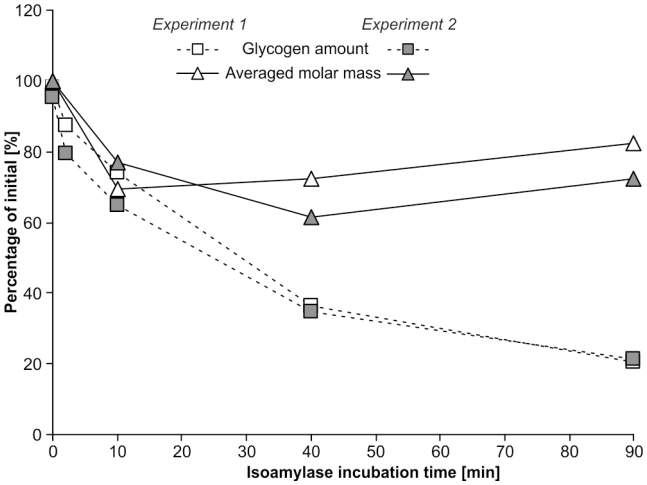

Figure 35. Change of averaged molecule size during isoamylolysis of glycogen

Averaged molar masses and amounts of glucosyl residues of glycogen are monitored during isoamylolysis of glycogen isolated from wild type mice. Values are given as % of the initial values of the same sample). Mean ± SD (n = 3, technical replica of glycogen determination, SD might be too small to be visualized). Two independent lines of experiments are shown.

A degradation of glycogen without alterations of the averaged molecule size can be explained by a sequential mode of isoamylase action. As illustrated in Figure 36, assuming such mode degradation

does not occur at the surface of all glycogen molecules simultaneously. This would decrease the averaged molecule size by decreasing the individual size of many glycogen molecules. Rather the enzymes complete the degradation of one molecule before acting on another. The number of molecules thereby decreases during degradation but the averaged molecule size remains constant if the enzyme has equal affinities towards molecules of all sizes. This seems to be largely the case during isoamylolysis of glycogen under the condition used in these experiments.

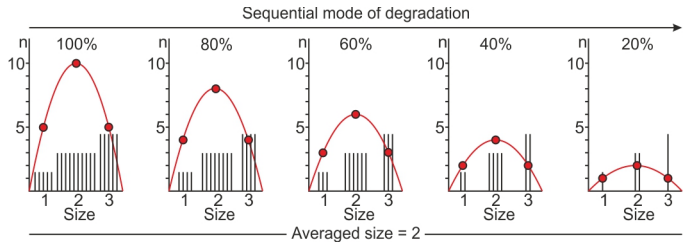

Figure 36. Illustration of the sequential mode of enzymatic glycogen degradation

Simplified alteration of glycogen size distribution during degradation assuming a sequential mode of enzymatic action. For simplification glycogen is assumed to consist of molecules with 3 distinct sizes that differ in number (indicated as black bars). Size distribution (circles interconnected by red line) is determined by number of molecules n (y-axis) at different molecule sizes (x-axis). If the enzyme has equal affinities towards molecules of all sizes and if enzymes complete the degradation of one molecule before acting on another (sequential mode) a simultaneous decrease of glycogen amount and the maintenance of the averaged molecule size is possible.

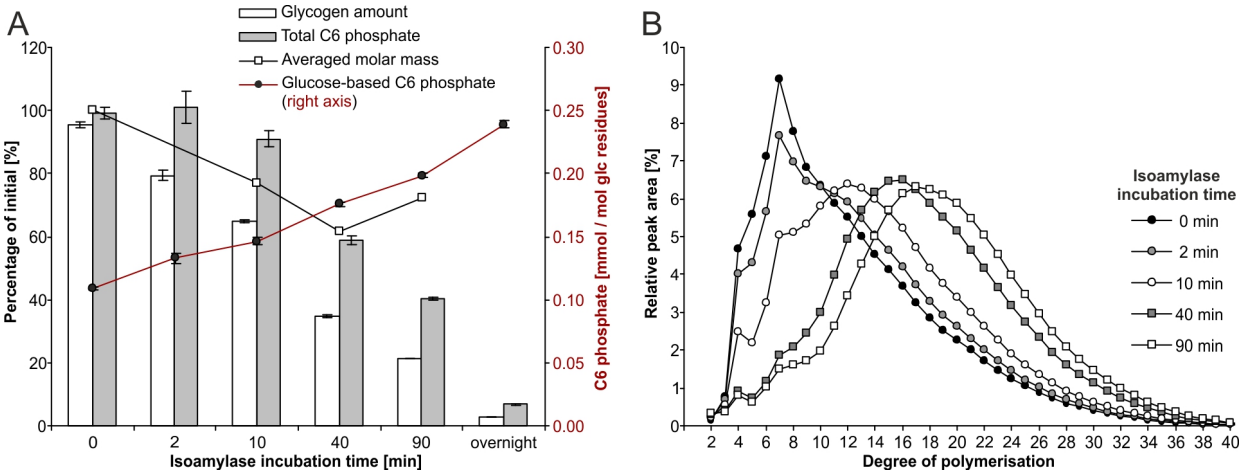

Figure 37. Molecule size and glucose-based C6 phosphate during gradual isoamylolysis of glycogen

The experimental design is outlined in Figure 31 (third approach). (A) Averaged molecule masses, amounts of glucosyl and G6P residues (each given as % of the initial values of glycogen; left scale) and glucose-based C6 phosphate levels (right scale) of glycogen retained by a 30 kDa filter during isoamylolysis. The release of 6-phosphoglucosyl residues takes place at much slower rate, resulting in an increase of glucose-based C6 phosphorylation in the partially degraded glycogen molecules. Mean ± SD (n = 3, technical replica; one of two independent experiments is shown, see Figure 35). (B) During isoamylolysis, the partially degraded glycogen was separated from released glucan chains and subjected to a second (exhaustive) debranching prior to HPAEC-PAD analysis. The chain pattern of partially degraded glycogen shifts towards higher DPs during gradual isoamylolysis. Together with the increased glucose-based G6P content (A), this result indicates that G6P residues occur more frequently in glycogen regions containing longer side chains.

During isoamylolysis, chain patterns of the residual glycogen were greatly altered. Smaller side chains were lost first and the remaining glycogen became enriched in longer side chains (Figure 37B). This enrichment also occurs at later stages of gradual isoamylolysis when the averaged molecule size remains largely unchanged. This indicates that isoamylase has a preference for those molecules that possess small side chains, and that apparently among all sizes of glycogen

molecules some consist of shorter others of longer side chains. The former are degraded first while the latter are initially enriched being only degraded at later stages of the isoamylolysis.
Interestingly, the glycogen being composed of longer side chains and, thus, being degraded at later stages of isoamylolysis showed increased glucose-based G6P content. This indicates that monoesterification at C6 positively correlates with chain length. Notwithstanding, glucan chains phosphorylated in C6 are to some extent removed during isoamylolysis indicating that 6-phosphoglucosyl residues also, but to a lesser extent, occur on glycogen molecules possessing smaller side chains (Figure 37A).

4 Discussion

Plants and animals store energy and reduced carbon as carbohydrates. Typically, transitory starch is built up in chloroplasts when sufficient light energy and CO_2 is available. Likewise, animals synthesize glycogen in the cells of various tissues when glucose is sufficiently provided as it is the case during feeding or in the first hours after food intake. Degradation of transitory starch occurs mainly during the night to maintain all vital metabolic processes by providing adequate amounts of energy and reduced carbon when photosynthesis is impossible. Similarly, products of glycogen degradation are used in the postabsorptive state. In muscle glycogen stores serve for fast local supply of energy when muscular activity is required. It is obvious that functionality of storage carbohydrate synthesis and degradation determine the vitality of plants and animals (Taiz and Zeiger, 2006; Zeeman *et al.*, 2010; Frayn, 2003; Villar-Palasi and Larner, 1968; Wolfsdorf and Weinstein, 2003).

The structures of both types of carbohydrate share major similarities but are also different in some aspects. Glycogen and the major component of starch, amylopectin, consist of branched polyglucan chains, the glucosyl residues of which are connected either by α-1,4 or α-1,6 glucosidic bonds. However, the differential arrangements of chains render glycogen molecules water-soluble while starch comprises water-insoluble particles. Due to the structural similarities, synthesis and degradation of transitory starch and glycogen are accomplished by a series of enzymatic activities that are also to some extend similar in plants and animals. Chain elongation, branching, and debranching are achieved by synthases, branching enzymes, and debranching enzymes, respectively (Zeeman *et al.*, 2010; Roach *et al.*, 2012). Differences lay for instance in the initiation of polyglucan synthesis and in the abundance of isoforms for each enzymatic function. Glycogen metabolism is often severely affected if one of the enzymes involved is defective since compensation by isoforms is usually impossible (Wolfsdorf and Weinstein, 2003). While glycogen synthesis requires glycogenin as both self-glucosylating and chain elongating enzyme (Krisman and Barengo, 1975; Roach *et al.*, 2012) starch *de novo* synthesis is probably accomplished by the concurrent action of more than one starch synthase isoform (Roldán *et al.*, 2007; Szydlowski *et al.*, 2009). Furthermore, while starch degradation relies mainly on hydrolytic enzymes (Fulton *et al.*, 2008) glycogen is believed to be mainly degraded using the phosphorolytic path (Roach *et al.*, 2012). However, in many animals (including humans) the hydrolytic pathway (though attributed to another compartment) is also established and necessary for functional glycogen metabolism (Matsui *et al.*, 1984; Reuser *et al.*, 1995).

Another structural feature of starch and glycogen has been found to play an important role in functional polyglucan metabolism. Phosphate esters were detected in both types of polyglucans already some decades ago (Hizukuri *et al.*, 1970; Tabata and Hizukuri, 1971; Fontana, 1980). Their abundance varies between polyglucans from different species and organs but is generally low. The degree of glucose-based phosphorylation in starch and glycogen is, however, in the same range (see 1.2.2).

Regarding starch metabolism the significance of this minor component was recognized when *Arabidopsis thaliana* mutants were analyzed that lacked enzymes involved in either phosphorylation or dephosphorylation of starch. These mutants typically possess a largely impaired starch turnover which results in starch accumulation and is closely associated with retardation of

growth (Yu *et al.*, 2001; Ritte *et al.*, 2006, Kötting *et al.*, 2005, 2009; Santelia *et al.*, 2011; Comparot-Moss *et al.*, 2010). Subsequent studies provided evidence that iterative phosphorylation and dephosphorylation at the starch granule surface affect the arrangement of chains and, thereby, most likely facilitate the action of hydrolytic enzymes (Edner *et al.*, 2007; Kötting *et al.*, 2009; Hejazi *et al.*, 2012a).

The assumed role of glycogen phosphate changed dramatically when it became clear that a severe form of human myoclonus epilepsy, Lafora disease, is the result of a defective enzyme (laforin) capable of glycogen dephosphorylation (Minassian *et al.*, 1998; Tagliabracci *et al.*, 2007). Patients lacking laforin progressively accumulate insoluble polyglucosan bodies (Lafora bodies) in many tissues including brain (de Siqueira, 2010). Lafora bodies are considered to be derived from precipitation of glycogen that is non-physiologically structured (Cavanagh, 1999; Minassian, 2001; Tiberia *et al.*, 2012; Roach *et al.*, 2012). Furthermore it was found that higher amounts of glycogen phosphate as observed in laforin-deficient mice lead to lower water solubility of glycogen (Tagliabracci *et al.*, 2008).

Thus, in the metabolism of both starch and glycogen phosphate esters seem to affect the physico-chemical properties of the respective polyglucan. It is possible that physico-chemical properties of polysaccharides are generally affected by phosphate. The presence of phosphate esters at carbon C6 of glucosyl residues in plant heteroglycans, as shown in this study (see 3.3.1), supports this assumption.

4.1 Phosphorylation sites in starch and glycogen

Already more than 40 years ago attempts were made to elucidate the glucosyl carbon position of phosphate esters in starch. In potato tuber starch the majority of phosphate was found to reside at C6, while a smaller proportion was identified at carbon C3. However, around 1% of phosphate was assigned to a third position, carbon C2 (Hizukuri *et al.*, 1970; Tabata and Hizukuri, 1971). These findings are now widely accepted as at least the ratio of C6 to C3 phosphate was confirmed in starches of different origins, such as potato tuber, *Curcuma* roots, cassava seeds, and leaves of *Arabidopsis thaliana (*see 1.2.2*)*. However, by the utilized techniques of ^{31}P-NMR and mass spectrometry the low amounts of C2 phosphate were not observed (Blennow *et al.*, 2000a; Haebel *et al.*, 2008; Ritte *et al.*, 2006).

Previous results concerning the carbon position of glycogen phosphate are partly contradictory. Fontana (1980) demonstrated the presence of glycogen phosphate esters and found that some are more acid labile than others. In hydrolysates components were found that co-migrated with authentic G6P. This together with the observed more acid labile phosphates suggests the presence of at least two phosphorylation sites. The acid labile ester was assigned to be a phosphodiester by Lomako *et al.* (1993). Recently, Tagliabracci *et al.* (2011) stated that exclusively phosphate monoesters are found at the carbon positions C2 and C3 of glycogen. The positions of phosphorylation certainly have implications for the enzymology responsible for phosphorylation and dephosphorylation. This concurs with the fact that in plants at least two enzymes, GWD and PWD, have evolved that specifically phosphorylate carbons C6 and C3, respectively (Ritte *et al.*, 2006). Likewise in plants not all enzymes capable of dephosphorylating phosphoglucans appear to hydrolyze monophosphate esters at both carbon positions (Santelia *et al.*, 2011). The presence and, thus, the conservation of many highly specific enzymes implies that phosphorylation at

different carbons is necessary and likely needs to be regulated separately, which is facilitated if distinct enzymes exist.

The most recent results on glycogen phosphorylation sites imply a strong difference regarding the enzymology of starch and glycogen phosphorylation and dephosphorylation as they state that phosphate is covalently bound to two carbon positions but the major phosphorylation site in starch (C6) is excluded. However, the functional equivalence of the plant enzyme SEX4 and laforin in animals, both sharing general structural features and the capability to remove phosphate from complex phosphorylated polyglucans (Worby *et al.*, 2006; Gentry *et al.*, 2007), indicates at least some similarity of phosphate metabolism in starch and glycogen.

Since the previous results on phosphorylation sites in glycogen are contradictory, the topic of glycogen phosphorylation, however, is closely related to a severe disease and, thus, very relevant, this study aimed to verify or falsify the currently assumed phosphorylation sites in glycogen.

4.1.1 Optimization of a sensitive assay for G6P determination in hydrolysates of carbohydrates

The absence or presence of C6 phosphate in glycogen is one crucial point for the decision whether or not phosphorylation is similar in starch and glycogen. Therefore a highly sensitive enzymatic assay was established to quantify G6P in hydrolysates of polysaccharides. It is based on the G6PDH-mediated conversion of G6P to 6-phosphogluconate under stoichiometric formation of NADPH which was subsequently coupled to a cycling system that yields formazan the formation rate of which correlates with the amount of G6P initially present in the assay mixture.

The principle of NADPH cycling has been described by Nisselbaum and Green (1969). Gibon *et al.* (2002) adopted this procedure for metabolite (including G6P) quantification in plant extracts. In this study the assay as based on the procedure described by Gibon *et al.* (2002) was optimized for measurement of very small amounts of G6P in the presence of high concentrations of non-target compounds (see 3.1.1). Hydrolysates of polyglycans consist largely of neutral sugars, i.e. glucose in starch and glycogen hydrolysates, arabinose and galactose in those of plant heteroglycans. Any effect of these highly abundant neutral sugars on the G6P determination can lead to severe analytical errors and has, thus, been carefully investigated.

Since Horne *et al.* (1970) reported an intrinsic glucose dehydrogenase activity in preparations of G6PDH several commercial G6PDH preparations were tested. For this purpose defined mixtures of authentic G6P and glucose were applied to the complete cycling assay procedure and the G6PDH preparation was varied. It was found that indeed the choice of G6PDH preparation is decisive for the unbiased and sensitive G6P determination in the presence of high concentrations of glucose. The preparation from yeast (Roche, grade I) was chosen since it showed no impact of glucose on the results of G6P determination if the glucose concentration exceeded that of G6P by 3 to 5 orders of magnitude (see 3.1.1.1).

Following a similar line, adding defined mixtures of authentic G6P, arabinose, and/or galactose to the cycling assay revealed that both neutral sugars also affect G6P determination when their concentration is too high (see 3.1.1.2). This effect was found to be deriving from a conversion occurring when assay mixtures with high arabinose and/or galactose underwent heat treatment at high pH (Figures 6 and 7). This concurs with the observation reported by Yang and Montgomery (1996) that reducing sugars (such as arabinose and galactose) undergo various types of reactions

at high concentrations in alkaline media. Since this treatment was, however, necessary for the destruction of excess $NADP^+$, the step could not simply be omitted. Instead a variation of the heat treatment conditions led to optimization as the total amount of arabinose and galactose could be increased by factor 8. This was sufficient to determine G6P in hydrolysates of plant heteroglycans (see 3.3.1).

Besides optimization of the cycling assay regarding the effects of highly abundant non-target compounds several attempts were made to improve its sensitivity for G6P determination. The G6P-based rate of formazan formation could be increased by raising the amount of G6PDH present during coenzyme cycling and by choosing $NADP^+$ instead of NAD^+ as coenzyme throughout the assay. Furthermore the deviation of technical replicas was significantly decreased by the introduction of an additional acid treatment step before the G6PDH-mediated G6P turnover. By raising the volume of the cycling reagent and by adding BSA, rates of formazan formation were linear for almost 2 hours. After optimization amounts of G6P as less as 0.5 pmol as well as slight changes of G6P amounts could be reliably detected. Thus, sensitivity of the cycling assay is approximately 6,000 fold higher than that of the conventional assay using the detection of NADPH at 340 nm (see 3.1.2).

Additionally in this study a procedure was developed that allowed a simple but standardized preparation of long-time stable stock solutions that are used to make the cycling reagent which then is only usable for a few hours. This facilitates coupling of NADPH cycling to various enzymatic reaction where target compounds are enzymatically converted under stoichiometric formation of NADPH. In this study versatility of the optimized cycling assay was exemplarily shown. G1P and G6P determined in leaf extracts from *Arabidopsis thaliana* using the cycling assay showed results indiscernible from those of the conventional enzymatic assay with NADPH determination at 340 nm (see 3.2). Likewise glucose was determined in hydrolysates of plant heteroglycans. All three applications benefit from the high sensitivity of the assay. In the case of metabolite determination very little fresh weight is needed per assay, and likewise only very little heteroglycan is necessary to determine the amount of glucosyl residues that usually accounts for only a very small proportion of the monomers (Fettke *et al.*, 2005a; see 3.2).

4.1.2 C6 phosphate is present in starch, plant heteroglycans, and glycogen

To validate the sensitive G6P assay with NADPH cycling various starches were analyzed. Hydrolysates of commercial potato tuber starch were subjected to the conventional enzymatic assay with NADPH detection at 340 nm and also to the optimized cycling assay. The measured glucose-based C6 monophosphate was indistinguishable between both assays indicating that the G6P determinations with the cycling assay are correct (see 3.3.2.1).

Furthermore hydrolysates of native starch isolated from *Curcuma* rhizome and *Arabidopsis thaliana* leaves were applied to the cycling assay (see 3.3.2.2). Glucose-based C6 phosphate values of the respective starch were compared with those of total phosphate. Both, the values for glucose-based C6 phosphorylation and the ratios of C6 to total phosphate were in the range of previously determined data determined in *Arabidopsis* and several other plant starches, respectively (see 1.2.2), which is another indication for correctness of absolute G6P values as determined by the cycling assay.

Especially regarding the question whether C6 phosphate is present in glycogen it is essential that the quantification method does not lead to false positive results which would indicate the apparent presence of C6 phosphate even in the absence of the target. When hydrolysates derived from starch of the *Arabidopsis thaliana* GWD knockout mutant (*sex1-8*) were subjected to the cycling assay, G6P was consistently below the limit of detection even though the maximum amount of starch was applied to the assay. This concurs with previous observations that when GWD, the enzyme responsible for starch phosphorylation at glucosyl carbon C6, is missing, the level of glucose-based C6 phosphorylation is extremely low (Ritte *et al.*, 2006). Thus, using the optimized cycling assay for G6P determination does not lead to G6P overestimation that is due to high glucose concentrations in the assay mixture (see 3.3.2.2). However, the glucose concentration should not exceed the maximum as determined during optimization (see above).

The high sensitivity of the optimized cycling assay also allowed the analysis of *Arabidopsis thaliana* heteroglycans (see 3.3.1). While only a minor fraction of the heteroglycan monomers comprise glucosyl residues the drastic changes in the abundance of those residues in mutant plants with altered starch metabolism point to a significant role of the cytosolic heteroglycans as glucosyl acceptor and donor (Fettke *et al.*, 2006, 2008). Interestingly, some of these glucosyl residues carry phosphate esters at carbon C6 as determined by the cycling assay in hydrolysates of the heteroglycans. The glucose-based C6 phosphate level is relatively high as it is similar to that of potato tuber starch (see 1.2.2). While the role of phosphate in heteroglycans is entirely uncertain, it is intriguing to see that phosphorylation obviously does not only occur in polyglucans but might be a feature of other polysaccharides as well. Where ever phosphorylation occurs questions arise about the underlying enzymology which in the case of cytosolic heteroglycans must remain uncovered here.

Finally the cycling assay was used to quantify G6P in hydrolysates of glycogen (see 3.3.3). Interestingly, glucosyl C6 phosphate is present in all glycogen preparations examined, the abundance varying between glycogens of different sources. Rabbit skeletal muscle glycogen showed the highest level of glucose-based C6 phosphate and was in the range of that of plant starch which also varies widely depending on the starch source. In mouse the abundance is generally lower and skeletal muscle glycogen contains more C6 phosphate than liver, where it was in fact at the limit of detection. However, its presence could be unambiguously proven by the occurrence of high amounts of G6P in hydrolysates of phosphoglucans enriched from amylolytically treated liver glycogen (see Table 8). Previously published values for glycogen total phosphate (see 1.2.2) reveal that glucosyl carbon C6 is a major phosphorylation site in glycogen. In rabbit muscle it accounts for 20-30% of the total phosphate while in mouse glycogen the proportion of C6 phosphate is smaller. Around 10% of mouse muscle glycogen phosphate is bound to C6 carbons 1-2% of which are only esterified in liver glycogen. Obviously the organ-specific changes in C6 phosphate are more rigorous than those of the total phosphate which may argue for a regulatory role of C6 phosphate though its relatively low abundance.

Additionally glycogen was analyzed in the mouse model of Lafora disease. In the absence of laforin (*Epm2a*$^{-/-}$) glucose-based C6 phosphate was 7 and 8 fold increased in glycogen of liver and skeletal muscle, respectively. When malin was knocked out (*Epm2b*$^{-/-}$) muscle glycogen likewise contained 8 times more C6 phosphate (see Table 8). Previous studies on glycogen from mice reported that total phosphate increases with age when laforin or malin are knocked out. Muscle glycogen of 9-12

month old LD mice possessed phosphate levels elevated as compared to wild type mice by 4 to 6 fold in laforin knockout mice and around 3 fold when malin was knocked out (Tagliabracci *et al.*, 2008; Tiberia *et al.*, 2012). In this study muscle glycogen analyzed was also obtained from 9-12 month old mice. The LD-related changes of C6 phosphate in muscle glycogen are therefore more pronounced than those of total phosphate. Thus, hyperphosphorylation of glucosyl carbon position C6 underlies Lafora disease but, furthermore, the changes in C6 phosphorylation more adequately reflect the drastic phenotype of the disease.

4.1.3 Determination of phosphorylation sites by NMR

The mere presence of C6 phosphate in glycogen contradicts recent publications that state the absence of C6 phosphate (Tagliabracci *et al.*, 2011; Roach *et al.*, 2012). An independent approach was, therefore, chosen to elucidate the phosphorylated carbon positions in glycogen. Amylolytically treated glycogen was first examined by 1D ^{31}P-NMR which already pointed to the existence of C6 phosphate when comparing with an equally treated sample of *Curcuma* starch and authentic G6P (see 3.4.1). However, assignment of other phosphorylated carbon positions and evaluating the possibility of a phosphodiester were not possible using this approach. Thus, phosphoglucans were carefully enriched under monitoring any loss of phosphate (see 3.4.2). Subsequently several techniques of 2D NMR were applied that finally prove the existence of phosphate monoesters at glucosyl carbons C2, C3, and C6 in glycogen. While the latter two positions concur with recent findings, the presence of C6 phosphate is new and was unambiguously demonstrated by two independent methods. Furthermore, C6 phosphate is not LD-, species-, or organ-specific as it was demonstrated in liver glycogen from *Epm2a*$^{-/-}$ mice and in that of wild type rabbit skeletal muscle (see 3.4.3.2; Nitschke *et al.*, 2013).

Though, using the well characterized starch from *Curcuma* rhizomes, glucosyl C2 phosphate was not detectable in NMR experiments performed in this study, the phosphorylated glucosyl carbon positions determined in glycogen are exactly those described for potato starch by Tabata and Hizukuri (1971, see 3.4.3.2). However, though the positions of phosphate on glucosyl residues in starch and glycogen seem to be rather similar, the stable abundance of each type of phosphate ester seems to differ between the two polyglucans. While C6 phosphate is most abundant phosphate ester in starch (see 1.2.2) this phosphorylation site accounts for a smaller proportion of total glycogen phosphate. A large proportion of glycogen phosphate seems to be highly labile under acid conditions (Fontana, 1980; Lomako *et al.*, 1993) which has also been shown for G2P (Tagliabracci, 2010) but not for G6P and G3P (Haebel *et al.*, 2008). This indicates that in glycogen, as opposed to starch, the labile C2 phosphate seems to represent a major proportion of total phosphate.

The results in this study reveal no evidence for the occurrence of any phosphodiester such as that proposed by Lomako *et al.* (1993; see 3.4.3.2). This concurs with the fact that the postulated transfer of G1P from UDPglucose to glycogen as mediated by a putative UDPglucose:glycogen glucose 1-phosphotransferase was never verified.

4.2 6-Phosphoglucosyl residues in glycogen – potential functional implications in glycogen metabolism

After uncovering laforin-deficiency as the major reason for Lafora disease it took a couple of years until laforin's function as a glycogen phosphatase was described (Minassian et al., 1998; Tagliabracci et al., 2007). Concurring with these findings glycogen hyperphosphorylation was assigned to be the immediate consequence of laforin-deficiency and thereby the ultimate structural basis of the disturbed glycogen metabolism in Lafora disease (Tagliabracci *et al.*, 2007). In fact laforin was soon proposed to be part of a corrective mechanism, such as known to exists for the synthesis of other biopolymers, e.g. nucleic acids (Tagliabracci *et al.*, 2008). This view implies that glycogen phosphate *per se* has no physiological function but is rather the result of a biochemical error that needs to be corrected. However, the results in this study suggest a regulatory function of glycogen phosphate in glycogen branching. Likewise they necessitate reconsidering the enzymology of glycogen phosphorylation.

4.2.1 Glycogen phosphate and branching

The relatively low abundance of 6-phosphoglucosyl residues in glycogen could argue for a minor role of this phosphorylation site in glycogen metabolism. However, this conclusion is hampered by at least two points: 1) the abundance of any phosphorylation site exclusively reflects a steady-state concentration while no information is available about the actual turnover at the particular phosphorylation site, 2) the hydroxyl group at glucosyl carbon C6 is involved in both branching and phosphorylation. Since branching is a major determinant of the physiological glycogen structure an interdependence of C6 phosphorylation, branching, and, thus, glycogen structure is conceivable.

The first argument is supported by the fact that in the case of Lafora disease C6 phosphate is more strongly altered than total phosphate (discussed in 4.1.2). In the disease state the phosphatase laforin is not functional and phosphate esters accumulate in glycogen. This study demonstrates that laforin is capable of removing phosphate from the carbon position C6 (see 3.3.4) implying that C6 phosphate accumulation is likely due to the absence of the so far only known glycogen phosphatase. The higher difference of C6 phosphate levels between disease and normal state may suggest a more rapid turnover at this phosphorylation site. Moreover, 6-phosphoglucosyl residues need not be evenly distributed among glycogen molecules. Some molecules could possess more C6 phosphate than others. Considering that isolated glycogen is usually a mixture of polyglucans from different cellular compartments, such as cytoplasm and lysosome, it is possible that abundance of C6 phosphate is compartment-specific or even acts as a signal for compartment-specific targeting of glycogen.

Thus, low averaged abundance of a specific phosphate ester does not necessarily exclude an essential role of this phosphorylation site. This is bolstered by the fact that for instance in wild type rice endosperm starch 6-phosphoglucosyl residues are not detectable. However, they seem to play a role as they are substantially increased (up to values in the range of leaf starch, see 1.2.2) in mutants lacking a starch branching enzyme (see 3.3.2.4). This implies that at least in starch C6 phosphate is subject of some kind of regulation, and that this regulation is connected to branching. This concurs with the results of previous studies that revealed elevated starch phosphate levels being closely associated with a low degree of branching. The latter was deduced from the linear

chain length pattern after debranching of the starch. Starches with higher proportions of longer chains appeared to contain more phosphate (Blennow *et al.*, 1998, 2000).

In this study a similar correlation was found when linear chain length patterns of muscle glycogen from wild type and LD mice were compared. Glycogen of both laforin- and malin-deficient mice consistently contains a higher proportion of longer chains while most short chains were reduced as compared to wild type (see 3.5). The effect was stronger in malin-deficient mice. Thus, since the levels of glycogen C6 phosphate were similarly high in both mutants, additional factors besides C6 phosphate seem to influence branching frequency. However, positive correlations of chain length and C6 phosphate are found in both starch and glycogen which reasons for a general principle in α-polyglucans.

The mechanisms underlying this correlation have yet to be elaborated, in starch and in glycogen. In glycogen elevated levels of phosphate as induced by laforin-deficiency seem to cause reduced branching. However, malin-deficiency also results in decreased branching. This could be explained by the hypothesis of a secondary deficiency in free active laforin. Tiberia *et al.* (2012) argue that laforin needs to be removed from glycogen after one event of dephosphorylation. In the absence of malin, laforin remains associated with glycogen resulting in the formation of Lafora bodies. Simultaneously the amount of free laforin capable of further glycogen dephosphorylation is reduced in the cytoplasm. Thus, hyperphosphorylation occurs and, as revealed in this study, decreased branching (see 3.5).

It is possible that glycogen branching is regulated through C6 esterification. This notion is supported by the results of gradual isoamylolysis of wild type muscle glycogen. At the beginning of the incubation chains released were quite short, later longer chains were released. This concurs with the findings of Palmer *et al.* (1983b) who did a similar experiment with oyster glycogen. The data let Palmer *et al.* (1983b) suggest that linear glucan chains are spatially distributed in glycogen molecules as it is conceivable that debranching proceeds from the periphery to the inner parts of the molecules. However, in this study the size distribution of glycogen was additionally monitored during gradual isoamylolysis (see 3.6.3). The results implied that isoamylase obviously has a mode of action different from that of α-amylase which indeed acts from periphery to central parts of glycogen (see 3.6.2). While isoamylolysis proceeds, the averaged molecule size remains rather constant implying that isoamylase follows a rather sequential mode of action. It largely completes degradation of one molecule before acting on another and removes glycogen molecules from all sizes without preferences for specific molecule sizes (see Figure 36).

Considering the length of chains released during degradation it seems isoamylase preferably degrades glycogen molecules containing short chains, releasing longer chains only at later stages of the incubation. Since the chain length distribution measured in native glycogen is very similar in glycogen molecules with different sizes the data suggest that among all sizes molecules exist that are composed of either longer or shorter chains. Interestingly, the molecules with the longest chains (degraded at later stages) contain the most C6 phosphate. Thus, the experiments reveal yet another indication of a positive correlation between chain length and C6 phosphorylation.

It is conceivable that Lafora disease leads to accumulation of C6 phosphate over many rounds of synthesis and degradation (Roach *et al.*, 2012) and thereby results in a higher proportion of less branched molecules. At one point, molecules with too long side chains might become insoluble and

precipitate as Lafora bodies which are known to mainly consist of glucans with reduced branching (Yokoi *et al.*, 1968; Sakai *et al.*, 1970).

Precipitation of glycogen in association with reduced branching is also observed in glycogen storage diseases with affected glycogen branching, such as Andersen's disease and adult polyglucosan body disease (Cavanagh, 1999). Considering the elevated C6 phosphate in endosperm starch of rice lacking starch branching enzyme it would be interesting to investigate whether C6 phosphate is also elevated in glycogen of GBE-deficient tissues. A higher abundance of 6-phosphoglucosyl residues would argue for a rather bidirectional dependency of C6 phosphate and branching. It is not inconceivable that by phosphorylation at carbon C6 the architecturally appropriate branching site is 'marked', and the branching event itself involves phosphatase-mediated dephosphorylation. This way the 'mark' is removed prior to glucosylation at C6 (branching). In the case of glycogen the absence of laforin prevents removal of the 'mark' from carbon C6, and thus prevents branching. If GBE is not functional the branching process is not initiated, and, thus, does not instigate the laforin co-action to remove the phosphate.

Other results in this study also point to a specific role of C6 phosphate during glycogen synthesis. During gradual α-amylolysis the averaged molecule size decreases in line with the remaining glycogen. The latter are successively enriched in 6-phosphoglucosyl residues (see 3.6.2). Since α-amylase-mediated hydrolysis of glucosidic linkages is unlikely to be hindered by the rare phosphate esters in glycogen (Posternak, 1951; Hizukuri *et al.*, 1970), due to sterical reasons degradation is likely to proceed from the periphery to the inner parts of the molecules. This is supported by the results of α-amylolysis performed on glycogen molecules labeled at the periphery (see 3.6.2). Thus, the data suggest a higher C6 phosphorylation in the more central regions of glycogen molecules which points to a role during the early stages of glycogen synthesis, probably to avoid inappropriate packing through erroneous branching. It is reasonable to assume that phosphate incorporation during starch synthesis (Nielsen *et al.*, 1994; Ritte *et al.*, 2004) serves a similar purpose.

4.2.2 Glycogen phosphate and molecule size

Besides branching another structural parameter of glycogen seems to be related to hyperphosphorylation. In this study the size distribution of glycogen molecules isolated from wild type and LD mice was investigated. The molecule sizes of glycogen from all three sources (wild type, *Epm2a*$^{-/-}$, and *Epm2b*$^{-/-}$) are distributed over at least 2 orders of magnitude. Thus, independent of the disease state rather small to rather large molecules exist. However, the averaged molecule size is significantly different in LD mice as compared to wild type (see 3.6.1). Interestingly, the two forms of LD have an opposite effect on the averaged molecule size of glycogen. While muscle glycogen molecules from laforin-deficient tissue are much smaller, those of malin-deficient tissue exceed those of wild type by factor 2.6. Thus, glycogen size seems not to be directly related to hyperphosphorylation which is, at least regarding glucosyl carbon position C6, similar in both forms of the disease. Furthermore, analysis of muscle glycogen fractions with varying averaged molecule sizes did not show differential amounts of C6 phosphate. Thus, within one glycogen preparation C6 phosphate does not correlate with molecule size which must therefore be determined by additional factors. However, it remains open whether the disease-related

hyperphosphorylation, possible even at carbon C6, has an at least indirect impact on the size of glycogen molecules.

It should be noted that the size distribution of glycogen molecules is likely affected by the metabolic state of the cells. Regarding muscle cells, glycogen is synthesized during periods of rest and is degraded to supply the cell with energy during periods of muscular activity (Villar-Palasi and Larner, 1968; Frayn, 2003). If at the time of sampling the metabolic state of muscle cells differed in wild type and the two variants of LD mice, the averaged size of glycogen molecules could also be largely affected. Furthermore, under the assumption that at the same metabolic state normal and LD glycogen have the same size distribution, the measured averaged size should be reflected by the glycogen content in the muscle. The amount of muscle glycogen in malin-deficient mice is only slightly yet significantly increased (Tiberia *et al.*, 2012). That of laforin-deficient mice is, however, several fold increased (Tagliabracci *et al.*, 2008). Thus, sampling of mouse tissue in different metabolic states can be ruled out to be the main reason of the differential sizes of glycogen molecules in wild type and LD mice.

Theoretically identical rates of glycogen synthesis could be realized by synthesizing either a low number of large molecules or a high number of adequately smaller molecules. Apparently malin- and laforin-deficiency induce or require an opposite strategy regarding the realization of glycogen synthesis. At this time one can only speculate about the immanent reason. In smaller molecules the relative number of glucan chains that are accessible to degrading enzymes is higher. It is possible that in the case of laforin-deficiency building more but smaller molecules is a strategy to compensate for a slower rate of glycogen degradation that could be the result of high amounts of covalently bound phosphate. Likewise in the case of malin-deficiency laforin remains associated to glycogen molecules as is believed to disturb the structure. This disturbance could not only lead to the formation of Lafora bodies as hypothesized by Tiberia *et al.* (2012) but could also restrict the access of degrading enzymes. This would imply that degradation of glycogen molecules is inefficient or incomplete, and resynthesis of glycogen molecules proceeds upon molecules incompletely degraded. Many rounds of incomplete glycogen degradation and resynthesis could lead to an increase in averaged molecule size.

4.2.3 Enzymology of glycogen phosphorylation

For years laforin was the only enzyme identified that is involved in glycogen phosphate metabolism. At least part of the enzymology of glycogen dephosphorylation was hence elucidated and widely accepted (Roach *et al.*, 2012). However, the question how phosphate is incorporated into glycogen remained unclear. Already two decades ago Lomako *et al.* (1993) postulated a phosphoglucosyl transfer from UDPglucose to glycogen but no enzyme could be identified then. The idea was pursued in the lab of Peter J. Roach where it was found that glycogen acquires radiolabeled phosphate during incubation with functional glycogen synthase (GS) and UDPglucose labeled in the β-phosphate position (phosphate adjacent to the glucosyl residue). According to their interpretation GS in one of approximately 10^4 cases transfers phosphorylated glucose instead of just glucose to glycogen and, thus, should be responsible for glycogen phosphorylation (Tagliabracci *et al.*, 2011). This view fitted well to the assumption that glycogen phosphate is a biochemical error and has no physiological function. The long known fact that GS does not exclusively transfer glucosyl residues from the respective UDP derivative to glycogen but also

galactose and glucosamin (Tarentino and Maley, 1976) additionally supports this view, since it is not implausible to assume that the limited flexibility of the GS active site could also be responsible for the phosphate-related error.

While Lomako *et al.* (1993) postulated the formation of a phosphodiester this type of phosphate ester was not found when Tagliabracci *et al.* (2011) performed NMR-studies on glycogen. Instead they exclusively observed monophosphate esters bound to glucosyl carbons C2 and C3. To consolidate C2 and C3 phosphorylation with the transfer of phosphorylated glucose from UDPglucose (where phosphate is bound to glucosyl carbon C1) a complex reaction mechanism had to be postulated that included the formation of glucose 1,X-cyclic phosphate with ester bonds at C1 and CX (C2 or C3) prior to the formation of a new glucosidic bond and the concurrent cleavage of the ester bond at C1. The result would be an incorporated glucosyl residue phosphorylated in C2 or C3. This proposed mechanism is supported by earlier publications that state a possible formation of glucose cyclic phosphates from UDPglucose (Paladini and Leloir, 1952; Nunez and Barker, 1976; Tagliabracci, 2010).

The inherent plausibility of these findings resulted in the now widely accepted view that phosphate is incorporated via an erratic side reaction of GS. Even with additional assumptions not all of the recent observations regarding glycogen phosphate can be explained using this model. The deviation of the actual phosphate amount found in glycogen and the low rate of apparent GS-mediated phosphate incorporation could be explained by the accumulation of phosphate in many rounds of glycogen synthesis and degradation (Tagliabracci *et al.*, 2011; Roach *et al.*, 2012). The progressive increase of glycogen phosphate as observed in laforin-deficient tissue supports this assumption. However, the phosphate amount is rather constant in wild type tissue (Tagliabracci *et al.*, 2007, 2008), implying that in the presence of laforin, glycogen phosphate is not accumulating but is still much more abundant than expectable by the rate of GS-mediated phosphate incorporation. Thus, another assumption must apply that would explain a differential phosphate incorporation by GS *in vivo* and *in vitro*. Furthermore, in the absence of laforin, muscle glycogen possesses much more phosphate than that in liver even though in both tissues the so called muscle GS (encoded by GYS1) is expressed (Nuttall *et al.*, 1994). If a differential expression of GYS1 in both tissues accounts for the variation in glycogen phosphate then at least it must be assumed that the liver-specific GS (encoded by GYS2) does not or only very little contribute to phosphate incorporation into liver glycogen. Alternatively one might assume that the GS-mediated phosphate incorporation is modulated in different tissues. However, to the best of my knowledge, there is no indication that stochastic events, such as an undesired side reaction that causes severe problems if not compensated, can be regulated. If the frequency of the side reaction can be regulated the need of the laforin-mediated glycogen dephosphorylation would be severely challenged.

The hypothesis of an exclusive GS-mediated phosphate incorporation is, however, completely unhinged by the findings of this study. First of all, the mere presence of 6-phosphoglucosyl residues, which has been unambiguously proven, is inconsistent with the mechanism proposed by Tagliabracci *et al.* (2011). For C2 phosphorylation, a five-membered cyclization (as in glucose 1,2 cyclic phosphate) was postulated to transfer the phosphate group from C1 to C2, and for C3 esterification a six-membered cyclization (as in glucose 1,3-cyclic phosphate; Tagliabracci *et al.*, 2011). As discussed by the authors and bolstered by previous data (Paladini and Leloir, 1952; Nunez and Barker, 1976), these cyclic structures were observed and are, thus, possible. However,

seven-membered cyclization, as required for transfer of phosphate from C1 to C6, has been reported impossible for glucose cyclic phosphates (Khorana *et al.*, 1957).

Furthermore, the uneven distribution of 6-phosphoglucosyl residues in glycogen molecules as presented in this study contradicts the hypothesis of glycogen phosphorylation by a mere stochastic event the occurrence of which dictates an even distribution of phosphate. Gradual α-amylolysis of wild type glycogen revealed, however, that C6 phosphate is more abundant in central parts of the glycogen molecules. Additionally, as indicated by the results of gradual isoamylolysis glycogen molecules exist among all sizes of molecules that are composed of glucan chains with differential averaged chain length. C6 phosphate tends to be more abundant in molecules possessing longer glucan chains. It is difficult to explain an uneven distribution of C6 phosphate by a side reaction of GS. Indeed the results rather point to a specific function of 6-phosphoglucosyl residues that is related to branching and/or to the early stages of glycogen synthesis (see 4.2.1).

One could argue that C6 is probably incorporated by another mechanism, but for both C2 and C3 GS-mediated incorporation is still feasible with some additional assumptions (see above). In fact there is no proof (yet) whether phosphate esters at C2 and C3 are also unevenly distributed in glycogen molecules. However, the existence of C6 phosphate very recently motivated reconsidering the experiments that resulted in the idea of the apparent GS-mediated phosphate incorporation. During careful reproduction of the experiments of Tagliabracci *et al.* (2011) a difficult to anticipate pitfall was identified. Apparently one main product of the classical GS reaction, UDP, non-covalently interacts with glycogen more strongly than UDPglucose. After incubation of glycogen with GS and [^{32}P] labeled UDPglucose a very minor proportion of UDP remained non-covalently attached to the glycogen and, thus, mimicked glycogen phosphorylation. The time-dependent increase of glycogen label during GS incubation is consistent with the concurrently increasing UDP concentration. In the absence of functional GS, of course, glycogen is not labeled due to the absence of vast amounts of labeled UDP. However, by gel chromatography UDP could be removed from glycogen avoiding the pitfall. Including this additional step of purification following apparent glycogen labeling no evidence of any phosphorylation of glycogen by GS was found (Nitschke *et al.*, 2013). Rather it seems GS exhibits high reaction specificity.

Likewise it was considered that glycogen phosphorylase (GP) could introduce phosphate, also by an erratic side reaction. As described by Klein *et al.* (1986) during phosphorolysis the electrophilic attack of orthophosphate is directed towards the C1 carbon of the terminal glucosyl residue yielding G1P and glycogen reduced by one glucosyl residue. If in some cases the attack would occur at C4 of the second glucosyl residue glucose would be released and phosphate be incorporated at C4 of the terminal glucosyl residue of glycogen. Neither the NMR-data presented in this study nor incubation experiments of glycogen, GP, and labeled orthophosphate did, after sufficient purification of glycogen, support GP-mediated phosphate incorporation at C4 (Nitschke *et al.*, 2013; see 3.4.3.2).

The findings presented in this study and in that of Nitschke *et al.* (2013) call for a complete reevaluation of the current view on glycogen phosphorylation. In fact they permit a wider view on putative roles of glycogen phosphate by opposing previous results that seemed to confirm glycogen phosphate to be a mere biochemical error. Rejecting the assumption of GS-mediated phosphate incorporation, it is again worthwhile to search for alternative biochemical ways of glycogen phosphorylation which for many reasons could be mediated by distinct phosphorylating enzymes as

it is realized in starch metabolism of plants. First, the biochemical reactions that introduce phosphate into amylopectin or glycogen should be similar, since both carbohydrates consist of branched α-1,4 glucan chains. Second, apparently the same hydroxyl groups are potentially esterified in starch and glycogen. Third, enzymes involved in starch phosphate metabolism are mainly specific with respect to the glucosyl carbon position they act on. For instance amylopectin is phosphorylated by at least two distinct dikinases which form phosphate esters specifically at either of the glucosyl carbons C6 (GWD) or C3 (PWD) (Ritte *et al.*, 2006). Likewise LSF2 removes phosphate esters preferentially from carbon C3 (Santelia *et al.*, 2011). Fourth, the phosphoglucan phosphatases SEX4 in plants and laforin in animals are most likely the products of two separate evolutionary fusion events, but still their function has been shown to be equivalent (Gentry *et al.*, 2007). This underlines the chemical similarity of amylopectin and glycogen, as functionally equivalent enzymes likely act on similar substrates, and it emphasizes the physiological importance of such function. In starch both the removal and the introduction of phosphate are vital for functional starch turnover (Hejazi *et al.*, 2012a). Now, this study provides evidence that glycogen phosphate may also be involved in essential processes, such as regulation of branching, that maintain the functionality of glycogen molecules. Thus, regarding the facts known about both starch and glycogen phosphate striking similarities are obvious. It is, therefore, considered highly likely that also in glycogen metabolism distinct enzymes are responsible for the incorporation of phosphate. This would facilitate the regulation of glycogen phosphorylation and for instance differential abundances of glycogen phosphate in various tissues could be explained independent of the presence of laforin.

To the best of my knowledge, yet no equivalents of the starch-related dikinases were found by *in silico* searches (Gentry *et al.*, 2009). Since GWD and PWD seem to have evolved specifically in the green lineage, it is difficult to predict the sequence characteristics of putative glycogen (di)kinases (Ball *et al.*, 2011).

4.3 6-phosphoglucosyl residues in glycogen – significance for Lafora disease research

Within only a few years, significant findings brought together the fields of phosphate-related starch and glycogen research and underline their significance regarding a severe form of epilepsy, Lafora disease, which has been assigned to mutations in genes encoding the phosphatase laforin (Minassian *et al.*, 1998) or the E3 ubiquitin ligase malin (Chan *et al.*, 2003a). Laforin is functionally equivalent to plant SEX4, either of which has been shown to dephosphorylate glycogen and amylopectin, respectively (Niitylä *et al.*, 2006; Worby *et al.*, 2006; Gentry *et al.*, 2007). In mammals and in plants the absence of the respective enzyme severely impairs polyglucan metabolism by defective polyglucan dephosphorylation (Niitylä *et al.*, 2006; Tagliabracci *et al.*, 2007, 2008; Kötting *et al.*, 2009). Thus, it became clear that covalent phosphate is an important factor in the metabolism of both starch and glycogen. This study provides further evidence that the role of phosphate is similar in starch and glycogen metabolism.

As patients of LD suffer from the consequences of insufficient removal of phosphate esters from glycogen, the inhibition of the enzyme(s) responsible for glycogen phosphorylation would be a possible treatment of the disease. While the knowledge about biochemical mechanisms of starch phosphorylation is already quite advanced (Hejazi *et al.*, 2012a), unfortunately, this is not the case

regarding glycogen. Only recently a possible mechanism of glycogen phosphorylation by GS was proposed. Accordingly, it was suggested to search for selective inhibitors of brain glycogen synthase (Tagliabracci *et al.*, 2011). Indeed this seems viable since a reduction of GS activity by the knockout of PTG (a protein that targets the GS-activator PP1 to GS) in *Epm2a*$^{-/-}$ mice results in near-complete disappearance of Lafora bodies which are believed to trigger the symptoms of Lafora disease (Turnbull *et al.*, 2011). These results do not necessarily imply the correctness of the proposed side reaction of GS, since the down-regulation of GS would certainly not alter the frequency of the erratic side reaction. Apparently the cellular glycogen level is significantly decreased by PTG knockout which most likely results in a lower probability of glycogen precipitation (Turnbull *et al.*, 2011). Furthermore it has been shown that overexpression of GS in mouse muscle leads to polyglucosan structures that are similar to LB (Pederson *et al.*, 2003). Thus, an alteration of the ratio between chain elongation and branching events seems to induce dramatic changes in glycogen structure and likely its physico-chemical properties. If, as suggested in this study, the absence of laforin leads to a lower branching frequency this insufficiency could be compensated by down-regulation of GS-mediated chain elongation.

The results of this study oppose the theory of a stochastic incorporation of phosphate into glycogen by GS and rather suggest the existence of one or more phosphorylating enzymes such as kinases or dikinases. Therefore, another treatment of the disease could be achieved by selectively inhibiting these enzymes. However, they must be identified first.

The presence of glycogen phosphorylating kinases or dikinases in tissue lysates can be proven by incubation of a suitable carbohydrate with for instance laforin-deficient muscle lysates and [^{32}P] labeled ATP. By using [^{32}P]ATP that is specifically labeled at the β- or γ-positions kinases and dikinases can be distinguished. Dikinases transfer the γ-phosphate group to water (yielding orthophosphate) and the β-group to the glucan to be phosphorylated (thus converting ATP to AMP), while kinases transfer the γ-phosphate to the target glucan and convert ATP to ADP. In either case incorporation of label into the carbohydrate indicates phosphorylation. The results can be confirmed by performing experiments using unlabeled ATP. Following incubation, putatively phosphorylated polyglucans are hydrolyzed and the sensitive cycling assay optimized in this study can be used to obtain unambiguous evidence for phosphorylation at C6. By wide variation of the carbohydrate substrate and the conditions used during incubation high rates of phosphorylation should be obtained. This way conditions can be defined under which interaction of the putative (di)kinase with its carbohydrate substrate might be sufficient to enable enrichment of carbohydrate binding proteins in affinity assays. Following SDS-PAGE the identification of carbohydrate binding proteins would certainly rely on tryptic digestion, MALDI-MS analysis, and data base search. Alternatively, following the optimization of a phosphate incorporation assay (see above) a human cDNA library screening could be performed. Any resultant protein candidate should be confirmed by an approach using RNAi inhibition of the candidate gene in cell culture. Comparing either the glycogen phosphate level or the glycogen phosphorylation activity in cell cultures with or without induction of the RNAi construct reveals whether or not the candidate is a glycogen phosphorylating enzyme.

Besides selective inhibition of GS or putative glycogen phosphorylating enzymes other approaches are viable as a treatment against LD. One aims for removal of Lafora bodies, the disorganized aggregates of malformed glycogen that precipitated, and the presence of which in neurons is believed to be the main cause for neurodegenerative symptoms of LD (Minassian, 2001; Duran *et*

al., 2012). Apparently, since they accumulated in the course of LD, Lafora bodies cannot (or at least not sufficiently) be digested by the cell's normal enzymes of glycogen catabolism. This is coherent with the fact that glycogen phosphorylase usually acts on soluble substrates and, being an exo-acting enzyme, its action is stalled by both covalent phosphate and branching points. However, it has been shown that Lafora bodies can be completely degraded by α-amylase (Nikaido *et al.*, 1971), the type of hydrolase that is also used for intestinal digestion of ingested (insoluble) starch granules. As underlined in this study, α-amylase is an endo-acting hydrolase the action of which on polyglucans is largely unaffected by rare phosphate esters or branching points (Posternak, 1951; Hizukuri *et al.*, 1970; Roberts and Whelan, 1960). It is, thus, reasonable to attempt removal of Lafora bodies by transient introduction of α-amylase into neurons, where they are not expressed constitutively. This could be realized by a carrier-system using a non-toxic variant of diphtheria toxin (DT) that specifically and efficiently crosses the blood-brain barrier through non-invasive, physiological mechanisms (Stenmark *et al.*, 1991). *In situ* α-amylolytic treatment of LB would also result in an unusually high amount of phosphorylated oligoglucans, as for instance observed in *Arabidopsis thaliana* SEX4 mutants. Since in LD patients a suitable phosphoglucan phosphatase is missing these phosphoglucans might persist in the cell with unpredictable pathological consequences. Thus, the introduction of a functional phosphoglucan phosphatase in addition to α-amylase could avoid this complication. Since it takes many years for first symptoms to occur in LD, the α-amylase (and phosphatase) delivery would not need to be done very often. A successful treatment could also be transferred to other glycogen storage diseases associated with polyglucosan body formation, such as adult polyglucosan body disease.

During any treatment that involves reduction of highly phosphorylated and, thus, malformed glycogen in cells, such as Lafora bodies, the glucose-based phosphate amount is likely to be decreased in the glycogen fraction. Thus, an assay to specifically measure glycogen phosphate could be used to monitor the progress of a treatment. As indicated in this study, in comparison to total phosphate, C6 phosphate shows greater relative difference between disease and normal state. Thus, observation of significant changes in glycogen phosphate levels, as caused by a successful treatment, is facilitated when abundance of C6 phosphate is monitored. By virtue of its high sensitivity, the cycling assay optimized in this study requires only very small amounts of sample. This renders the assay a suitable diagnostic tool even in cell culture experiments with neuronal cells that have been reported to contain only very small amounts of glycogen (Vilchez *et al.*, 2007). Likewise investigations of glycogen C6 phosphate with high temporal resolution are possible, as exemplarily shown for *Chlamydomonas reinhardtii* cells (see 3.3.2.3). This could help to elucidate timely alterations of glycogen phosphate in order to further characterize its metabolic function.

Any disease-related research should aim to finally find a cure or at least a treatment that reduces the fatal consequences of the disease. However, often results of fundamental research prove to be extremely valuable even though the initial aim was entirely unrelated to diseases. Very likely Tabata and Hizukuri, who first characterized the phosphorylated glucosyl carbons in potato starch, did not guess that polyglucan phosphate could be very closely related to a severe disease. However, they and many researchers after them carried on, successively shedding light on the significance of this minor covalent modification. One should note, that they were probably also encouraged by the existence of several industrial applications of starch with differential levels of phosphate. Already, while the biochemical source of starch phosphate was still unknown, efforts

were made to determine the exact location of phosphate in starch particles (Takeda and Hizukuri, 1982), to examine phosphate-related effects on the starch structure and properties (Muhrbeck and Tellier, 1991; Lim and Seib, 1993; Blennow *et al.*, 1998, 2000, 2001), and to fathom possibilities of phosphate incorporation into starch (Nielsen *et al.*, 1994). Likewise after the description of covalent phosphate in glycogen (Fontana, 1980), phosphate-related research on glycogen was merely fundamental (Lomako *et al.*, 1993, 1994). Phosphate was assigned to be one of the minor components in glycogen, and the physiological relevance was far from clear (Manners, 1991; Lomako *et al.*, 1994).

Within the last 15 years the view on phosphate in polyglucans changed dramatically. Today it is unmistakably clear that functional regulation of polyglucan phosphorylation is essential both in plants and animals. In starch research it is now widely accepted that phosphate esters are introduced for specific reasons, e.g. to facilitate enzymatic action at the starch surface by affecting the arrangement of glucan chains. The results of this study, moreover, present further evidence that phosphorylation plays a crucial role in the regulation of branching. By elucidating the correct pattern of glycogen phosphate ester positions and especially by unambiguously proving the existence of C6 phosphate in glycogen this study opposes the current view that phosphate in glycogen is a mere biochemical error that, if not corrected by laforin, has fatal consequences. It proposes a role of phosphate in regulation of glycogen branching, one major determinant of glycogen structure, and points to the existence of specific glycogen phosphorylating enzymes. Thus, it changes the current view on glycogen phosphate which implies new possibilities of Lafora disease treatment.

5 Summary

Functional metabolism of storage carbohydrates is vital to plants and animals. The water-soluble glycogen in animal cells and the amylopectin which is the major component of water-insoluble starch granules residing in plant plastids are chemically similar as they consist of α-1,6 branched α-1,4 glucan chains. Synthesis and degradation of transitory starch and of glycogen are accomplished by a set of enzymatic activities that to some extend are also similar in plants and animals. Chain elongation, branching, and debranching are achieved by synthases, branching enzymes, and debranching enzymes, respectively. Similarly, both types of polyglucans contain low amounts of phosphate esters whose abundance varies depending on species and organs. Starch is selectively phosphorylated by at least two dikinases (GWD and PWD) at the glucosyl carbons C6 and C3 and dephosphorylated by the phosphatase SEX4 and SEX4-like enzymes. In Arabidopsis insufficiency in starch phosphorylation or dephosphorylation results in largely impaired starch turnover, starch accumulation, and often in retardation of growth. In humans the progressive neurodegenerative epilepsy, Lafora disease, is the result of a defective enzyme (laforin) that is functional equivalent to the starch phosphatase SEX4 and capable of glycogen dephosphorylation. Patients lacking laforin progressively accumulate unphysiologically structured insoluble glycogen-derived particles (Lafora bodies) in many tissues including brain. Previous results concerning the carbon position of glycogen phosphate are contradictory. Currently it is believed that glycogen is esterified exclusively at the carbon positions C2 and C3 and that the monophosphate esters, being incorporated via a side reaction of glycogen synthase (GS), lack any specific function but are rather an enzymatic error that needs to be corrected.

In this study a versatile and highly sensitive enzymatic cycling assay was established that enables quantification of very small G6P amounts in the presence of high concentrations of non-target compounds as present in hydrolysates of polysaccharides, such as starch, glycogen, or cytosolic heteroglycans in plants. Following validation of the G6P determination by analyzing previously characterized starches G6P was quantified in hydrolysates of various glycogen samples and in plant heteroglycans. Interestingly, glucosyl C6 phosphate is present in all glycogen preparations examined, the abundance varying between glycogens of different sources. Additionally, it was shown that carbon C6 is severely hyperphosphorylated in glycogen of Lafora disease mouse model and that laforin is capable of removing C6 phosphate from glycogen. After enrichment of phosphoglucans from amylolytically degraded glycogen, several techniques of two-dimensional NMR were applied that independently proved the existence of 6-phosphoglucosyl residues in glycogen and confirmed the recently described phosphorylation sites C2 and C3. C6 phosphate is neither Lafora disease- nor species-, or organ-specific as it was demonstrated in liver glycogen from laforin-deficient mice and in that of wild type rabbit skeletal muscle. The distribution of 6-phosphoglucosyl residues was analyzed in glycogen molecules and has been found to be uneven. Gradual degradation experiments revealed that C6 phosphate is more abundant in central parts of the glycogen molecules and in molecules possessing longer glucan chains. Glycogen of Lafora disease mice consistently contains a higher proportion of longer chains while most short chains were reduced as compared to wild type.

Together with results recently published (Nitschke *et al.*, 2013) the findings of this work completely unhinge the hypothesis of GS-mediated phosphate incorporation as the respective reaction

mechanism excludes phosphorylation of this glucosyl carbon, and as it is difficult to explain an uneven distribution of C6 phosphate by a stochastic event. Indeed the results rather point to a specific function of 6-phosphoglucosyl residues in the metabolism of polysaccharides as they are present in starch, glycogen, and, as described in this study, in heteroglycans of Arabidopsis. In the latter the function of phosphate remains unclear but this study provides evidence that in starch and glycogen it is related to branching. Moreover a role of C6 phosphate in the early stages of glycogen synthesis is suggested. By rejecting the current view on glycogen phosphate to be a stochastic biochemical error the results permit a wider view on putative roles of glycogen phosphate and on alternative biochemical ways of glycogen phosphorylation which for many reasons are likely to be mediated by distinct phosphorylating enzymes as it is realized in starch metabolism of plants. Better understanding of the enzymology underlying glycogen phosphorylation implies new possibilities of Lafora disease treatment.

6 References

Abid, G., Silue, S., Muhovski, Y., Jacquemin, J.-M., Toussaint, A., and Baudoin, J.-P. (2009). Role of myo-inositol phosphate synthase and sucrose synthase genes in plant seed development. Gene 439, 1-10.

Alonso, A., Sasin, J., Bottini, N., Friedberg, I., Osterman, A., Godzik, A., Hunter, T., Dixon, J., and Mustelin, T. (2004). Protein tyrosine phosphatases in the human genome. Cell 117, 699-711.

Anderson, W.B., and Nordlie, R.C. (1968). Glucose dehydrogenase activity of yeast glucose 6-phosphate dehydrogenase. I. Selective stimulation by bicarbonate, phosphate, and sulfate. Biochemistry *7*, 1479-1485.

Antonio, C., Larson, T., Gilday, A., Graham, I., Bergström, E., and Thomas-Oates, J. (2008). Hydrophilic interaction chromatography/electrospray mass spectrometry analysis of carbohydrate-related metabolites from Arabidopsis thaliana leaf tissue. Rapid Communications in Mass Spectrometry 22, 1399-1407.

Asatsuma, S., Sawada, C., Itoh, K., Okito, M., Kitajima, A., and Mitsui, T. (2005). Involvement of α-Amylase I-1 in Starch Degradation in Rice Chloroplasts. Plant and Cell Physiology 46, 858-869.

Ball, S.G. (2002). The Intricate Pathway of Starch Biosynthesis and Degradation in the Monocellular Alga Chlamydomonas reinhardtii. Australian Journal of Chemistry 55, 49-59.

Ball, S., Colleoni, C., Cenci, U., Raj, J.N., and Tirtiaux, C. (2011). The evolution of glycogen and starch metabolism in eukaryotes gives molecular clues to understand the establishment of plastid endosymbiosis. Journal of Experimental Botany *62*, 1775-1801.

Baunsgaard, L., Lutken, H., Mikkelsen, R., Glaring, M.A., Pham, T.T., and Blennow, A. (2005). A novel isoform of glucan, water dikinase phosphorylates pre-phosphorylated alpha-glucans and is involved in starch degradation in Arabidopsis. Plant J 41, 595-605.

Berg, J.M., Tymoczko, J.L., and Stryer, L. (2003). Biochemie. 5th edition (Heidelberg, Berlin: Spektrum Akademischer Verlag GmbH).

Berger, S., Braun, S., and Kalinowski, H.-O. (1993). NMR-Spectroskopie von Nichtmetallen. Band 3. 31P-NMR-Spektroskopie. (Stuttgart, New York: Georg Thieme Verlag).

Blauth, S.L., Yao, Y., Klucinec, J.D., Shannon, J.C., Thompson, D.B., and Guiltinan, M.J. (2001). Identification of Mutator Insertional Mutants of Starch-Branching Enzyme 2a in Corn. Plant Physiology 125, 1396-1405.

Blauth, S.L., Kim, K.N., Klucinec, J., Shannon, J.C., Thompson, D., and Guiltinan, M. (2002). Identification of Mutator insertional mutants of starch-branching enzyme 1 (sbe1) in Zea mays L. Plant Molecular Biology 48, 287-297.

Blennow, A., Bay-Smidt, A.M., Olsen, C.E., and Moller, B.L. (2000a). The distribution of covalently bound phosphate in the starch granule in relation to starch crystallinity. Int J Biol Macromol 27, 211-218.

Blennow, A., Engelsen, S.B., Munck, L., and Moller, B.L. (2000b). Starch molecular structure and phosphorylation investigated by a combined chromatographic and chemometric approach. Carbohydrate Polymers 41, 163-174.

Blennow, A., Mette Bay-Smidt, A., and Bauer, R. (2001). Amylopectin aggregation as a function of starch phosphate content studied by size exclusion chromatography and on-line refractive index and light scattering. International Journal of Biological Macromolecules 28, 409-420.

Blennow, A., and Engelsen, S.B. (2010). Helix-breaking news: fighting crystalline starch energy deposits in the cell. Trends Plant Sci 15, 236-240.

Brooks, G.A., and Gaesser, G.A. (1980). End points of lactate and glucose metabolism after exhausting exercise. J Appl Physiol 49, 1057-1069.

Brown, B.I., and Brown, D.H. (1966). Lack of an alpha-1,4-glucan: alpha-1,4-glucan 6-glycosyl transferase in a case of type IV glycogenosis. Proceedings of the National Academy of Sciences 56, 725-729.

Browner, M.F., Nakano, K., Bang, A.G., and Fletterick, R.J. (1989). Human muscle glycogen synthase cDNA sequence: a negatively charged protein with an asymmetric charge distribution. Proceedings of the National Academy of Sciences 86, 1443-1447.

Bruno, C., van Diggelen, O.P., Cassandrini, D., Gimpelev, M., Giuffrè, B., Donati, M.A., Introvini, P., Alegria, A., Assereto, S., Morandi, L., Mora, M., Tonoli, E., Mascelli, S., Traverso, M., Pasquini, E., Bado, M., Vilarinho, L., van Noort, G., Mosca, F., DiMauro, S., Zara, F., and Minetti, C. (2004). Clinical and genetic heterogeneity of branching enzyme deficiency (glycogenosis type IV). Neurology 63, 1053-1058.

Buléon, A., Colonna, P., Planchot, V., and Ball, S. (1998a). Starch granules: structure and biosynthesis. International Journal of Biological Macromolecules 23, 85-112.

Buléon, A., Gérard, C., Riekel, C., Vuong, R., and Chanzy, H. (1998b). Details of the Crystalline Ultrastructure of C-Starch Granules Revealed by Synchrotron Microfocus Mapping. Macromolecules 31, 6605-6610.

Cameron, J.M., Levandovskiy, V., MacKay, N., Utgikar, R., Ackerley, C., Chiasson, D., Halliday, W., Raiman, J., and Robinson, B.H. (2009). Identification of a novel mutation in GYS1 (muscle-specific glycogen synthase) resulting in sudden cardiac death, that is diagnosable from skin fibroblasts. Molecular Genetics and Metabolism 98, 378-382.

Carpenter, S., and Karpati, G. (1981). Sweat gland duct cells in Lafora disease: diagnosis by skin biopsy. Neurology 31, 1564-1568.

Carpenter, M., Joyce, N., Butler, R., Genet, R., and Timmerman-Vaughan, G. (2012). A mass spectrometric method for quantifying C3 and C6 phosphorylation of starch. Analytical Biochemistry 431, 115-119.

Caspar, T., Huber, S.C., and Somerville, C. (1985). Alterations in Growth, Photosynthesis, and Respiration in a Starchless Mutant of Arabidopsis thaliana (L.) Deficient in Chloroplast Phosphoglucomutase Activity. Plant Physiol 79, 11-17.

Caspar, T., Lin, T.P., Kakefuda, G., Benbow, L., Preiss, J., and Somerville, C. (1991). Mutants of Arabidopsis with Altered Regulation of Starch Degradation. Plant Physiol 95, 1181-1188.

Cavanagh, J.B. (1999). Corpora-amylacea and the family of polyglucosan diseases. Brain Res Brain Res Rev 29, 265-295.

Chan, E.M., Bulman, D.E., Paterson, A.D., Turnbull, J., Andermann, E., Andermann, F., Rouleau, G.A., Delgado-Escueta, A.V., Scherer, S.W., and Minassian, B.A. (2003a). Genetic mapping of a new Lafora progressive myoclonus epilepsy locus (EPM2B) on 6p22. J Med Genet 40, 671-675.

Chan, E.M., Young, E.J., Ianzano, L., Munteanu, I., Zhao, X., Christopoulos, C.C., Avanzini, G., Elia, M., Ackerley, C.A., Jovic, N.J., Bohlega, S., Andermann, E., Rouleau, G.A., Delgado-Escueta, A.V., Minassian, B.A., and Scherer, S.W. (2003b). Mutations in NHLRC1 cause progressive myoclonus epilepsy. Nat Genet 35, 125-127.

Chan, E.M., Omer, S., Ahmed, M., Bridges, L.R., Bennett, C., Scherer, S.W., and Minassian, B.A. (2004a). Progressive myoclonus epilepsy with polyglucosans (Lafora disease): evidence for a third locus. Neurology 63, 565-567.

Chan, E.M., Ackerley, C.A., Lohi, H., Ianzano, L., Cortez, M.A., Shannon, P., Scherer, S.W., and Minassian, B.A. (2004b). Laforin preferentially binds the neurotoxic starch-like polyglucosans, which form in its absence in progressive myoclonus epilepsy. Human Molecular Genetics 13, 1117-1129.

Chen, D., and Dou, Q.P. (2010). The Ubiquitin-Proteasome System as a Prospective Molecular Target for Cancer Treatment and Prevention. Curr Protein Pept Sci 11, 459-470.

Cheng, A., Zhang, M., Okubo, M., Omichi, K., and Saltiel, A.R. (2009). Distinct mutations in the glycogen debranching enzyme found in glycogen storage disease type III lead to impairment in diverse cellular functions. Human Molecular Genetics 18, 2045-2052.

Chia, T., Thorneycroft, D., Chapple, A., Messerli, G., Chen, J., Zeeman, S.C., Smith, S.M., and Smith, A.M. (2004). A cytosolic glucosyltransferase is required for conversion of starch to sucrose in Arabidopsis leaves at night. Plant J 37, 853-863.

Cho, M.-H., Lim, H., Shin, D.H., Jeon, J.-S., Bhoo, S.H., Park, Y.-I., and Hahn, T.-R. (2010). Role of the plastidic glucose translocator in the export of starch degradation products from the chloroplasts in Arabidopsis thaliana. New Phytologist 190, 101-112.

Christiansen, C., Hachem, M.A., Glaring, M.A., Viksø-Nielsen, A., Sigurskjold, B.W., Svensson, B., and Blennow, A. (2009). A CBM20 low-affinity starch-binding domain from glucan, water dikinase. FEBS Letters 583, 1159-1163.

Conlee, R.K., Hickson, R.C., Winder, W.W., Hagberg, J.M., and Holloszy, J.O. (1978). Regulation of glycogen resynthesis in muscles of rats following exercise. Am J Physiol 235, R145-150.

Comparot-Moss, S., Kotting, O., Stettler, M., Edner, C., Graf, A., Weise, S.E., Streb, S., Lue, W.L., MacLean, D., Mahlow, S., Ritte, G., Steup, M., Chen, J., Zeeman, S.C., and Smith, A.M. (2010). A putative phosphatase, LSF1, is required for normal starch turnover in Arabidopsis leaves. Plant Physiol 152, 685-697.

Cook, A.G., Johnson, L.N., and McDonnell, J.M. (2005). Structural characterization of Ca2+/CaM in complex with the phosphorylase kinase PhK5 peptide. FEBS Journal 272, 1511-1522.

Critchley, J.H., Zeeman, S.C., Takaha, T., Smith, A.M., and Smith, S.M. (2001). A critical role for disproportionating enzyme in starch breakdown is revealed by a knock-out mutation in Arabidopsis. The Plant Journal 26, 89-100.

Currais, A., Hortobagyi, T., and Soriano, S. (2009). The neuronal cell cycle as a mechanism of pathogenesis in Alzheimer's disease. Aging (Albany NY) 1, 363-371.

Delatte, T., Trevisan, M., Parker, M.L., and Zeeman, S.C. (2005). Arabidopsis mutants Atisa1 and Atisa2 have identical phenotypes and lack the same multimeric isoamylase, which influences the branch point distribution of amylopectin during starch synthesis. The Plant Journal 41, 815-830.

Delatte, T., Umhang, M., Trevisan, M., Eicke, S., Thorneycroft, D., Smith, S.M., and Zeeman, S.C. (2006). Evidence for distinct mechanisms of starch granule breakdown in plants. J Biol Chem 281, 12050-12059.

Dent, P., Lavoinne, A., Nakielny, S., Caudwell, F.B., Watt, P., and Cohen, P. (1990). The molecular mechanism by which insulin stimulates glycogen synthesis in mammalian skeletal muscle. Nature 348, 302-308.

Denyer, K., Johnson, P., Zeeman, S., and Smith, A.M. (2001). The control of amylose synthesis. Journal of Plant Physiology 158, 479-487.

Drochmans, P. (1962). Morphologie du glycogène: Etude au microscope électronique de colorations négatives du glycogène particulaire. Journal of Ultrastructure Research 6, 141-163.

Dumez, S., Wattebled, F., Dauvillee, D., Delvalle, D., Planchot, V., Ball, S.G., and D'Hulst, C. (2006). Mutants of Arabidopsis Lacking Starch Branching Enzyme II Substitute Plastidial Starch Synthesis by Cytoplasmic Maltose Accumulation. The Plant Cell Online 18, 2694-2709.

Duran, J., Tevy, M.F., Garcia-Rocha, M., Calbo, J., Milan, M., and Guinovart, J.J. (2012). Deleterious effects of neuronal accumulation of glycogen in flies and mice. EMBO Mol Med 4, 1-11.

Edner, C., Li, J., Albrecht, T., Mahlow, S., Hejazi, M., Hussain, H., Kaplan, F., Guy, C., Smith, S.M., Steup, M., and Ritte, G. (2007). Glucan, water dikinase activity stimulates breakdown of starch granules by plastidial beta-amylases. Plant Physiol 145, 17-28.

Edwards, T.A., Wilkinson, B.D., Wharton, R.P., and Aggarwal, A.K. (2003). Model of the Brain Tumor-Pumilio translation repressor complex. Genes & Development 17, 2508-2513.

Ercan-Fang, N., Taylor, M.R., Treadway, J.L., Levy, C.B., Genereux, P.E., Gibbs, E.M., Rath, V.L., Kwon, Y., Gannon, M.C., and Nuttall, F.Q. (2005). Endogenous effectors of human liver glycogen phosphorylase modulate effects of indole-site inhibitors. American Journal of Physiology - Endocrinology And Metabolism 289, E366-E372.

Farkas, I., Hardy, T.A., Goebl, M.G., and Roach, P.J. (1991). Two glycogen synthase isoforms in Saccharomyces cerevisiae are coded by distinct genes that are differentially controlled. Journal of Biological Chemistry 266, 15602-15607.

Fettke, J., Eckermann, N., Poeste, S., Pauly, M., and Steup, M. (2004). The glycan substrate of the cytosolic (Pho 2) phosphorylase isozyme from Pisum sativum L.: identification, linkage analysis and subcellular localization. Plant J 39, 933-946.

Fettke, J., Eckermann, N., Tiessen, A., Geigenberger, P., and Steup, M. (2005a). Identification, subcellular localization and biochemical characterization of water-soluble heteroglycans (SHG) in leaves of Arabidopsis thaliana L.: distinct SHG reside in the cytosol and in the apoplast. Plant J *43*, 568-585.

Fettke, J., Poeste, S., Eckermann, N., Tiessen, A., Pauly, M., Geigenberger, P., and Steup, M. (2005b). Analysis of cytosolic heteroglycans from leaves of transgenic potato (Solanum tuberosum L.) plants that under- or overexpress the Pho 2 phosphorylase isozyme. Plant Cell Physiol 46, 1987-2004.

Fettke, J., Chia, T., Eckermann, N., Smith, A., and Steup, M. (2006). A transglucosidase necessary for starch degradation and maltose metabolism in leaves at night acts on cytosolic heteroglycans (SHG). Plant J *46*, 668-684.

Fettke, J., Nunes-Nesi, A., Alpers, J., Szkop, M., Fernie, A.R., and Steup, M. (2008). Alterations in cytosolic glucose-phosphate metabolism affect structural features and biochemical properties of starch-related heteroglycans. Plant Physiol 148, 1614-1629.

Fettke, J., Hejazi, M., Smirnova, J., Hochel, E., Stage, M., and Steup, M. (2009a). Eukaryotic starch degradation: integration of plastidial and cytosolic pathways. J. Exp. Bot., erp054.

Fettke, J., Malinova, I., Eckermann, N., and Steup, M. (2009b). Cytosolic heteroglycans in photoautotrophic and in heterotrophic plant cells. Phytochemistry 70, 696-702.

Fettke, J., Leifels, L., Brust, H., Herbst, K., and Steup, M. (2012a). Two carbon fluxes to reserve starch in potato (Solanum tuberosum L.) tuber cells are closely interconnected but differently modulated by temperature. Journal of Experimental Botany.

Fettke, J., Fernie, A.R., and Steup, M. (2012b). Transitory starch and its degradation in higher plant cells. In Starch: Origins, Structure and Metabolism. I.J. Tetlow, ed. (London: Society of Experimental Biology), pp. 311-374.

Fincher, G.B. (1989). Molecular and Cellular Biology Associated with Endosperm Mobilization in Germinating Cereal Grains. Annual Review of Plant Physiology and Plant Molecular Biology 40, 305-346.

Fiske, C.H., and Subbarow, Y. (1925). THE COLORIMETRIC DETERMINATION OF PHOSPHORUS. Journal of Biological Chemistry 66, 375-400.

Fontana, J.D. (1980). The presence of phosphate in glycogen. FEBS Lett 109, 85-92.

Frayn, K.N. (2003). Metabolic Regulation - A Human Perspective. 2nd edition (Oxford: Blackwell Science Ltd, Blackwell Publishing).

Friebolin, H. (1992). Ein- und zweidimensionale NMR-Spektroskopie. 2. Auflage (Weinheim, Basel, Cambridge, New York: VCH Verlagsgesellschaft mbH).

Frunder, H. (1954). Metabolism of diphosphopyridine-dihydrodiphosphopyridine nucleotide concentrations in fatty liver. Hoppe Seylers Z Physiol Chem 297, 267-277.

Fujita, N., Yoshida, M., Asakura, N., Ohdan, T., Miyao, A., Hirochika, H., and Nakamura, Y. (2006). Function and Characterization of Starch Synthase I Using Mutants in Rice. Plant Physiology 140, 1070-1084.

Fujita, N., Yoshida, M., Kondo, T., Saito, K., Utsumi, Y., Tokunaga, T., Nishi, A., Satoh, H., Park, J.-H., Jane, J.-L., Miyao, A., Hirochika, H., and Nakamura, Y. (2007). Characterization of SSIIIa-Deficient Mutants of Rice: The Function of SSIIIa and Pleiotropic Effects by SSIIIa Deficiency in the Rice Endosperm. Plant Physiology 144, 2009-2023.

Fujita, N., and Nakamura, Y. (2012). Distinct and overlapping functions of starch synthase isoforms. In Starch: Origins, Structure and Metabolism. I.J. Tetlow, ed. (London: Society for Experimental Biology), pp. 115-140.

Fulton, D.C., Stettler, M., Mettler, T., Vaughan, C.K., Li, J., Francisco, P., Gil, M., Reinhold, H., Eicke, S., Messerli, G., Dorken, G., Halliday, K., Smith, A.M., Smith, S.M., and Zeeman, S.C. (2008). Beta-AMYLASE4, a noncatalytic protein required for starch breakdown, acts upstream of three active beta-amylases in Arabidopsis chloroplasts. Plant Cell 20, 1040-1058.

Gallant, D.J., Bouchet, B., and Baldwin, P.M. (1997). Microscopy of starch: evidence of a new level of granule organization. Carbohydrate Polymers 32, 177-191.

Ganesh, S., Delgado-Escueta, A.V., Sakamoto, T., Avila, M.R., Machado-Salas, J., Hoshii, Y., Akagi, T., Gomi, H., Suzuki, T., Amano, K., Agarwala, K.L., Hasegawa, Y., Bai, D.-S., Ishihara, T., Hashikawa, T., Itohara, S., Cornford, E.M., Niki, H., and Yamakawa, K. (2002). Targeted disruption of the EPM2A gene causes formation of Lafora inclusion bodies, neurodegeneration, ataxia, myoclonus epilepsy and impaired behavioral response in mice. Human Molecular Genetics 11, 1251-1262.

Ganesh, S., Tsurutani, N., Suzuki, T., Hoshii, Y., Ishihara, T., Delgado-Escueta, A.V., and Yamakawa, K. (2004). The carbohydrate-binding domain of Lafora disease protein targets Lafora polyglucosan bodies. Biochem Biophys Res Commun 313, 1101-1109.

Garz, A., Sandmann, M., Rading, M., Ramm, S., Menzel, R., and Steup, M. (2012). Cell-to-Cell Diversity in a Synchronized Chlamydomonas Culture As Revealed by Single-Cell Analyses. Biophys J *103*, 1078-1086.

Gentry, M.S., Worby, C.A., and Dixon, J.E. (2005). Insights into Lafora disease: malin is an E3 ubiquitin ligase that ubiquitinates and promotes the degradation of laforin. Proc Natl Acad Sci U S A 102, 8501-8506.

Gentry, M.S., Dowen, R.H., Worby, C.A., Mattoo, S., Ecker, J.R., and Dixon, J.E. (2007). The phosphatase laforin crosses evolutionary boundaries and links carbohydrate metabolism to neuronal disease. The Journal of Cell Biology *178*, 477-488.

Gentry, M.S., Dixon, J.E., and Worby, C.A. (2009). Lafora disease: insights into neurodegeneration from plant metabolism. Trends in Biochemical Sciences *34*, 628-639.

Gérard, C., Colonna, P., Buléon, A., and Planchot, V. (2001). Amylolysis of maize mutant starches. Journal of the Science of Food and Agriculture 81, 1281-1287.

Gibon, Y., Vigeolas, H., Tiessen, A., Geigenberger, P., and Stitt, M. (2002). Sensitive and high throughput metabolite assays for inorganic pyrophosphate, ADPGlc, nucleotide phosphates, and glycolytic intermediates based on a novel enzymic cycling system. Plant J *30*, 221-235.

Giddings, J.C. (1993). Field-flow fractionation: analysis of macromolecular, colloidal, and particulate materials. Science *260*, 1456-1465.

Gilbert, A., Robins, R.J., Remaud, G.r.S., and Tcherkez, G.G.B. (2012). Intramolecular 13C pattern in hexoses from autotrophic and heterotrophic C3 plant tissues. Proceedings of the National Academy of Sciences 109, 18204-18209.

Girard, J.-M., Lê, K.H.D., and Lederer, F. (2006). Molecular characterization of laforin, a dual-specificity protein phosphatase implicated in Lafora disease. Biochimie 88, 1961-1971.

Glaring, M.A., Zygadlo, A., Thorneycroft, D., Schulz, A., Smith, S.M., Blennow, A., and Baunsgaard, L. (2007). An extra-plastidial alpha-glucan, water dikinase from Arabidopsis phosphorylates amylopectin in vitro and is not necessary for transient starch degradation. J Exp Bot 58, 3949-3960.

Glock, G.E., and McLean, P. (1955). The determination of oxidized and reduced diphosphopyridine nucleotide and triphosphopyridine nucleotide in animal tissues. Biochem J 61, 381-388.

Goldsmith, E., Sprang, S., and Fletterick, R. (1982). Structure of maltoheptaose by difference Fourier methods and a model for glycogen. Journal of Molecular Biology 156, 411-427.

Guan, H., Li, P., Imparl-Radosevich, J., Preiss, J., and Keeling, P. (1997). Comparing the Properties of Escherichia coli Branching Enzyme and Maize Branching Enzyme. Archives of Biochemistry and Biophysics 342, 92-98.

Gunja-Smith, Z., Marshall, J.J., Mercier, C., Smith, E.E., and Whelan, W.J. (1970). A revision of the Meyer-Bernfeld model of glycogen and amylopectin. FEBS Lett 12, 101-104.

Gunja-Smith, Z., Marshall, J.J., and Smith, E.E. (1971). Enzymatic determination of the unit chain length of glycogen and related polysaccharides. FEBS Letters 13, 309-311.

Günther, H. (1992). NMR-Spektroskopie. Grundlagen, Konzepte und Anwendungen der Protonen und Kohlenstoff-13 Kernresonanz-Spektroskopie in der Chemie. 3. Auflage (Stuttgart, New York: Georg Thieme Verlag).

Haebel, S., Hejazi, M., Frohberg, C., Heydenreich, M., and Ritte, G. (2008). Mass spectrometric quantification of the relative amounts of C6 and C3 position phosphorylated glucosyl residues in starch. Anal Biochem *379*, 73-79.

Hansen, P.I., Spraul, M., Dvortsak, P., Larsen, F.H., Blennow, A., Motawia, M.S., and Engelsen, S.B. (2009). Starch phosphorylation--maltosidic restrains upon 3'- and 6'-phosphorylation investigated by chemical synthesis, molecular dynamics and NMR spectroscopy. Biopolymers 91, 179-193.

Hatakeyama, S., and Nakayama, K.I. (2003). U-box proteins as a new family of ubiquitin ligases. Biochemical and Biophysical Research Communications 302, 635-645.

Hejazi, M., Fettke, J., Haebel, S., Edner, C., Paris, O., Frohberg, C., Steup, M., and Ritte, G. (2008). Glucan, water dikinase phosphorylates crystalline maltodextrins and thereby initiates solubilization. Plant J 55, 323-334.

Hejazi, M., Fettke, J., Paris, O., and Steup, M. (2009). The two plastidial starch-related dikinases sequentially phosphorylate glucosyl residues at the surface of both the A- and B-allomorph of crystallized maltodextrins but the mode of action differs. Plant Physiol. 150, 962-976.

Hejazi, M., Fettke, J., Kotting, O., Zeeman, S.C., and Steup, M. (2010). The Laforin-Like Dual-Specificity Phosphatase SEX4 from Arabidopsis Hydrolyzes Both C6- and C3-Phosphate Esters Introduced by Starch-Related Dikinases and Thereby Affects Phase Transition of {alpha}-Glucans. Plant Physiol. 152, 711-722.

Hejazi, M., Fettke, J., and Steup, M. (2012a). Starch phosphorylation and dephosphorylation: the consecutive action of starch-related dikinases and phosphatases. In Starch: Origins, Structure and Metabolism. I.J. Tetlow, ed. (London: Society of Experimental Biology), pp. 279-310.

Hejazi, M., Steup, M., and Fettke, J. (2012b). The plastidial glucan, water dikinase (GWD) catalyses multiple phosphotransfer reactions. FEBS J 279, 1953-1966.

Hess, H.H., and Derr, J.E. (1975). Assay of inorganic and organic phosphorus in the 0.1-5 nanomole range. Anal Biochem *63*, 607-613.

Hizukuri, S., Tabata, S., Kagoshima, and Nikuni, Z. (1970). Studies on Starch Phosphate Part 1. Estimation of glucose-6-phosphate residues in starch and the presence of other bound phosphate(s). Starch - Stärke 22, 338-343.

Hizukuri, S. (1986). Polymodal distribution of the chain lengths of amylopectins, and its significance. Carbohydrate Research 147, 342-347.

Holzer, H., Goldschmidt, S., Lamprecht, W., and Helmreich, E. (1954). Determination of stationary concentrations of intermediate substances. I. Determination of stationary concentrations of diphosphopyridine-dihydrodiphosphopyridine nucleotide in living cells and tissues. Hoppe Seylers Z Physiol Chem 297, 1-18.

Hurley, T.D., Walls, C., Bennett, J.R., Roach, P.J., and Wang, M. (2006). Direct detection of glycogenin reaction products during glycogen initiation. Biochemical and Biophysical Research Communications 348, 374-378.

Hussain, H., Mant, A., Seale, R., Zeeman, S., Hinchliffe, E., Edwards, A., Hylton, C., Bornemann, S., Smith, A.M., Martin, C., and Bustos, R. (2003). Three Isoforms of Isoamylase Contribute Different Catalytic Properties for the Debranching of Potato Glucans. The Plant Cell Online 15, 133-149.

Imberty, A., Buléon, A., Tran, V., and Péerez, S. (1991). Recent Advances in Knowledge of Starch Structure. Starch - Stärke 43, 375-384.

Itaya, K., and Ui, M. (1966). A new micromethod for the colorimetric determination of inorganic phosphate. Clin Chim Acta 14, 361-366.

Jenkins, P.J., Cameron, R.E., and Donald, A.M. (1993). A Universal Feature in the Structure of Starch Granules from Different Botanical Sources. Starch - Stärke 45, 417-420.

Jeon, J.-S., Ryoo, N., Hahn, T.-R., Walia, H., and Nakamura, Y. (2010). Starch biosynthesis in cereal endosperm. Plant Physiology and Biochemistry 48, 383-392.

Khorana, H.G., Tener, G.M., Wright, R.S., and Moffatt, J.G. (1957). Cyclic Phosphates. III. Some General Observations on the Formation and Properties of Five-, Six- and Seven-membered Cyclic Phosphate Esters. Journal of the American Chemical Society 79, 430-436.

Kirkman, B.R. and Whelan, W.J. (1986). Glucosamine is a normal component of liver glycogen. FEBS Letters 194, 6-11.

Klein, H.W., Im, M.J., and Palm, D. (1986). Mechanism of the phosphorylase reaction. European Journal of Biochemistry 157, 107-114.

Kollberg, G., Tulinius, M.r., Gilljam, T., Ã–stman-Smith, I., Forsander, G., Jotorp, P., Oldfors, A., and Holme, E. (2007). Cardiomyopathy and Exercise Intolerance in Muscle Glycogen Storage Disease 0. New England Journal of Medicine 357, 1507-1514.

Kötting, O., Pusch, K., Tiessen, A., Geigenberger, P., Steup, M., and Ritte, G. (2005). Identification of a novel enzyme required for starch metabolism in Arabidopsis leaves. The phosphoglucan, water dikinase. Plant Physiol *137*, 242-252.

Kötting, O., Santelia, D., Edner, C., Eicke, S., Marthaler, T., Gentry, M.S., Comparot-Moss, S., Chen, J., Smith, A.M., Steup, M., Ritte, G., and Zeeman, S.C. (2009). STARCH-EXCESS4 Is a Laforin-Like Phosphoglucan Phosphatase Required for Starch Degradation in Arabidopsis thaliana. Plant Cell, tpc.108.064360.

Krisman, C.R., and Barengo, R. (1975). A Precursor of Glycogen Biosynthesis: α-1,4-Glucan-Protein. European Journal of Biochemistry 52, 117-123.

Kuhl, A., and Lorenzen, H. (1964). Handling and Culturing of Chlorella. In Methods in Cell Physiology. D.M. Prescott, ed. (New York, USA: Academic Press Inc.), pp. 159-166.

Kuipers, A.G.J., Jacobsen, E., and Visser, R.G.F. (1994). Formation and Deposition of Amylose in the Potato Tuber Starch Granule Are Affected by the Reduction of Granule-Bound Starch Synthase Gene Expression. The Plant Cell Online 6, 43-52.

Lafora, G.R., and Glueck, B. (1911). Beitrag zur Histopathologie der myoklonischen Epilepsie. Zeitschrift für die gesamte Neurologie und Psychiatrie 6, 1-14.

Lehninger, A., Nelson, D., and Cox, M. (2001). Lehninger Biochemie. 3rd edition (Berlin, Heidelberg, New York: Springer-Verlag).

Lim, S., Seib, P. A. (1993). Location of Phosphate Esters in a Wheat Starch Phosphate by [31]P-Nuclear Magnetic Resonance Spectroscopy. Cereal Chem. 70, 145-152.

Lin, T.-P., Caspar, T., Somerville, C., and Preiss, J. (1988). Isolation and Characterization of a Starchless Mutant of Arabidopsis thaliana (L.) Heynh Lacking ADPglucose Pyrophosphorylase Activity. Plant Physiology 86, 1131-1135.

Lin, A., Mu, J., Yang, J., and Roach, P.J. (1999). Self-Glucosylation of Glycogenin, the Initiator of Glycogen Biosynthesis, Involves an Inter-subunit Reaction. Archives of Biochemistry and Biophysics 363, 163-170.

Lindeboom, N., Chang, P.R., and Tyler, R.T. (2004). Analytical, Biochemical and Physicochemical Aspects of Starch Granule Size, with Emphasis on Small Granule Starches: A Review. Starch - Stärke 56, 89-99.

Lohi, H., Ianzano, L., Zhao, X.-C., Chan, E.M., Turnbull, J., Scherer, S.W., Ackerley, C.A., and Minassian, B.A. (2005a). Novel glycogen synthase kinase 3 and ubiquitination pathways in progressive myoclonus epilepsy. Human Molecular Genetics 14, 2727-2736.

Lohi, H., Young, E.J., Fitzmaurice, S.N., Rusbridge, C., Chan, E.M., Vervoort, M., Turnbull, J., Zhao, X.-C., Ianzano, L., Paterson, A.D., Sutter, N.B., Ostrander, E.A., André, C., Shelton, G.D., Ackerley, C.A., Scherer, S.W., and Minassian, B.A. (2005b). Expanded Repeat in Canine Epilepsy. Science 307, 81.

Lomako, J., Lomako, W.M., Whelan, W.J., and Marchase, R.B. (1993). Glycogen contains phosphodiester groups that can be introduced by UDPglucose: glycogen glucose 1-phosphotransferase. FEBS Lett 329, 263-267.

Lomako, J., Lomako, W.M., Kirkman, B.R., and Whelan, W.J. (1994). The role of phosphate in muscle glycogen. Biofactors *4*, 167-171.

Lovering, R., Hanson, I.M., Borden, K.L., Martin, S., O'Reilly, N.J., Evan, G.I., Rahman, D., Pappin, D.J., Trowsdale, J., and Freemont, P.S. (1993). Identification and preliminary characterization of a protein motif related to the zinc finger. Proceedings of the National Academy of Sciences 90, 2112-2116.

Lowenstein, D.H., Bleck, T., and Macdonald, R.L. (1999). It's Time to Revise the Definition of Status Epilepticus. Epilepsia 40, 120-122.

Lowry, O.H., Passonneau, J.V., Schulz, D.W., and Rock, M.K. (1961). The measurement of pyridine nucleotides by enzymatic cycling. J Biol Chem 236, 2746-2755.

Lowry, O.H., and Passonneau, J.V., eds. (1972). A flexible system of enzymatic analysis. (New York: Academic Press).

Lu, Y., and Sharkey, T. (2004). The role of amylomaltase in maltose metabolism in the cytosol of photosynthetic cells. Planta 218, 466-473.

Lunn, J.E., and MacRae, E. (2003). New complexities in the synthesis of sucrose. Current Opinion in Plant Biology 6, 208-214.

Manners, D.J. (1991). Recent developments in our understanding of glycogen structure. Carbohydrate Polymers 16, 37-82.

Marchand, I., Chorneyko, K., Tarnopolsky, M., Hamilton, S., Shearer, J., Potvin, J., and Graham, T.E. (2002). Quantification of subcellular glycogen in resting human muscle: granule size, number, and location. Journal of Applied Physiology 93, 1598-1607.

Marshall, J.J., Tipson, R.S., and Derek, H. (1974). Application of Enzymic Methods to the Structural Analysis of Polysaccharides: Part I. In Advances in Carbohydrate Chemistry and Biochemistry (Academic Press), pp. 257-370.

Martin, G.E., and Zektzer, A.S. (1988). Two-Dimensional NMR Methods for Establishing Molecular Connectivity. A Chemist's Guide to Experiment Selection, Performance, and Interpretation. (New York: VCH Publishers, Inc.).

Matsui, H., Sasaki, M., Takemasa, E., Kaneta, T., and Chiba, S. (1984). Kinetic Studies on the Substrate Specificity and Active Site of Rabbit Muscle Acid α-Glucosidase. Journal of Biochemistry 96, 993-1004.

McVerry, P.H., and Kim, K.-H. (1974). Purification and kinetic mechanism of rat liver glycogen synthase. Biochemistry 13, 3505-3511.

Meléndez, R., Meléndez-Hevia, E., and Canela, E.I. (1999). The Fractal Structure of Glycogen: A Clever Solution to Optimize Cell Metabolism. Biophysical journal *77*, 1327-1332.

Meléndez-Hevia, E., Waddell, T.G., and Shelton, E.D. (1993). Optimization of molecular design in the evolution of metabolism: the glycogen molecule. Biochem J *295 (Pt 2)*, 477-483.

Mikkelsen, R., Baunsgaard, L., and Blennow, A. (2004). Functional characterization of alpha-glucan,water dikinase, the starch phosphorylating enzyme. Biochem J 377, 525-532.

Minassian, B.A., Lee, J.R., Herbrick, J.A., Huizenga, J., Soder, S., Mungall, A.J., Dunham, I., Gardner, R., Fong, C.Y., Carpenter, S., Jardim, L., Satishchandra, P., Andermann, E., Snead, O.C., 3rd, Lopes-Cendes, I., Tsui, L.C., Delgado-Escueta, A.V., Rouleau, G.A., and Scherer, S.W. (1998). Mutations in a gene encoding a novel protein tyrosine phosphatase cause progressive myoclonus epilepsy. Nat Genet 20, 171-174.

Minassian, B.A. (2001). Lafora's disease: towards a clinical, pathologic, and molecular synthesis. Pediatr Neurol *25*, 21-29.

Mordoh, J., Krisman, C.R., and Leloir, L.F. (1966). Further studies on high molecular weight liver glycogen. Archives of Biochemistry and Biophysics 113, 265-272.

Morrison, W.R. (1964). A fast, simple and reliable method for the microdetermination of phosphorus in biological materials. Analytical Biochemistry 7, 218-224.

Muhrbeck, P., and Tellier, C. (1991). Determination of the Posphorylation of Starch from Native Potato Varieties by 31P NMR. Starch - Stärke 43, 25-27.

Nakamura, Y. (2002). Towards a Better Understanding of the Metabolic System for Amylopectin Biosynthesis in Plants: Rice Endosperm as a Model Tissue. Plant and Cell Physiology 43, 718-725.

Nakayama, A., Yamamoto, K., and Tabata, S. (2001). Identification of the Catalytic Residues of Bifunctional Glycogen Debranching Enzyme. Journal of Biological Chemistry 276, 28824-28828.

Newsholme, P., Angelos, K.L., and Walsh, D.A. (1992). High and intermediate affinity calmodulin binding domains of the alpha and beta subunits of phosphorylase kinase and their potential role in phosphorylation-dependent activation of the holoenzyme. Journal of Biological Chemistry 267, 810-818.

Nielsen, T.H., Wischmann, B., Enevoldsen, K., and Moller, B.L. (1994). Starch Phosphorylation in Potato Tubers Proceeds Concurrently with de Novo Biosynthesis of Starch. Plant Physiol 105, 111-117.

Niittylä, T., Messerli, G., Trevisan, M., Chen, J., Smith, A.M., and Zeeman, S.C. (2004). A Previously Unknown Maltose Transporter Essential for Starch Degradation in Leaves. Science 303, 87-89.

Niittyla, T., Comparot-Moss, S., Lue, W.L., Messerli, G., Trevisan, M., Seymour, M.D., Gatehouse, J.A., Villadsen, D., Smith, S.M., Chen, J., Zeeman, S.C., and Smith, A.M. (2006). Similar protein phosphatases control starch metabolism in plants and glycogen metabolism in mammals. J Biol Chem 281, 11815-11818.

Nikaido, T., Austin, J., and Stukenbrok, H. (1971). Studies in Myoclonus Epilepsy III. The Effects of Amylolytic Enzymes on the Ultrastructure of Lafora Bodies. Journal of Histochemistry & Cytochemistry 19, 382-385.

Nishi, A., Nakamura, Y., Tanaka, N., and Satoh, H. (2001). Biochemical and genetic analysis of the effects of amylose-extender mutation in rice endosperm. Plant Physiol *127*, 459-472.

Nisselbaum, J.S., and Green, S. (1969). A simple ultramicro method for determination of pyridine nucleotides in tissues. Anal Biochem *27*, 212-217.

Nitschke, F., Wang, P., Schmieder, P., Girard, G-M., Awrey, D.E., Wang, T., Israelian, J., Zhao, X., Turnbull, J., Heydenreich, M., Kleinpeter, E., Steup, M., and Minassian, B.A. (2013). Hyperphosphorylation of glucosyl C6 carbons and altered structure of glycogen in the neurodegenerative epilepsy Lafora disease. Cell Metabolism. In press.

Nunez, H.A., and Barker, R. (1976). The metal ion catalyzed decomposition of nucleoside diphosphate sugars. Biochemistry 15, 3843-3847.

Nuttall, F.Q., Gannon, M.C., Bai, G., and Lee, E.Y.C. (1994). Primary Structure of Human Liver Glycogen Synthase Deduced by cDNA Cloning. Archives of Biochemistry and Biophysics 311, 443-449.

Paladini, A.C., and Leloir, L.F. (1952). Studies on uridine-diphosphate-glucose. Biochem J 51, 426-430.

Palmer, T.N., Macaskie, L.E., and Grewel, K.K. (1983a). The unit-chain distribution profiles of branched (1,4)-α-d-glucans. Carbohydrate Research 114, 338-342.

Palmer, T.N., Macaskie, L.E., and Grewal, K.K. (1983b). Spatial distribution of unit chains in glycogen. Carbohydrate Research 115, 139-150.

Patel, S., Doble, B.W., MacAulay, K., Sinclair, E.M., Drucker, D.J., and Woodgett, J.R. (2008). Tissue-Specific Role of Glycogen Synthase Kinase 3Î² in Glucose Homeostasis and Insulin Action. Molecular and Cellular Biology 28, 6314-6328.

Patron, N.J., and Keeling, P.J. (2005). Common Evolutionary Origin of Starch Biosynthetic Enzymes in Green and Red Algae. Journal of Phycology 41, 1131-1141.

Peat, S., Roberts, P.J.P., and Whelan, W.J. (1952). The Occurrence of Fructose in Rabbit-Liver Glycogen. Biochem J 51, XVII.

Pederson, B.A., Cheng, C., Wilson, W.A., and Roach, P.J. (2000). Regulation of Glycogen Synthase: Identification of Residues Involved in Regulation by the Allosteric Ligand Glucose 6-P and by Phosphorylation. Journal of Biological Chemistry 275, 27753-27761.

Pederson, B.A., Csitkovits, A.G., Simon, R., Schroeder, J.M., Wang, W., Skurat, A.V., and Roach, P.J. (2003). Overexpression of glycogen synthase in mouse muscle results in less branched glycogen. Biochemical and Biophysical Research Communications 305, 826-830.

Pérez, S., and Bertoft, E. (2010). The molecular structures of starch components and their contribution to the architecture of starch granules: A comprehensive review. Starch - Stärke *62*, 389-420.

Perich, J.W., and Johns, R.B. (1988a). Di-tert-butyl N,N-Diethylphosphoramidite. A New Phosphitylating Agent for the Efficient Phosphorylation of Alcohols. Synthesis *1988*, 142-144.

Perich, J.W., and Johns, R.B. (1988b). Di-t-butyl N, N-diethylphosphoramidite and dibenzyl N, N-diethylphosphoramidite. Highly reactive reagents for the 'phosphite-triester' phosphorylation of serine-containing peptides. Tetrahedron Letters *29*, 2369-2372.

Pulido, R., and Hooft van Huijsduijnen, R. (2008). Protein tyrosine phosphatases: dual-specificity phosphatases in health and disease. FEBS J 275, 848-866.

Qi, Y., Kawano, N., Yamauchi, Y., Ling, J., Li, D., and Tanaka, K. (2005). Identification and cloning of a submergence-induced gene OsGGT (glycogenin glucosyltransferase) from rice (Oryza sativa L.) by suppression subtractive hybridization. Planta 221, 437-445.

Rahman, S., Kosar-Hashemi, B., Samuel, M.S., Hill, A., Abbott, D.C., Skerritt, J.H., Preiss, J., Appels, R., and Morell, M.K. (1995). The Major Proteins of Wheat Endosperm Starch Granules. Functional Plant Biology 22, 793-803.

Raju, G.P., Li, H.-C., Bali, D.S., Chen, Y.-T., Urion, D.K., Lidov, H.G.W., and Kang, P.B. (2008). A Case of Congenital Glycogen Storage Disease Type IV With a Novel GBE1 Mutation. Journal of Child Neurology 23, 349-352.

Reschiglian, P., Zattoni, A., Roda, B., Michelini, E., and Roda, A. (2005). Field-flow fractionation and biotechnology. Trends in biotechnology *23*, 475-483.

Reuser, A.J.J., Kroos, M.A., Hermans, M.M.P., Bijvoet, A.G.A., Verbeet, M.P., Van Diggelen, O.P., Kleijer, W.J., and Van Der Ploeg, A.T. (1995). Glycogenosis type II (acid maltase deficiency). Muscle & Nerve 18, S61-S69.

Ritte, G., Eckermann, N., Haebel, S., Lorberth, R., and Steup, M. (2000). Compartmentation of the Starch-Related R1 Protein in Higher Plants13. Starch - Stärke *52*, 145-149.

Ritte, G., Lloyd, J.R., Eckermann, N., Rottmann, A., Kossmann, J., and Steup, M. (2002). The starch-related R1 protein is an alpha -glucan, water dikinase. Proc Natl Acad Sci U S A *99*, 7166-7171.

Ritte, G., Scharf, A., Eckermann, N., Haebel, S., and Steup, M. (2004). Phosphorylation of transitory starch is increased during degradation. Plant Physiol 135, 2068-2077.

Ritte, G., Heydenreich, M., Mahlow, S., Haebel, S., Kotting, O., and Steup, M. (2006). Phosphorylation of C6- and C3-positions of glucosyl residues in starch is catalyzed by distinct dikinases. FEBS Lett *580*, 4872-4876.

Roach, P.J., Depaoli-Roach, A.A., Hurley, T.D., and Tagliabracci, V.S. (2012). Glycogen and its metabolism: some new developments and old themes. Biochem J *441*, 763-787.

Roberts, P.J., and Whelan, W.J. (1960). The mechanism of carbohydrase action. 5. Action of human salivary alpha-amylase on amylopectin and glycogen. Biochem. J. 76, 246-253.

Rodriguez, I.R., and Whelan, W.J. (1985). A novel glycosyl-amino acid linkage: rabbit-muscle glycogen is covalently linked to a protein via tyrosine. Biochem Biophys Res Commun 132, 829-836.

Roldán, I., Wattebled, F., Mercedes Lucas, M., Delvallé, D., Planchot, V., Jiménez, S., Pérez, R., Ball, S., D'Hulst, C., and Mérida, Á. (2007). The phenotype of soluble starch synthase IV defective mutants of

Arabidopsis thaliana suggests a novel function of elongation enzymes in the control of starch granule formation. The Plant Journal 49, 492-504.

Romero, P.A., Smith, E.E., and Whelan, W.J. (1980). Glucosamine as a substitute for glucose in glycogen metabolism. Biochem Int 1, 1-9.

Rover, L., Fernandes, J.C.B., Neto, G.d.O., Kubota, L.T., Katekawa, E., and Serrano, S.H.P. (1998). Study of NADH Stability Using Ultraviolet-Visible Spectrophotometric Analysis and Factorial Design. Analytical Biochemistry *260*, 50-55.

Rybicka, K.K. (1996). Glycosomes - the organelles of glycogen metabolism. Tissue and Cell 28, 253-265.

Sakai, M., Austin, J., Witmer, F., and Trueb, L. (1970). Studies in myoclonus epilepsy (Lafora body form): II. Polyglucosans in the systemic deposits of myoclonus epilepsy and in corpora amylacea. Neurology 20, 160.

Santelia, D., Kötting, O., Seung, D., Schubert, M., Thalmann, M., Bischof, S., Meekins, D.A., Lutz, A., Patron, N., Gentry, M.S., Allain, F.H.T., and Zeeman, S.C. (2011). The Phosphoglucan Phosphatase Like Sex Four2 Dephosphorylates Starch at the C3-Position in Arabidopsis. The Plant Cell Online.

Satoh, H., Nishi, A., Yamashita, K., Takemoto, Y., Tanaka, Y., Hosaka, Y., Sakurai, A., Fujita, N., and Nakamura, Y. (2003). Starch-Branching Enzyme I-Deficient Mutation Specifically Affects the Structure and Properties of Starch in Rice Endosperm. Plant Physiology 133, 1111-1121.

Satoh, H., Shibahara, K., Tokunaga, T., Nishi, A., Tasaki, M., Hwang, S.-K., Okita, T.W., Kaneko, N., Fujita, N., Yoshida, M., Hosaka, Y., Sato, A., Utsumi, Y., Ohdan, T., and Nakamura, Y. (2008). Mutation of the Plastidial α-Glucan Phosphorylase Gene in Rice Affects the Synthesis and Structure of Starch in the Endosperm. The Plant Cell Online 20, 1833-1849.

Sawilowsky, S.S. (2002). Fermat, Schubert, Einstein, and Behrens-Fisher:The Probable Difference Between Two Means When σ_1^2 unequal to σ_2^2. Journal of Modern Applied Statistical Methods *1*, 461-472.

Schächtele, C., and Steup, M. (1986). α-1,4-Glucan phosphorylase forms from leaves of spinach (Spinacia oleracea L.) I. In situ localization by indirect immunofluorescence. Planta 167, 444-451.

Schmidt, R.F., and Thews, G. (1997). Physiologie des Menschen. 27th edition (Berlin, Heidelberg, New York: Springer Verlag).

Schoch, T.J. (1942). Fractionation of Starch by Selective Precipitation with Butanol. Journal of the American Chemical Society 64, 2957-2961.

Schochet, S.S., Jr., McCormick, W.F., and Zellweger, H. (1970). Type IV glycogenosis (amylopectinosis). Light and electron microscopic observations. Arch Pathol 90, 354-363.

Serratosa, J.M., Gomez-Garre, P., Gallardo, M.E., Anta, B., de Bernabe, D.B., Lindhout, D., Augustijn, P.B., Tassinari, C.A., Malafosse, R.M., Topcu, M., Grid, D., Dravet, C., Berkovic, S.F., and de Cordoba, S.R. (1999). A novel protein tyrosine phosphatase gene is mutated in progressive myoclonus epilepsy of the Lafora type (EPM2). Hum Mol Genet 8, 345-352.

Shimomura, S., Nagai, M., and Fukui, T. (1982). Comparative Glucan Specificities of Two Types of Spinach Leaf Phosphorylase. Journal of Biochemistry 91, 703-717.

Silbernagl, S., and Lang, F. (1998). Taschenatlas der Pathophysiologie. (Stuttgart: Georg Thieme Verlag).

Singh, D.G., Lomako, J., Lomako, W.M., Whelan, W.J., Meyer, H.E., Serwe, M., and Metzger, J.W. (1995). β-Glucosylarginine: a new glucose-protein bond in a self-glucosylating protein from sweet corn. FEBS Letters 376, 61-64.

Singh, S., and Ganesh, S. (2009). Lafora progressive myoclonus epilepsy: A meta-analysis of reported mutations in the first decade following the discovery of the EPM2A and NHLRC1 genes. Human Mutation 30, 715-723.

Singh, S., and Ganesh, S. (2012). Phenotype variations in Lafora progressive myoclonus epilepsy: possible involvement of genetic modifiers[quest]. J Hum Genet 57, 283-285.

Sinnott, M.L. (2007). Carbohydrate Chemistry and Biochemistry: Structure and Mechanism. (Cambridge: RSC Publishing).

de Siqueira, L.F.M. (2010). Progressive myoclonic epilepsies: review of clinical, molecular and therapeutic aspects. Journal of Neurology 257, 1612-1619.

Slack, F.J., and Ruvkun, G. (1998). A novel repeat domain that is often associated with RING finger and B-box motifs. Trends in Biochemical Sciences 23, 474-475.

Smith, A.M. (2001). The biosynthesis of starch granules. Biomacromolecules 2, 335-341.

Stanley, D., Fitzgerald, A.M., Farnden, K.J.F., and MacRae, E.A. (2002). Characterisation of putative α-amylases from apple (Malus domestica) and Arabidopsis thaliana. Biologia 57/Suppl. 11, 137-148.

Stapleton, D., Nelson, C., Parsawar, K., McClain, D., Gilbert-Wilson, R., Barker, E., Rudd, B., Brown, K., Hendrix, W., O'Donnell, P., and Parker, G. (2010). Analysis of hepatic glycogen-associated proteins. Proteomics 10, 2320-2329.

Stenmark, H., Moskaug, J.O., Madshus, I.H., Sandvig, K., and Olsnes, S. (1991). Peptides fused to the amino-terminal end of diphtheria toxin are translocated to the cytosol. The Journal of Cell Biology 113, 1025-1032.

Streb, S., Eicke, S., and Zeeman, S.C. The simultaneous abolition of three starch hydrolases blocks transient starch breakdown in Arabidopsis. J Biol Chem 287, 41745-41756.

Sueoka, N. (1960). Mitotic Replication of Deoxyribonucleic Acid in Chlamydomonas Reinhardi. Proc Natl Acad Sci U S A *46*, 83-91.

Sullivan, M.A., Vilaplana, F., Cave, R.A., Stapleton, D., Gray-Weale, A.A., and Gilbert, R.G. (2010). Nature of α and β Particles in Glycogen Using Molecular Size Distributions. Biomacromolecules 11, 1094-1100.

Sun, L., and Chen, Z.J. (2004). The novel functions of ubiquitination in signaling. Current Opinion in Cell Biology 16, 119-126.

Szydlowski, N., Ragel, P., Raynaud, S., Lucas, M.M., Roldán, I., Montero, M., Munoz, F.J., Ovecka, M., Bahaji, A., Planchot, V., Pozueta-Romero, J., D'Hulst, C., and Mérida, Á. (2009). Starch Granule Initiation in Arabidopsis Requires the Presence of Either Class IV or Class III Starch Synthases. The Plant Cell Online.

Tabata, S., and Hizukuri, S. (1971). Studies on Starch Phosphate. Part 2. Isolation of Glucose 3-Phosphate and Maltose Phosphate by Acid Hydrolysis of Potato Starch. Starch - Stärke 23, 267-272.

Tabata, S., Nagata, K., and Hizukuri, S. (1975). Studies on Starch Phosphates. Part 3. On the Esterified Phosphates in Some Cereal Starches. Starch - Stärke 27, 333-335.

Tagliabracci, V.S., Turnbull, J., Wang, W., Girard, J.M., Zhao, X., Skurat, A.V., Delgado-Escueta, A.V., Minassian, B.A., Depaoli-Roach, A.A., and Roach, P.J. (2007). Laforin is a glycogen phosphatase, deficiency of which leads to elevated phosphorylation of glycogen in vivo. Proc Natl Acad Sci U S A 104, 19262-19266.

Tagliabracci, V.S., Girard, J.M., Segvich, D., Meyer, C., Turnbull, J., Zhao, X., Minassian, B.A., DePaoli-Roach, A.A., and Roach, P.J. (2008). Abnormal Metabolism of Glycogen Phosphate as a Cause for Lafora Disease. J. Biol. Chem. *283*, 33816-33825.

Tagliabracci, V.S. (2010). Metabolism of the Covalent Phosphate in Glycogen. Doctorate thesis. Department of Biochemistry & Molecular Biology (Indiana University).

Tagliabracci, V.S., Heiss, C., Karthik, C., Contreras, C.J., Glushka, J., Ishihara, M., Azadi, P., Hurley, T.D., Depaoli-Roach, A.A., and Roach, P.J. (2011). Phosphate Incorporation during Glycogen Synthesis and Lafora Disease. Cell Metab *13*, 274-282.

Taiz, L., and Zeiger, E. (2006). Plant Physiology. 4th edition (Sunderland, MA: Sinauer Associates, Inc.).

Takeda, Y., and Hizukuri, S. (1982). Location of phosphate groups in potato amylopectin. Carbohydrate Research 102, 321-327.

Takeda, Y., Hizukuri, S., and Juliano, B.O. (1987). Structures of rice amylopectins with low and high affinities for iodine. Carbohydrate Research 168, 79-88.

Tanaka, Y., Minagawa, S., and Akazawa, T. (1967). Association of Enzyme Proteins with Starch Granules in Rice Grains. Starch - Stärke 19, 206-212.

Tarentino, A.L. and Maley, F. (1976). Direct evidence that D-galactosamine incorporation into glycogen occurs via UDP-glucosamine. FEBS Letters 69, 175-178.

Tatge, H., Marshall, J., Martin, C., Edwards, E.A., and Smith, A.M. (1999). Evidence that amylose synthesis occurs within the matrix of the starch granule in potato tubers. Plant, Cell & Environment 22, 543-550.

Teitelbaum, R.C., Ruby, S.L., and Marks, T.J. (1980). A resonance Raman/iodine Moessbauer investigation of the starch-iodine structure. Aqueous solution and iodine vapor preparations. Journal of the American Chemical Society 102, 3322-3328.

Tiberia, E., Turnbull, J., Wang, T., Ruggieri, A., Zhao, X.C., Pencea, N., Israelian, J., Wang, Y., Ackerley, C.A., Wang, P., Liu, Y., and Minassian, B.A. (2012). Increased Laforin and Laforin Binding to Glycogen Underlie Lafora Body Formation in Malin-deficient Lafora Disease. J Biol Chem 287, 25650-25659.

Turnbull, J., Wang, P., Girard, J.M., Ruggieri, A., Wang, T.J., Draginov, A.G., Kameka, A.P., Pencea, N., Zhao, X., Ackerley, C.A., and Minassian, B.A. (2010). Glycogen hyperphosphorylation underlies lafora body formation. Ann Neurol 68, 925-933.

Turnbull, J., DePaoli-Roach, A.A., Zhao, X., Cortez, M.A., Pencea, N., Tiberia, E., Piliguian, M., Roach, P.J., Wang, P., Ackerley, C.A., and Minassian, B.A. (2011). PTG depletion removes Lafora bodies and rescues the fatal epilepsy of Lafora disease. PLoS Genet *7*, e1002037.

Twyman, R.M. (2005). Nuclear magnetic resonance spectroscopy-applicable elements: Phosphorus-31. In Encyclopedia of Analytical Science. P. Worsfold, A. Townshend, and C. Poole, eds. (London UK: Elsevier Science), pp. 278-286.

Umemoto, T., Yano, M., Satoh, H., Shomura, A., and Nakamura, Y. (2002). Mapping of a gene responsible for the difference in amylopectin structure between japonica-type and indica-type rice varieties. Theoretical and Applied Genetics 104, 1-8.

Utsumi, Y., and Nakamura, Y. (2006). Structural and enzymatic characterization of the isoamylase1 homo-oligomer and the isoamylase1-isoamylase2 hetero-oligomer from rice endosperm. Planta 225, 75-87.

Valles-Ortega, J., Duran, J., Garcia-Rocha, M., Bosch, C., Saez, I., Pujadas, L., Serafin, A., Cañas, X., Soriano, E., Delgado-García, J.M., Gruart, A., and Guinovart, J.J. (2011). Neurodegeneration and functional impairments associated with glycogen synthase accumulation in a mouse model of Lafora disease. EMBO Molecular Medicine 3, 667-681.

Vereb, G., and Bot, G. (1979). Regulation of heart specific phosphorylase a by AMP, glucose6-phosphate and glucose. International Journal of Biochemistry 10, 697-703.

Verhue, W., and Hers, H.G. (1966). A study of the reaction catalyzed by the liver branching enzyme. Biochem. J. 99, 222-227.

Vilchez, D., Ros, S., Cifuentes, D., Pujadas, L., Valles, J., Garcia-Fojeda, B., Criado-Garcia, O., Fernandez-Sanchez, E., Medrano-Fernandez, I., Dominguez, J., Garcia-Rocha, M., Soriano, E., Rodriguez de Cordoba, S., and Guinovart, J.J. (2007). Mechanism suppressing glycogen synthesis in neurons and its demise in progressive myoclonus epilepsy. Nat Neurosci 10, 1407-1413.

Villar-Palasi, C., and Larner, J. (1968). The hormonal regulation of glycogen metabolism in muscle. In Vitamins and Hormones. R.S. Harris, Wool, I.G., Loraine, J.A., ed. (New York: Academic Press, Inc.), pp. 65-118.

Visser, R.G.F., Somhorst, I., Kuipers, G.J., Ruys, N.J., Feenstra, W.J., and Jacobsen, E. (1991). Inhibition of the expression of the gene for granule-bound starch synthase in potato by antisense constructs. Molecular and General Genetics MGG 225, 289-296.

Waffenschmidt, S., and Jaenicke, L. (1987). Assay of reducing sugars in the nanomole range with 2,2'-bicinchoninate. Anal Biochem *165*, 337-340.

Walker, G.J., and Whelan, W.J. (1960). The mechanism of carbohydrase action. 8. Structures of the muscle-phosphorylase limit dextrins of glycogen and amylopectin. Biochem. J. 76, 264-268.

Wang, J., Stuckey, J.A., Wishart, M.J., and Dixon, J.E. (2002). A Unique Carbohydrate Binding Domain Targets the Lafora Disease Phosphatase to Glycogen. Journal of Biological Chemistry 277, 2377-2380.

Wang, W., Parker, G.E., Skurat, A.V., Raben, N., DePaoli-Roach, A.A., and Roach, P.J. (2006). Relationship between glycogen accumulation and the laforin dual specificity phosphatase. Biochemical and Biophysical Research Communications 350, 588-592.

Wang, W., Lohi, H., Skurat, A.V., DePaoli-Roach, A.A., Minassian, B.A., and Roach, P.J. (2007). Glycogen metabolism in tissues from a mouse model of Lafora disease. Archives of Biochemistry and Biophysics 457, 264-269.

Wanson, J.-C., and Drochmans, P. (1968). RABBIT SKELETAL MUSCLE GLYCOGEN: A Morphological and Biochemical Study of Glycogen β-Particles Isolated by the Precipitation-Centrifugation Method. The Journal of Cell Biology 38, 130-150.

Weber, A., Servaites, J.C., Geiger, D.R., Kofler, H., Hille, D., Groner, F., Hebbeker, U., and Flugge, U.I. (2000). Identification, purification, and molecular cloning of a putative plastidic glucose translocator. Plant Cell 12, 787-802.

Weinstein, D.A., Correia, C.E., Saunders, A.C., and Wolfsdorf, J.I. (2006). Hepatic glycogen synthase deficiency: An infrequently recognized cause of ketotic hypoglycemia. Molecular Genetics and Metabolism 87, 284-288.

Weise, S., Weber, A.M., and Sharkey, T. (2004). Maltose is the major form of carbon exported from the chloroplast at night. Planta 218, 474-482.

WHO (2006). Neurological disorders: public health challenges. (Geneva, Switzerland: World Health Organisation).

Wikman, J., Larsen, F.H., Motawia, M.S., Blennow, A., and Bertoft, E. (2011). Phosphate esters in amylopectin clusters of potato tuber starch. International Journal of Biological Macromolecules 48, 639-649.

Wilson, W.A., Roach, P.J., Montero, M., Baroja-Fernández, E., Muñoz, F.J., Eydallin, G., Viale, A.M., and Pozueta-Romero, J. (2010). Regulation of glycogen metabolism in yeast and bacteria. FEMS Microbiology Reviews 34, 952-985.

Wolfsdorf, J., and Weinstein, D. (2003). Glycogen Storage Diseases. Reviews in Endocrine and Metabolic Disorders 4, 95-102.

Worby, C.A., Gentry, M.S., and Dixon, J.E. (2006). Laforin, a Dual Specificity Phosphatase That Dephosphorylates Complex Carbohydrates. J. Biol. Chem. 281, 30412-30418.

Yamamoto, K., Sawada, S., and Onogaki, T. (1973). Properties of Rice Starch Prepared by Alkali Method with Various Conditions. Journal of the Japanese Society of Starch Science *20*, 99-104.

Yamamoto, K., Sawada, S., and Onogaki, T. (1981). Effects of Quality and Quantity of Alkaline Solution on the Properties of the Rice Starch. Journal of the Japanese Society of Starch Science *28*, 241-244.

Yang, B.Y., and Montgomery, R. (1996). Alkaline degradation of glucose: effect of initial concentration of reactants. Carbohydrate Research 280, 27-45.

Yao, Y., Thompson, D.B., and Guiltinan, M.J. (2004). Maize Starch-Branching Enzyme Isoforms and Amylopectin Structure. In the Absence of Starch-Branching Enzyme IIb, the Further Absence of Starch-Branching Enzyme Ia Leads to Increased Branching. Plant Physiology 136, 3515-3523.

Yokoi, S., Austin, J., Witmer, F., and Sakai, M. (1968). Studies in myoclonus epilepsy (lafora body form): I. isolation and preliminary characterization of lafora bodies in two cases. Archives of Neurology 19, 15-33.

Yu, T.S., Kofler, H., Hausler, R.E., Hille, D., Flugge, U.I., Zeeman, S.C., Smith, A.M., Kossmann, J., Lloyd, J., Ritte, G., Steup, M., Lue, W.L., Chen, J., and Weber, A. (2001). The Arabidopsis sex1 mutant is defective in the R1 protein, a general regulator of starch degradation in plants, and not in the chloroplast hexose transporter. Plant Cell 13, 1907-1918.

Yu, T.-S., Zeeman, S.C., Thorneycroft, D., Fulton, D.C., Dunstan, H., Lue, W.-L., Hegemann, B., Tung, S.-Y., Umemoto, T., Chapple, A., Tsai, D.-L., Wang, S.-M., Smith, A.M., Chen, J., and Smith, S.M. (2005). α-Amylase Is Not Required for Breakdown of Transitory Starch in Arabidopsis Leaves. J. Biol. Chem. 280, 9773-9779.

Zeeman, S.C., Northrop, F., Smith, A.M., and Rees, T. (1998). A starch-accumulating mutant of Arabidopsis thaliana deficient in a chloroplastic starch-hydrolyzing enzyme. Plant J 15, 357-365.

Zeeman, S.C., Tiessen, A., Pilling, E., Kato, K.L., Donald, A.M., and Smith, A.M. (2002). Starch synthesis in Arabidopsis. Granule synthesis, composition, and structure. Plant Physiol 129, 516-529.

Zeeman, S.C., Thorneycroft, D., Schupp, N., Chapple, A., Weck, M., Dunstan, H., Haldimann, P., Bechtold, N., Smith, A.M., and Smith, S.M. (2004). Plastidial alpha-glucan phosphorylase is not required for starch degradation in Arabidopsis leaves but has a role in the tolerance of abiotic stress. Plant Physiol 135, 849-858.

Zeeman, S.C., Smith, S.M., and Smith, A.M. (2007). The diurnal metabolism of leaf starch. Biochem J 401, 13-28.

Zeeman, S.C., Kossmann, J., and Smith, A.M. (2010). Starch: its metabolism, evolution, and biotechnological modification in plants. Annu Rev Plant Biol *61*, 209-234.

Zhang, X., Colleoni, C., Ratushna, V., Sirghie-colleoni, M., James, M., and Myers, A. (2004). Molecular characterization demonstrates that the Zea mays gene sugary2 codes for the starch synthase isoform SSIIa. Plant Molecular Biology 54, 865-879.

Zimm, B.H. (1948). The Scattering of Light and the Radial Distribution Function of High Polymer Solutions. The Journal of Chemical Physics *16*, 1093-1099.

Zmudzka, B., and Shugar, D. (1964). Preparation and chemical and enzymic properties of cyclic phosphates of D-glucopyranose and synthesis of derivates of N-(D-glucopyranosyl) pyridine. Acta Biochimica Polonica *11*, 509-525.

Zolnierowicz, S. (2000). Type 2A protein phosphatase, the complex regulator of numerous signaling pathways. Biochem Pharmacol 60, 1225-1235.

Acknowledgements

I would like to thank Prof. Dr. Martin Steup for introducing me to such an interesting topic, for his continuous support during all stages of this work, and his help with the smaller and bigger problems of scientific work. Discussions with him were always helpful and encouraging. I am thankful for being introduced to our collaborators at the Hospital for Sick Children, Toronto, and for helping me in numerous ways during the collaboration.

I would like to thank our collaborators and friends, Prof. Dr. Berge Minassian and Dr. Peixiang Wang, for putting so much trust into my work and for mind-setting and open discussions. I truly appreciate that they acquainted me with the 'red side' of polyglucan phosphorylation. Furthermore my deep thanks goes to Prof. Dr. Berge Minassian for his continuous and generous support of my work.

I thank Prof. Dr. Erich Kleinpeter for allowing me to use the facilities of his group. Especially, I want to mention Dr. Matthias Heydenreich who was always ready to perform apparently endless NMR experiments and to discuss the derived data. I'm thankful for his significant contributions to this work. Finally I want to express my thanks for introducing me to Dr. Peter Schmieder.

My deep thanks goes to Dr. Peter Schmieder, who designed and performed many crucial NMR experiments for this work. Moreover he never got tired to answer my question and help me to broaden my knowledge on NMR. This work would have been impossible without him.

I would like to thank PD Dr. Joerg Fettke for his constant support during my work. His advise was always very helpful and his criticism constructive.

I want to say thanks to the present and former members of the department of plant physiology who provided a good and productive atmosphere for scientific work and were always helpful in word and deed. Especially, I would like to mention Dr. Mahdi Hejazi and Madeleine Wilsky, who helped me with isolation of huge amounts of *Curcuma* starch.

I would like to thank Dr. Gerhard Ritte for kindly providing seeds of the *Arabidopsis thaliana* mutant *sex1-8* and samples of G3P and M6P.

I thank Prof. Dr. Yasunori Nakamura for kindly providing endosperm starch of wild type and EM10 rice.

Finally, I want to express my deep thanks to my wife, my family, and my friends, who always encouraged and supported me in many ways during the last years.